

Microbial degradation of crude oil at high pressure

Vom Promotionsausschuss der
Technischen Universität Hamburg-Harburg
zur Erlangung des akademischen Grades
Doktorin der Naturwissenschaften (Dr. rer. nat.)
genehmigte Dissertation

von
Martina Schedler

aus
Rostock

2016

1. Gutachter: Prof. Dr. rer. nat. Rudolf Müller
2. Gutachter: Prof. Dr.-Ing. Michael Schlüter
Vorsitzender des Prüfungsausschusses: Prof. Dr.-Ing. Stefan Heinrich

Tag der mündlichen Prüfung: 22.11.2016

urn:nbn:de:gbv:830-88215925



This work is licensed under a Creative Commons Attribution-NonCommercial 4.0 International License (CC BY-NC 4.0).

Danksagung

Mein Dank gebührt an erster Stelle Prof. Dr. Rudolf Müller für die Möglichkeit am Institut für Technische Biokatalyse an diesem spannenden und anspruchsvollen Thema arbeiten zu dürfen. Ich möchte mich herzlich bei ihm bedanken für seine großzügige Unterstützung, die zahlreichen anregenden Diskussionen, wertvollen Ratschläge und seine Herzlichkeit.

Ich möchte auch Prof. Dr. Michael Schlüter danken für die Übernahme des Zweitgutachtens sowie Prof. Dr. Stefan Heinrich für die Bereitschaft, den Vorsitz des Prüfungsausschusses zu übernehmen.

Von ganzem Herzen möchte ich Dr. Ana Gabriela Valladares Juárez danken für die fachliche und moralische Unterstützung, die schöne Zeit im Labor, unsere Teamarbeit und Freundschaft.

Auch Nuttapol Noirungsee, Eva Mong Su und Miriam Aßmann danke ich herzlich für ihre Hilfe, Verlässlichkeit, Freundschaft und den Spaß, den wir zusammen hatten.

Allen Partnern des Hochdruck-Projektes an der TUHH, Prof. Dr. Giselher Gust, Prof. Dr. Michael Schlüter, Prof. Dr. Andreas Liese, Prof. Dr. Dieter Krause, Katrin Laqua, Karen Malone, Dr. Paul Bubenheim, Steffen Hackbusch und Juan Viamonte Dominguez, danke ich für die erfolgreiche Zusammenarbeit.

Des Weiteren danke ich Dr. Sara Lincoln, Dr. David Lindo-Atichati, Prof. Dr. Thomas Oldenburg und Dr. Jagos Radovic für die erfolgreiche Kooperation. Darüber hinaus möchte ich Dr. Sara Lincoln, Dr. Patrick Schwing, Prof. Dr. Wade Jeffrey und Prof. Dr. Joe Lepo danken für das Zurverfügungstellen der bakteriellen Stämme und Tiefseesedimente. Ebenso bedanke ich mich bei Prof. Dr. Giselher Gust, Prof. Dr. Rudolf Eggers und Dr. Philip Jaeger für das Zurverfügungstellen der Hochdruckreaktoren. Auch allen anderen C-IMAGE Projektpartnern, insbesondere Prof. Dr. Steven Murawski, Prof. Dr. David Hollander, Sherryl Gilbert und Prof. Dr. Hans-Peter Grossart, danke ich herzlich für ihre Unterstützung.

Allen Studentinnen und Studenten, mit denen ich am Hochdruck-Projekt zusammenarbeiten durfte, danke ich sehr für ihre Arbeit und ihren Einsatz: Robert Hiessl, Alexandra Buck-Emden, Sabrina Felicitas Jesch, Lisa Sophie Egger, Alexander Kromm, José Manuel Jiménez Juárez, Judit Martín Juárez, Nneka Maryrose Enwena und Hari Spandana

Kadimesetty. Ebenso möchte ich den BTA-Auszubildenden, die ich betreuen durfte, Mareike Jaeckel, Sophia Kummer, Alexander Eichhorst und Jana Ohletz, für ihre Hilfe danken.

Besonderer Dank gilt Thi Lien Tieu-Schröder und Andreas Meyer für ihre verlässliche Hilfe und Beratung bei allen technischen Herausforderungen und Fragen.

Allen Kollegen vom Institut für Technische Biokatalyse möchte ich herzlich danken für ihre Hilfsbereitschaft, das herzliche Miteinander und eine schöne Zeit am ITB.

Großer Dank gilt meinem Freund Johannes für seine beständige Unterstützung, Liebe und Geduld während dieser besonderen Zeit.

Meinen Eltern, meiner Familie und meinen Freunden danke ich sehr für ihre Motivation und den steten Rückhalt.

Nicht zuletzt danke ich der Gulf of Mexico Research Initiative und C-IMAGE für die Finanzierung dieses Projektes.

Summary

Knowledge about effects of high pressure on the growth of crude oil-degrading bacteria and their degradation capabilities has been scarce up to now. With the expansion of drilling in deeper and deeper waters and the ever-present risk of accidental oil spills, this knowledge becomes increasingly important.

In this work, the development of incubation systems, designed to simulate deep sea conditions in the laboratory, allowed to study biodegradation of crude oil and its components under *in situ* pressure conditions.

The ability of bacterial model strains to grow on and degrade several crude oil components was analysed at high pressure. Three of these strains were isolated from environmental samples and one model strain was isolated from a Gulf of Mexico deep-sea sediment sample. The chosen crude oil components were representatives of the main fractions of crude oil. As reference, the strains were tested at ambient pressure.

Growth and alkane-degradation capability of *Rhodococcus qingshengii* TUHH-12, a model degrader of saturated, linear hydrocarbons, at high pressure were only slightly different from growth and degradation capability at ambient pressure. The strain grew well with n-hexadecane at 147 bar at a rate of 0.162 h^{-1} , although slightly slower than at 1 bar at a rate of 0.364 h^{-1} . The n-hexadecane was degraded at a rate of 0.035 mM/h at 1 bar compared to a slightly lower rate of 0.019 mM/h at 147 bar.

In contrast, pressures of up to 88 bar had little effect on the growth of the tested model degrader of polycyclic aromatic hydrocarbons, *Sphingobium yanoikuyae* B1, with naphthalene, whereas above this pressure growth decreased and no growth occurred at 120 bar or more. Nevertheless, the degradation of naphthalene continued even at more than 120 bar, although it was degraded at a lower rate and not completely. After 75 h at 139 bar, 96.6% of the naphthalene was converted at a rate of 0.054 mM/h , whereas at 1 bar 100% of the naphthalene was converted at a rate of 0.064 mM/h . Salicylic acid, a metabolite of the naphthalene degradation pathway, was accumulated in the culture medium in incubations at high pressure, suggesting that the second part of the naphthalene

degradation pathway was inhibited. The effect of high pressure on growth with glucose as sole carbon source was similar to the effect on growth with naphthalene. At 156 bar, no growth occurred with glucose, whereas at 1 bar the strain grew well. Of the initial glucose after 45.5 h 10.4% was converted at 156 bar and 43.7% was converted at 1 bar, suggesting that a central cell function of *S. yanoikuyae* B1 was also inhibited by high pressure.

The aromatic hydrocarbon degraders *Rhodococcus wratislaviensis* Tol3 and *Dietzia aurantiaca* C7.oil.2 showed an enhanced growth on toluene in incubations at high pressure compared to growth at ambient pressure. At 154 bar, *R. wratislaviensis* Tol3 reached 8×10^4 to 1×10^6 -fold higher final cell numbers than at 1 bar and *D. aurantiaca* C7.oil.2 showed a 1.8×10^4 -fold higher final cell number at 142 bar than at 1 bar. Most probably, this resulted from changes of vapour pressure of toluene induced by the elevated total pressure.

Moreover, the influence of high pressure on the degradation of crude oil and natural gas by bacterial communities from Gulf of Mexico deep-sea surface sediments was investigated. High pressure was found to have enhancing or inhibiting effects on crude oil degradation by bacterial communities, dependent on the analysed sediment and its sampling time. Furthermore, high pressure changed the composition of the communities in sediments that degrade crude oil and natural gas.

In conclusion, the effect of high pressure on degradation behaviour and growth was dependent on the respective investigated microorganisms and carbon sources.

In the course of this thesis, several high pressure reactor systems were tested, their advantages and disadvantages were investigated and the requirements for the construction of a new, improved high pressure reactor system were described. For instance, a system for online-measurement of the hydrocarbon concentration or a continuous gas exchange would be helpful. Moreover, different online oxygen and carbon dioxide measurement systems were tested and resulting from this, a new prototype oxygen sensor for measurement at high pressure was developed in cooperation with two companies.

This thesis proved that pressure is an important factor in the bacterial degradation of hydrocarbons and cannot be neglected when estimating the biodegradation and ultimate fate of oil released in the deep sea.

Zusammenfassung

Bis heute ist nur wenig über die Effekte bekannt, die hoher Druck auf das Wachstum und die Erdöl-Abbaufähigkeit von Bakterien hat. Mit zunehmender Zahl von Bohrungen an immer tiefer gelegenen Stellen des Meeresbodens und der damit verbundenen ständigen Gefahr von Unfällen, die zum Austritt großer Mengen Erdöls führen können, wird dieses Wissen zunehmend wichtig. Öl-abbauende Bakterien können dazu beitragen, Ölbelastungen auf Ökosysteme zu minimieren.

Im Rahmen dieser Arbeit konnten mithilfe speziell entwickelter Inkubationssysteme Tiefsee-Bedingungen simuliert und so der biologische Abbau von Erdöl und dessen Komponenten unter *in situ* Druckbedingungen im Labor untersucht werden.

Es wurden drei Modell-Bakterienstämme, isoliert aus Umweltproben, und ein Modell-Stamm, isoliert aus einer Tiefseesedimentprobe aus dem Golf von Mexiko, hinsichtlich ihrer Fähigkeit untersucht, unter Hochdruckbedingungen mit verschiedenen Erdölkomponenten als einziger Kohlenstoffquelle zu wachsen und diese abzubauen. Die gewählten Kohlenwasserstoffe waren Vertreter der wichtigsten Fraktionen des Erdöls. Zum Vergleich wurden die Stämme parallel unter atmosphärischem Umgebungsdruck (1 bar) inkubiert.

Das Wachstum und die Fähigkeit zum Alkan-Abbau von *Rhodococcus qingshengii* TUHH-12, einem Modell-Abbauer von gesättigten, linearen Kohlenwasserstoffen, waren unter Umgebungsdruck nur geringfügig verschieden von Wachstum und Alkan-Abbaufähigkeit unter hohem Druck. Der Stamm wuchs gut auf n-Hexadekan bei 147 bar mit einer Rate von 0.162 h^{-1} , wenn auch etwas schlechter als bei 1 bar mit einer Rate von 0.364 h^{-1} . Der Abbau von n-Hexadekan bei 147 bar war mit 0.019 mM/h etwas langsamer als bei 1 bar mit 0.035 mM/h .

Im Gegensatz dazu war das Wachstum des getesteten polycyclische Aromaten-abbauenden Modell-Stamms *Sphingobium yanoikuyae* B1 auf Naphthalin bei hohen Drücken von bis zu 88 bar nur wenig beeinflusst, aber bei 120 bar oder höheren Drücken wuchs der Stamm nicht. Dennoch wurde Naphthalin selbst bei mehr als 120 bar abgebaut, wenn auch mit einer geringeren Rate und unvollständig. Nach 75 h bei 139 bar waren 96.6% des

Naphthalins umgesetzt mit einer Rate von 0.054 mM/h, während bei 1 bar 100% des Naphthalins mit einer Rate von 0.064 mM/h umgesetzt wurden. In Inkubationen unter hohem Druck konnte nachgewiesen werden, dass Salizylsäure, ein Metabolit des Naphthalin Abbauwegs, akkumulierte, was darauf hindeutet, dass der zweite Teil des Naphthalin Abbauwegs inhibiert wurde. Hoher Druck hatte eine ähnliche Wirkung auf das Wachstum mit Glukose als einziger Kohlenstoffquelle wie auf das Wachstum mit Naphthalin. Während der Stamm bei 156 bar nicht wuchs, konnte bei 1 bar Wachstum beobachtet werden. Bei 156 bar wurden nach 45.5 h 10.4% der anfänglichen Glukose umgesetzt, während es bei 1 bar 43.8% Glukose waren. Dies lässt darauf schließen, dass zusätzlich eine zentrale Zell-Funktion von *S. yanoikuyae* B1 inhibiert wurde.

Die untersuchten Aromaten-abbauenden Modell-Stämme *Rhodococcus wratislaviensis* Tol3 und *Dietzia aurantiaca* C7.oil.2 zeigten ein verstärktes Wachstum auf Toluol unter hohem Druck im Vergleich zum Wachstum bei Umgebungsdruck. Bei 154 bar erreichte *R. wratislaviensis* Tol3 eine 8×10^4 bis 1×10^6 -fach höhere finale Zellzahl als bei 1 bar und *D. aurantiaca* C7.oil.2 erreichte eine 1.8×10^4 -fach höhere finale Zellzahl bei 142 bar als bei 1 bar. Als Ursache wird die Druck-induzierte Veränderung des Dampfdrucks von Toluol vermutet.

Darüber hinaus wurde der Einfluss von hohem Druck auf den Abbau von Erdöl und Erdgas durch Bakteriengemeinschaften aus Sedimentproben aus dem Golf von Mexico untersucht. Hoher Druck hatte fördernde oder hemmende Auswirkungen auf den Erdöl-Abbau durch die Bakteriengemeinschaften, abhängig von dem analysierten Sediment und dem Zeitpunkt der Sediment-Probennahme. Der hohe Druck änderte außerdem die Zusammensetzung der bakteriellen Gemeinschaft.

Es kann geschlussfolgert werden, dass der Effekt von hohem Druck auf das bakterielle Wachstum und das Abbauverhalten von den jeweiligen untersuchten Mikroorganismen und der jeweiligen getesteten Kohlenstoffquelle abhängig ist.

Mehrere Hochdruck-Reaktorsysteme wurden im Laufe der Arbeit getestet, ihre Vor- und Nachteile wurden untersucht und Anforderungen an ein neues, verbessertes Hochdruck-Reaktorsystem konnten beschrieben werden. Beispielsweise wären ein System zur Messung der Kohlenwasserstoff-Konzentration oder ein kontinuierlicher Gasaustausch hilfreich. Darüber hinaus, wurden verschiedene Online-Sauerstoff- und -Kohlenstoffdioxid-

Messsysteme getestet und als Ergebnis wurde in Zusammenarbeit mit zwei Firmen ein neuer Prototyp-Sensor zum Messen von Sauerstoff unter hohem Druck entwickelt.

Mit dieser Arbeit konnte gezeigt werden, dass der Druck großen Einfluss auf den bakteriellen Abbau von Kohlenwasserstoffen hat und in Untersuchungen des biologischen Erdölabbaus in der Tiefsee nicht vernachlässigt werden kann.

Contents

1	Introduction.....	1
1.1	The Deepwater Horizon oil spill	1
1.1.1	Corexit® and oil plumes.....	1
1.1.2	Marine snow	4
1.1.3	The Gulf of Mexico Research Initiative.....	6
1.2	Crude oil biodegradation	7
1.2.1	Crude oil and its components.....	7
1.2.2	Hydrocarbon-degrading microorganisms.....	9
1.2.3	Hydrocarbon degradation and metabolic pathways.....	10
1.2.4	Aerobic biodegradation of crude oil from the Deepwater Horizon oil spill.....	18
1.3	High pressure in the deep sea	21
1.3.1	Deep-sea conditions	22
1.3.2	Effects of high pressure	22
1.3.3	Adaptation of deep-sea microorganisms to high pressure	27
1.4	Objectives of this thesis.....	28
2	Materials and methods	30
2.1	Chemicals.....	30
2.2	Equipment	30
2.3	Microorganisms	35
2.3.1	Bacterial strains	35
2.3.2	Bacterial communities from deep-sea sediments.....	36
2.4	Liquid and solid culture media	37
2.5	Storage of bacteria	37

2.6	Substrates	37
2.7	Biodegradation experiments at ambient and high pressure in different reactor systems	38
2.7.1	Experiments in 160 mL high pressure reactors and ambient pressure reference reactors.....	41
2.7.2	Cultivation of bacterial strains in the 1 L high pressure reactor at ambient and high pressure	43
2.7.3	Cultivation of bacterial strains in the high pressure reactor with screw-piston mechanism at elevated oxygen partial pressure	43
2.7.4	Experiments in view cell reactor No. 1 at ambient and high pressure	44
2.7.5	Cultivation of bacterial communities from GoM deep-sea sediments in view cell reactor No. 2 at ambient and high pressure.....	45
2.8	Analysis of bacterial growth and substrate degradation	46
2.8.1	Determination of cell density with the Neubauer chamber	46
2.8.2	Determination of cell density by plate counting.....	47
2.8.3	Determination of optical density.....	47
2.8.4	Determination of pH value	48
2.8.5	Analysis of hydrocarbons by gas chromatography-mass spectrometry	48
2.8.6	Analysis of α -D-glucose concentration.....	49
2.8.7	Determination of salicylic acid concentration.....	49
2.8.8	Detection of hydroxylated intermediates of naphthalene conversion.....	49
2.8.9	Determination of oxygen consumption and carbon dioxide production	51
2.9	Sequencing of 16S rRNA genes.....	51
2.9.1	Amplification of DNA by Colony Polymerase Chain Reaction	51
2.9.2	Agarose gel electrophoresis	52
2.9.3	Purification and determination of DNA concentration of products from Polymerase Chain Reaction	52

2.9.4	Sequencing.....	52
2.10	Community analysis via Denaturing Gradient Gel Electrophoresis	52
2.10.1	Filtration	53
2.10.2	DNA extraction	53
2.10.3	Amplification of DNA by PCR	54
2.10.4	Denaturing Gradient Gel Electrophoresis	54
3	Results.....	56
3.1	Development, construction and setup of high pressure equipment	56
3.1.1	The 160 mL high pressure reactors and ambient pressure reference reactors	56
3.1.2	The 1 L high pressure reactor	61
3.1.3	The high pressure reactor with screw-piston mechanism for mechanical pressurisation	64
3.1.4	The high pressure view cell reactor No. 1	69
3.1.5	The high pressure view cell reactor No. 2	71
3.2	Online analytics: Test of different O ₂ and CO ₂ online measurement systems.....	72
3.2.1	The oxygen sensors from Ocean Optics GmbH	73
3.2.2	The oxygen sensor Fibox 3 and the carbon dioxide sensor pCO ₂ mini from PreSens Precision Sensing GmbH	74
3.2.3	The oxygen measurement system VisiSens™ from PreSens Precision Sensing GmbH.....	75
3.2.4	The oxygen prototype sensor from PreSens Precision Sensing GmbH and Eurotechnica GmbH.....	77
3.3	Biodegradation of n-alkanes at ambient and high pressure	77
3.3.1	Degradation of n-hexadecane by <i>R. qingshengii</i> TUHH-12 at ambient and high pressure	78
3.3.2	Growth of <i>R. qingshengii</i> TUHH-12 with n-tetracosane at ambient and high pressure	82

3.3.3	Growth of <i>R. qingshengii</i> TUHH-12 with n-decane at ambient and high pressure	84
3.3.4	Degradation of n-hexadecane by <i>D. aurantiaca</i> C7.oil.2 at ambient and high pressure	87
3.3.5	Influence of Corexit® EC9500A on growth and biodegradation capability of <i>R. qingshengii</i> TUHH-12 at ambient and high pressure	88
3.4	Biodegradation of aromatic hydrocarbons at ambient and high pressure	92
3.4.1	Growth of <i>R. wratislaviensis</i> Tol3 with toluene at ambient and high pressure	92
3.4.2	Growth of <i>R. wratislaviensis</i> Tol3 with toluene at different pressures from 1 to 154 bar	93
3.4.3	Degradation of α -D glucose by <i>R. wratislaviensis</i> Tol3 at different pressures from 1 to 154 bar	94
3.4.4	Investigation of the influence of toluene concentration on the growth of <i>R. wratislaviensis</i> Tol3	95
3.4.5	Growth of <i>D. aurantiaca</i> C7.oil.2 with toluene at ambient and high pressure at 4°C	96
3.5	Biodegradation of a PAH at ambient and high pressure	97
3.5.1	Degradation of naphthalene by <i>S. yanoikuyae</i> B1 at ambient and high pressure.	98
3.5.2	Incubation of naphthalene without bacteria at ambient and high pressure	99
3.5.3	Degradation of naphthalene by <i>S. yanoikuyae</i> B1 at different pressures from 1 to 130 bar	100
3.5.4	Investigation of O ₂ consumption and CO ₂ production by <i>S. yanoikuyae</i> B1 growing with naphthalene at ambient and high pressure	101
3.5.5	Analysis of brown culture medium from incubation of <i>S. yanoikuyae</i> B1 with naphthalene at high pressure	102
3.5.6	Degradation of salicylic acid by <i>S. yanoikuyae</i> B1 at ambient and high pressure	104

3.5.7	Degradation of α -D glucose by <i>S. yanoikuyae</i> B1 at ambient and high pressure	104
3.5.8	Influence of Corexit® EC9500A on degradation of naphthalene by <i>S. yanoikuyae</i> B1 at ambient and high pressure	105
3.5.9	Growth of <i>S. yanoikuyae</i> B1 on Corexit® EC9500A at ambient and high pressure	109
3.6	Biodegradation of Louisiana sweet crude oil and natural gas by bacterial communities from deep-sea sediments at ambient and high pressure	109
3.6.1	Comparison of the activity of bacterial communities from deep-sea sediments from 2010 and 2013 at different incubation conditions	110
3.6.2	Degradation of Louisiana sweet crude oil by bacterial communities from 2010 and 2013 sediments at ambient and high pressure	114
3.6.3	Degradation of natural gas and crude oil by bacterial communities from a 2010 sediment at ambient and high pressure	119
4	Discussion	122
4.1	Development and optimisation of the high pressure reactors	122
4.1.1	Optimisation of the oxygen concentration in a high pressure reactor for aerobic biodegradation	122
4.1.2	Suggestions for the design of an ideal reactor for biodegradation experiments under deep-sea conditions	123
4.2	Biodegradation of n-alkanes at ambient and high pressure	125
4.2.1	Degradation of n-hexadecane, n-tetracosane and n-decane by <i>R. qingshengii</i> TUHH-12 and <i>D. aurantiaca</i> C7.oil.2 at ambient and high pressure	125
4.2.2	Influence of Corexit® EC9500A on n-hexadecane degradation by <i>R. qingshengii</i> TUHH-12 at ambient and high pressure	128
4.3	Biodegradation of an aromatic hydrocarbon at ambient and high pressure	129
4.3.1	Growth of <i>R. wratislaviensis</i> Tol3 and <i>D. aurantiaca</i> C7.oil.2 with toluene at ambient and high pressure	129

4.4	Biodegradation of a PAH at ambient and high pressure	132
4.4.1	Degradation of naphthalene by <i>S. yanoikuyae</i> B1 at ambient and high pressure.	132
4.4.2	Influence of Corexit® EC9500A on degradation of naphthalene by <i>S. yanoikuyae</i> B1 at ambient and high pressure	138
4.5	Biodegradation of Louisiana sweet crude oil and natural gas by bacterial communities from deep-sea sediments at ambient and high pressure	139
4.5.1	Comparison of the activity of bacterial communities from deep-sea sediments from 2010 and 2013 at different incubation conditions.....	139
4.5.2	Degradation of Louisiana sweet crude oil by bacterial communities from 2010 and 2013 sediments at ambient and high pressure.....	140
4.5.3	Degradation of natural gas and crude oil by bacterial communities from a 2010 sediment at ambient and high pressure	143
5	Conclusion.....	145
6	References	147
	Appendix.....	171

List of abbreviations and symbols

Abbreviations

APS	ammonium persulfate
BP	British Petroleum
bp	base pairs
BSA	bovine serum albumin
C_{av}	average of cell counts in one large square of the Neubauer counting chamber
CFU	colony forming unit
CFU_{av}	average colony forming unit count
C-IMAGE	Center for Integrated Modeling and Analysis of Gulf Ecosystems
CTAB	cetyltrimethylammonium bromide
DCM	dichloromethane
DF	dilution factor
DGGE	Denaturing Gradient Gel Electrophoresis
DNA	deoxyribonucleic acid
DOSS	dioctylsulfosuccinate
DR	decrease rate of hydrocarbon concentration
DSMZ	Deutsche Sammlung von Mikroorganismen und Zellkulturen GmbH
DWH	Deepwater Horizon
e.g.	for example
EPS	extracellular polysaccharide
eV	electronvolt
g	gram
g	gravity
g/L	gram per litre
GC-MS	gas chromatography-mass spectrometry
GoM	Gulf of Mexico
GoMRI	Gulf of Mexico Research Initiative

GRIIDC	The Gulf of Mexico Research Initiative Information and Data Cooperative
h	hour
HPLC	high performance liquid chromatography
kb	kilobase
km	kilometre
L	litre
LB	Luria Bertani
<i>log</i>	logarithm
mM	millimolar
M	molar
m	metre
MMII	minimal mineral medium II
mg	milligram
min	minute
mL	millilitre
mM	millimolar
mm	millimetre
MOSSFA	Marine Oil Snow Sedimentation and Flocculent Accumulation
Mt	megaton
μL	microlitre
μm	micrometre
N	normality
N	north
NADH	Nicotinamide adenine dinucleotide hydride
ng/μL	nanogram per microlitre
nm	nanometre
No.	number
OD	optical density
OMAs	oil-mineral aggregates
PAH	polycyclic aromatic hydrocarbon
PCR	Polymerase Chain Reaction
PEG	polyethyleneglycol

pmol/ μ L	picomol per microlitre
PSU	Pennsylvania State University
<i>R.</i>	<i>Rhodococcus</i>
rDNA	ribosomal deoxyribonucleic acid
rRNA	ribosomal ribonucleic acid
RT	room temperature
rpm	revolutions per minute
<i>S.</i>	<i>Sphingobium</i>
sp.	species
sec	second
TAE	tris-acetate-EDTA
TEMED	tetramethylethylenediamine
TUHH	Hamburg University of Technology
u/ μ L	Unit per microlitre
USF	University of South Florida
UV	ultraviolet
v/v	volume per volume
V	volt
VOC	volatile organic compound
vs.	versus
W	west
w/v	weight per volume
w/w	weight per weight

Symbols

Δ	Delta: symbol for difference
ΔG	Gibbs free energy
e	Euler's number
μ	growth rate
x_1 and x_2	first and second measured cell density or hydrocarbon concentration
t_1 and t_2	first and second point in time

1 Introduction

1.1 The Deepwater Horizon oil spill

The starting points of this thesis were the Deepwater Horizon (DWH) oil spill and the subsequent, natural and anthropogenic processes in the Gulf of Mexico (GoM). On 20 April 2010, the DWH oil drilling rig exploded resulting in the largest accidental marine oil spill in history. Approximately 170 to 310 million kg natural gas and about 780 million litres (4.9 million barrels) of light sweet crude oil from the Macondo oil field were discharged through a high pressure jet into the deep sea of the GoM. On 15 July, the wellhead of the rig, where the oil was released, was capped after 87 days (Atlas and Hazen 2011, Kimes *et al.* 2014, King *et al.* 2015). The wellhead was located 77 km offshore at 1,525 m depth (Atlas and Hazen 2011, Montagna *et al.* 2013), where the pressure is 152.5 bar. About 10.1 ± 2 million kg hydrocarbons per day were released into the GoM (Ryerson *et al.* 2012). Of the Macondo reservoir fluid mass, 62% was liquid crude oil and 38% was natural gas (Ryerson *et al.* 2011).

In November 2010, Lehr *et al.* released the DWH Oil Budget Calculator Technical Documentation, giving an estimation of the crude oil's fate. Until 14 July 2010, 41% of the crude oil has been cleaned up by human response activities, namely direct recovery from the well, *in situ* burning, skimming or chemical dispersion, and 37% by natural processes such as natural dispersion, evaporation and dissolution. The fate of the remaining 22% of the crude oil was unaccounted for. This oil was supposed to persist on or just below the water surface as light sheen or weathered tar balls, to be biodegraded, to be washed ashore and collected from the shore, or to be buried in sand and sediments and may resurface over time (Ramseur 2010).

1.1.1 Corexit® and oil plumes

As a primary strategy to mitigate the impacts of the blowout, 5.2 million litres of two chemical dispersants, Corexit® EC9527 and Corexit® EC9500A, were applied at the water surface. In addition, for the first time in history, 2.9 million litres of Corexit® EC9500A were directly injected into the flow of gas and oil at the wellhead (Atlas and Hazen 2011,

Kujawinski *et al.* 2011). Dispersants are composed of surfactants and hydrocarbon-based solvents (Kujawinski *et al.* 2011). They are applied to break down the oil into tiny droplets by reducing its surface tension (Brakstad 2008). On the one hand, this results in a dispersion of the oil in the water column, which prevents it from rising to the water surface, building large slicks and contaminating the shoreline (Atlas and Hazen 2011, Kujawinski *et al.* 2011). On the other hand, dispersants increase the surface-to-volume ratios of oil droplets. As a primary aim of applying dispersants, this should result in an enhanced availability of oil to microorganisms and a stimulation of crude oil biodegradation (Atlas and Hazen 2011, Brakstad 2008).

Much research has been done on the environmental fate of chemical dispersants, on their effects on bacteria and microbial community structure and function, as well as on the ability of bacteria to degrade dispersed oil and dispersants (e.g. Campo *et al.* 2013, Bælum *et al.* 2012, Hamdan and Fulmer 2011, Kleindienst *et al.* 2015a, Kujawinski *et al.* 2011, Lindstrom and Braddock 2002, Overholt *et al.* 2016). However, the ability of dispersants to reduce oil spill impacts still remains unclear and is a subject of debate (Kleindienst *et al.* 2016, Prince *et al.* 2016). Similarly, the fate of dispersants is unclear. While Prince *et al.* (2016) suggested that dispersants may have short-term debits, White *et al.* (2014) found long-term persistence of Corexit® in Gulf-ecosystems of about 4 years. In addition, the impacts of dispersants in high pressure environments are still poorly understood.

The dispersant-induced reduction of oil droplet sizes may have increased the crude oil's residence time in the water column (Socolofsky *et al.* 2015). Thus, the direct injection of Corexit® EC9500A at the wellhead, as well as natural dispersion, may have facilitated the formation of plumes of dispersed hydrocarbons in the water column (National Commission on the BP Deepwater Horizon Oil Spill and Offshore Drilling 2011). In May and June 2010, a large plume was detected at 1,000 to 1,200 m below sea level, located at the southwest of the DWH wellhead. The plume consisted of huge amounts of gas and oil, which remained in the deep sea (Camilli *et al.* 2010, Diercks *et al.* 2010, Hazen *et al.* 2010, Schrope 2010, Yvon-Lewis *et al.* 2011, Zhang *et al.* 2011). Moreover, separate hydrocarbon plumes were found at other directions to the spill site in the deep sea (Valentine *et al.* 2010). However, Aman *et al.* (2015) stated that only up to 3% more oil would have reached the sea surface without the

injection of dispersants at the wellhead and thus, even without the application of Corexit[®], the plume would have formed (Daly *et al.* 2016).

Only a low flux of methane (CH₄) to the atmosphere was detected (Yvon-Lewis *et al.* 2011), but the majority of the methane was dissolved and suspended in the deep ocean at >800 m (Kessler *et al.* 2011, McNutt *et al.* 2012). Methane was found to be the most abundant hydrocarbon in the deep-water plumes (Kessler *et al.* 2011, Reddy *et al.* 2012, Valentine *et al.* 2010). Furthermore, among the low molecular weight alkanes (C₁–C₅) high contents of ethane and propane were enriched in the plumes (Joye *et al.* 2011b, Reddy *et al.* 2012). The most abundant hydrocarbon compounds higher than C₅ were benzene, toluene, ethylbenzene as well as m-, p- and o- xylenes, which can be summarised as BTEX (Reddy *et al.* 2012, Valentine *et al.* 2010). Moreover, high levels of polycyclic aromatic hydrocarbons (PAHs) were found in the deep sea plumes (Diercks *et al.* 2010). Ryerson *et al.* (2012) estimated that about 69% of the deep plume mass was made up of readily soluble hydrocarbons and the remaining 31% of the deep plume mass was made up of oil droplets.

Besides moving through the deep sea in form of plumes, a part of the discharged crude oil, namely the large droplets with high proportions of PAHs and heavier hydrocarbons, rose to the sea surface, where it formed surface slicks with an overall area of up to 180,000 km² (Atlas and Hazen 2011, Kimes *et al.* 2014). This oil was weathered and washed ashore along the northeastern coast of the GoM, contaminating marshes and beaches (Joye *et al.* 2014, Michel *et al.* 2013). Another part of the released oil settled down to the sea floor and contaminated sediments close to the wellhead (Atlas and Hazen 2011, Liu *et al.* 2012, Romero *et al.* 2015, Sammarco *et al.* 2013, Valentine *et al.* 2014). The “dirty bathtub ring” hypothesis is a possible transport pathway of hydrocarbons to the sea floor. This hypothesis suggests that hydrocarbons were deposited on the sea floor due to direct contact between continental slope surface sediments (at 1,000 to 1,200 m depth) and hydrocarbons from the deep plume, which were moved by deep currents (Romero *et al.* 2015, Schrope 2013, Schwing *et al.* 2015, Valentine *et al.* 2014). Another proposed oil sedimentation pathway is the interaction of crude oil with sediment mineral particles in the water column. The emerging oil-mineral aggregates (OMAs) rapidly sank to the sea floor (Chanton *et al.* 2015, Daly *et al.* 2016).

In conclusion, most of the light alkanes (C_1 – C_3) and water-soluble aromatic BTEX hydrocarbons were trapped in the deep water column, whereas the rather water-insoluble crude oil components were transported to the sea surface or deposited on the sea floor (Reddy *et al.* 2012). McNutt *et al.* (2012) estimated that over 2 million barrels of oil (318 million litres) and essentially all the released methane did not reach the sea surface and remained in the deep sea. One year after the DWH spill, the oil, deposited in sediments near the wellhead, was only slightly to moderately degraded since short-chained n-alkanes (C_{10} – C_{15}), BTEX and C_3 -benzenes were still present (Liu *et al.* 2012).

1.1.2 Marine snow

The DWH oil spill was followed by an unusually large microbially mediated formation of flocs of marine snow in May 2010 (Passow *et al.* 2012). Marine snow consists of macroscopic aggregates of organic and inorganic particles including living bacteria and phytoplankton, detritus, fecal pellets and bio-minerals (Alldredge and Silver 1988, Passow *et al.* 2012). Marine snow is a common phenomenon in marine ecosystems and a hotspot for nutrients and hence microbial activity (Azam and Malfatti 2007, Ziervogel *et al.* 2012). Previous to the DWH spill, such floc formations have not been reported in association with degradation of crude oil (Bælum *et al.* 2012). Following the DWH spill, marine snow was formed due to different processes: mucus web production through activities of bacterial oil degraders, coagulation of oil components with suspended matter and aggregation of phytoplankton with oil droplets (Passow *et al.* 2012). In addition, extracellular polysaccharides (EPS), which can be produced by certain hydrocarbon-degrading bacteria, probably enhanced the hydrocarbon emulsification and formation of oil aggregates in the GoM after the DWH spill (Gutierrez *et al.* 2013a). These flocs of marine snow were found to be present at the sea surface and the upper water column in the weeks after the blowout (Joye *et al.* 2014). During summer of 2010, the oil-associated particles rapidly vanished from view, sank and settled to the sea floor around the Macondo wellhead, as depicted in Figure 1.1. During sinking, the sticky marine snow interacted with crude oil droplets. In addition, it transported other particles (such as organisms, detritus or other organic matter) to depths and thus may have purged the water column. With high sedimentation and accumulation rates this sinking event potentially resulted in a “dirty flocculent blizzard” phenomenon (Brooks *et al.* 2015,

Joye *et al.* 2014, Passow *et al.* 2012, Passow 2014, Romero *et al.* 2015, Schrope 2013, Ziervogel *et al.* 2012).

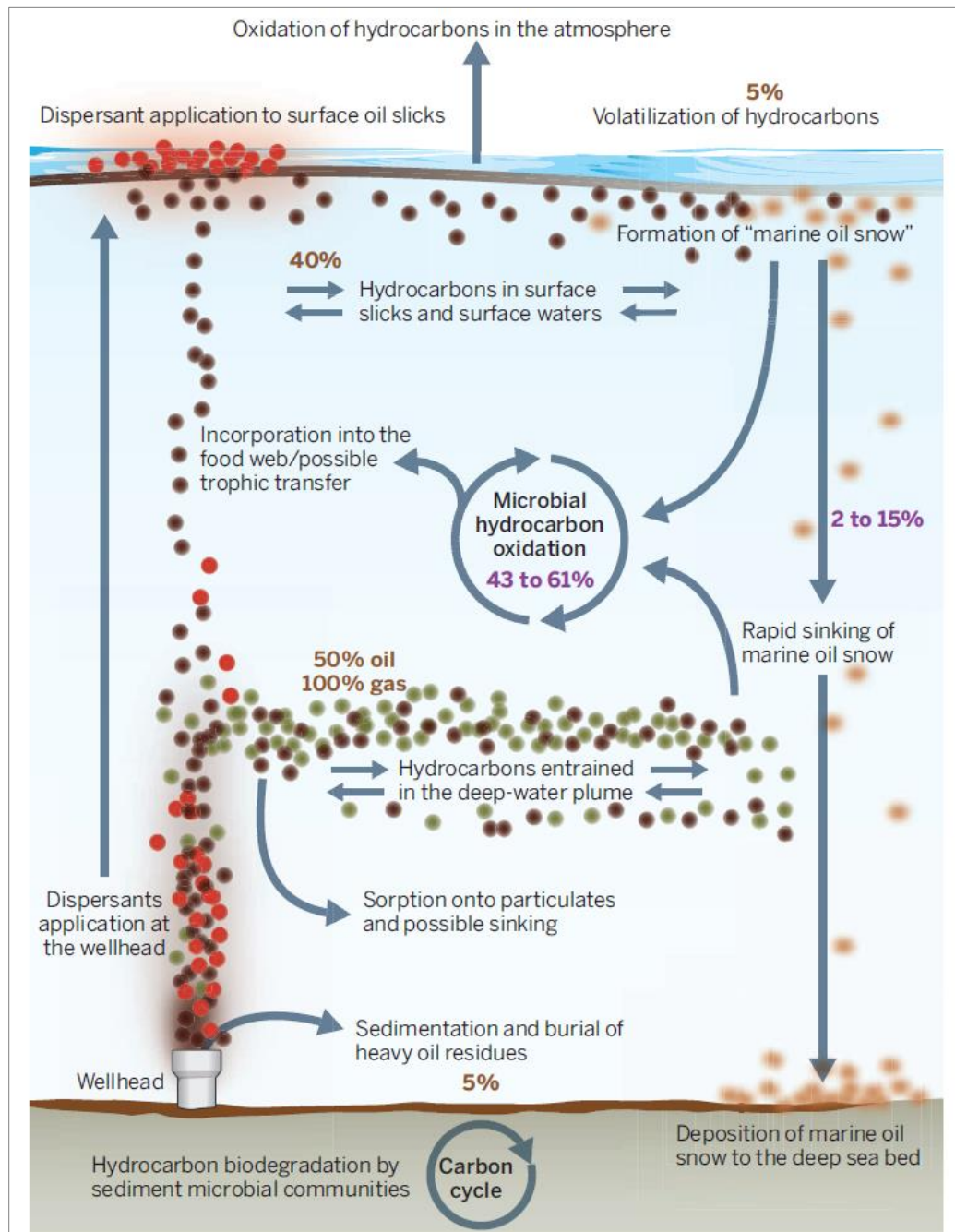


Figure 1.1: Proposed distribution (brown percentages) of the DWH gas (green circles) and oil (brown circles) under addition of dispersants (red circles). The long-term fate (purple percentages) is only known for 45 to 76% of the hydrocarbons. Not shown in the picture is that part of the oil which was deposited on beaches or coastal marshes (figure from Joye 2015).

In conclusion, this MOSSFA (Marine Oil Snow Sedimentation and Flocculent Accumulation) process (Daly *et al.* 2016), in addition to the direct deposition of oil onto the sediment's surface (as described in the previous subsection), may explain the fate of some of the oil that was unaccounted for in the DWH Oil Budget Calculator Technical Documentation by Lehr *et al.* (2010) (Mason *et al.* 2014). Valentine *et al.* (2014) estimated that 1.8 to 14.4% of the oil, discharged from the DWH wellhead, was transported to the sea bottom, whereas Chanton *et al.* (2015) give an estimation of 0.5 to 9.1%. Valentine *et al.* (2014) stated that the source of the oil on the deep-sea sediment's surface were most likely the oil plumes rather than the oil slick at the sea surface.

1.1.3 The Gulf of Mexico Research Initiative

In May 2010, British Petroleum (BP plc), to whom the DWH drilling rig was leased, committed a \$500 million grant over a 10-year period to create the independent research program named Gulf of Mexico Research Initiative (GoMRI). The program is conducted primarily in the Gulf Coast states of the USA. The aim of this program is to study the impacts of the oil, dispersed oil and dispersants on the ecosystems and human health in the GoM and the affected coastal states. Ultimately, GoMRI wants to improve the society's ability to understand, respond to and mitigate the impacts of oil spills (<http://gulfresearchinitiative.org>). In the first funding period 8 and in the second funding period 12 research consortia were awarded. In both periods, each lasting three years, C-IMAGE (Center for Integrated Modeling and Analysis of Gulf Ecosystems) was one of those awarded consortia. C-IMAGE, now C-IMAGE II, is a research consortium of 19 international institutions, which aims to improve the understanding of the processes and mechanisms involved in the marine blowouts and their environmental consequences (<http://www.marine.usf.edu/c-image/>). Within this consortium, at the Hamburg University of Technology (TUHH), high pressure experimentation is carried out to study the hydrodynamic behaviour and, as described in this thesis, the biodegradation of crude oil and its components at artificial deep-sea conditions. Particular attention is paid to the deep-sea condition of high pressure, since the DWH oil spill was the first blowout of a deep-sea oil exploration well to date (Hollander *et al.* 2010).

The present thesis was made possible by a grant from The Gulf of Mexico Research Initiative/C-IMAGE. Data are publicly available through the Gulf of Mexico Research Initiative Information & Data Cooperative (GRIIDC) at <https://data.gulfresearchinitiative.org> (doi: 10.7266/N7930R5K).

1.2 Crude oil biodegradation

As described in the following subsections, crude oil and its vast number of components can be degraded by specialised hydrocarbon-degrading microorganisms in metabolic pathways. In the aftermath of the DWH spill, the majority of the crude oil was rapidly aerobically biodegraded, resulting in changes of the bacterial community composition of the GoM ecosystems (Atlas and Hazen 2011, Dubinsky *et al.* 2013, Kimes *et al.* 2014). The aerobic biodegradation of the DWH oil was subject of this thesis.

1.2.1 Crude oil and its components

For millions of years hydrocarbons have been part of the earth's biosphere (Prince *et al.* 2010). Crude oil, deposited in subsurface reservoirs, is often associated with natural gas, as they have similar origins (Rojey and Jaffret 1997). Crude oil and natural gas derived from organic materials of animal or plant origin (e.g. zooplankton or algae) that settled to the sea floor millions of years ago. Over time, the debris was covered by mud and soil that changed into rock. The organic material fossilised under influence of high pressures and temperatures and was changed to coal, crude oil and/or natural gas. Thus, natural gas can occur with crude oil and also alone. Its principal component is methane. In small percentages, some high molecular weight alkanes up to C₅ and non-hydrocarbon constituents, such as carbon dioxide, nitrogen, hydrogen sulfide and helium, can be found (Speight 2007).

Crude oil is an extremely complex mixture of more than 17,000 distinct chemical compounds (Marshall and Rodgers 2003). Crude oil consists nearly exclusively of the elements hydrogen and carbon. Less than 3% is made up by nitrogen, sulfur and oxygen. Less than 1% is composed of phosphorus and heavy metals (Hassanshahian and Cappello 2013). Within the oil's complexity, several fractions of hydrocarbons can be defined: the saturated (or aliphatic) fraction, the aromatic fraction and the more polar asphaltic fractions

of resins and asphaltenes (Atlas 1981, Head *et al.* 2006). The saturated fraction includes nonpolar linear n-alkanes, branched alkanes and cyclic saturated hydrocarbons (cycloalkanes). The aromatic fraction consists of more polarisable hydrocarbons with one or more aromatic rings. The resins and asphaltenes have polar substituents. In contrast to resins, asphaltenes are insoluble in an excess of heptane or pentane (Fan and Buckley 2002).

The crude oil's constituents differ substantially in their chemical and physical properties, e.g. solubility and volatility, which influence their biodegradation susceptibility and environmental fate (Head *et al.* 2006, Redmond and Valentine 2012). For instance, the hydrocarbon's vapour pressure, which is the pressure of the vapour over a liquid at equilibrium, is increasing with decreasing carbon number and thus the lightest volatile organic compounds (VOCs) are evaporating rapidly when they reach the sea surface (Ryerson *et al.* 2011).

The composition of crude oils varies substantially and is dependent on the location and age of the oil field. Moreover, crude oils can be classified according to their relative proportions of high molecular weight constituents (Hassanshahian and Cappello 2013). Light oils have a high content of saturated and aromatic hydrocarbons (low molecular weight constituents) and a lower proportion of resins and asphaltenes (high molecular weight constituents). In contrast, heavy oils are high in resins and asphaltenes and have a low content of saturated and aromatic hydrocarbons, since they are the result of anaerobic biodegradation processes *in situ* in the oil reservoirs (Head *et al.* 2006). Changes in the crude oil composition, which are induced by chemical or biological processes, are referred to as weathering (Atlas 1981).

The world's largest receptors of hydrocarbon pollutants are the oceans (Atlas 1981). However, oil released into the oceans may not only have anthropogenic sources, but also natural oil seeps lead to a continuous input of oil in the environment. An estimated amount of about 1.3 Mt oil per year was released in the marine environment from 1990 to 1999. Of this oil, about 47% can be ascribed to natural seeps, whereas the remaining 53% originated from anthropogenic activities. These are for instance related to extraction, transportation and consumption of crude oil or its refined products (National Research Council 2003).

1.2.2 Hydrocarbon-degrading microorganisms

Hydrocarbons are relatively stable molecules that can, however, be source of energy and carbon for microorganisms, which are able to activate and metabolise them (Prince *et al.* 2010). Due to the continuous input of oil into the oceans through natural seeps, indigenous microorganisms with capability to degrade hydrocarbons have evolved over millions of years, so that by now almost 200 hydrocarbon-degrading genera (including bacterial, cyanobacterial, algal and fungal genera) are described (Yakimov *et al.* 2007, Brakstad 2008). However, hydrocarbons in the environment are mainly degraded by bacteria and fungi (Leahy and Colwell 1990). Nearly 80 hydrocarbon-utilising bacterial genera are described, which are ubiquitous in the terrestrial and aquatic ecosystems (Head *et al.* 2006, Leahy and Colwell 1990). In 1946, ZoBell reported on the ability of microorganisms to utilise hydrocarbons as sole source of energy and carbon. He stated that such microorganisms are of great diversity and are able to oxidise hydrocarbons at diverse environmental conditions. They are referred to as hydrocarbonoclastic microorganisms.

Biodegradation is the major method for treating oil spills naturally in the environment (Prince, 1993). Each hydrocarbonoclastic bacterial species is highly specialised in degrading a small range of oil components and thus an appropriate bacterial population of hydrocarbon-degrading bacteria is needed for efficient biodegradation of crude oil (Ron and Rosenberg 2014, Rosenberg *et al.* 1998). As concluded in the review of Head *et al.* (2006), the diversity of bacterial communities decreases with oil contamination and bioremediation, which is ascribable to a selection for specialised hydrocarbon-degrading bacteria.

Described specialised bacteria, which are able to grow in pure culture with hydrocarbons as sole source of carbon and energy, are primarily in the phyla Actinobacteria, Bacteroidetes, Firmicutes and Protoeobacteria. The majority of the currently described genera of hydrocarbon-degrading bacteria are in the very large phylum of Proteobacteria. However, only organisms that can be isolated in pure culture were taken into consideration here (Prince *et al.* 2010). Bacteria often cooperate to metabolise substrates (McInerney *et al.* 2008) and grow in consortia, which are beneficial for all (Allen and Banfield 2005, Brenner *et al.* 2008). Thus, only a very small part of microorganisms can be cultivated in pure culture and the diversity of hydrocarbon-degrading bacteria must be considerably underestimated (Prince *et al.* 2010).

1.2.3 Hydrocarbon degradation and metabolic pathways

Since hydrocarbons have a very low water solubility, bacteria need to come into direct contact with them and usually grow on the hydrocarbon droplet's surface. To increase the oil-water interphase, most hydrocarbon-degraders produce low-molecular, extracellular and cell-bound compounds (biosurfactants) to emulsify the substrate (Fuchs 1999, Müller 2006, Rosenberg *et al.* 1998). Hydrocarbons with high molecular weight, which have poor and slow water solubility, are taken up in form of microdroplets. Microbes with high cell-surface hydrophobicity can adhere to these insoluble hydrocarbons. In contrast, hydrocarbons up to C₈ are soluble enough to be taken up by bacteria without high cell-surface hydrophobicity via diffusion (Fuchs 1999, Rosenberg *et al.* 1998).

Aerobic biodegradation of hydrocarbons is initiated by mono- and dioxygenases (Kimes *et al.* 2014). In microorganisms, which are specialised in hydrocarbon-oxidation, these oxygenases are membrane-bound and group-specific. This means that some oxygenases are specialised in oxidation of various alkanes and others in oxidation of aromatics (Rosenberg *et al.* 1998). Possibly, all aerobic organisms have some basic hydrocarbon metabolism due to nonspecific oxygenases (Prince *et al.* 2010). The genes coding for the enzymes of the hydrocarbon degradation pathways may be located on plasmids (Fuchs 1999, Müller 2006).

In addition to aerobic biodegradation processes, especially in marine sediments, the anaerobic hydrocarbon biodegradation is important (Coates *et al.* 1997, Kimes *et al.* 2014). To utilise hydrocarbons, anaerobic microorganisms use nitrate, iron(III) or sulfate as electron acceptor. Furthermore, there are phototrophic, methanogenic, denitrifying and nitrate-ammonifying bacteria, which can degrade hydrocarbons at anoxic conditions (Heider and Schühle 2013).

The rates of natural hydrocarbon degradation by bacteria in marine environments are slow (Atlas and Bartha 1972) and in some cases degradation is not complete (Müller 2006). Reasons for this can be unsuitable conditions such as a limited availability of oxygen, nitrogen and phosphorus, an improper pH value, the usually low number of hydrocarbon degraders, the toxicity of some crude oil constituents, a limited oil-water interphase or suboptimal temperatures (Atlas and Bartha 1972, Müller 2006, Ron and Rosenberg 2014, Rosenberg *et al.* 1998). The various hydrocarbons in a crude oil mixture are degraded at different rates. Usually, the smaller, less substituted hydrocarbons are degraded at a higher

rate than the larger hydrocarbons with higher number of substituted groups (Redmond and Valentine 2012). Furthermore, the saturated and aromatic hydrocarbons are degraded preferentially in the environment, whereas the polar fractions are more resistant to biodegradation (Head *et al.* 2006). Thus, resins and asphaltenes have almost unnoticeable degradation rates (Atlas and Hazen 2011). The saturated hydrocarbons make up the largest mass-fraction of crude oil. Hence, their depletion is of high importance for the clean-up of the environment. However, in the long term, aromatic hydrocarbons and polar fractions are environmentally significant due to their higher toxicity and persistency (Head *et al.* 2006).

1.2.3.1 Alkanes

In general, in a mixture of hydrocarbons, aliphatic hydrocarbons and in particular the saturated n-alkanes are considered to be degraded most readily (Kator *et al.* 1971, Atlas 1981, Fuchs 1999).

The degradation of methane and other C₁ hydrocarbons is restricted to a few specialised microorganisms referred to as obligate aerobic methylotrophs. Within this group, methanotrophic microorganisms can oxidise methane to carbon dioxide with methane monooxygenase, which is contained in internal membrane systems, and molecular oxygen. As shown in Figure 1.2, in intermediate steps methanol, formaldehyde and formate are built and subsequently oxidised. Similarly, only a limited number of bacteria are able to degrade C₂–C₈ hydrocarbons (Fuchs 1999).

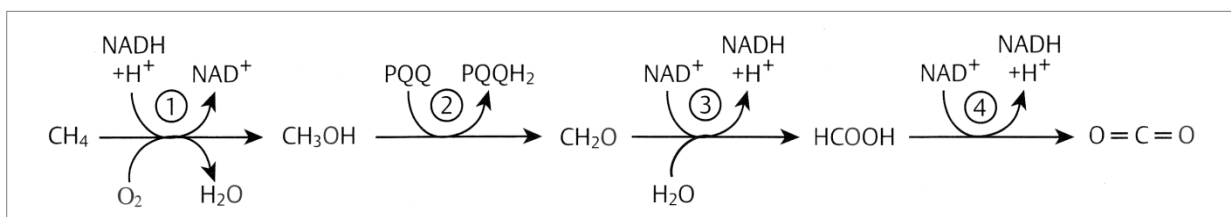


Figure 1.2: Oxidation of methane. Reactions are catalysed by following enzymes: (1) methane monooxygenase, (2) methanol dehydrogenase, (3) formaldehyde dehydrogenase and (4) formate dehydrogenase (figure from Fuchs 1999).

Usually, the C₁₀–C₁₈ alkanes are degraded best and saturated alkanes are favored over the unsaturated ones. The aerobic degradation of all n-alkanes, e.g. n-decane, n-hexadecane or n-tetracosane, starts with oxidation of the terminal methyl group to the respective alcohol, alkane-1-ol, by an n-alkane monooxygenase (see Figure 1.3). The alcohol is subsequently oxidised by an alcohol dehydrogenase to the aldehyde, which is afterwards oxidised to the carboxylic acid by an aldehyde dehydrogenase. This fatty acid is degraded

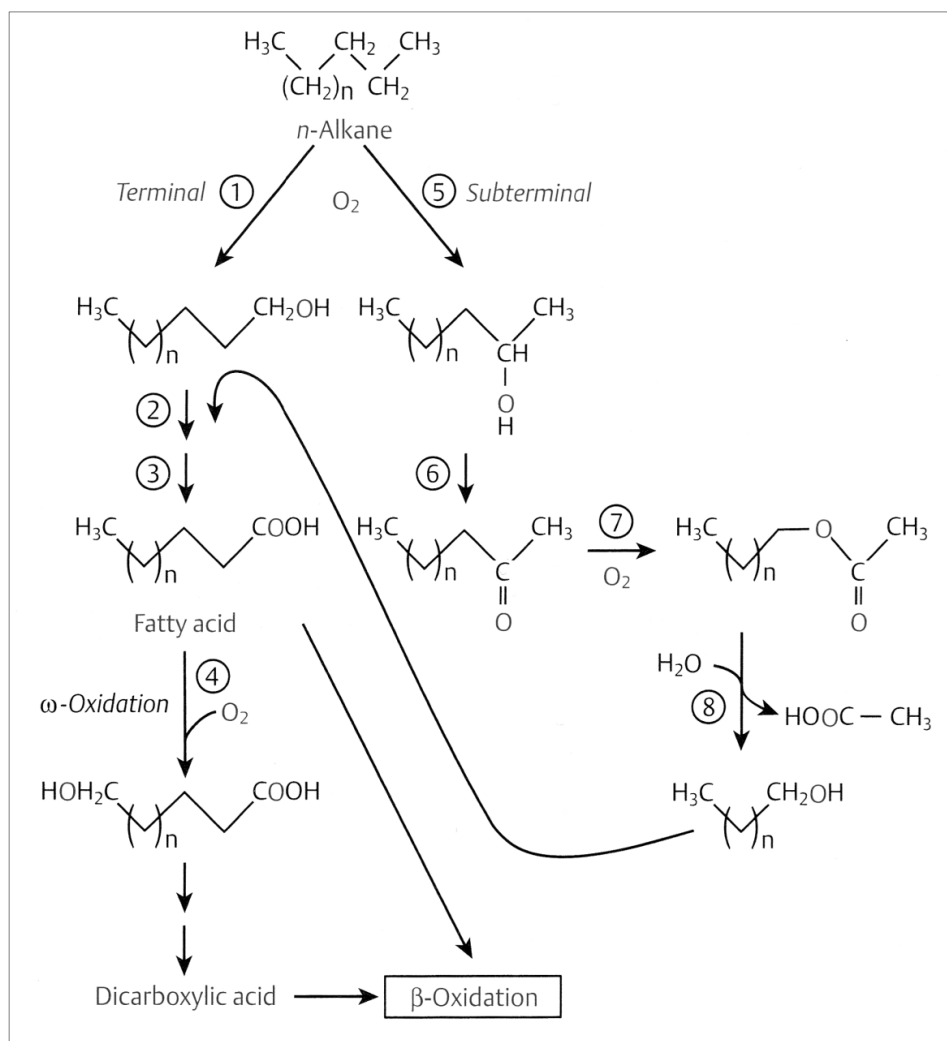


Figure 1.3: Basic metabolism of n-alkanes, where following enzymes are involved: (1) n-alkane monooxygenase, (2) alcohol dehydrogenase, (3) aldehyde dehydrogenase, (4), (5), (7) monooxygenases, (6) secondary alcohol dehydrogenase and (8) acetyltransferase (figure from Fuchs 1999).

through β -oxidation. In some organisms, the subterminal oxidation at C_2 by a monooxygenase is possible and yields the secondary alcohol, which is oxidised to the ketone (Fuchs 1999, Müller 2006). A monooxygenase then oxidises the ketone to the acetyl ester, which is subsequently hydrolysed to the alcohol and acetate. The alcohol is oxidised to the fatty acid. Degradation of branched alkanes is more slowly and happens via the α -oxidation at both ends (Fuchs 1999).

Aliphatic hydrocarbons can be degraded anaerobically by sulfate-, nitrate-, or iron(III)-reducing bacteria, where the addition of fumarate to the terminal methyl group is a crucial step (Spormann and Widdel 2000).

1.2.3.2 Aromatic hydrocarbons

In general, the aerobic biodegradation of aromatics requires molecular oxygen to (1) introduce hydroxyl groups for the activation of the aromatic hydrocarbon and (2) to subsequently cleave the aromatic ring (Fuchs 1999, Müller 2006, Pérez-Pantoja *et al.* 2010). In both key steps oxygenases play the main role (Pérez-Pantoja *et al.* 2010). The aerobic biodegradation of substituted aromatics is composed of an upper, peripheral pathway and a lower, central pathway. The former leads to the formation of partially-oxidised, central, aromatic intermediates (Müller 2006). The most common central intermediates are catechol or protocatechuate, but some aromatic hydrocarbons are degraded via gentisate (Fuchs 1999). In the following lower pathway, an oxygen molecule is introduced into these activated, dihydroxylated, aromatic molecules by a dioxygenase. Thus, the aromatic ring is cleaved oxygenolytically either at the *ortho*- (between the hydroxyl groups) or at the *meta*-position (adjacent to the hydroxyl groups) (Müller 2006). As shown in Figure 1.4, in the *ortho*-cleavage pathway, which is also referred to as β -keto adipate pathway, catechol or protocatechuate are degraded via the common intermediate β -keto adipate to acetyl-CoA and succinate, which are products of the citric acid cycle (Fuchs 1999, Müller 2006, Stanier and Ornston 1973). In the *meta*-cleavage pathway catechol is oxidised to 2-hydroxymuconic acid semialdehyde, whereas protocatechuate is oxidised to 2-hydroxy-4-carboxymuconic acid semialdehyde (Figure 1.5). End products of this *meta*-cleavage pathway are pyruvate, formate and acetaldehyde, which are intermediates in central metabolic pathways (Fuchs 1999, Stanier and Ornston 1973).

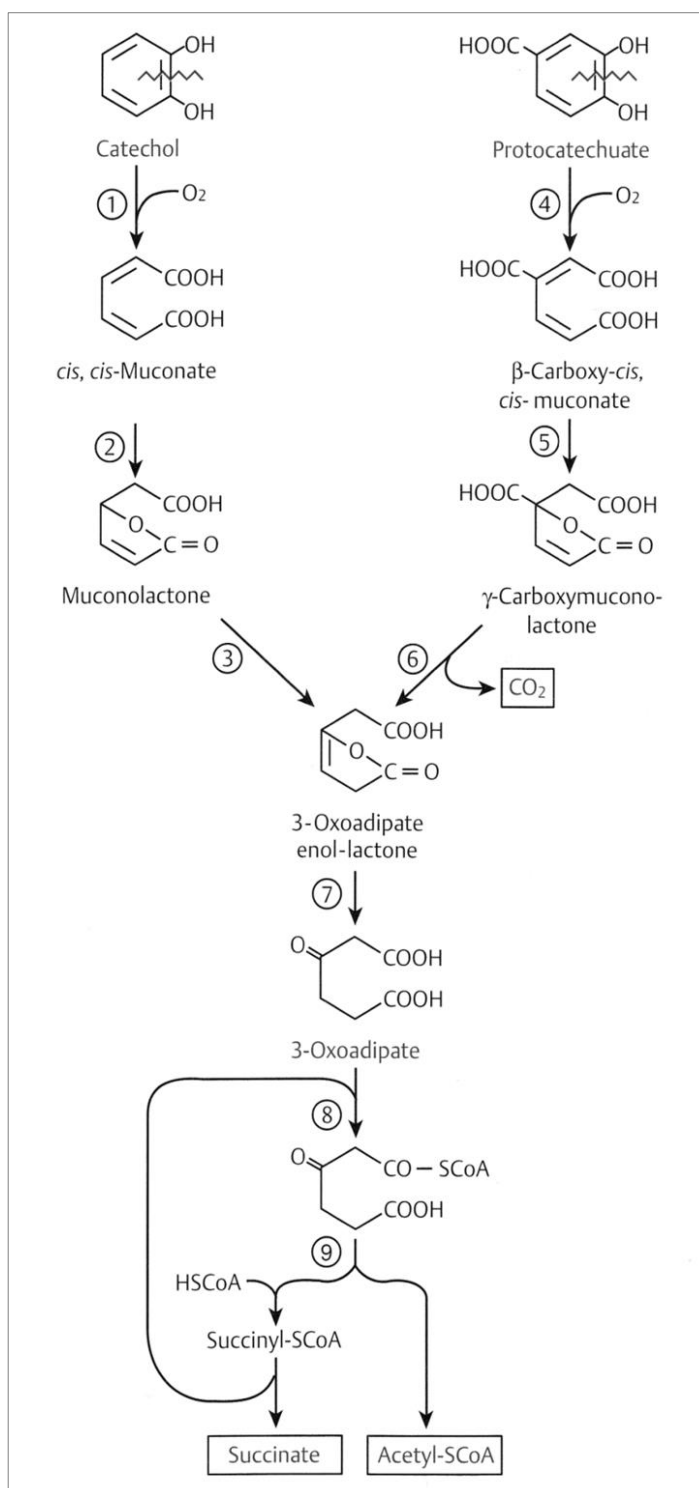


Figure 1.4: The *ortho*-cleavage pathway. Involved enzymes: (1) catechol 1,2-dioxygenase, (2) muconate-lactonising enzyme, (3) muconolactone isomerase, (4) protocatechuate 3,4-dioxygenase, (5) β -carboxymuconate-lactonising enzyme, (6) γ -carboxymuconolactone decarboxylase, (7) 3-oxoadipate enol-lactone hydrolase, (8) 3-oxoadipate succinyl-CoA transferase and (9) 3-oxoadipate-CoA thiolase (3-oxoadipate = β -ketoadipate).

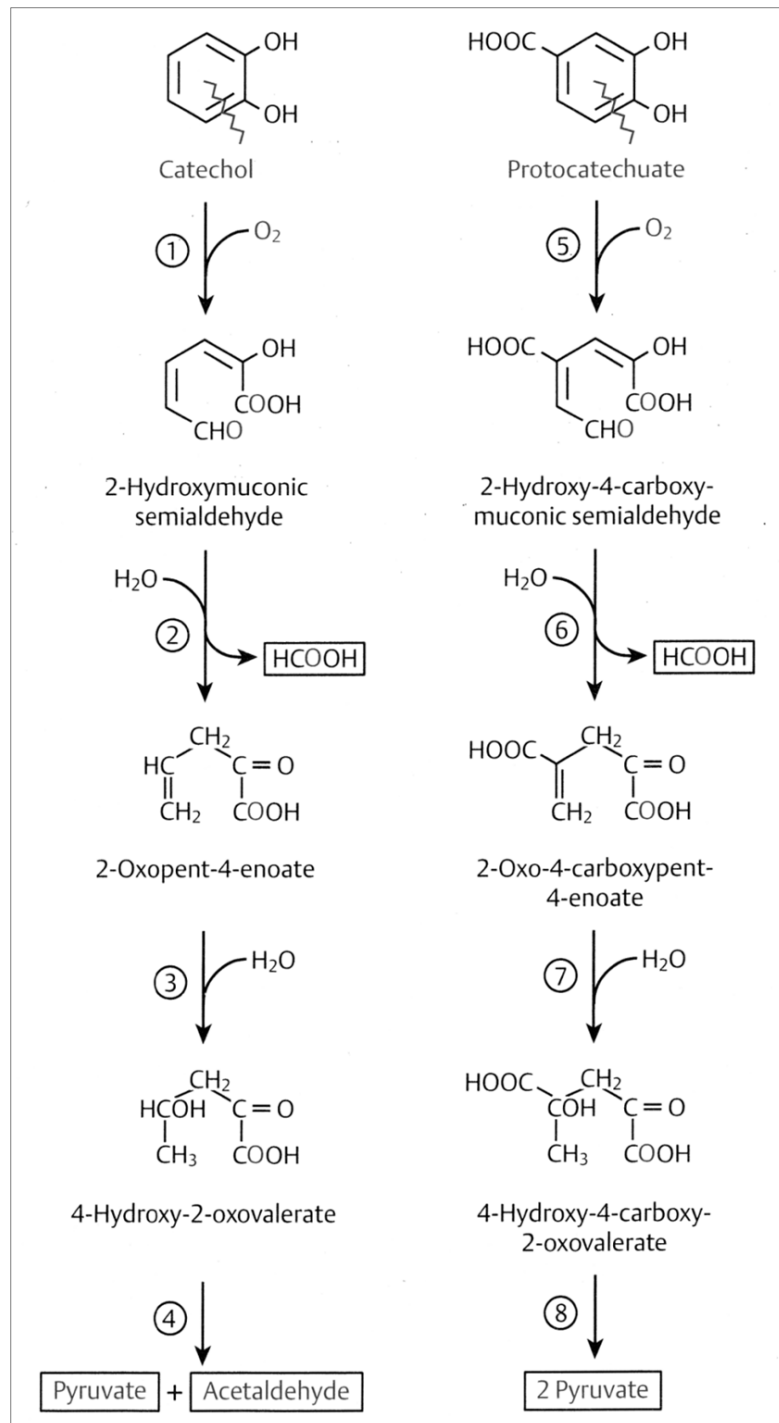


Figure 1.5: The *meta*-cleavage pathway. Involved enzymes: (1) catechol 2,3-dioxygenase, (2) 2-hydroxymuconic semialdehyde hydrolase, (3) 2-oxopent-4-enoic acid hydrolase, (4) 4-hydroxy-2-oxovalerate aldolase, (5) protocatechuate 4,5-dioxygenase, (6) 2-hydroxy-4-carboxymuconic semialdehyde hydrolase, (7) 2-oxo-2-carboxypent-4-enoic acid hydrolase and (8) 4-hydroxy-4-carboxy-2-oxovalerate aldolase (figures from Fuchs 1999).

For substituted aromatic hydrocarbons, such as toluene or xylene, either the substituent is split off or modified and then the ring is degraded, or the substituted aromatic hydrocarbon is degraded as if it is not substituted and substituted end-products are built. For toluene two possible degradation pathways are prevailing (Figure 1.6). In the first common route the methyl group is oxidised via the alcohol and the aldehyde to the acid. This benzoic acid is decarboxylated oxidatively and catechol is built, which is further metabolised usually via the *meta*-cleavage pathway. In the alternative route, via toluene-*cis*-dihydrodiol, 3-methylcatechol is built, which is cleaved at the *meta*-position. Subsequently, instead of formic acid, acetic acid is split off (Müller 2006).

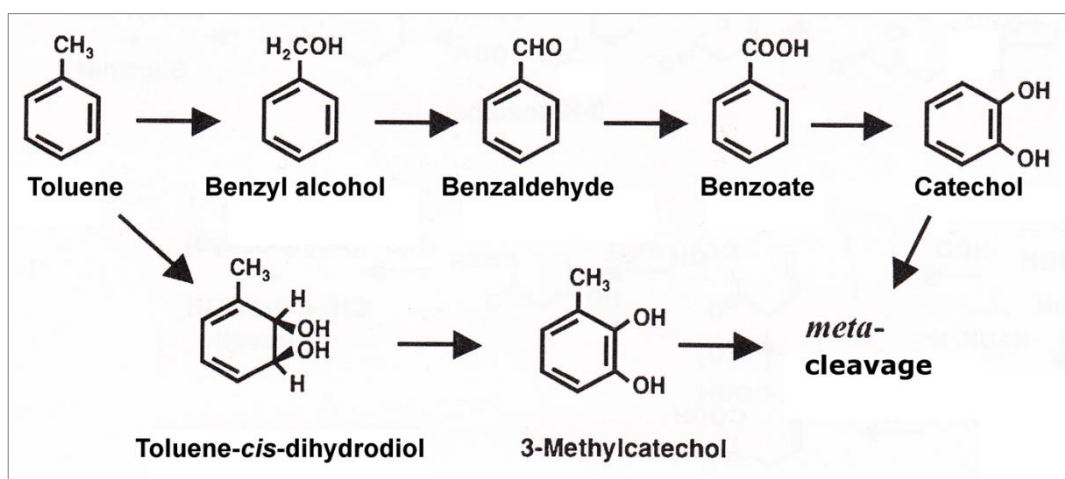


Figure 1.6: Two aerobic degradation pathways of toluene: via oxidation of the substituent and via oxidation of the aromatic ring (figure adapted from Müller 2006).

In the anaerobic degradation of aromatic hydrocarbons usually the aromatic ring is hydrogenated stepwise and derivatives of cyclohexane are built, which are cleaved hydrolytically (Müller 2006).

1.2.3.3 Polycyclic aromatic hydrocarbons

Polycyclic aromatic hydrocarbons (PAHs) contain two or more fused aromatic rings in linear, angular or cluster arrangements (Cerniglia 1984). They are ubiquitously distributed throughout the environment and can be of petrogenic, pyrogenic and biogenic source (e.g. lignin). Since several PAHs have been considered to be carcinogens, their biodegradation is of particular interest (Seo *et al.* 2009).

For aerobic degradation of PAHs there are three possibilities: (1) the complete mineralisation to carbon dioxide and biomass by bacteria, (2) the co-metabolic transformation by fungi and bacteria, which leads to partial oxidation of the ring and usually to accumulation of partially oxidised metabolites and (3) the unspecific, radical, extracellular oxidation, where radicals are built that further react non-specifically and produce undefined polymeric compounds. In this way white rot fungi are able to degrade xenobiotic substances and lignin (Müller 2006).

Naphthalene is degraded completely to carbon dioxide and biomass by specialised bacteria. At first, it is oxidised by a dioxygenase to *cis*-1,2-dihydroxy-1,2-dihydronaphthalene, which is converted to 1,2-dihydroxynaphthalene by a dehydrogenase. The 1,2-dihydroxynaphthalene is subsequently *meta*-cleaved, pyruvate is split off and salicylaldehyde is built. This is oxidised to salicylic acid, which can be oxidised to catechol and is degraded in the *meta*-cleavage pathway (Figure 1.7) (Cerniglia 1984, Müller 2006). Additionally, coumarin, 1,2-naphthoquinone, 1-naphthol and 2-naphthol were reported to be intermediates of the naphthalene metabolism (Abbott and Gledhill 1971, Agteren *et al.* 1998, Seo *et al.* 2009). The degradation of other PAHs, such as anthracene or phenanthrene, takes place in a similar way (Müller 2006).

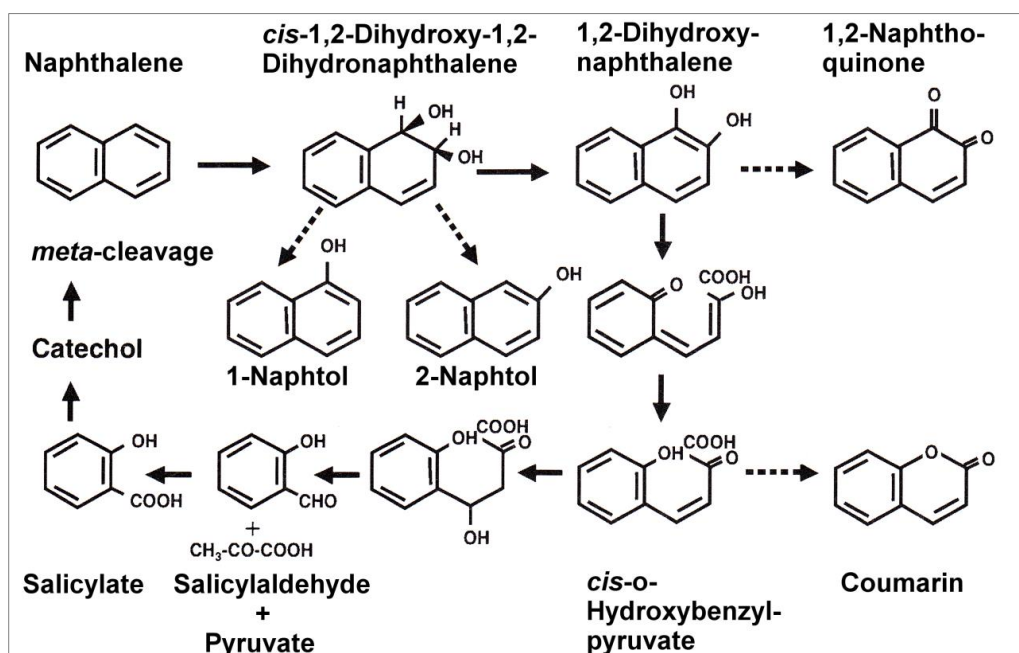


Figure 1.7: Aerobic degradation pathway of naphthalene (figure adapted from Müller 2006).

1.2.4 Aerobic biodegradation of crude oil from the Deepwater Horizon oil spill

Much research has been done on biodegradation of crude oil, in particular in the marine environment (e.g. Atlas 1981, Colwell and Walker 1977, Head *et al.* 2006, Leahy and Colwell 1990, Yakimov *et al.* 2007). Since 2010, the number of studies, especially in context of the DHW incident, is rising (e.g. Bælum *et al.* 2012, Hazen *et al.* 2010, Kessler *et al.* 2011, Kleindienst *et al.* 2015a, Passow 2014).

In the DWH spill, oil-adapted indigenous microorganisms responded rapidly to the oil and thus played a significant role in reducing the environmental impact of the oil (Atlas and Hazen 2011). From the discharged hydrocarbons, probably 43 to 61% have been microbially oxidised (Joye 2015). A substantial proportion of hydrocarbons in the plumes was converted to biomass (about 0.8 to 2×10^{10} mol carbon) (Shiller and Joung 2012), resulting in bacterial blooms. These blooms, which indicate that indigenous oil-degrading bacteria were enriched by the high supply of released hydrocarbons in the oil plumes, were observed in the months following the DHW accident (Bælum *et al.* 2012, Hazen *et al.* 2010, Kessler *et al.* 2011, Redmond and Valentine 2012, Valentine *et al.* 2010 and 2012).

The biodegradation rates of crude oil and gaseous hydrocarbons in the plumes were debated (Daley *et al.* 2016). While Camilli *et al.* (2010) suggested very low biodegradation of the hydrocarbon plume (requiring many months), Hazen *et al.* (2010) suggested fast hydrocarbon biodegradation at 5°C (oil half-lives in order of days) and reported high cell densities in the plume compared to outside the plume. Hazen *et al.* (2010) gave several reasons for this: (1) The oil from the DWH blowout was light crude oil, which can be more readily biodegraded than heavy crude oil, (2) the particle size of the oil droplets dispersed in the deep plume was small and (3) an oil-adapted bacterial community was already stimulated by oil leaks from natural deep-sea seeps in the GoM. Similarly, Kimes *et al.* (2014) and King *et al.* (2015) concluded in their reviews that the overall response of the microbial community to the oil and gas was rapid and robust.

Corexit® was found to have differing effects on the biodegradation rates. For instance, Bælum *et al.* (2012) found no negative effects of Corexit® EC9500A on growth of indigenous bacteria and an improved oil degradation in enrichment experiments. Kleindienst *et al.* (2015a) reported that crude oil biodegradation of a microbial community was either suppressed or not stimulated when dispersants were added. Overholt *et al.* (2016),

however, found both dispersants-induced inhibition as well as dispersants-induced stimulation of oil degradation and growth of certain model oil degraders. Corexit® EC9500A is a mixture of hydrocarbons (50%), glycols (40%) and dioctylsulfosuccinate (DOSS) (10%) (Bælum *et al.* 2012). These components can be degraded as well (Bælum *et al.* 2012, Campo *et al.* 2013, Chakraborty *et al.* 2012, Kleindienst *et al.* 2015a, Lindstrom and Braddock 2002, Lindstrom *et al.* 1999, Overholt *et al.* 2016).

The oil plumes were found to be associated with a decrease in dissolved oxygen concentration (oxygen anomaly), which was supposed to be caused by microbial respiration during the hydrocarbon degradation (Hazen *et al.* 2010, Joye *et al.* 2011b). Kessler *et al.* (2011) reported that within 120 days a bloom of methanotrophic bacteria in the deep sea metabolised almost all the released methane and that this event was accounting for the anomalous oxygen depression in the plume. However, this interpretation was subject of debate (Crespo-Medina *et al.* 2014, Joye *et al.* 2011a). Other gases, such as ethane and propane, were also degraded rapidly in the plume (King *et al.* 2015). Valentine *et al.* (2010) reported that rapid microbial respiration of propane and ethane, mainly by *Colwellia* (Redmond and Valentine 2012), was responsible for up to 70% of the oxygen depletion and that these hydrocarbon gases were the primary drivers of microbial respiration early in the spill.

1.2.4.1 Succession of the bacterial community composition

The bacterial community composition in the deep-sea plumes as well as other GoM locations changed over time and space in response to the varying oil composition and quantity (see Figure 1.8) (Atlas and Hazen 2011, Dubinsky *et al.* 2013, Kimes *et al.* 2014). The communities were dominated by a few types of Gammaproteobacteria (Dubinsky *et al.* 2013, Hazen *et al.* 2010, Redmond and Valentine 2012, Valentine *et al.* 2010).

Introduction

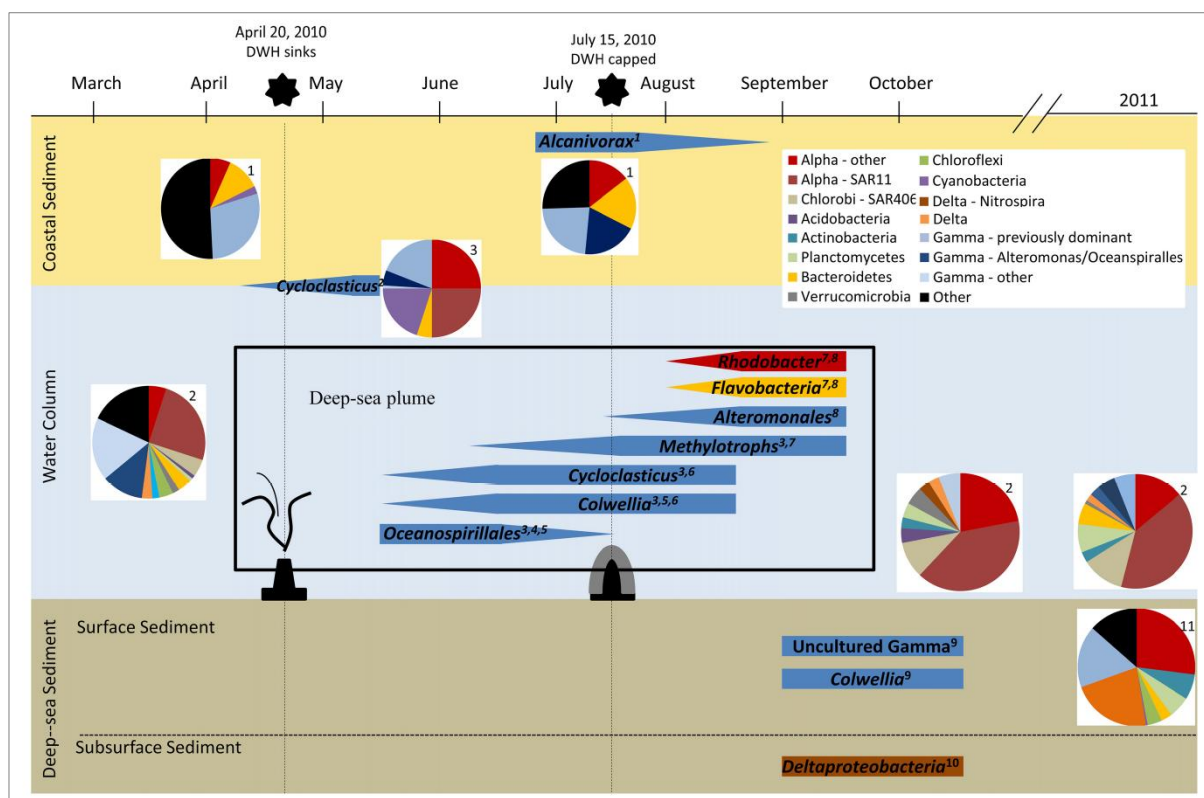


Figure 1.8: Changes in dominant members of the GoM microbial communities in response to the DWH oil spill (figure from Kimes *et al.* 2014).

During unmitigated flow of crude oil from the wellhead early in the spill, from end of May to beginning of June 2010, which resulted in high concentrations of n-alkanes and cycloalkanes, the dominating taxa in the deep-sea plumes were Oceanospirillales and *Pseudomonas*, which are alkane degraders (Dubinsky *et al.* 2013, Hazen *et al.* 2010, Mason *et al.* 2012, Redmond and Valentine 2012). In early June 2010, hydrocarbons were partially captured at the wellhead, hydrocarbon concentrations decreased and the amount of BTEX relative to alkanes increased. During this time, there was a shift in the plume community to dominance of *Colwellia*, *Cycloclasticus*, *Pseudoalteromonas* and *Thalossomonas*, which are capable of degradation of hydrocarbon gases (propane and ethane) or degradation of aromatic hydrocarbons (Dubinsky *et al.* 2013, Redmond and Valentine 2012, Valentine *et al.* 2010). After the well shut-in in mid-July 2010, the community in the dissolved oxygen anomaly of the water column was dominated by methylotrophs of the taxa Methylococcaceae (methane oxidisers), *Methylophaga* and Methylophilaceae (both secondary consumers of C₁ compounds) (Kessler *et al.* 2011, Kimes *et al.* 2014), as well as

Flavobacteria, Rhodobacteraceae and Alteromonadaceae, which are degraders of high molecular weight hydrocarbons and of complex organic matter (Dubinsky *et al.* 2013, Kessler *et al.* 2011). They probably scavenged organic matter and cell biomass from the decaying bacterial bloom (King *et al.* 2015).

Similarly, the bacterial community in the oil-contaminated deep-sea sediments responded to the oil from the DWH blowout. Mason *et al.* (2014) found highly oil-contaminated surface sediments to be most abundant with an uncultivated Gammaproteobacterium and a *Collwellia* species. In contrast, Liu and Liu (2013) found mainly Gammaproteobacteria (*Methylococcus*, *Vibrio* and *Pseudomonas*), Alphaproteobacteria (*Methylobacterium*), Flavobacteria and Acidobacteria.

Oiled coastal sands were also dominated by members of the class Gammaproteobacteria, such as *Alcanivorax*, *Marinobacter*, *Pseudomonas* and *Acinetobacter* (Kostka *et al.* 2011). Oil-contaminated coastal salt marshes were found to be dominated by Proteobacteria, Bacteroides, Actinobacteria and Firmicutes (Beazley *et al.* 2012).

In oil-contaminated surface waters a dominance of Gammaproteobacteria (including *Marinobacter*, *Alcanivorax*, *Pseudomonas* and *Alteromonas*), Alphaproteobacteria and Cyanobacteria was reported (Liu and Liu 2013, Redmond and Valentine 2012). However, Yang *et al.* (2014) found Gammaproteobacterium *Cycloclasticus* to be dominant in surface-water samples.

In conclusion, oil acted as a strong selective force to stimulate particular, specialised, oil-degrading bacteria and reduced the community diversity (Head *et al.* 2006). The response of bacterial communities to the oil probably depended on the respective environmental conditions (Liu and Liu 2013).

1.3 High pressure in the deep sea

Particular attention of this work was paid to the harsh conditions present in the deep sea at the DWH well head, especially to the high pressure. As described in the following subsection, high pressure can cause numerous effects on bacterial cells and their components. However, deep-sea bacteria developed various mechanisms of adaptation to withstand the extreme pressure.

1.3.1 Deep-sea conditions

Deep-sea environments are characterised by extreme conditions such as high hydrostatic pressure. The deep sea starts at a depth of 1,000 m (Fang *et al.* 2010, Jannasch and Taylor 1984). Hydrostatic pressure is defined as a function of the weight of water above a surface at a given depth (Fang *et al.* 2010). In water the hydrostatic pressure rises 1 bar for every 10 m in depth below the water surface (Jannasch and Taylor 1984). At the deepest site existing in the ocean, at 10,994 m (± 40 m) in the Mariana Trench, pressure is 1,100 bar (Abe and Horikoshi 2001, Gardner and Armstrong 2011). At the sea bottom around the DWH well the pressure is about 150 bar.

In addition to high pressure, other extreme conditions, such as low nutrient concentrations and low temperatures, are present in the deep sea (Prieur and Marteinsson 1998). In the oceans temperature is decreasing with depth until the thermocline is reached at 30 to 100 m below surface. Below the thermocline almost constant temperatures of 3°C ($\pm 1^\circ\text{C}$) are present (Jannasch and Taylor 1984). An exception are hydrothermal vents, where temperatures of up to 400°C are reached (Horikoshi 1998). In the GoM, below a depth of 700 m the temperature is 2 to 5°C (Atlas and Hazen 2011). The ocean's salinity varies between 34.3 and 35.1 g/L and pH varies between 7.5 and 8.0 (Nagata *et al.* 2010). Light and thus photosynthesis occur up to a depth of 300 m below the water surface of the oceans (Jannasch and Taylor 1984).

1.3.2 Effects of high pressure

The extreme pressure conditions can affect microorganisms, living in the deep sea. In general, high pressure effects are driven by changes of volume. When pressure is increased the equilibrium of a reaction will be shifted to the side that occupies the smallest volume according to the principle of Le Chatelier and Braun. Thus, increase of pressure can accelerate or decelerate reactions depended on whether the reaction is accompanied by a volume decrease or increase (Abe and Horikoshi 2001, Follonier *et al.* 2012).

As stated previously, the ability of microorganisms to degrade crude oil is dependent on the composition of the present hydrocarbons. However, there is evidence that the degradation ability is also dependent on temperature. According to the Arrhenius law reactions are accelerated when temperature is increasing. This implies that all processes of

life are slowed down when temperature is decreasing (Atlas 1975, Madigan and Martinko 2009). In addition, microbial growth in the deep-sea environment is affected by an interdependence of temperature and pressure (Horikoshi 1998). ZoBell and Johnson (1949) showed that low temperatures strengthened the retarding effects of high pressure on bacterial growth, while at high temperatures the effects were less pronounced. Louvado *et al.* (2015) proposed that high pressure and low temperatures may synergistically reduce PAH biodegradation by hindering PAH uptake due to reduction in membrane permeability and by inactivation of essential enzymes due to conformational changes.

Pressures of up to 10 bar are affecting microorganisms only indirectly by raising the gas solubility (e.g. of oxygen or carbon dioxide). According to Henry's law the concentration of a dissolved gas is increased when its partial pressure in the gas phase is increased. This can lead to accumulation of reactive oxygen species in the cell, which may damage nucleic acids, proteins and lipids (Cabiscol *et al.* 2000, Follonier *et al.* 2012, Wiebe and Gaddy 1940).

As shown in Figure 1.9, high pressure can have various effects on bacterial cell components, associated cellular processes (such as protein synthesis, membrane activity and transport processes), enzymatic reactions and regulation of gene expression.

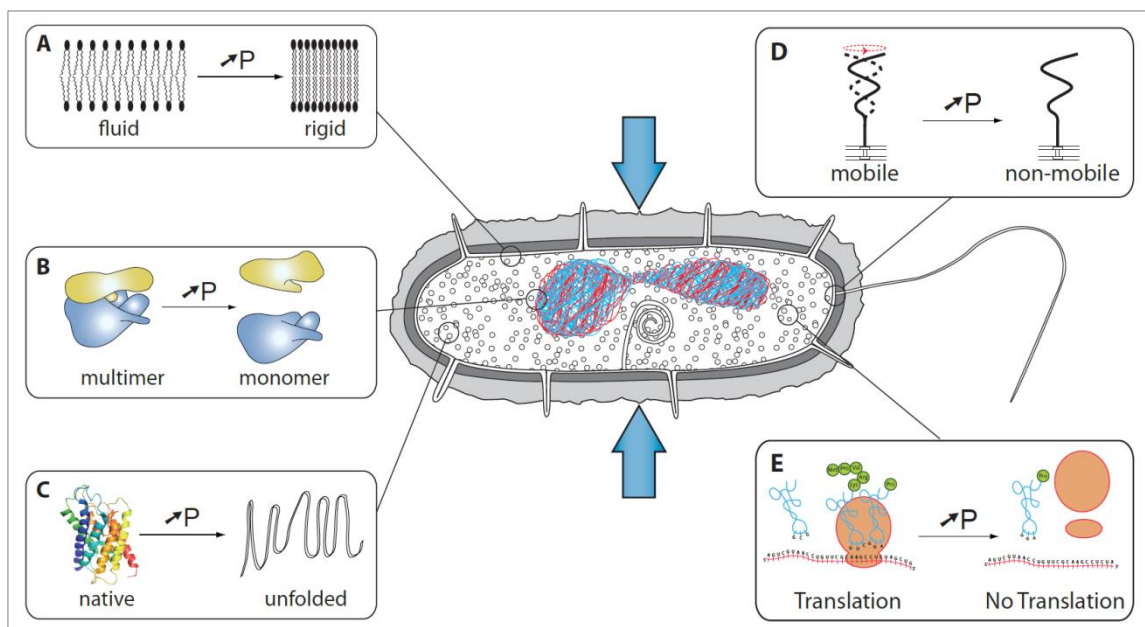


Figure 1.9: Effects of high pressure on bacterial cell components such as (A) lipid membranes, (B) multimeric proteins, (C) protein structure, (D) motility and (E) protein synthesis (figure from Oger and Jebbar 2010).

The majority of these direct pressure effects were reported to start at more than 200 bar (Follonier *et al.* 2012):

- The structure of small molecules (such as peptides, saccharides and lipids) as well as the primary structure of macromolecules (such as proteins, polysaccharides and nucleic acids) are not changed by high pressure, since covalent bonds are not affected, at least not at less than 10,000 bar (Follonier *et al.* 2012, Mozhaev *et al.* 1996). However, high pressure is predominantly disrupting weak, non-covalent bonds. Thus, high pressure can affect the conformation of macromolecules as well as their interactions (multimer association), which influences their functionality in the cells (Follonier *et al.* 2012, Mota *et al.* 2013, Oger and Jebbar 2010).
- Proteins are among the most pressure-sensitive parts of the cell (Oger and Jebbar 2010) and they are affected in their stability and structure (Abe and Horikoshi 2001). High pressure can have stabilising as well as destabilising effects on protein structure (Follonier *et al.* 2012), depending on the respective initial pressure and temperature (Balny *et al.* 1997, Eisenmenger and Reyes-De-Corcuera 2009). The pressure-temperature phase diagram of the native/denatured protein equilibrium (Figure 1.10) has an elliptic shape. In general, up to approximately 1,000 bar the

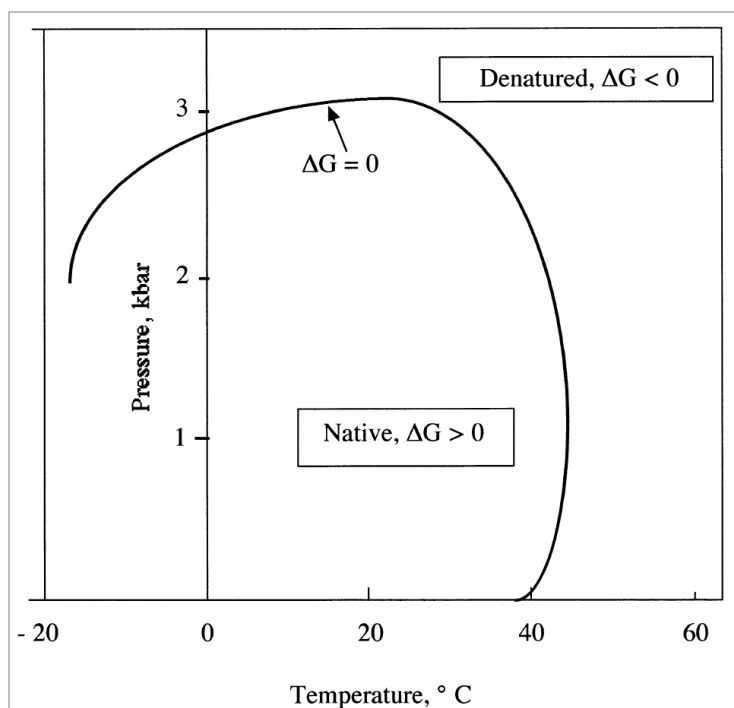


Figure 1.10: Pressure-temperature diagram for protein denaturation. The region inside the elliptical shape corresponds to native protein conformation, the region outside corresponds to denatured conformation. The regions are separated by a zone of reversible denaturation, where ΔG (Gibbs free energy) = 0 (Follonier *et al.* 2012, figure from Balny *et al.* 1997).

temperature of protein denaturation is increasing and when pressure increases more, the denaturation temperature will decrease (Balny *et al.* 1997).

The conformation of enzymes can be modified by pressure, which can have consequences for their substrate affinity and reaction rates (Follonier *et al.* 2012). Multimeric enzymes are inhibited by high pressure since their protein multimers dissociate into single units (Penniston 1971). This effect on the quaternary structure of multimeric proteins occurs at pressures of about 2,000 bar, while at pressures of more than 4,000 bar most proteins tend to unfold and denature (Aertsen *et al.* 2009).

- Synthesis of proteins stops at 588 to 600 bar, as ribosomes dissociate (Gross *et al.* 1993, Yayanos and Pollard 1969). However, this process is reversible under certain conditions in *Escherichia coli* and as soon as the pressure is released the protein synthesis can proceed (Niven *et al.* 1999). The dissociation of ribosomes is supposed to be one of the major reasons for growth inhibition at high pressure (Niven *et al.* 1999).
- Nucleic acids are stabilised by high pressure, since hydrogen bonds are stabilised. This may be problematic for replication and transcription, where single-strand DNA is required (Macgregor 2002, Oger and Jebbar 2010). An inhibition of DNA synthesis was reported to occur at 500 bar in *E. coli*. The RNA synthesis was found to be totally inhibited at 770 bar in *E. coli* (Yayanos and Pollard 1969).
- Lipid membranes are highly sensitive to high pressure (Oger and Jebbar 2010). When pressure is increased, the melting point of lipids is raised and the membrane gels or crystallises (Kato *et al.* 2002, Wirsen *et al.* 1986). This may result in decrease of the membrane's fluidity, reduced membrane transport and a disruption of the permeability of the cell membrane for water-soluble proteins (Hauben *et al.* 1996, Kato *et al.* 2002, Oger and Jebbar 2010). However, optimal fluidity is essential for maintenance of various membrane functions (Wirsen *et al.* 1986). The change of membrane fluidity was reported to occur at 1,000 bar or lower (Kato *et al.* 2002). Loss of membrane integrity was found to occur between 1,000 and 2,000 bar in *E. coli* (Pagán and Mackey 2000).

- Cell division and growth in cell size (formation of biomass) of *E. coli* were found to be inhibited by pressures of about 200 to 500 bar. However, cell division was more retarded than the growth in cell size. The cells showed the tendency to grow in filamentous shape at increased pressures (ZoBell and Cobet 1962, 1964).
- The motility of *E. coli* was inhibited at a pressure of about 100 bar, as described by Meganathan and Marquis (1973).

Predominantly, *E. coli* was used as model organism in studies on pressure effects, mentioned above. However, absolute values of critical pressures may vary from one organism to another. The extent of cell damage may depend not only on the organisms' degree of pressure tolerance but also on the duration of pressure exposure and other environmental conditions (Mota *et al.* 2013).

Up to now, only a few reports are available investigating the effects of high pressure on biodegradation by deep-sea bacteria. Mostly, they do not concentrate on the degradation of hydrocarbons but of organic matter, detritus or glucose. These studies found inhibiting as well as enhancing effects of high pressure (see e.g. Jannasch *et al.* 1971, Turley and Lochte 1990, ZoBell and Johnson 1949). However, as oil companies are exploring the oceans for more oil and deep-water drilling expands, the knowledge on how high pressure affects biodegradation of crude oil is increasingly important. Nevertheless, only a limited number of studies focused on this issue to date. Bowles *et al.* (2011) found that a pressure of 100 bar increased anaerobic methane oxidation rates by microbial communities from deep-sea sediments. Schwarz *et al.* (1974 and 1975) reported that a microbial community from deep-sea sediment utilised n-hexadecane at a much lower rate under *in situ* pressure of 506.6 bar than under ambient pressure (= atmospheric pressure of 1 bar). Grossi *et al.* (2010) found no significant influence of high pressure (of 350 bar) on the n-hexadecane degradation and growth of the deep-sea strain *Marinobacter hydrocarbonoclasticus*. However, the lipid composition of the cells was affected by high pressure. Recently, Scoma *et al.* (2016) reported that pressures of already 50 and 100 bar reduced significantly growth yields of two surface-water strains (*Alcanivorax jadensis* KS_339 and *A. dieselolei* KS_293) tested with n-dodecane. However, cell viability was not affected by high pressure, indicating that cell division processes were slowed down. At 100 bar, the carbon dioxide production, as an indirect measure of the n-dodecane degradation, was not affected at high pressure in strain *A. dieselolei* KS_293. Despite the pressure-induced differences in growth and hydrocarbon

utilisation reported in these studies, oil biodegradation research has been conducted predominantly at surface pressure to date. Thus, obtained results may not be applicable to the deep ocean. Bowles *et al.* (2011) emphasised that for accurate analysis of deep-sea microbial processes, *in situ* conditions such as high pressure need to be considered. In the present thesis this issue was revisited.

1.3.3 Adaptation of deep-sea microorganisms to high pressure

In the deep sea many microorganisms are extremophiles such as halophiles (organisms that need at least 1 M salt for growth), psychrophiles (organisms with optimal growth temperature of 10°C or lower and maximal growth temperature of 20°C), thermophiles (organisms that can grow at temperatures from 60°C to 85°C) and piezophiles (Horikoshi and Bull 2010, Kato 1999). In 1949, ZoBell and Johnson started to investigate the effects of elevated pressure on the activity of marine and terrestrial bacteria. They coined the term “barophilic” (also termed piezophilic from Greek *piezein*, to press), which describes bacteria with optimal growth at more than 1 bar or bacteria that need increased pressure for growth (Abe and Horikoshi 2001, Kato 1999, Nogi 2008, ZoBell and Johnson 1949). Piezophilic bacteria show best growth at >400 bar (Horikoshi 1998). Some of them, obligatory piezophiles, even cannot grow at 1 bar (Nogi 2008). Piezotolerant bacteria in turn grow best at 1 bar, but are also able to grow at elevated pressures of 300 to 500 bar (Abe and Horikoshi 2001, Nogi 2008). In contrast, piezosensitive bacteria are susceptible to high pressure (Abe and Horikoshi 2001). They were described to stop growth completely at pressures of 300 to 500 bar (Nogi 2008). Most of the bacteria adapted to the deep sea are not only piezotolerant or piezophilic but also psychrophilic (Horikoshi 1998). Piezophilic and piezotolerant bacteria are adapted to high pressure conditions in many ways:

- The modification of the structure of biomolecules, such as enzymes, is one adaptation mechanism to maintain the binding capacity for their substrates and minimise the effects of pressure (Oger and Jebbar 2010, Madigan and Martinko 2009).
- The increase of the amount of unsaturated fatty acids in their membranes is another adaptation mechanism of organisms that grow at elevated pressures (DeLong and Yayanos 1985, Wirsen *et al.* 1986). This diminishes the packing density and the

melting points of the lipid molecules and thus helps to maintain fluidity of membranes at high pressures (DeLong and Yayanos 1985, Madigan and Martinko 2009). This high pressure response (termed “homeoviscous” adaptation) is analogous to membrane adaptations to low temperatures (DeLong and Yayanos 1985).

- The change of the protein composition of the cell wall is another way to adapt to high pressure (Madigan and Martinko 2009). The moderate psychrophilic piezophile *Photobacterium profundum* SS9 was found to synthesise the protein *OmpH* for transport of nutrients in the outer membrane exclusively at high pressure (Bartlett *et al.* 1989). This was the first identification of a pressure-regulated gene product (Abe and Horikoshi 2001).
- The adjustment of the gene expression to high pressure and expression of high-pressure-specific genes is another strategy (Oger and Jebbar 2010). Microorganisms from deep-sea environments can respond to high pressure by inducing the synthesis of specific stress proteins (Kato 1999). This pressure-induced regulation of gene expression shares similarities with cold-shock and heat-shock responses (Follonier *et al.* 2012). When *E. coli* was incubated at 553 bar, it was found to upregulate certain cold-shock and heat-shock-proteins as well as many proteins, which only appear in response to pressure (Welch *et al.* 1993). Heat-shock proteins can help to refold or degrade misfolded proteins (Arsène *et al.* 2000), while cold-shock proteins interact directly or indirectly with DNA, RNA or ribosomes to decrease the synthesis of macromolecules (Madigan and Martinko 2009).

1.4 Objectives of this thesis

The aim of this thesis was to examine the biodegradation of crude oil at the sea floor around the DWH well in the GoM. The harsh conditions ruling in this environment make it difficult to study oil-degradation mechanisms *in situ*. By simulating artificial deep-sea conditions using high pressure reactors in the laboratory it is possible to control different factors such as temperature, salinity, substrate concentration or pressure separately. In context of this work, two pressure regimes were compared: the atmospheric pressure of 1 bar and the pressure of 150 bar, the latter corresponding to the DWH’s well depth. The effects of high pressure on aerobic, bacterial crude oil degradation were investigated.

However, crude oil is one of the most complex mixtures of organic compounds on earth (Head *et al.* 2006). Hence, to simplify the approach initially, different representatives of the main fractions of crude oil were chosen to be analysed at high pressure. n-Decane, n-hexadecane and n-tetracosane were chosen as representatives of the n-alkanes. Toluene served as a representative of aromatic oil components and naphthalene was used as a representative of PAHs.

Because no bacterial isolates were available from the GoM during the major part of this work, several bacterial model strains were chosen for biodegradation experiments. Their ability to degrade hydrocarbons at ambient pressure was already known and in this thesis they were tested under high pressure conditions. *Rhodococcus qingshengii* TUHH-12 was used as a model degrader of different alkanes, *Sphingobium yanoikuyae* B1 was used as a model degrader of the PAH naphthalene and *Rhodococcus wratislaviensis* Tol3 was used as a model degrader of the aromatic hydrocarbon toluene. Among other species of the genera *Rhodococcus* and *Sphingobium*, also *R. qingshengii* and *S. yanoikuyae* had already been isolated from sediments sampled in the deep sea (Colquhoun *et al.* 1998, Cui *et al.* 2008, Heald *et al.* 2001, Peng *et al.* 2008, Tapilatu *et al.* 2010, Wang and Gu 2006). Moreover, *Rhodococcus* sp. and *Sphingobium* sp. were identified in sediment samples collected in May 2011, about 2 and 6 km away from the wellhead of the DWH (Liu and Liu 2013).

In addition, one indigenous bacterial strain, *Dietzia aurantiaca* C7.oil.2, isolated from a GoM sediment sample, was examined for its ability to degrade n-hexadecane and toluene.

Furthermore, bacterial communities from sediments, sampled at different times and different sites in the GoM, were incubated with crude oil and natural gas under high pressure conditions.

Moreover, it was investigated how biodegradation under high pressure is influenced by the dispersant Corexit® EC9500A, which was applied in the DWH oil spill to mitigate the impacts of the oil on the environment.

The ultimate proposal of this thesis was to achieve a deeper insight into the crude oil biodegradation processes in the deep sea. The resulting degradation rates, obtained under field conditions, are valuable for the improvement of models that simulate and predict the fate of the spilled oil in the deep sea.

2 Materials and methods

2.1 Chemicals

Used chemicals were purchased from following companies: Sigma-Aldrich Chemie GmbH (Munich, Germany), Carl Roth GmbH + Co. KG (Karlsruhe, Germany), Merck KGaA (Darmstadt, Germany) and Fluka Feinchemikalien GmbH (Neu-Ulm, Germany). Nitrogen gas was supplied by Linde AG (Munich, Germany).

Louisiana sweet crude oil (request ID 10384) was obtained from the Knox Storage Archive Facility (Fort Collins, Colorado, USA) and was a surrogate oil from the Marlin platform of the Dorado field, which is about 37 km northeast of the DWH platform. This oil is chemically and toxicologically similar to the Macondo field oil (Reference oil team 2012).

The dispersant Corexit® EC9500A was obtained from the company Nalco (Naperville, Illinois, USA).

For Polymerase Chain Reaction (PCR) following chemicals were used:

- Taq DNA Polymerase Kit (PEQLAB, VWR International GmbH, Erlangen, Germany)
- Primers (biomers.net, Ulm, Germany)
- Agarose (SERVA Electrophoresis GmbH, Heidelberg, Germany)
- SYBR® Green I Nucleic acid gel stain (Lonza, Rockland, Maine, USA)
- peqGOLD 1kb DNA Ladder (PEQLAB Biotechnology GmbH, Erlangen, Germany)
- 6x loading dye (PEQLAB Biotechnology GmbH, Erlangen, Germany)
- Gene JET PCR Purification Kit #K0702 (Thermo Fisher Scientific Germany BV & Co. KG, Braunschweig, Germany)

2.2 Equipment

Laboratory equipment used in this study is listed in Table 2.1, high pressure equipment is listed in Table 2.2 and online monitoring systems for oxygen (O₂) and carbon dioxide (CO₂) are listed Table 2.3.

Table 2.1: Laboratory equipment used in this thesis.

Equipment		Manufacturer
Super-Nuova Multiplate Stirrer		Thermo Fisher Scientific Germany BV & Co. KG, Braunschweig, Germany
Shaker CERTOMAT® R		B. Braun Melsungen AG, Melsungen, Germany
Incubators	Köttermann® 2737	Köttermann GmbH & Co KG, Uetze/Hänigsen, Germany
	Memmert GTR0214	Memmert GmbH + Co. KG, Schwabach, Germany
pH meter CG 812		Schott Geräte, Hofheim, Germany
Ultrasonicator Sonorex RK 106 S (ultrasonic waterbath)		BANDELIN electronic GmbH & Co. KG, Berlin, Germany
Glassware, flasks, vials		Schott AG , Mainz, Germany; Glasgerätebau Ochs Laborfachhandel e.K., Bovenden / Lenglern, Germany
Uvikon Spectrophotometer		Kontron AG, Zurich, Switzerland
Milli-Q Water Purification System		Millipore, Massachusetts, USA
Microscope Axioskop		Carl Zeiss AG, Oberkochen, Germany
Gas chromatography-mass spectrometry (Hewlett-Packard 5890 Series II gas chromatograph, Agilent HP-5MS column [30 m x 0.25 mm], Hewlett-Packard 5971A mass selective detector)		Hewlett-Packard GmbH, Böblingen, Germany; Agilent Technologies Deutschland GmbH, Frankfurt, Germany
Centrifuge Biofuge_13 and Megafuge 1.0R		Heraeus Instruments GmbH, Hanau, Germany
Varioklav® Steam Steriliser 250T and 500 EP Z		HP Medizintechnik GmbH, Oberschleißheim, Germany

Table continued on next page.

Table 2.1 - continued

Solvent evaporator (Rotavapor R-200, Heating Bath B-491, Vacuum Controller V-805, Pump Vac V-513)		BÜCHI Labortechnik GmbH, Essen, Germany
Water baths	Ecoline RE106	LAUDA DR. R. WOBSE GMBH & CO. KG, Lauda-Königshofen, Germany
	SW23	Julabo GmbH, Seelbach, Germany
Rocking table Model 3013		Gesellschaft für Labortechnik mbH, Burgwedel, Germany
Neubauer chamber (0.02 mm depth, 0.0025 mm ²)		Glaswarenfabrik Karl Hecht GmbH & Co KG, Sondheim v. d. Rhön, Germany
PCR equipment	Thermocycler PCR Sprint	Hybraid Limited, Ashford, UK
	UV fluorescence table ECX-20-11	PEQLAB Biotechnology GmbH, Erlangen, Germany
	Gel documentation DP-CF-011-C	PEQLAB Biotechnology GmbH, Erlangen, Germany
	Agarose gel chamber Horizon58	Life Technologies, Gibco BRC, Gaithersburg, Maryland, USA
Denaturing Gradient Gel Electrophoresis (DGGE) equipment	Electrophoresis system	Biorad Laboratories, California, USA
	Gradient mixer GM25	Scie-Plas Ltd., Cambridge, UK
	Pump 323Du/D	Watson-Marlow Limited, Falmouth, Cornwall, UK
Tray cell for measurement of DNA concentration		Hellma GmbH & Co. KG, Müllheim, Germany
Breeze [®] 2 for measurement of glucose concentration		Bayer AG, Leverkusen, Germany
Mounting for 160 mL high pressure reactors		Workshop TUHH

Table continued on next page.

Table 2.1 - continued

Filling hose and mounting for pressurisation of the 160 mL high pressure reactors	Technik Service Andreas Meyer, Lindau Germany
NanoDrop™ 2000c Spectrophotometer	Thermo Fisher Scientific Germany BV & Co. KG (Braunschweig, Germany)

Table 2.2: High pressure equipment used in this thesis.

Reactor	Quantity	Maximum pressure (bar)	Volume (mL)	Manufacturer
160 mL high pressure reactors ¹ (one of them was formerly equipped with a screw-piston mechanism for mechanical pressurisation)	10	400	~ 160	Technik Service Andreas Meyer, Lindau Germany
Ambient pressure reference reactors	10	1	~ 160	Workshop TUHH
High pressure reactor with screw-piston mechanism for mechanical pressurisation ¹	1	400	30	Technik Service Andreas Meyer, Lindau, Germany
High pressure view cell reactor No. 1 (HP-VC 300) with mechanical spindle pump ²	1	300	25	Reactor: Eurotechnica GmbH, Bargteheide, Germany; spindle pump: SITEC-Sieber Engineering AG, Zurich, Switzerland

Table continued on next page.

¹ Five of the 160 mL high pressure reactors and the high pressure reactor with screw-piston mechanism were kindly provided by Prof. Dr. Giselher Gust, former Institute of Ocean Engineering, now Institute of Product Development and Mechanical Engineering Design, TUHH

² Kindly lent by Dr. Philip Jaeger, Eurotechnica GmbH, Germany

Table 2.2 - continued

High pressure view cell reactor No. 2 ³	1	400	100	SITEC-Sieber Engineering AG, Zurich, Switzerland
1 L high pressure reactor	1	300	1,000	Technik Service Andreas Meyer, Lindau, Germany

Table 2.3: Oxygen and carbon dioxide measurement systems used in this thesis.

Equipment	Maximal pressure (bar)	Manufacturer
O ₂ sensor with former HIOXY T1000, now FOSPOR coating formulation for measurement at high pressure	200	Ocean Optics GmbH, Ostfildern, Germany
O ₂ sensors with FOXY or FOSPOR coating formulation for measurement at ambient pressure	1	Ocean Optics GmbH, Ostfildern, Germany
O ₂ sensor Fibox 3 ⁴	Not specified	PreSens Precision Sensing GmbH, Regensburg, Germany
CO ₂ sensor pCO ₂ mini ⁴	Not specified	PreSens Precision Sensing GmbH, Regensburg, Germany
VisiSens TM systems for measurement of O ₂ and CO ₂ ⁴	Not specified	PreSens Precision Sensing GmbH, Regensburg, Germany
O ₂ prototype sensor for measurement at high pressure ⁵	200	Cooperation of PreSens Precision Sensing GmbH, Regensburg, Germany and Eurotechnica GmbH, Bargteheide, Germany

³ Kindly lent by Prof. Dr. Rudolf Eggers and Dr. Philip Jaeger, Institute of Thermal Separation Processes, TUHH

⁴ Kindly lent by PreSens Precision Sensing GmbH, Germany

⁵ Kindly lent by PreSens Precision Sensing GmbH, Germany and Dr. Philip Jaeger, Eurotechnica GmbH, Germany

2.3 Microorganisms

2.3.1 Bacterial strains

Hydrocarbon-degrading model strains used for this work were (1) *Rhodococcus qingshengii* TUHH-12, (2) *Rhodococcus wratislaviensis* Tol3, (3) *Sphingobium yanoikuyae* B1 and (4) *Dietzia aurantiaca* C7.oil.2. As a reference strain *Escherichia coli* K12 DH5 α , purchased from DSMZ (DSM No. 6897), was used.

R. qingshengii TUHH-12, a degrader of alkanes, was isolated in our laboratory from seawater samples collected beneath an ice cap by Prof. Dr. Hauke Trinks (TUHH) during an expedition to Spitzbergen, Norway. The genome of this strain was sequenced by Lincoln *et al.* 2015. The strain was deposited in the open collection of the DSMZ (DSM No. 46766).

Tol3, a degrader of aromatic hydrocarbons, was isolated in our laboratory from water samples collected from the Elbe River. The strain was identified as *Rhodococcus wratislaviensis* by sequencing the 16S rRNA gene.

S. yanoikuyae B1, a degrader of several aromatic and polycyclic aromatic hydrocarbons, was originally isolated from polluted stream samples by Gibson *et al.* 1973. The strain was purchased from DSMZ (DSM No. 6900).

The strain C7.oil.2 was isolated from sediment material that was sampled at a temperature of 18.5°C and a depth of 121 m at a sampling site located at the coordinates 29° 49.998' N 86° 40.002' W in the GoM. C7.oil.2 was one of ten strains⁶ that were isolated from sediments sampled at different GoM sites in October 2012. The strain C7.oil.2 was found to grow on Louisiana sweet crude oil, n-hexadecane, n-tetracosane and phenanthrene. Moreover, it was able to grow on agar as sole carbon and energy source. The strain was identified as *Dietzia* sp. by Davis (2014). During work on the present thesis it was identified more precisely as *Dietzia aurantiaca* using 16S rDNA sequencing. *D. aurantiaca* C7.oil.2 and another strain, were the only two (out of the ten) strains that could be successfully recultivated in our laboratory (Bachelor thesis of José Manuel Jiménez Juárez 2015).

⁶ Kindly provided by Prof. Dr. Wade Jeffrey and Prof. Dr. Joe Lepo from University of West Florida, USA

2.3.2 Bacterial communities from deep-sea sediments

Several deep-sea sediment cores were collected in the GoM close to the blowout site during annual cruises after the DWH oil spill. Material from the top of the sampled sediment cores were used in this study as source of bacterial communities that are capable of aerobic oil degradation. The used sediments⁷ are listed in the following Table 2.4. They had different contents of water. Thus, since different sediments were compared in the experiments, dry weight of the sediments had been determined previously and sediments were diluted with sterile water to adjust them to an equal dry-to-wet weight ratio.

Table 2.4: Deep-sea sediments used in this thesis.

Sedi- ment No.	Sample name (cruise- site)	Depth in core (mm)	Core lati- tude (N)	Core longi- tude (W)	Water depth (m)	Core date	Media	Notes
2	WB-1110- MC-DSH08	0-10	29° 7.255'	87° 51.927'	1143	Dec. 2010	Sediment	Time-series site (Desoto Canyon), USF
3	WB-1110- MC-DSH10	0-10	28° 58.6'	87° 53.4'	1520	Dec. 2010	Sediment	Time-series site (Desoto Canyon), USF
4	WB-1103- BC-DSH10	Surface scrape	28° 58.6'	87° 53.4'	1520	Aug. 2010	Sediment/ Water	Earliest sample, USF
8	WB-0813- MC-DSH10	0-50				Aug. 2013	Sediment	PSU

⁷ Kindly provided by Dr. Patrick Schwing and Prof. Dr. David Hollander from University of South Florida (USF), USA and Prof. Dr. Katherine Freeman and Dr. Sara Lincoln from Pennsylvania State University (PSU), USA

2.4 Liquid and solid culture media

R. qingshengii TUHH-12 and *D. aurantiaca* C7.oil.2 were cultivated in minimal mineral medium II (MMII) consisting of 2.6 g Na_2HPO_4 , 1.33 g KH_2PO_4 , 1 g $(\text{NH}_4)_2\text{SO}_4$ and 0.20 g $\text{MgSO}_4 \times 7 \text{H}_2\text{O}$ dissolved in 1,000 mL of demineralised water. The medium was adjusted to pH 7 and autoclaved. To that, 5 mL of trace element solution and 1 mL of vitamin solution were added. The trace element and vitamin solutions were prepared according to the DSMZ methanogenium medium 141 (DSMZ 2012a). The trace element solution was autoclaved and the vitamin solution was filter sterilised. For plate counting agar plates with Luria Bertani (LB) medium were used.

R. wratislaviensis and *S. yanoikuyae* B1 were cultivated in Brunner mineral medium, which was prepared as described in DSMZ medium 457 (DSMZ 2012b). For plate counting agar plates with LB or R2A medium (DSMZ medium 830, DSMZ 2012c) were used.

Bacterial communities from deep-sea sediments were cultivated in MMII with or without 3% (w/v) NaCl (pH 8). For plate counting LB medium with or without 3% NaCl was used.

All media were sterilised by autoclaving at 121°C for 20 min. To prepare the media HPLC-grade water was used. For solidification 15 g/L of agar was added to the medium prior to autoclaving.

2.5 Storage of bacteria

All strains were kept on mineral medium agar plates. For long time preservation a culture of each strain was stored in cryo-vials (Roti® store, Karl Roth GmbH) at -80°C. Sediments used as inoculum in oil-degradation experiments were stored at -20°C.

2.6 Substrates

As sole source of carbon the mineral media were supplemented with different n-alkanes, aromatics or PAHs. Used model alkanes were n-decane ($\text{C}_{10}\text{H}_{22}$), n-hexadecane ($\text{C}_{16}\text{H}_{34}$) and n-tetracosane ($\text{C}_{24}\text{H}_{50}$). Toluene (C_7H_8) served as a model aromatic oil compound and the bicyclic naphthalene (C_{10}H_8) served as a model PAH. The concentration of the respective hydrocarbon in the medium was adjusted to 1 mM or 3 mM, or to such a concentration that the total carbon mass equaled the carbon mass in the medium adjusted to an n-hexadecane concentration of 1 mM. The liquid hydrocarbons (n-hexadecane and n-decane) were added

directly to the liquid media or plated directly on the solid agar media. Solid hydrocarbons (naphthalene and n-tetracosane) were dissolved in the organic solvents n-hexane or acetone. A certain volume of this stock solution was then added to the culture medium. After evaporation of the organic solvent, the liquid medium and the bacterial inoculum were added. For incubation of agar plates, naphthalene was provided via vapour diffusion. Similarly, toluene was provided via vapour diffusion for both cultivations on liquid and solid media. For the vapour diffusion, an open supply beaker, which contained the substrate, was placed in the reactor or in an air-tight desiccator, in which the bacterial culture was incubated (200 μ L liquid toluene per litre gas volume).

In order to determine the ability of a strain to grow on a non-toxic substrate at high pressure conditions, its growth on α -D-glucose was tested. For that, 1% (w/v) α -D-glucose was added to the culture medium.

In order to investigate the capability of *S. yanoikuyae* B1 to grow on salicylic acid, which is an intermediate of the naphthalene degradation pathway, the culture medium was supplemented with 1.63 mM of salicylic acid.

To investigate the influence of the dispersant Corexit[®] EC9500A on the bacterial growth and hydrocarbon degradation, experiments were set up with Corexit[®] EC9500A added to a culture medium containing either n-hexadecane or naphthalene at a dispersant-to-hydrocarbon ratio of 1:10 (w/w). Furthermore, degradation of Corexit[®] EC9500A as sole source of carbon (0.024 μ L/mL medium) was tested.

In experiments, where bacterial communities from sediments were used as inoculum, the MMII medium was supplemented with 0.1% (v/v) Louisiana sweet crude oil.

2.7 Biodegradation experiments at ambient and high pressure in different reactor systems

As described in the following subsections, in preparation for the high pressure biodegradation experiments different steps had to be carried out dependent on the respective reactor system, hydrocarbon substrate and bacterial inoculum. The following Table 2.5 gives an overview of how these parameters were combined in the experiments carried out in this thesis.

Table 2.5: Summary of all microorganisms, substrates, media and reactors used in this thesis.

Microorganism	Substrate	Medium		Reactor	Probe
		For cultivation and storage	For plate counting		
<i>R. qingshengii</i> TUHH-12	- n-Decane	- MMIII	LB	- 160 mL high pressure reactor with screw-piston mechanism for mechanical pressurisation - 160 mL high pressure reactor + ambient pressure reference reactors - High pressure reactor with screw-piston mechanism for mechanical pressurisation	O ₂ sensors from Ocean Optics GmbH
	- n-Hexadecane - n-Tetracosane - α -D Glucose - n-Hexadecane + Corexit® EC9500A - Corexit® EC9500A	- LB			
<i>E. coli</i>	α -D Glucose	- MMIII - LB	LB	High pressure reactor with screw-piston mechanism for mechanical pressurisation	

Table continued on next page.

Table 2.5 - continued

<i>D. aurantiaca</i> C7.oil.2	- n-Hexadecane - Toluene	MMill	LB	- 160 mL high pressure reactors + ambient pressure reactors - 1 L high pressure reactor	Prototype O ₂ sensor
<i>R. wratislaviensis</i> Tol3	- Toluene - α -D Glucose	Brunner mineral medium	LB	160 mL high pressure reactors + ambient pressure reference reactors	O ₂ sensors from Ocean Optics GmbH
<i>S. yanoikuyae</i> B1	- Naphthalene - Salicylic acid - α -D Glucose - Naphthalene + Corexit® EC9500A - Corexit® EC9500A	Brunner mineral medium	R2A medium	- 160 mL high pressure reactors + ambient pressure reference reactors - High pressure view cell reactor No. 1 - 1 L high pressure reactor	O ₂ sensor Fibox 3 + pCO ₂ mini from PreSens Precision Sensing GmbH
Bacterial communities from sediments	- Louisiana sweet crude oil - Natural gas	MMill with or without 3% (w/v) NaCl	LB with or without 3% (w/v) NaCl	- High pressure view cell reactor No. 1 - High pressure view cell reactor No. 2 - 160 mL high pressure reactors + ambient pressure reference reactors	- O ₂ sensor Fibox 3 + pCO ₂ mini from PreSens Precision Sensing GmbH - VisiSens™ O ₂ and CO ₂ sensors from PreSens - O ₂ sensors from Ocean Optics GmbH

Experiments were repeated as follows. If in an experiment no effect of high pressure on growth and hydrocarbon degradation was found, no further replications were made. If in an experiment an effect of high pressure on growth and hydrocarbon degradation was found, the experiment was replicated at least one more time. In repetitive experiments the initial cell density was adjusted to the same value as in previous experiments (1×10^5 CFU/mL for *R. qingshengii* TUHH-12, 5×10^4 CFU/mL for *R. wratislaviensis* Tol3, 1×10^6 CFU/mL for *S. yanoikuyae* B1, 1×10^7 CFU/mL for *E. coli* and 4×10^6 CFU/mL for *D. aurantiaca* C7.oil.2). However, because of not exactly matching sampling times and slightly differing inoculation cell densities, calculated rates of growth and hydrocarbon degradation varied slightly. For the diagrams in the Results Chapter, the most representative replication was selected.

2.7.1 Experiments in 160 mL high pressure reactors and ambient pressure reference reactors

To ensure sterile conditions in the experiments in 160 mL high pressure reactors and ambient pressure reference reactors, the bacteria were cultivated in autoclavable glass vials, instead of directly in the reactors. The glass vials were covered with aluminium foil. At the beginning of this thesis, one 80 mL vial was put into one reactor. In later experiments, three 10 mL vials were put into one reactor. The latter option allowed replicative sampling under the same conditions.

2.7.1.1 Cultivation of bacterial strains in 160 mL high pressure and ambient pressure reference reactors

In preparation for the experiments in the ten 160 mL high pressure reactors and ten ambient pressure reference reactors, a preculture of the hydrocarbon-degrading strain growing with the hydrocarbon was set up one to four days prior to the experiment. The preculture was shaken at 110 rpm and incubated at room temperature (RT).

For cultivation of the bacterial strains in the reactors, 20 mL MMII was filled in 80 mL glass vials or 5 mL of the medium was filled in 10 mL vials. The medium was supplemented with a single hydrocarbon as carbon source and inoculated with 10% (v/v) of a grown preculture of the respective bacterial strain. In case of a blank experiment no inoculum was added. An initial 1 mL sample was taken for analysis of cell growth (point in time 0 h). After

placing the vials inside the 160 mL high pressure reactors, these were closed and nitrogen gas was introduced to pressurise up to 150 bar (corresponding to a depth of 1,500 m at the DWH well). Since it was not feasible to adjust the pressure in all ten 160 mL high pressure reactors to exactly the same value, always the mean value of pressures in all reactors of one experiment is given in the Results Chapter and in the Discussion Chapter. To avoid bursting of the aluminium foils while pressurisation, they were perforated 5 times with a cannula prior to closing the 160 mL high pressure reactors. As control, ten ambient pressure reference reactors were run simultaneously at 1 bar. The cultures in the reactors were incubated at RT or at 4°C and mixed with magnetic stirrers at 200 rpm.

One 160 mL high pressure reactor and one ambient pressure reference reactor was connected to an oxygen sensor from Ocean Optics GmbH (Ostfildern, Germany) to continuously monitor the oxygen partial pressure. All reactors were started simultaneously. The reactors were opened successively and for each point in a diagram one reactor was sacrificed. The last reactor was incubated until a constant level of oxygen was observed.

Before reactors containing n-hexadecane were depressurised and opened, they were cooled at 4°C for 5 h to minimise the evaporation of the substrate. After opening of a reactor the vial containing the culture was put into an ultrasonic bath, to disrupt cell clumps. Then, a 1 mL sample (from the vigorously mixed culture) was taken for analysis of bacterial growth. To determine the substrate concentration, the non-metabolised hydrocarbon was extracted from the remaining medium with n-hexane and was then analysed via gas chromatography-mass spectrometry.

2.7.1.2 Cultivation of bacterial communities from GoM deep-sea sediments in 160 mL high pressure and ambient pressure reference reactors

For incubation of bacterial communities from deep-sea sediments with crude oil in the 160 mL high pressure reactors and ambient pressure reference reactors, 50 mL of MMII was filled into the 80 mL vials and supplemented with 50 µL of Louisiana sweet crude oil. The culture was inoculated with 1 mL of diluted sediment No. 8 (WB-0813-MC-DSH10). In order to compare the incubation of this sediment with the incubation of sediment No. 4, sediment No. 8 was diluted with sterile water to adjust it to an equal weight ratio of dry to wet sediment as in 1 mL of sediment No. 4. The vials were placed into the 160 mL high pressure

reactors and these were pressurised to 150 bar and incubated at RT as described above. As control, ambient pressure reference reactors were run simultaneously at 1 bar.

2.7.2 Cultivation of bacterial strains in the 1 L high pressure reactor at ambient and high pressure

In preparation of an experiment in the 1 L high pressure reactor, all non-autoclavable parts of the reactor, which came in contact with bacterial culture, were incubated in 70% (v/v) ethanol for about 1 h, to ensure sterile conditions. Afterwards, they were dried for 1 h.

A sterile 250 mL glass bottle, capped with aluminium foil, was filled with 200 mL mineral medium, supplemented with 1.77 mM naphthalene or 1 mM n-hexadecane and inoculated with a grown preculture of *S. yanoikuyae* B1 or *D. aurantiaca* C7.oil.2, constituting 10% (v/v) of the total volume. The bottle was placed inside the reactor and the aluminium foil was perforated. The reactor was closed, pressurised to 150 bar with nitrogen gas and incubated at RT and 200 rpm. As control the 1 L high pressure reactor was run subsequently at 1 bar.

To monitor the reaction, the decrease of oxygen inside the reactor was measured online by connecting it to the prototype sensor constructed by companies Eurotechnica GmbH (Bargteheide, Germany) and PreSens Precision Sensing GmbH (Regensburg, Germany) (see Chapter 3.2.4).

Samples for analysis of cell growth were taken from the culture medium prior to and after the experiment. Additionally, during the course of an experiment, samples were taken through a dedicated valve. After subsampling, the reactor was repressurised with nitrogen gas.

2.7.3 Cultivation of bacterial strains in the high pressure reactor with screw-piston mechanism at elevated oxygen partial pressure

No sterile glass vial could be used in the high pressure reactor with screw-piston mechanism. Thus, in preparation for the experiment, the reactor was cleaned and autoclaved or incubated with 70% (v/v) ethanol for 1 h.

After evaporation of the ethanol, 10 mL of MMII or LB medium was inoculated with 10% (v/v) of a grown preculture of *R. qingshengii* TUHH-12 or *E. coli*. A sample was taken to analyse the initial cell density. The culture was filled into the reactor. For cultivation of *R.*

qingshengii TUHH-12, MMII was supplemented with 1 mM n-hexadecane or complex LB medium was used. For cultivation of *E. coli*, MMII was supplemented with 1% (w/v) α -D glucose or complex LB medium was used. The reactor was pressurised manually to different pressures up to 131 bar by screwing the piston into the reactor. Thus, certain oxygen partial pressures were adjusted. Taking subsamples was possible through a valve during incubation. Pressure losses were compensated via screwing the piston. The culture was incubated for 3.5 h at 37°C (*E. coli*) or 24 h at RT (*R. qingshengii* TUHH-12) on a rocking table. To intensify the mixing, a sterilised glass marble was added. After incubation, the reactor was depressurised and the end sample for analysis of growth was taken.

2.7.4 Experiments in view cell reactor No. 1 at ambient and high pressure

No sterile glass vial could be used in the high pressure view cell reactor No. 1. Thus, in preparation for an experiment at high pressure, the high pressure view cell reactor and all connecting parts needed to be cleaned and disinfected with 70% (v/v) ethanol. The reactor was rinsed with HPLC-grade H₂O and 70% (v/v) ethanol with a pump (Watson-Marlow Limited, Falmouth, Cornwall, UK). Afterwards, the reactor was incubated with 70% (v/v) ethanol for 1 h. Finally, the remaining ethanol was left to evaporate.

2.7.4.1 Cultivation of a bacterial strain in view cell reactor No. 1 at ambient and high pressure

For an experiment in the view cell reactor No. 1, a certain volume of a stock solution, consisting of naphthalene dissolved in acetone, was dropped on a sterile cover slip (20 x 20 mm), resulting in 1.77 mM naphthalene. After evaporation of the solvent, the cover slip was placed into the reactor and the windows were closed. The reactor was filled with 4.5 mL mineral medium and inoculated with 10% (v/v) of a grown preculture of *S. yanoikuyae* B1. An initial sample for analysis of cell growth was taken. Finally, after all valves and screwing connections were closed, the reactor was either left at ambient pressure or pressurised to 150 bar with nitrogen gas.

Since the decrease of oxygen and increase of carbon dioxide corresponds to the degradation of hydrocarbons, the O₂ and CO₂ partial pressures in the reactor were

measured online using the Fibox 3 and pCO₂ mini systems (PreSens Precision Sensing GmbH, Regensburg, Germany).

Samples were taken through a valve during incubation. Pressure losses were compensated via refilling the reactor with fresh medium using a spindle pump or via repressurisation with nitrogen gas. After incubation for at least 143 h at RT, the reactor was depressurised and the end sample for analysis of growth was taken.

2.7.4.2 Cultivation of bacterial communities from GoM deep-sea sediments in view cell reactor No. 1 at ambient and high pressure

For oil-degradation experiments with bacterial communities from different deep-sea sediments, the view cell reactor No. 1 was operated as described above, but 12.5 µL crude oil and an equivalent of 12.5 mg dry sediment were added to a small, sterilised glass container. This container was placed into the reactor, the windows were closed and the reactor was filled with 12.5 mL MMII or MMII + 3% NaCl. The reactor was either left at ambient pressure or pressurised. The reactor was incubated at 5°C or RT. The reactor was opened after oxygen and carbon dioxide reached a constant level.

2.7.5 Cultivation of bacterial communities from GoM deep-sea sediments in view cell reactor No. 2 at ambient and high pressure

No sterile glass vial could be used in the high pressure view cell reactor No. 2. Thus, to ensure sterile culture conditions, prior to an experiment the high pressure view cell reactor was cleaned and disinfected with 70% (v/v) ethanol.

After evaporation of the ethanol, half of the reactor was filled with 50 mL of MMII. Then, 50 µL of Louisiana sweet crude oil or 180 mL of natural gas (a hydrocarbon mixture consisting primarily of methane) was added. As inoculum 1 ml slurry of sediment No. 4 (WB1103-BC-DSH10) was used. For a blank experiment no inoculum was added. An initial sample was taken to count the cell density. To avoid oxygen limitations, 2.8 bar of compressed air was filled into the reactor. The reactor was either additionally pressurised with nitrogen gas to 150 bar or it was left at ambient pressure. The incubation was carried out at RT.

The O₂ and CO₂ concentrations in the reactor were measured online using the chemical-optical sensor system VisiSens™ (PreSens Precision Sensing GmbH, Regensburg, Germany).

The incubation was terminated when a constant level of oxygen or carbon dioxide was observed. Then, the reactor was depressurised and a final sample was taken.

2.8 Analysis of bacterial growth and substrate degradation

After incubation in the high pressure reactors, samples were taken from the culture medium. They were analysed for bacterial growth (see Chapters 2.8.1, 2.8.2 and 2.8.3), substrate degradation (see Chapters 2.8.4, 2.8.5, 2.8.6, 2.8.7 and 2.8.8), oxygen consumption and carbon dioxide production (see Chapter 2.8.9).

2.8.1 Determination of cell density with the Neubauer chamber

Samples from the culture medium were taken prior to, during and after an experiment. The cell density of a sample was determined by counting living as well as dead cells using a light microscope at 400x magnification and a Neubauer counting chamber (depth = 0.02 mm). This chamber has a grid of lines forming 16 large squares. The volume of a large square is 8×10^{-7} mL. Each large square is subdivided into 16 small squares (area of a small square = 0.0025 mm^2). For each sample, cells in four large squares were counted and the average count was calculated. The number of counted cells per one large square was 20 to 200 cells. For cultures with higher density, the cell suspension needed to be diluted with saline solution (0.9% [w/v] NaCl). Using following formula the cell density was determined:

$$\text{cell density (cells/mL)} = \frac{C_{av}}{DF \times 8 \times 10^{-7} \text{ mL}} \quad (2.1)$$

Here C_{av} is the average number of cells counted in four large squares and DF is the dilution factor of the sample.

In addition to the determination of the cell density by use of the Neubauer chamber, each sample was also analysed using other methods, which are described in the following subsections.

2.8.2 Determination of cell density by plate counting

The cell density in most diagrams of the Results Chapter is represented in CFU/mL. To determine colony forming units (CFU), samples of a single strain culture were serially diluted in saline solution (0.9% [w/v] NaCl) and 5 μ L of the dilution were dropped on complex media agar plates in triplicate. Samples from incubations of sediments were ultrasonicated in a water bath to detach cells from sediments. Subsequently, 100 μ L of a dilution was spread on an agar plate. After incubation at RT for 1 to 4 days the colonies were counted. Plate counting is a method for determination of the density of viable cells. However, it has to be taken into account that one CFU can originate from one or several cells. The cell density was calculated according to following equation.

$$\text{cell density (CFU/mL)} = \frac{CFU_{av} \times 1,000}{DF \times 5} \quad (2.2)$$

Here CFU_{av} is the average of the colony forming units counted in three 5 μ L drops and DF is the dilution factor of the sample.

The growth rate of a model strain on a certain substrate was calculated from the exponential growth phase using following equation:

$$\mu (h^{-1}) = \frac{\log x_2 - \log x_1}{\log e \times (t_2 - t_1)} \quad (2.3)$$

Here μ is the growth rate and x_1 and x_2 are the measured cell densities at points in time t_1 and t_2 .

2.8.3 Determination of optical density

After determinations of cell density, the optical density (OD₆₀₀) of the samples was analysed by spectrophotometry at a wavelength of 600 nm.

2.8.4 Determination of pH value

The pH value of the samples was measured to monitor changes during growth. The pH value of the medium is defined by dissolved acids and bases, and their corresponding salts. If, for instance, salts are consumed or acids and CO₂ are produced from hydrocarbons, the decreasing pH value reveals to which extent hydrocarbons were degraded.

2.8.5 Analysis of hydrocarbons by gas chromatography-mass spectrometry

After the cultivation in the reactor and subsequent sampling for determination of cell growth as described in the previous subsections, the concentration of the not-metabolised hydrocarbon was analysed by gas chromatography-mass spectrometry (GC-MS). Thus, the degree of biodegradation was quantified. For this, a Hewlett-Packard 5890 Series II gas chromatograph (GC), equipped with an Agilent HP-5MS column of 30 m length and 0.25 mm internal diameter, was used. The GC was coupled to a Hewlett-Packard 5971A mass selective detector.

The complete remaining culture medium was extracted with 5 mL of n-hexane. An internal standard (0.2 mM) was added to the solvent. For analysis of n-hexadecane as well as n-tetracosane, n-dodecane was added as internal standard. For analysis of naphthalene and n-decane, n-hexadecane was added as internal standard. An aliquot from the upper, apolar phase, containing the hydrocarbon, was injected into the GC-MS. The split ratio was 28:1 and helium served as carrier gas.

For quantification of n-hexadecane, n-decane and naphthalene, the injector temperature had a gradient from 80°C to 200°C at a rate of 0.5°C/sec and a final 3.5 min hold at 200°C. The oven temperature was increased from initially 80°C to a final temperature of 200°C at a rate of 15°C/min and was finally held for 1 min at 200°C. For quantification of n-tetracosane, the injector temperature had a gradient from 150°C to 280°C at a rate of 0.5°C/sec and a final hold at 280°C for 3.5 min. The oven temperature was increased from initially 150°C to 280°C at a rate of 15°C/min with a final 2 min hold at 280°C.

The mass spectrometer was set to full scan mode from 50 to 650 amu. The MS transfer line temperature was kept at 320°C and the ion source temperature at 180°C.

The hydrocarbon concentration decrease rate was calculated from the exponential phase of the degradation curve according to following equation:

$$DR \text{ (mM/h)} = \frac{x_1 - x_2}{t_2 - t_1} \quad (2.4)$$

Here DR is the decrease rate of the hydrocarbon concentration. x_1 and x_2 are the measured hydrocarbon concentrations at points in time t_1 and t_2 .

2.8.6 Analysis of α -D-glucose concentration

To measure the concentration of non-metabolised α -D-glucose in samples, the blood glucose monitoring system Breeze[®] 2 (Bayer AG, Leverkusen, Germany) was used according to the instruction manual.

2.8.7 Determination of salicylic acid concentration

To measure the concentration of remaining, not metabolised salicylic acid, samples from the culture medium were centrifuged at 13,000 rpm for 5 min. The supernatant was diluted with Brunner mineral medium (1:10). The absorbance was measured at 296 nm in a spectrophotometer, since at this wavelength salicylic acid has an absorbance maximum. By using a standard curve, the salicylic acid concentration in the samples was determined.

2.8.8 Detection of hydroxylated intermediates of naphthalene conversion

2.8.8.1 Colourimetric determination of hydroxylated intermediates of naphthalene conversion

The colourimetric method described by Arnow (1937) was used to detect hydroxylated intermediates in the conversion of naphthalene. The samples were centrifuged for 3 min at 13,000 rpm and a 200 μ L aliquot of the supernatant was supplemented with 200 μ L of the following reagents in the given order: 0.5 N HCl, nitrite/molybdate reagent and 1 N NaOH. After addition of each reagent, the solution was mixed well. For the nitrite/molybdate reagent, 1 g of NaNO₂ and 1.375 g of NaMoO₄ x 2 H₂O was dissolved in 10 mL H₂O. After acidification with HCl and addition of nitrite/molybdate reagent, a yellow colour appeared. After addition of NaOH, a red colour appeared, which pointed to presence of dihydroxylated compounds such as catechol or 1,2-dihydroxynaphthalene. If monohydroxylated compounds, such as salicylate or monohydroxynaphthalene, were present, the solution

remained yellow. When the solution was measured spectrophotometrically, a peak occurred at 512 nm in the spectrogram in the presence of catechol or 1,2-dihydroxynaphthalene.

2.8.8.2 Determination of naphthalene conversion intermediates by gas chromatography-mass spectrometry

For an analysis of the naphthalene conversion intermediates, a bigger amount of culture medium was needed to extract the hydrocarbons. Therefore, 200 mL of a *S. yanoikuyae* B1 culture, incubated with 1.77 mM naphthalene at high pressure in the 1 L high pressure reactor, was prepared as described in Chapter 2.7.2. After 9 days, the reactor was depressurised, opened and a 1 mL sample was taken for analysis of cell growth.

Afterwards, the remaining culture medium was treated by acid-base extraction as follows. At neutral pH-value, 66 mL dichloromethane (DCM) was added to the culture medium in a separating funnel. After shaking of the funnel, the two phases separated and the bottom DCM extract was collected. The procedure was repeated with 44 mL and then 22 mL of DCM. Afterwards, the pH of the medium was changed to 2 by adding 1 M HCl and the extraction was repeated with 66 mL, 44 mL and 22 mL of DCM. Finally, the pH value was changed to 10 with 1 M NaOH and the culture medium was extracted once with 66 mL of DCM. All extracts were combined and the solvent amount was reduced to almost dryness in a solvent evaporator (BÜCHI Labortechnik GmbH, Essen, Germany) at 100 rpm, 25°C water bath temperature and 330 to 500 mbar vacuum.

For analysis by GC-MS, the extract was sent to project partners Prof. Dr. Thomas Oldenburg and Dr. Jagos Radovic from University of Calgary, Canada. From the extract 10 µL were diluted with DCM to a resulting volume of 500 µL and of this 1 µL was injected in the GC-MS. The split ratio was 28:1 and Helium served as carrier gas with a constant flow of 1.1 mL/min. The initial oven temperature was kept at 40°C for 5 min, was then increased at a rate of 4°C/min to 325°C and was finally held for 15 min. The mass spectrometer was conducted in full scan mode from 50 to 550 amu and electron ionisation was at 70 eV. The interface and transfer line temperature was kept at 300°C and the ion source temperature at 230°C. A solvent delay of 5 min was adjusted. Using a standard solution with known concentration of deuterated naphthalene (D8-N) the hydrocarbon concentrations were quantified relative to it.

2.8.9 Determination of oxygen consumption and carbon dioxide production

Different systems for measurement of oxygen and carbon dioxide were used and evaluated. They are described in detail in Chapter 3.2. The oxygen consumption rate and carbon dioxide production rate were calculated from the exponential phases of the oxygen or carbon dioxide curves using following formulas:

$$RO_2 = \frac{x_2 - x_1}{t_2 - t_1} \quad (2.5)$$

Here RO_2 (in % O_2 /h or mM/h) is the oxygen consumption rate. x_1 and x_2 are the measured oxygen concentrations/partial pressures at points in time t_1 and t_2 .

$$RCO_2 = \frac{x_2 - x_1}{t_2 - t_1} \quad (2.6)$$

Here RCO_2 (in % CO_2 /h or mM/h) is the carbon dioxide production rate. x_1 and x_2 are the measured carbon dioxide concentrations/partial pressures at points in time t_1 and t_2 .

2.9 Sequencing of 16S rRNA genes

To determine the identity of the Tol3 strain and to verify the identity of the C7.oil.2 strain, the 16S rDNA was amplified, purified and sequenced.

2.9.1 Amplification of DNA by Colony Polymerase Chain Reaction

To amplify the DNA by Colony Polymerase Chain Reaction (Colony PCR), the peqlab Taq DNA Polymerase Kit (PEQLAB Biotechnology GmbH, Erlangen, Germany) was used. Per PCR reaction, 10 μ L of 10x reaction buffer S, 6 μ L of 25 mM $MgCl_2$, 2 μ L of 10 mM dNTP Mix, 0.5 μ L of 100 pmol/ μ L 341F primer, 0.5 μ L of 100 pmol/ μ L 907R primer, 0.6 μ L of 250 u/ μ L Taq polymerase, 20 μ L of Enhancer Solution P and 60.4 μ L of H_2O were mixed with a few cells of a single colony in a PCR tube. The sequences of used primers, specific for 16S rDNA, were 341f: 5'-CCT ACG GGA GGC AGC AG-3' and 907r: 5'-CCG TCA ATT CMT TTG AGT TT-3'.

The cycling program consisted of an initial denaturation step at 94°C for 2 min, followed by 30 cycles of 94°C for 30 sec (denaturation), 52°C for 45 sec (elongation) and 72°C for 1.5

min (annealing). Finally, an elongation step at 72°C for 9 min was conducted. The program ended with holding the temperature at 4°C.

2.9.2 Agarose gel electrophoresis

To confirm the success of the PCR, the PCR products were analysed by agarose gel electrophoresis. For that, 10 µL of a PCR product was mixed with 2 µL of 6x loading dye and loaded on a 1% (w/v) agarose gel. As reference, a 1 kb DNA ladder was loaded on the gel. The gel was run in 1x TAE buffer at 90 V. The gel was stained with SYBR® Green, which was diluted with 1x TAE buffer (1 µL/1 mL), and subsequently analysed under UV light. The expected fragments had a length of about 500 bp.

2.9.3 Purification and determination of DNA concentration of products from Polymerase Chain Reaction

The PCR products were purified using the Gene JET PCR Purification Kit #K0702 from Thermo Fisher Scientific Germany BV & Co. KG (Braunschweig, Germany). The DNA concentration was analysed using the Tray Cell from Hellma GmbH & Co. KG (Müllheim, Germany) at 260 nm.

2.9.4 Sequencing

The samples were sent to Seqlab - Sequence Laboratories Göttingen GmbH (Göttingen, Germany) to be sequenced. The obtained nucleotide sequences were entered in EzTaxon database (<http://www.ezbiocloud.net/eztaxon>) to align the sequences and to identify the bacterial strains.

2.10 Community analysis via Denaturing Gradient Gel Electrophoresis

Denaturing Gradient Gel Electrophoresis (DGGE) is a genetic fingerprinting method to separate DNA fragments of equal length and different sequences from each other. This technique can be used to compare the diversity of microbial communities and to monitor population dynamics (Muyzer *et al.* 1993, Muyzer 1999).

By PCR of nucleic acid from environmental samples, DNA-fragments of the same length but different DNA sequences can be generated, which represent diverse dominant microbial

species. By DGGE, these DNA-fragments can be separated in a polyacrylamide gel with a gradient of the DNA-denaturing agents urea and formamide. Due to the species-specific sequence differences, the fragments denature at different denaturant concentrations and stop migrating in the gel, resulting in a specific band pattern. Theoretically, each band represents a different strain, which is present in the microbial community (Muyzer *et al.* 1993, Muyzer 1999).

During the work on this thesis, the DGGE was carried out at the Leibniz-Institute of Freshwater Ecology and Inland Fisheries (IGB) in Neuglobsow, Department Experimental Limnology, Stechlin, Germany with the friendly assistance of Prof. Dr. Hans-Peter Grossart. In preparation for the DGGE, samples from the culture medium, which contained bacterial communities from sediments, needed to be filtrated to fractionate the bacteria. Subsequently, DNA was extracted and amplified.

2.10.1 Filtration

At first, a 5.0 µm polycarbonate filter was used, to separate the particle-attached bacteria. Subsequently, the flow-through was filtrated with a 0.2 µm polycarbonate filter, to trap the bacteria that were unattached. The filters were cut into small pieces and put into Eppendorf tubes.

2.10.2 DNA extraction

The DNA extraction was performed according to the protocol, described by Nercessian *et al.* (2005), with some slight modifications. The filters, 0.5 g of 0.1 mm zirconia-silica beads (BioSpec Products Inc., Bartlesville, Oklahoma, USA) and 0.5 g of 0.7 mm zirconia-silica beads were suspended in 750 µL of extraction buffer. The extraction buffer was a mixture of equal volumes of 10% (w/v) CTAB (cetyltrimethylammonium bromide) in 1.6 M NaCl and 0.2 M phosphate buffer, pH 8. Then, 75 µL of 10% (w/v) sodium dodecyl sulfate, 75 µL of 10% (w/v) lauroyl sarcosine and 750 µL phenol-chloroform-isoamyl alcohol (25:24:1) were added. The mixture was vortexed at 2850 rpm for 10 min and then centrifuged at 16,000x *g* for 10 min at 4°C. The upper, aqueous phase was mixed with an equal volume of phenol-chloroform-isoamyl alcohol and centrifuged at 16,000x *g* for 10 min at 4°C. Two volumes of PEG/NaCl, which is a mixture of 1.6 M NaCl and 30% (w/v) PEG 6000 (polyethylenglycol 6000), were

added and nucleic acids were precipitated for 2 h at RT. After centrifugation at 17,000x *g* for 75 to 90 min at 4°C, the pellet was washed with 1 mL cold 75% (v/v) ethanol and again centrifuged at 17,000x *g* at 4°C for 10 min. The pellet was dried and resuspended in 20 µL of sterile, nuclease-free water.

The concentration of the extracted DNA was determined using the NanoDrop™ 2000c Spectrophotometer from Thermo Fisher Scientific Germany BV & Co. KG (Braunschweig, Germany) and the DNA was diluted to 20 ng/µL.

2.10.3 Amplification of DNA by PCR

The 16S rRNA gene was amplified. Per PCR reaction, 5 µL of 10x PCR buffer, 3 µL of 50 mM MgCl₂, 5 µL of 2.5 mM dNTP Mix, 0.5 µL of 20 pmol/µL 341f-GC primer, 0.5 µL of 20 pmol/µL 803r primer, 2 µL of 30 mg/mL BSA (bovine serum albumin), 31.5 µL of H₂O, 2 µL of 20 ng/µL DNA and 0.5 µL of 1 u/µL Taq polymerase were mixed in a PCR tube. The sequences of the used primers, specific for 16S rDNA, were 341f-GC: 5'-CGC CCG CCG CGC CCC GCG CCC GTC CCG CCG CCC CCG CCC GCC TAC GGG AGG CAG CAG-3' and 803r: 5'-CTA CCA GGG TAT CTA ATC C-3'.

The cycling program consisted of an initial denaturation step at 95°C for 3 min, followed by 30 cycles of 95°C for 1 min (denaturation), 54°C for 1 min (elongation) and 72°C for 2 min (annealing). Finally, an elongation step at 72°C for 10 min was conducted. The program ended with holding the temperature at 4°C.

The products of the PCR were verified via agarose gel electrophoresis. Of each amplification, 5 µL DNA were mixed with 1 µL 6x loading dye and loaded on a 1.5% (w/v) agarose gel. The gel was run and stained according to Chapter 2.9.2.

2.10.4 Denaturing Gradient Gel Electrophoresis

An acrylamide/bisacrylamide gel with a denaturant gradient was prepared. To catalyse the polymerisation of the acrylamide solutions into gel matrices, APS (ammonium persulfate) and TEMED (tetramethylethylenediamine) were added to the stock solutions immediately before pouring the gel. With help of a gradient mixer and a pump, the 7% acrylamide/bisacrylamide stock solutions with 40 and 65% urea/formamide were poured into the glass plate assembly. After polymerisation, a 0% denaturant cap gel was poured on

top of the gradient gel with a comb to create the sample wells. From the PCR-product, 20–25 μL were mixed with 6x loading dye (5:1) and loaded on the gel with a Hamilton syringe. The gel was run in 1x TAE buffer at 100 V and 60°C for 18–22 h. The gel was stained with SYBR® Green, which was diluted with 1x TAE buffer (1 $\mu\text{L}/1\text{ mL}$), and subsequently analysed under UV light. Bands could be cut out from the gel, reamplified and sequenced.

3 Results

With different high pressure reactors, the degradation of various hydrocarbons by model strains and the degradation of crude oil and natural gas by deep-sea communities was investigated under high pressure conditions. An overview of all experiments, which were carried out in this thesis, can be found in Table A.1 in the Appendix.

3.1 Development, construction and setup of high pressure equipment

During work on this thesis, different reactor systems were used for high pressure biodegradation experiments. In the following subsections, their development, construction and setup are described, and their advantages and disadvantages are evaluated.

3.1.1 The 160 mL high pressure reactors and ambient pressure reference reactors

The first 160 mL high pressure reactor, which was used to study high pressure biodegradation of oil components at the Institute of Technical Biocatalysis, was developed by and kindly lent from the former Institute of Ocean Engineering of the TUHH (now Institute of Product Development and Mechanical Engineering Design) in cooperation with Technik Service Andreas Meyer (Lindau, Germany). This reactor was made of a stainless steel cylinder, capped with bronze lids. The reactor was mechanically pressurised by a piston, which was screwed into the reactor. The reactor had a volume of 160 mL. For taking subsamples over the course of the incubation, a needle valve was installed. Subsampling at high pressure through the needle valve resulted in a pressure loss, which was readjusted mechanically by screwing the piston into the reactor. This reactor, which was originally designed for transport of liquids under high pressure, was adapted for biological experiments. A connected manometer indicated the pressure (Figure 3.1). The culture inside was mixed by a steel ball in the reactor, which was moved by rocking the whole reactor horizontally on a rocking table. To minimise the risk of contaminations, the system was autoclaved apart from heat-sensitive parts such as gaskets and the manometer.

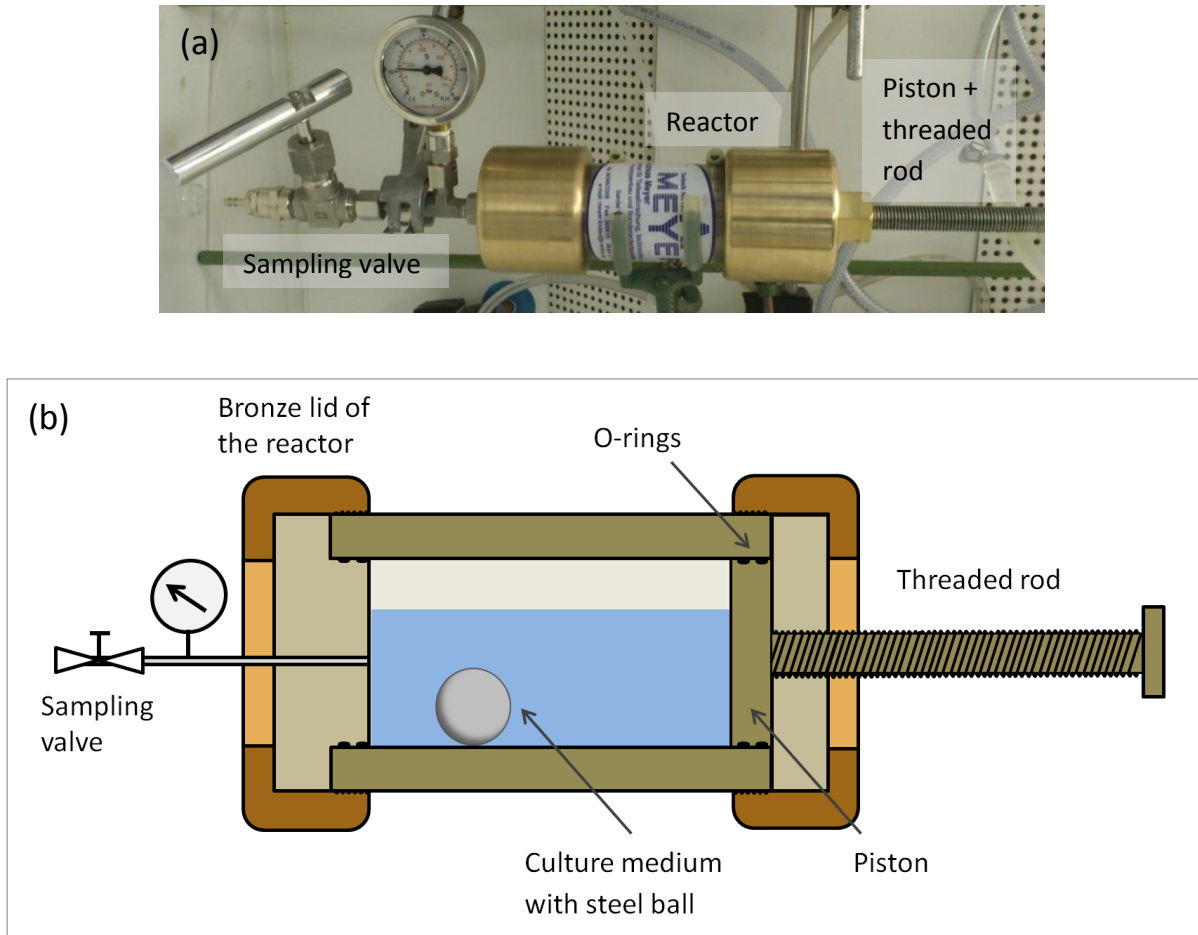


Figure 3.1: (a) The 160 mL high pressure reactor with mechanical pressure build-up via a screw-piston mechanism. (b) Construction scheme.

In early experiments, the reactor was filled completely with mineral medium, inoculated with 10% (v/v) *R. qingshengii* TUHH-12 preculture and supplemented with 1 mM n-hexadecane. The reactor was incubated at RT and 1 bar. No growth was observed in comparison to growth of a control culture in an Erlenmeyer flask (Figure 3.2 a and c). This can be explained by a lack of dissolved oxygen in the medium in the reactor, which is needed by aerobic bacteria to degrade n-hexadecane. In addition, mixing the culture with a rocking steel ball was not sufficient, as n-hexadecane was not mixed efficiently and stayed only on the surface of the medium.

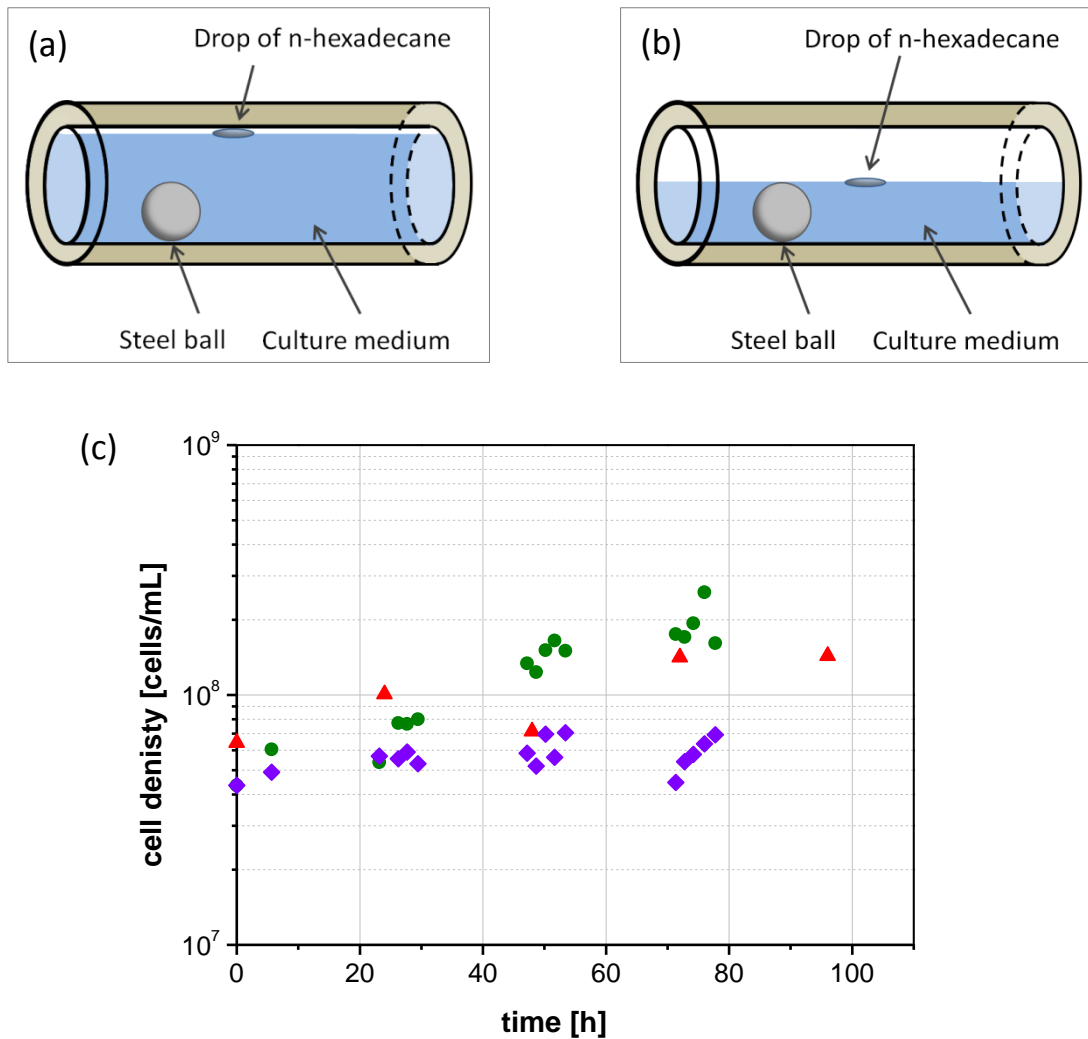


Figure 3.2: Scheme of (a) a completely filled reactor and (b) a half-filled reactor. (c) Cell density (cells/mL) of *R. qingshengii* TUHH-12 growing with n-hexadecane at 1 bar and RT: in an Erlenmeyer flask (●), in a completely filled reactor (◆) and in a half-filled reactor (▲) (Bachelor thesis of Katharina Hauf 2012).

In the subsequent experiment, the reactor was filled half with culture medium, inoculated with *R. qingshengii* TUHH-12, and half with air (Figure 3.2 b and c) and incubated under the same conditions as in the previous experiment. Cell growth was observed resulting from a better supply with oxygen. In addition, the steel ball, now moving in a smaller culture volume, could do a better mixing of the culture. Thus, a better distribution and dissolution of n-hexadecane and oxygen in the medium was ensured. This result emphasises the importance of a sufficient air supply for the degradation of hydrocarbons by aerobic bacteria.

The next step was to test the bacterial growth at high pressure. Thus, the reactor was filled half with culture medium, inoculated with *R. qingshengii* TUHH-12, and half with air. The reactor was pressurised mechanically to 150 bar by screwing the piston. No cell growth was observed. This result can be explained by an increase of the oxygen partial pressure above the limits tolerated by bacteria due to the mechanical pressurisation (see also Chapter 3.1.3).

This 160 mL high pressure reactor with mechanical pressurisation had another disadvantage. Oil as well as oil components are nearly insoluble in water, forming an immiscible two-phase system. Therefore, no representative, homogeneous subsamples could be taken through the needle valve to measure the substrate degradation.

To optimise the 160 mL high pressure reactor for biological experiments, several modifications were carried out. Firstly, a quick lock connection was installed, which allows pressurisation with nitrogen gas up to a maximal pressure limit of 400 bar. This pressurisation system, on the one hand, required less muscle power compared to the system with a screw-piston mechanism. On the other hand, by introducing the inert gas nitrogen, the oxygen and carbon dioxide partial pressures were kept constant and equivalent to the partial pressures of the gases at ambient atmosphere. Thus, a toxic increase of these gases in the reactor was avoided. Secondly, since oil components are nearly insoluble in water and stirring rates affect biodegradation, efficient mixing was necessary for microbial degradation. Therefore, the reactor was modified to be able to stand vertically on a magnetic stirrer and the culture was mixed at defined rates with a stirring bar. Thirdly, to ensure sterile cultivation conditions, 80 mL glass vials, which fit into the reactor and can be autoclaved, were manufactured. Alternatively, the reactor was equipped with three autoclavable 10 mL glass vials for generating samples in triplicate. Usage of such glass vials was very convenient and time-saving compared to cleaning and autoclaving the whole reactor. Finally, to circumvent the above-described problems with subsampling for analysis of the hydrocarbon concentration, nine additional 160 mL high pressure reactors were built by Technik Service Andreas Meyer (Lindau, Germany) (Figure 3.3 a). In an experiment, these ten 160 mL high pressure reactors were started at the same time, were run in parallel and were depressurised one by one at different times. Thus, for each point in a diagram one reactor was sacrificed and the culture medium was analysed. Besides, operating a set of ten reactors in parallel avoided subsampling at high pressure and de-/repressurisation cycles.

Moreover, this sampling method avoided the problem of valves that were blocked and damaged by sediments, as it was experienced in the high pressure view cell reactors (see Chapters 3.1.4 and 3.1.5).

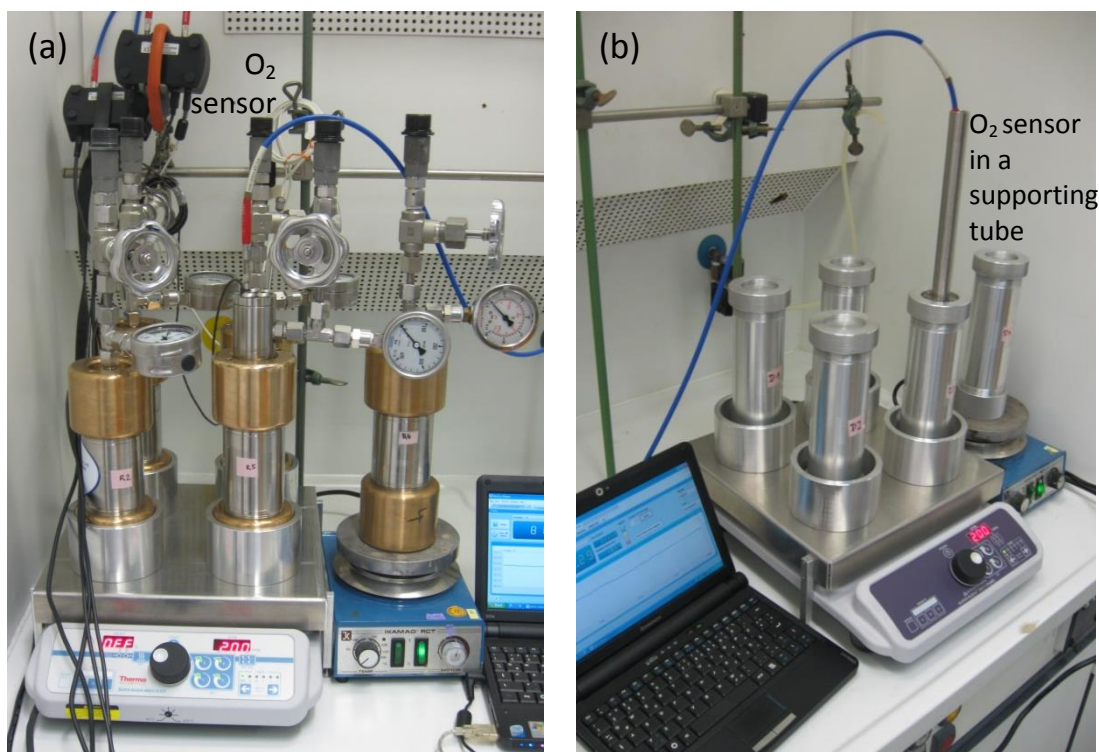


Figure 3.3: (a) The 160 mL high pressure reactors and (b) the ambient pressure reference reactors on magnetic stirrers. One reactor was equipped with an oxygen sensor respectively.

In addition, ten ambient pressure reference reactors were built by the workshop of the TUHH (Figure 3.3 b). They were made from aluminium and had the same geometry as the 160 mL high pressure reactors. They were used for simultaneous control biodegradation experiments at atmospheric pressure. For one point in a diagram, one 160 mL high pressure reactor and one ambient pressure reference reactor was opened. Within the set of ten 160 mL high pressure reactors and ten ambient pressure reference reactors, one reactor of each type was equipped with an oxygen sensor from Ocean Optics GmbH (Ostfildern, Germany), as described in Chapter 3.2.1 (Figure 3.4). This approach of parallel incubation in several 160 mL high pressure and ambient pressure reference reactors was very effective but time- and resource-intensive.

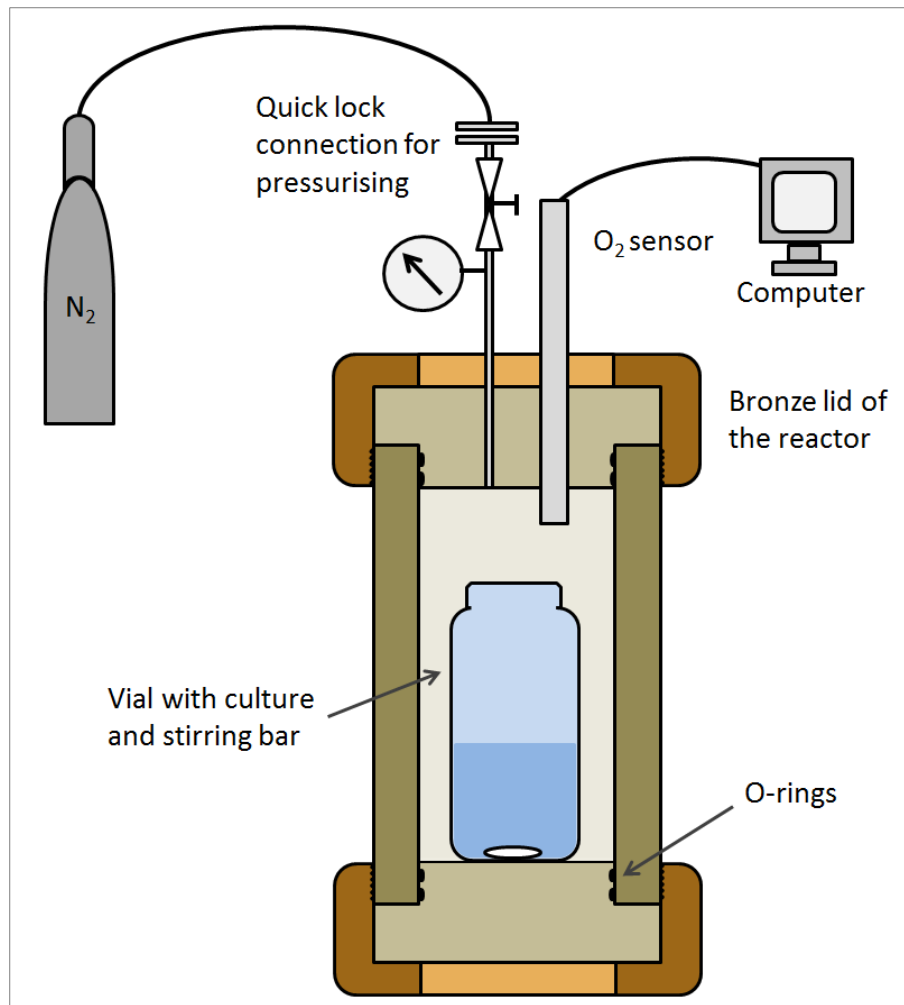


Figure 3.4: Construction scheme of a 160 mL high pressure reactor. Only one out of ten 160 mL high pressure reactors was equipped with an oxygen sensor from Ocean Optics GmbH.

3.1.2 The 1 L high pressure reactor

A high pressure reactor with a larger volume was built by Technik Service Andreas Meyer (Lindau, Germany) and tested in biodegradation experiments at high pressure. The design was similar to the smaller 160 mL high pressure reactors, but it had a volume of 1 L (Figure 3.5 a). Additionally, the lid had two connections: the first for installation of an oxygen prototype sensor (described in Chapter 3.2.4) and the second for introducing nitrogen gas to pressurise up to a maximum pressure of 300 bar.

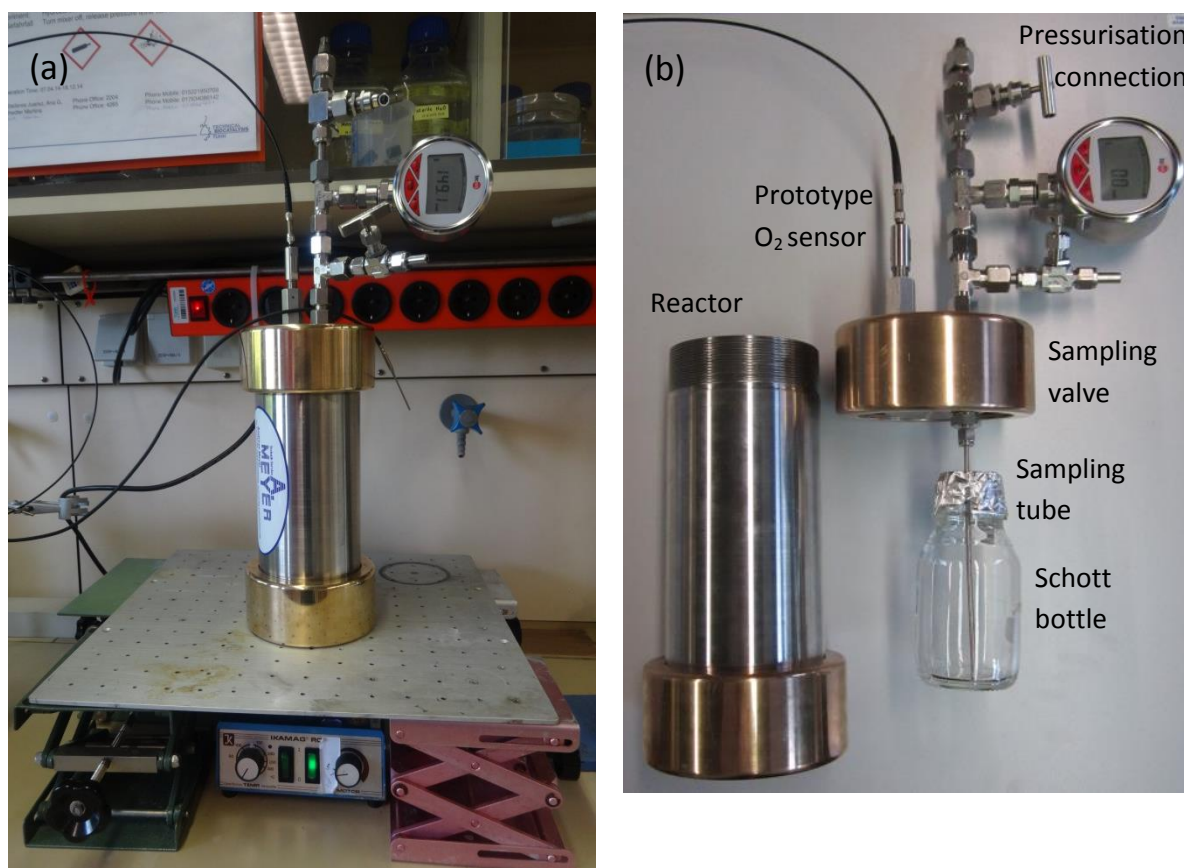


Figure 3.5: The high pressure reactor with volume of 1 L in (a) assembled state on a magnetic stirrer and in (b) disassembled state. The prototype oxygen sensor from companies PreSens Precision Sensing GmbH and Eurotechnica GmbH is installed.

As shown in Figure 3.5 b and Figure 3.6, this second connection could be upgraded by installing a valve with a T-piece for taking subsamples while the experiment was running. A sampling tube was connected with the hole in the lid. This tube reached into the culture medium in a sterilised 250 ml glass bottle. For subsampling at 150 bar, the sampling valve was opened carefully and at first about 5 mL medium, which is the volume of media that stuck unstirred in the tubings above the culturing bottle, were discarded. Then, a defined sample volume was taken using a syringe connected to the valve. Then, the valve was closed again. Since subsampling at 150 bar resulted in a pressure loss, the reactor was repressurised with nitrogen gas. Using this subsampling mechanism, it was possible to analyse the growth of a culture at high pressure without sacrificing a reactor.

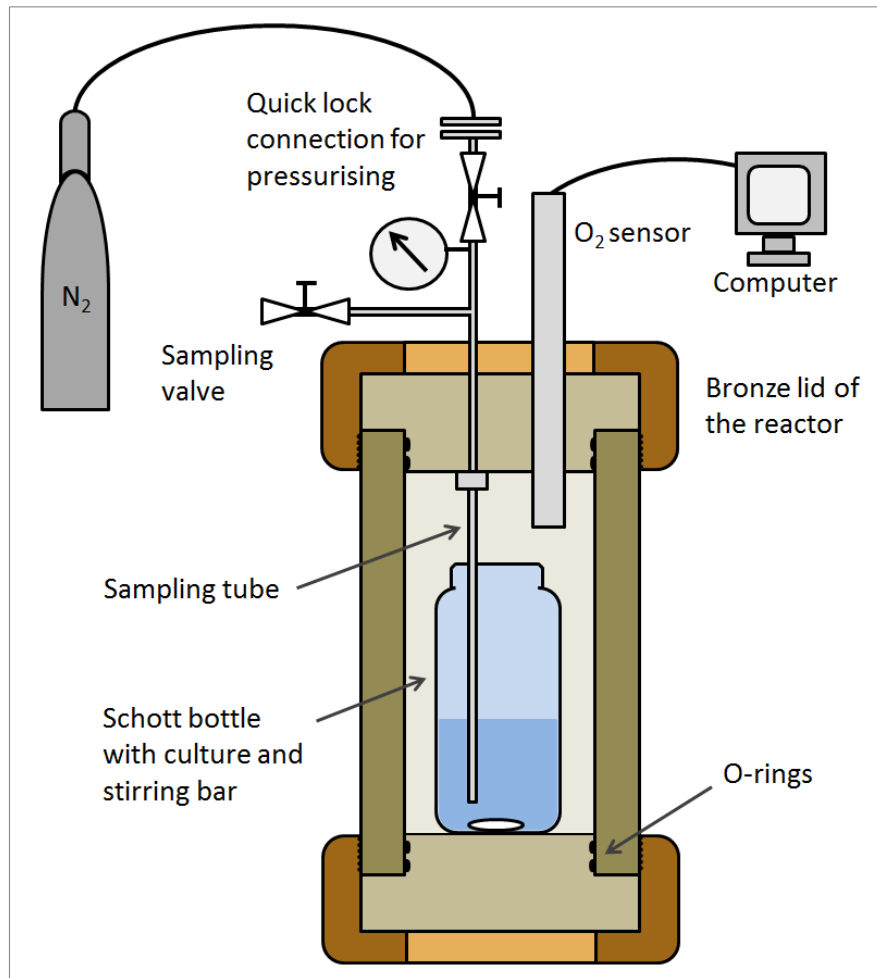


Figure 3.6: Construction scheme of the 1 L high pressure reactor.

However, subsampling at 1 bar was difficult, since a negative pressure arose. To balance this negative pressure simultaneously while sampling, it would have been useful to refill the reactor with nitrogen gas with help of a syringe and thus replace the sampled medium volume. For this reason, a third connection in the lid would have been needed (see Figure 3.7). With help of this extra connection, also the pressure loss while subsampling at high pressure could be compensated precisely using a mechanical spindle pump. Moreover, it would be more practical if the sampling valve would not be integrated into the pressurisation connection, but in a fourth port in the lid. Thus, withdrawing gas from the reactor while subsampling could be avoided.

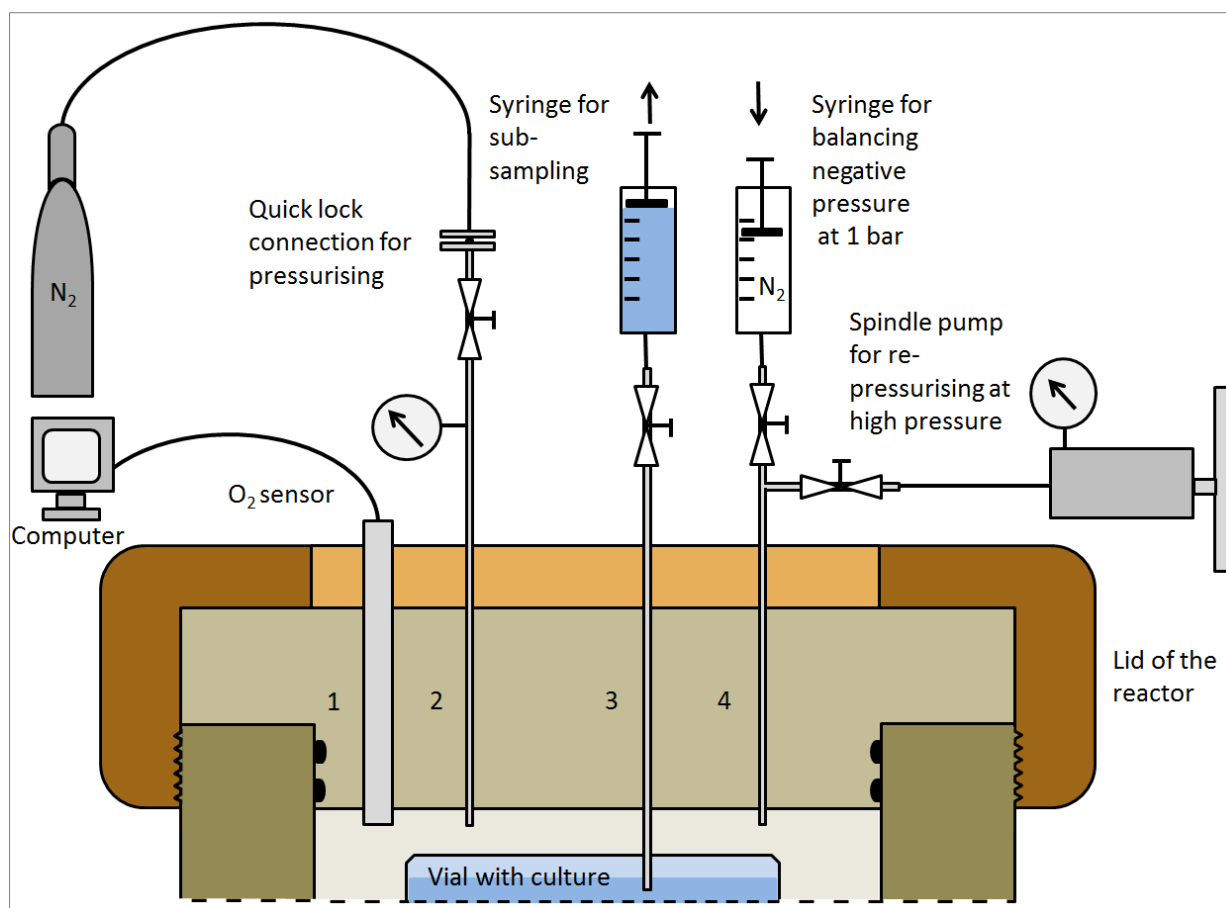


Figure 3.7: Suggested setup of an improved lid for the 1 L high pressure reactor with four connections in the lid for (1) the oxygen prototype sensor, (2) pressurisation with N_2 , (3) subsampling and (4) balancing pressure losses due to subsampling.

This reactor system had another disadvantage. As already described in the previous subsection, subsampling for analysis of oil (-components) concentration was not feasible with a one-pot system. Hence, an online hydrocarbon measurement system would be needed.

3.1.3 The high pressure reactor with screw-piston mechanism for mechanical pressurisation

As derived from experiments described in Chapter 3.1.1, a sufficient volume of air and thus a sufficient supply of oxygen was needed in high pressure cultivation, to ensure optimal growth conditions for aerobic hydrocarbon-degrading bacteria. If there was too little oxygen, aerobic bacteria could not degrade hydrocarbons and no significant growth was

observed. Too much oxygen, however, had harmful effects for bacteria. Oxygen partial pressures of 2 to 10.1 bar were described to be toxic for most aerobic bacteria (Bean 1945). Reason for toxicity is the emergence of reactive oxygen species in the cell. These are able to damage or inhibit the function of proteins, lipids and DNA (Cabisco 2000).

A stainless steel high pressure reactor with a screw-piston mechanism for mechanical pressurisation constructed by Technik Service Andreas Meyer (Lindau, Germany) was used to evaluate the influence of elevated oxygen partial pressures on n-hexadecane degradation. The critical oxygen partial pressure, above which growth of n-hexadecane degrader *R. qingshengii* TUHH-12 was completely inhibited, was determined. For comparison, the oxygen tolerance of *E. coli* was also tested. The reactor, which is shown in Figure 3.8, consisted of a stainless steel cylinder with a small volume of 30 mL. By screwing a bronze piston mechanically into the reactor, total pressure as well as oxygen partial pressure and thus dissolved oxygen concentration in the medium were elevated. The reactor had a maximal pressure limit of 400 bar. A connected valve allowed subsampling of the reactor during incubation. Pressure losses were compensated by screwing the piston. Another advantage of this reactor system was that due to its small size it could be easily disassembled and (apart from the manometer) autoclaved. The culture was mixed by a glass marble inside of the reactor, which was moved by rocking the whole reactor horizontally on a rocking table.

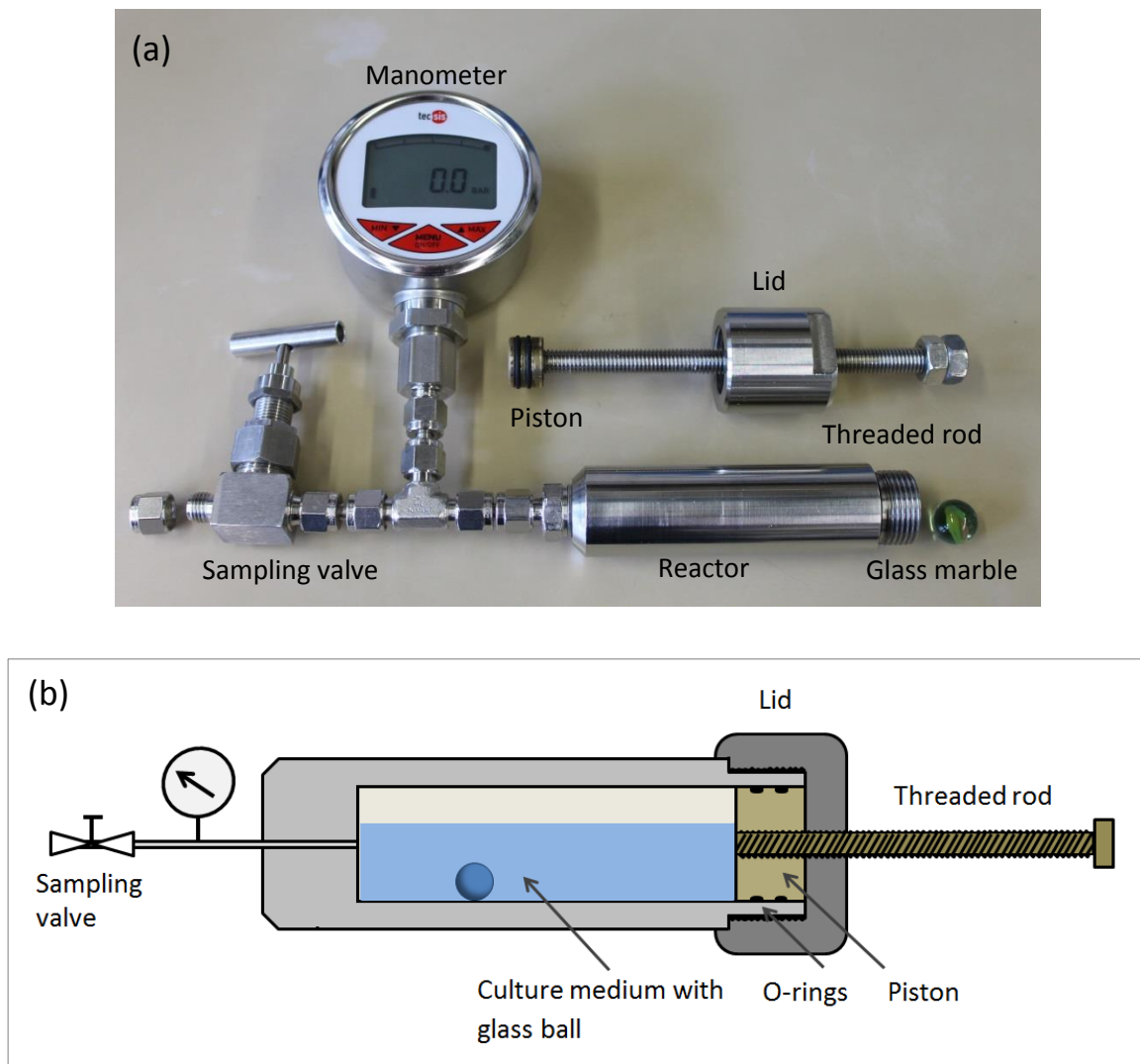


Figure 3.8: (a) High pressure reactor with screw-piston mechanism for mechanical pressurisation. (b) Construction scheme.

As shown in Figure 3.9 a, for *R. qingshengii* TUHH-12 a critical oxygen partial pressure of 2.73 bar was determined, above which no growth on MMII with 1 mM n-hexadecane was observed. However, growth on LB medium showed a slightly different critical oxygen partial pressure point of 2.81 bar (Figure 3.9 b). Growth of *E. coli* on complex LB medium was inhibited at an oxygen partial pressure of 26.46 bar and at 0.63 bar on MMII supplemented with 1% (w/v) α -D glucose (Figure 1.10 a and b). Thus, it was shown that the oxygen partial pressure tolerated was dependent on the strain and the culture medium. The results of the experiment made clear that for testing the effects of high pressure on the bacterial growth and degradation behaviour, mechanical pressurisation of the reactor was not suitable.

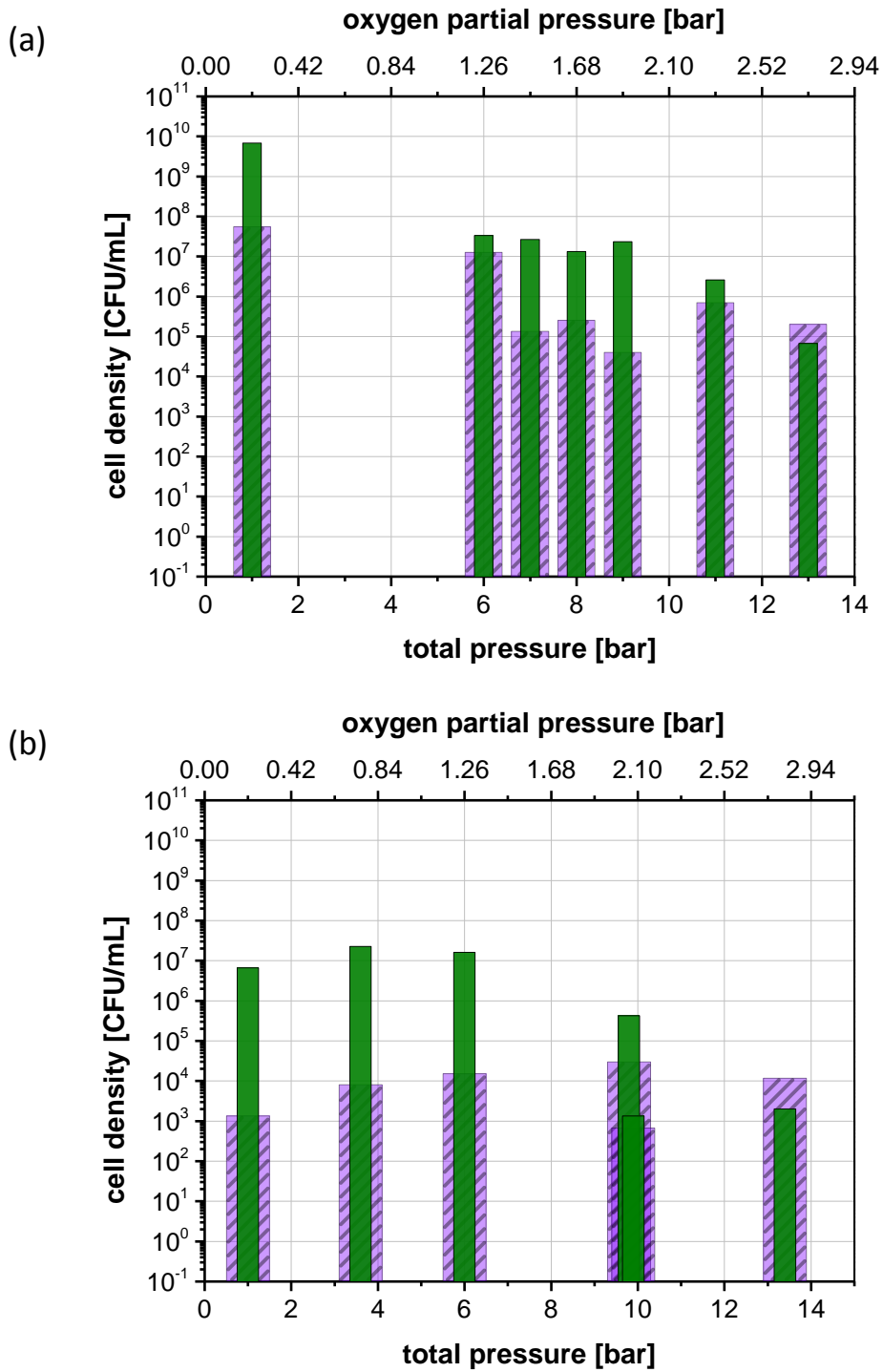


Figure 3.9: Starting cell density (purple striped columns, in CFU/mL) and end cell density (green columns, in CFU/mL) at different oxygen partial pressures in incubations of *R. qingshengii* TUHH-12 growing on (a) MMII supplemented with 1 mM n-hexadecane or on (b) LB medium after 24 h of incubation at RT ([a]: Bachelor thesis of Lisa Sophie Egger 2013, [b]: Bachelor thesis of Alexander Kromm 2014).

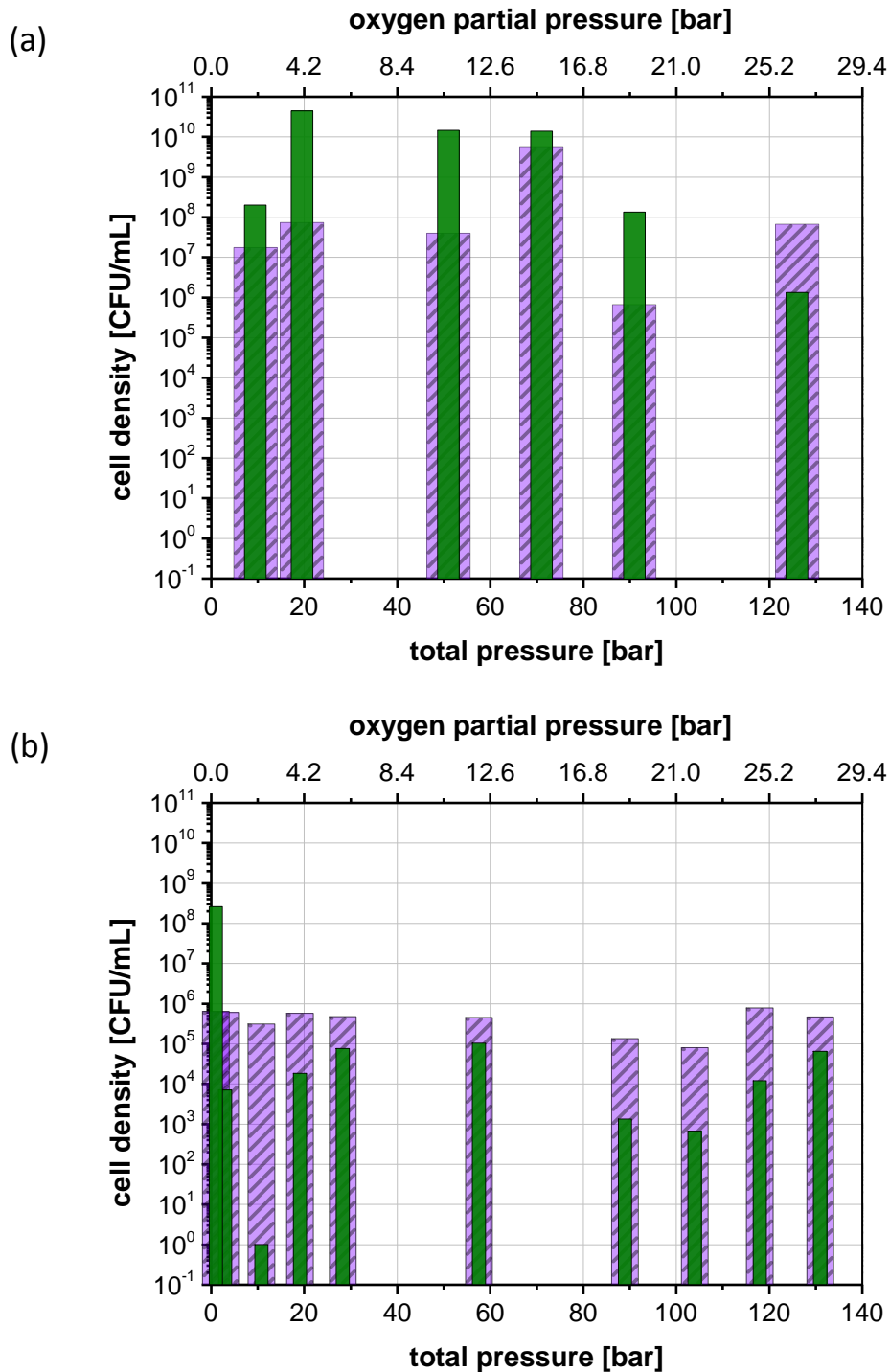


Figure 3.10: Starting (purple striped columns, in CFU/mL) and end cell density (green columns, in CFU/mL) at different oxygen partial pressures in incubations of *E. coli* growing on (a) LB medium or on (b) MMII supplemented with glucose after 3.5 h of incubation at 37°C ([a]: Bachelor thesis of Lisa Sophie Egger 2013, [b]: Bachelor thesis of Alexander Kromm 2014).

3.1.4 The high pressure view cell reactor No. 1

Another type of high pressure reactor, constructed by Eurotechnica GmbH (Bargteheide, Germany), was tested for biodegradation experiments at high pressure (Figure 3.11). This 25 mL high pressure view cell reactor (HP-VC 300) had two sapphire windows for non-invasive online measurement using the fiber optic O₂ sensor Fibox 3 and the CO₂ sensor pCO₂ mini from PreSens Precision Sensing GmbH (Regensburg, Germany), as described in Chapter 3.2.2. The high pressure view cell reactor was pressurised with nitrogen gas. A maximal pressure of 300 bar was allowed. The reactor was equipped with a cooling jacket, which was connected to a water bath, to ensure constant temperature.

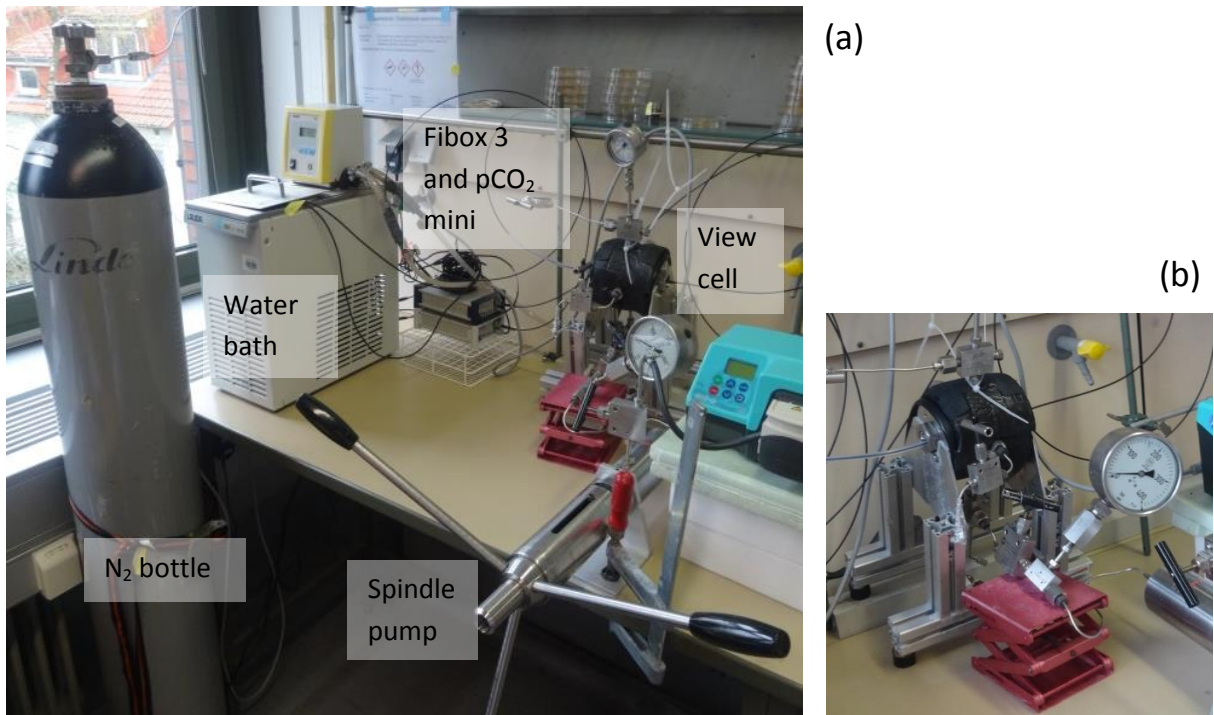


Figure 3.11: (a) High pressure view cell reactor No. 1 (HP-VC 300) connected to a water bath, a N₂ gas bottle, the Fibox 3 and the pCO₂ mini systems from PreSens Precision Sensing GmbH. (b) High pressure view cell reactor No. 1.

An advantage of this system was the possibility of subsampling at high pressure through a valve at the side of the reactor, as depicted in Figure 3.12. However, always before taking a sample, a small volume of the culture had to be discarded, to rinse the valve tubings. For compensating the pressure loss, the reactor was repressurised with nitrogen gas or it was

repressurised manually with fresh medium using a connected mechanical spindle pump. For subsampling at 1 bar, the spindle pump was pressurised to about 10 bar. Then the valve that connected the pump with the reactor and the sampling valve were opened carefully. However, when sediments were used, subsampling through the valve was not feasible, since it blocked and broke the valve. To overcome this problem, instead of filling the sediments and the oil directly into the reactor, both were filled into a small glass container, which fitted into the reactor.

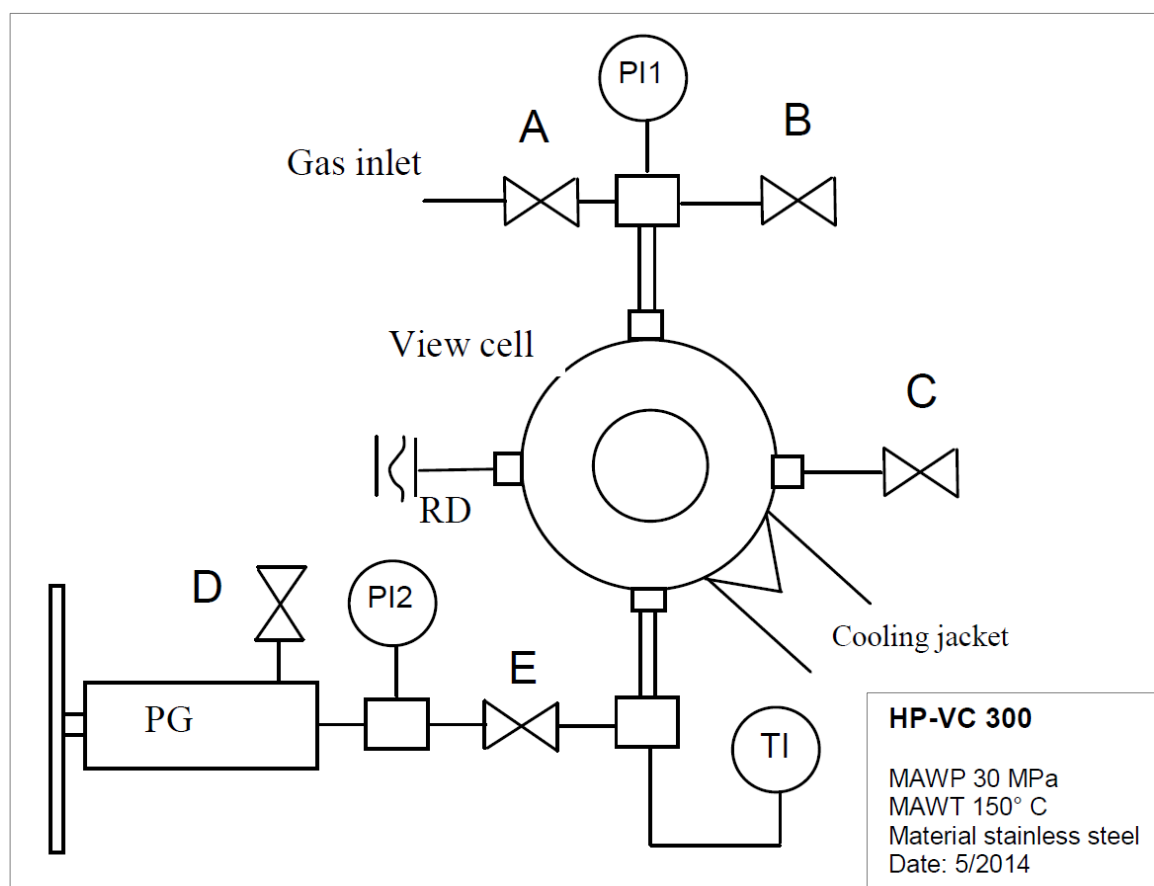


Figure 3.12: Construction scheme of high pressure view cell reactor No. 1: (PG) spindle pump, (A–E) valves ([C] sampling valve, [D] medium input and [E] valve that connects the pump with the reactor), (PI1 and PI2) manometers and (RD) rupture disk (Operating Manual HP-VC 300, version 5/2014, Eurotechnica GmbH).

A disadvantage of this system was that the culture inside the reactor could not be stirred, leading to a heterogeneous distribution of microorganisms within the reactor content. Since it had heat sensitive parts, the high pressure view cell reactor could not be autoclaved, but it

was disinfected by rinsing and incubating with 70% (v/v) ethanol. Unfortunately, this procedure did not ensure total sterility, so that from time to time contaminations were observed when analysing the cell growth.

3.1.5 The high pressure view cell reactor No. 2

A high pressure view cell reactor from SITEC-Sieber Engineering AG (Zurich) was tested. This high pressure view cell reactor, which is shown in Figure 3.13 and Figure 3.14, consisted of a 100 mL stainless steel cylinder with one sapphire window on each side. The windows were used to measure oxygen and carbon dioxide using the Fibox 3 and pCO₂ mini system or the VisiSensTM system from PreSens Precision Sensing GmbH (Regensburg, Germany), as described in Chapters 3.2.2 and 3.2.3. The steel cylinder was pressurised with nitrogen gas (maximal pressure limit: 300 bar). The cylinder was surrounded by a cooling jacket, which was connected to a water bath, to incubate the culture at a constant temperature. No stirring of the culture and no subsampling of the reactor was feasible. Instead, samples were

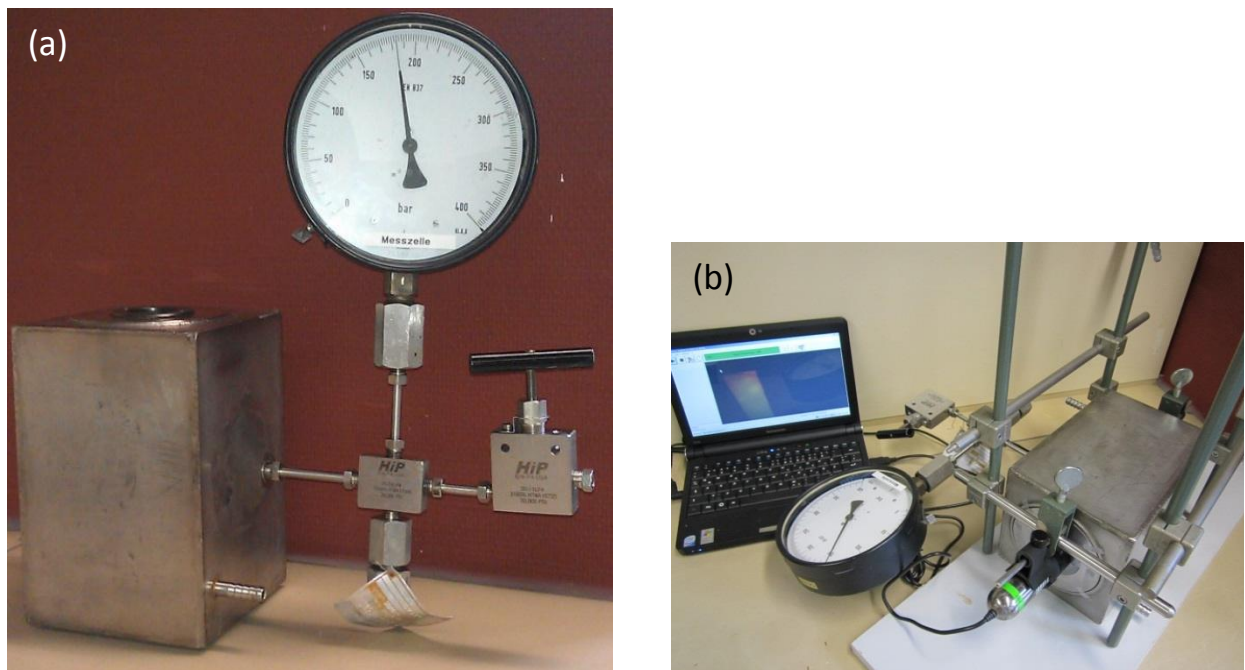


Figure 3.13: (a) High pressure view cell reactor No. 2 from SITEC-Sieber Engineering AG (Zurich), (b) with VisiSensTM CO₂ measurement system from PreSens Precision Sensing GmbH.

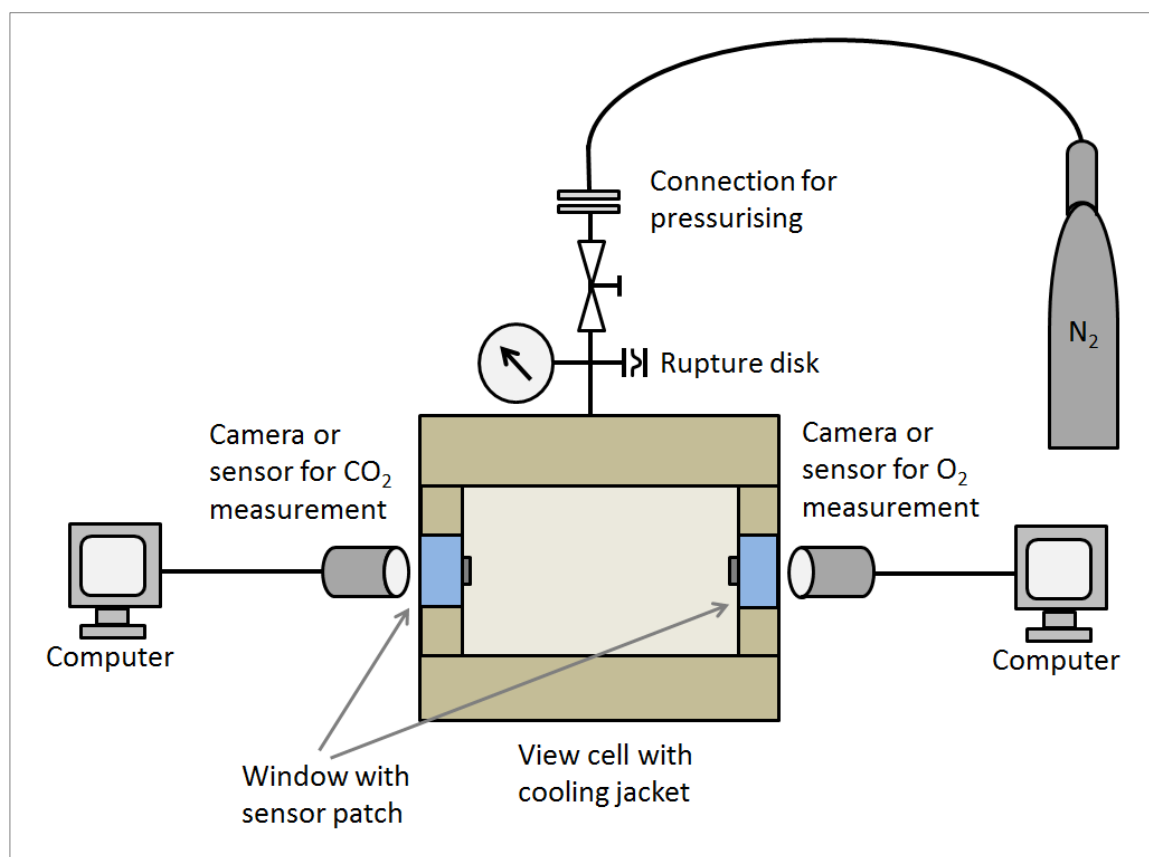


Figure 3.14: Construction scheme High pressure view cell reactor No. 2.

taken at beginning and end of the experiment. Instead of autoclaving, only spraying the reactor with 70% (v/v) ethanol was possible to decontaminate it. Thus, there was a risk of contaminations.

3.2 Online analytics: Test of different O₂ and CO₂ online measurement systems

The analysed bacterial strains and cultures were degrading oil and oil components aerobically, which means oxygen was needed as electron acceptor when hydrocarbons were oxidised. Thus, the bacterial consumption of oxygen and the production of carbon dioxide are related to the rate of hydrocarbon biodegradation. Monitoring these values continuously in the reactors gave an insight into the rate of biodegradation and the experimental effort was minimised substantially. In this thesis, different optical oxygen and carbon dioxide measurement systems were used in various biodegradation experiments at different pressure conditions. To the best of my knowledge, this was the first time that

oxygen and carbon dioxide were measured online during crude oil biodegradation at high pressure in the laboratory. In the following subsections, the systems used are described and their advantages and disadvantages are discussed.

3.2.1 The oxygen sensors from Ocean Optics GmbH

One 160 mL high pressure reactor and one ambient pressure reference reactor were equipped with a fiber optic oxygen sensor from Ocean Optics GmbH (Ostfildern, Germany). With their help it was possible to control the course of an experiment and the experimental effort was reduced. In an experiment, the 160 mL high pressure reactor and the ambient pressure reference reactor that were equipped with the sensors were run until the oxygen reached a constant level. The remaining reactors were opened at different points in the course of the incubation to determine the cell density and remaining substrate concentration. The continuous monitoring of oxygen was used to facilitate the decision of when to sacrifice reactors for taking samples. The oxygen sensors were fitted into the lid of the reactors and measured the oxygen partial pressure in the gaseous phase above the culture medium. Other gases should not affect the oxygen reading. One oxygen sensor, resistant to high pressure, had a HIOXY T1000 coating formulation and after refurbishment, it had a FOSPOR coating formulation. For monitoring the oxygen consumption at ambient pressure, several oxygen sensors with FOXY-R or FOSPOR coating formulation were used.

All coating types were applying the principle of photoluminescence quenching using an oxygen-sensitive ruthenium or Pt-porphyrin compound, trapped in the coating at the tip of the probe. The fluorescence signal of these fluorescent dyes was excited by light of a specific wavelength and was quenched in the presence of oxygen molecules. The degree of quenching was measured and correlated with the partial pressure of oxygen in the coating, which was in dynamic equilibrium with the oxygen in the gaseous phase (Ocean Optics GmbH 2012).

For two-point calibration of the Hioxy- and Foxy-coated probes, the 0% oxygen point was obtained by incubating the sensor in a reactor filled with 100% nitrogen gas and the 100% oxygen point was obtained by incubating in atmospheric gas composition. For FOSPOR-coated sensors a company delivered multipoint calibration with included temperature compensation was used. The O₂ values were collected with the software NeoFox Viewer.

However, during work on this thesis, it was often difficult to reproduce oxygen decrease curves with help of oxygen probes from Ocean Optics GmbH. According to the manufacturer, in particular the HIOXY coating was resistant to hydrocarbons (Ocean Optics GmbH 2012). However, in bacterial hydrocarbon degradation experiments all sensor and coating types sometimes showed a peak at the beginning of the oxygen curve, mostly with a maximum at 20 to 50 h of incubation and of variable height (e.g. see Figure 3.18 b). A possible explanation for this artefact could be the diffusion of the hydrocarbon into the coating of the probe, disturbing the measurement. Sometimes nearly no oxygen partial pressure decrease or even an increase of oxygen was observed although oxygen-consuming bacteria were growing. Operating different Ocean Optics probes, which were calibrated equally, at the same experimental conditions did not result in equal oxygen depletion curves. Moreover, a strong temperature dependence of the oxygen measurement (e.g. fluctuations of temperature in a day-night rhythm) was observed. Very often, the Neofox Viewer software crashed so that data were not saved and were lost. Resulting from these issues, it was only in a few cases possible to obtain reliable oxygen degradation curves with the help of the O₂ sensor system from Ocean Optics GmbH.

3.2.2 The oxygen sensor Fibox 3 and the carbon dioxide sensor pCO₂ mini from PreSens Precision Sensing GmbH

The fiber optic oxygen sensor Fibox 3 and the carbon dioxide sensor pCO₂ mini from PreSens Precision Sensing GmbH (Regensburg, Germany) were non-invasive measurement systems. In order to use these sensors, a high pressure view cell reactor with windows was needed. The oxygen- and carbon dioxide-sensitive sensor spots were glued on the inner side of the windows, where the reaction took place, the sensor was mounted on the outer side of the windows. The oxygen sensor was intended for measurements in the gas phase. Thus, the spot was not in direct contact with the culture medium. The carbon dioxide sensor was constructed for measuring in solutions. However, it could measure CO₂ in the gas phase if humidity was high and constant. If sensor patches were reused too often, they detached partially or completely from the window, when air bubbles or liquid intruded between the glass and the patch. Each sensor spot was delivered with specific pre-calibration data. At the beginning of an experiment, the ambient pressure and temperature needed to be adjusted

to set the initial values of O₂ or CO₂ partial pressure. The values were collected with the software Universal pCO₂View and OxyView PST3 (PreSens Precision Sensing GmbH, Regensburg, Germany). This system had integrated temperature compensation. Like the probes from Ocean Optics GmbH, it was using the principle of luminescence quenching by molecular oxygen. However, in comparison to the Ocean Optics GmbH system, the system from PreSens Precision Sensing GmbH was more reliable.

3.2.3 The oxygen measurement system VisiSens™ from PreSens Precision Sensing GmbH

Another system from PreSens Precision Sensing GmbH (Regensburg, Germany), the VisiSens™ system for measurement of O₂ and CO₂, was tested in high pressure experiments. These chemical-optical systems consisted of a sensing foil (sensor foil SF-RPSu4 for detecting O₂ and foil SF-CD1R for CO₂), which needed to be glued to the inner side of a window in a high pressure view cell reactor, and a camera (camera DU01 for O₂ and camera DU03 for CO₂), which was mounted on the outer side of the window. The sensing foil was in direct contact with the culture medium. Oxygen could be measured in liquid and gaseous phase, whereas carbon dioxide could only be measured in liquid phase.

The system was based on the principle of fluorescence ratiometric imaging. The optical sensor foil contained an analyte-sensitive dye and a reference dye. The analyte-sensitive dye was excited by a light-emitting diode, integrated in the camera, and emitted fluorescence of varying intensity depending on the O₂ or CO₂ concentrations. The reference dye emitted fluorescence of constant intensity (Brochure: Imaging Solutions-VisiSens).

Like the previously described systems from PreSens Precision Sensing GmbH, this VisiSens™ system was non-invasive. The sensing foil was separated from the electronics, which led to the advantage of convenient applicability at extreme conditions. The images were recorded and analysed with the software VisiSens™ AnalytiCal 1 for O₂ and AnalytiCal 3 for CO₂.

To calibrate the sensors via two-point calibration method, the sensor foil was incubated in sodium dithionite solution to obtain the 0% O₂ point and in air-saturated water for the 100% O₂ point. For CO₂ calibration, a solution from 0 to 60 mg/L CO₂ was used.

Stirring of the culture was not possible, resulting in depth strata with different O₂ and CO₂ concentrations in the reactor at different points in time of the incubation. Thus, in the

images, taken by the camera (see Figure 3.15), the oxygen depletion and carbon dioxide production were observed to start at the bottom of the reactor and to rise to the interface of air and water. Hence, by using the VisiSensTM system, the temporal and spatial changes in the oxygen and carbon dioxide concentrations in an incubation were monitored (Valladares Juárez *et al.* 2015). In the experiment described in Chapter 3.6.2, the top of the sensor patch was placed in the gas phase and the bottom part in liquid medium in the half filled high pressure view cell reactor No. 2. A decrease in oxygen concentration resulted in a change of colour of the patch from light to dark (Figure 3.15). For calculation of gas concentrations, only the lower part of the sensing foil was used.

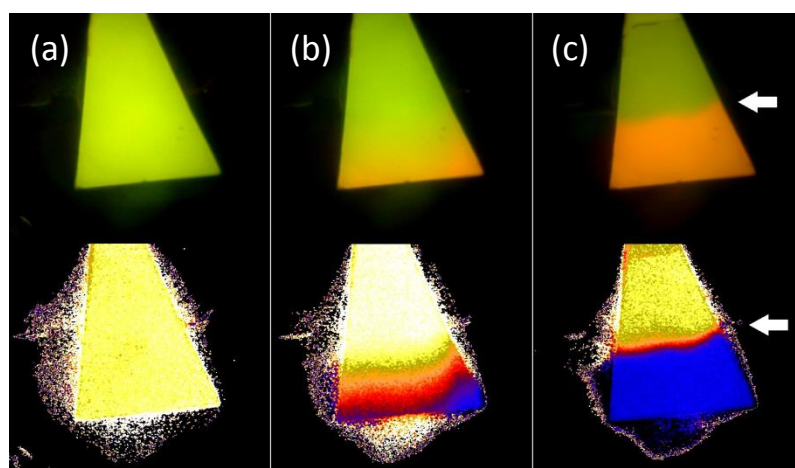


Figure 3.15: Images of an oxygen-sensing patch taken with VisiSensTM camera during incubation of a deep-sea sediment with crude oil in high pressure view cell reactor No. 2. The upper images are unprocessed and the lower images are processed photos at (a) start, (b) middle and (c) end time of the experiment. The arrows indicate the gas-liquid interphase (Valladares Juárez *et al.* 2015).

As already described by Valladares Juárez *et al.* (2015), several challenges had to be dealt with, when working with the VisiSensTM system. Prior to this work, this system had never been tested at high pressures and the calibration could not be corrected for effects of pressure on the sensor's chemistry. To avoid disturbance of the signal by light, the whole setup was covered with dark plastic foil during measurements. Nevertheless, sensitivity of the camera to light as well as accidental movements of the camera could have been responsible for peaks in the O₂ and CO₂ values. Disturbances of the measurement were also induced by detachment of the sensing foil from the window, when high pressure was

applied and gas or liquid spread between foil and glass (Valladares Juárez *et al.* 2015). However, this system yielded reliable results.

3.2.4 The oxygen prototype sensor from PreSens Precision Sensing GmbH and Eurotechnica GmbH

During this thesis, in a cooperation of the companies PreSens Precision Sensing GmbH and Eurotechnica GmbH, an oxygen sensor was developed, which involved the experiences gained with the sensors described in Chapters 3.2.1, 3.2.2 and 3.2.3. This prototype sensor combined the oxygen measurement principle from PreSens Precision Sensing GmbH and the technological knowledge of high pressure applications of Eurotechnica GmbH. The sensor met all requirements for measuring the bacterial oxygen consumption. The oxygen-sensitive sensor spot was glued to the tip of the probe, whose fiber was embedded in a pressure-resistant stainless-steel housing. This system was installed in the 1 L high pressure reactor. The sensor was hydrocarbon resistant and could measure at pressures up to 200 bar. Function at higher pressures was not tested yet. First tests with this sensor, which is shown in Figure 3.16, provided reliable and reproducible oxygen curves.



Figure 3.16: Oxygen prototype sensor constructed by companies PreSens Precision Sensing GmbH and Eurotechnica GmbH.

3.3 Biodegradation of n-alkanes at ambient and high pressure

R. qingshengii TUHH-12 was used as a model bacterium for testing the degradation of n-alkanes at ambient pressure in ambient pressure reference reactors and at high pressure in 160 mL high pressure reactors. As representatives of the alkanes n-hexadecane, n-decane and n-tetracosane were chosen. The influence of Corexit® EC9500A on the degradation of n-hexadecane was investigated. The strain *D. aurantiaca* C7.oil.2 was isolated from deep-sea

sediments, which were sampled in the GoM, and served as an indigenous model degrader of n-hexadecane.

3.3.1 Degradation of n-hexadecane by *R. qingshengii* TUHH-12 at ambient and high pressure

R. qingshengii TUHH-12 was incubated with 1 mM n-hexadecane at 1 bar in ambient pressure reference reactors and at 147 bar in 160 mL high pressure reactors at RT. Cell growth as well as substrate degradation were analysed. This bacterial model strain, which was originally isolated from samples collected at ambient pressure, was found to degrade and grow with n-hexadecane at ambient as well as at high pressure. At 1 bar, the growth rate, in the exponential phase from 17 to 43 h, was 0.364 h^{-1} , whereas the strain showed a slightly lower growth rate of 0.162 h^{-1} , in the exponential growth phase lasting from 16 to 44 h, when incubated at 147 bar (Figure 3.17). At the end, in the stationary phase, a slightly higher cell density was reached in the ambient-pressure incubation than in the high pressure incubation. The degradation rate of n-hexadecane (in the exponential phase from 17 to 43 h) at 1 bar was 0.035 mM/h, compared to a slightly lower rate of degradation of 0.019 mM/h at 147 bar (from 16 to 44 h). The oxygen consumption rates of 1.73% O_2/h (from 27 to 46 h) at 1 bar and 0.82% O_2/h (from 24 to 44 h) at 147 bar correlated with the substrate degradation rates. The results of this subsection were published in Schedler *et al.* 2014.

Only 19 to 46% of oxygen was consumed in the incubations with 1 mM n-hexadecane. In comparison, when the culture medium was supplemented with 3 mM n-hexadecane instead of 1 mM n-hexadecane, the oxygen was used up completely (Figure 3.18). In Figure 3.18 b, an initial peak of oxygen partial pressure is visible, most probably resulting from diffusion of the hydrocarbon into the oxygen-sensitive coating at the tip of the probe. The oxygen decrease curves correlated with the n-hexadecane degradation curves. The oxygen consumption rate at 1 bar was with 2.12% O_2/h (from 32 to 58 h) slightly lower than the rate at 150 bar with 2.65% O_2/h (from 22 to 44 h). For calculation of growth rate and n-hexadecane degradation rate there were not enough data points in the exponential phase.

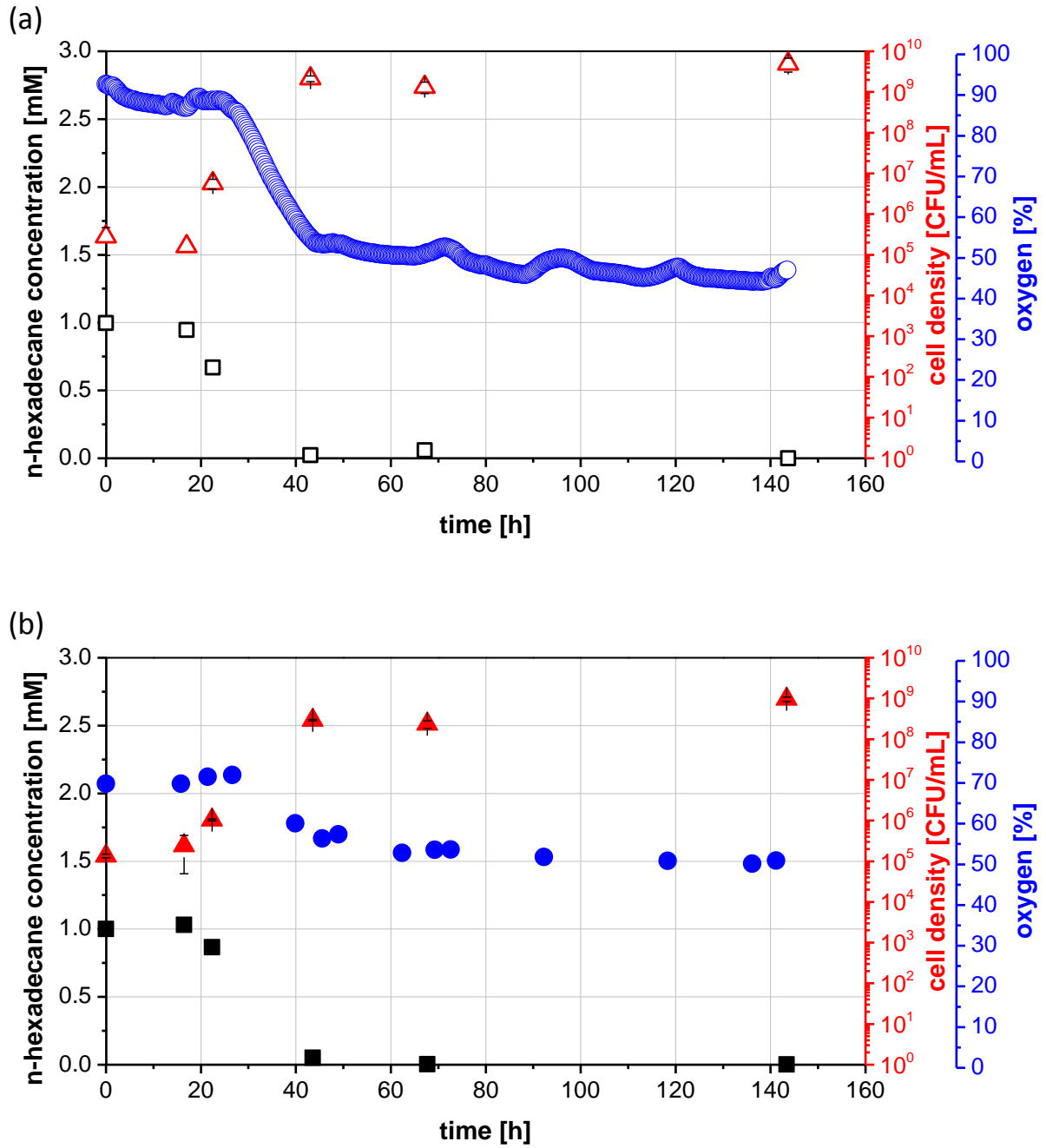


Figure 3.17: Degradation of 1 mM n-hexadecane by *R. qingshengii* TUHH-12 at RT at (a) 1 bar vs. (b) 147 bar. Cell density (CFU/mL) was investigated at 1 bar (Δ) and 147 bar (\blacktriangle). n-Hexadecane concentration (mM) was investigated at 1 bar (\square) and 147 bar (\blacksquare). Oxygen partial pressure (%) was measured at 1 bar (\circ) and 147 bar (\bullet) total pressure with O_2 sensors from Ocean Optics GmbH in the gaseous phase. 100% of oxygen corresponds to 20.95% oxygen in air. Cell density was determined in triplicate and standard deviations are shown.

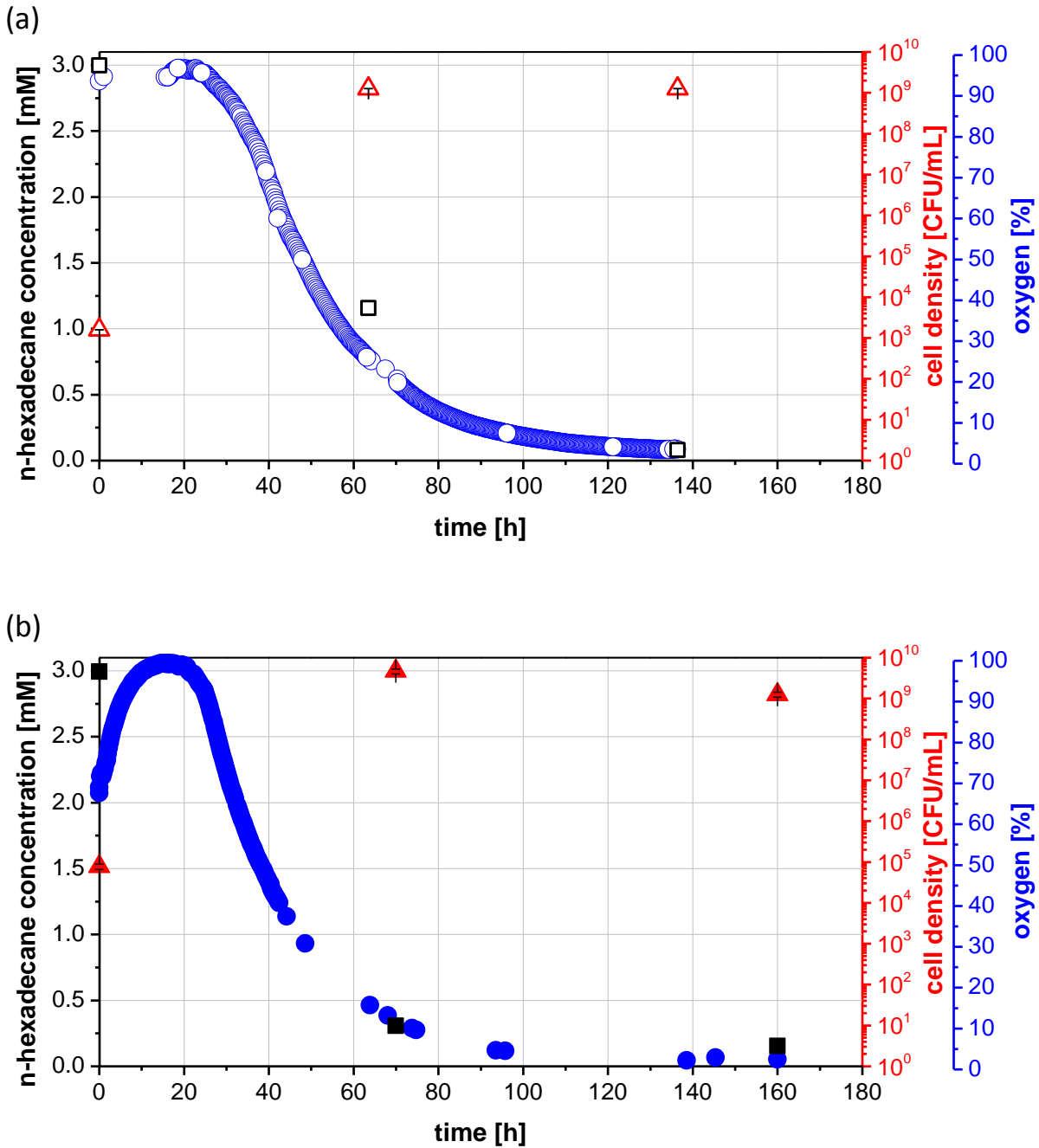


Figure 3.18: Degradation of 3 mM n-hexadecane by *R. qingshengii* TUHH-12 at RT at (a) 1 bar vs. (b) 150 bar. Cell density (CFU/mL) was investigated at 1 bar (Δ) and 150 bar (\blacktriangle). n-Hexadecane concentration (mM) was investigated at 1 bar (\square) and 150 bar (\blacksquare). Oxygen partial pressure (%) was measured at 1 bar (\circ) and 150 bar (\bullet) total pressure with Ocean Optics O₂ sensors in the gaseous phase. 100% of oxygen corresponds to 20.95% oxygen in air. Cell density was determined in triplicate and standard deviations are shown.

3.3.1.1 Incubation of n-hexadecane without inoculum at ambient and high pressure

To verify the influence of high pressure on the concentration of n-hexadecane, control experiments without bacterial inoculum were carried out at RT in the 160 mL high pressure reactors and ambient pressure reference reactors. As shown in Figure 3.19, at ambient pressure the n-hexadecane concentration only decreased at a very slow rate of 0.0034 mM/h, whereas at high pressure the n-hexadecane concentration decreased more rapidly at a rate of 0.011 mM/h.

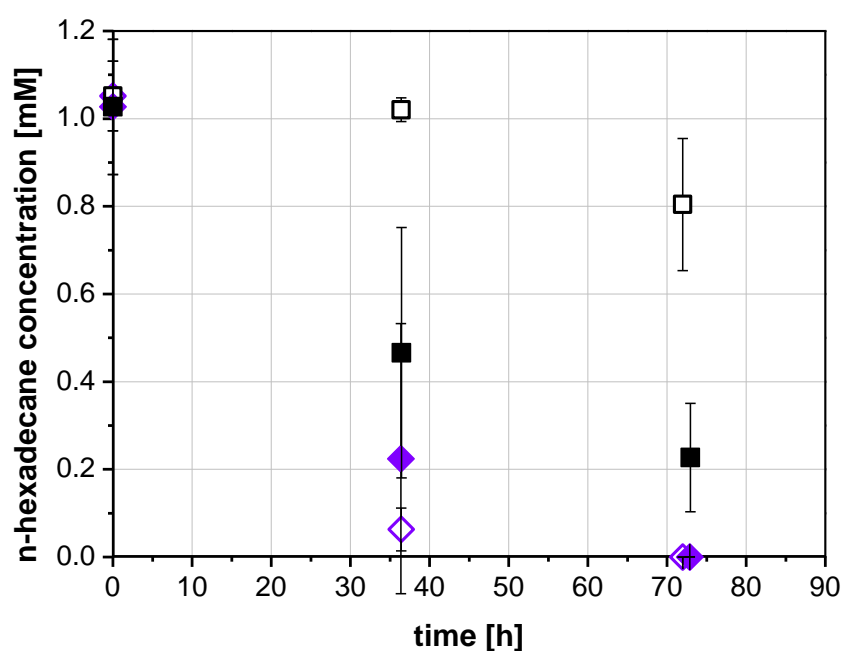


Figure 3.19: Concentration of n-hexadecane (mM) in MMII at RT during incubation of initially 1 mM n-hexadecane without bacterial inoculum at 1 bar (□) and 135 bar (■), compared to incubation of 1 mM n-hexadecane with bacterial inoculum (*R. qingshengii* TUHH-12) at 1 bar (◇) and 135 bar (◆). Shown n-hexadecane concentrations are the mean of analysis of three reactors, respectively. Standard deviations are shown.

To minimise losses of n-hexadecane at high pressure, the 160 mL high pressure reactors as well as the ambient pressure reference reactors were cooled for 5 h at 4°C prior to depressurisation and opening. As shown in Figure 3.20, at 152 bar the n-hexadecane concentration still slowly decreased, however, at a much slower rate (0.0067 mM/h) than when the 160 mL high pressure reactors were not cooled. In the cooled ambient pressure reference reactors with a decreasing rate of 0.0004 mM/h nearly no n-hexadecane was lost.

In consequence, in all experiments determining the degradation of n-hexadecane all reactors were cooled at 4°C for 5 h prior to depressurisation and opening of the reactors.

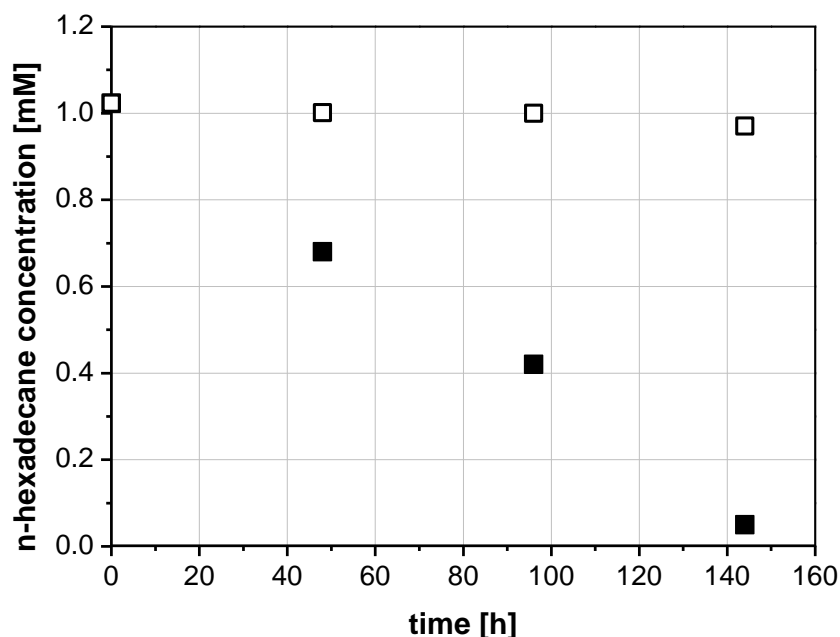


Figure 3.20: Concentration of n-hexadecane (mM) during incubation of initially 1 mM n-hexadecane at RT in MMIII without bacterial inoculum at 1 bar (□) and 152 bar (■). The reactors were cooled at 4°C for 5 h before they were depressurised and opened.

3.3.2 Growth of *R. qingshengii* TUHH-12 with n-tetracosane at ambient and high pressure

Another alkane tested was n-tetracosane. Its degradation by *R. qingshengii* TUHH-12 was investigated in the 160 mL high pressure reactors at 146 bar and the ambient pressure reference reactors at 1 bar at RT, as shown in Figure 3.21. At 1 bar, the strain seemed to grow slightly faster (rate of 0.209 h^{-1} , from 0 to 38 h) than at 146 bar with a growth rate of 0.099 h^{-1} (from 0 to 45 h). Moreover, oxygen curves showed a higher oxygen consumption rate ($2.30\% \text{ O}_2/\text{h}$, from 43 to 70 h) at 1 bar than at 146 bar with an oxygen consumption rate of $0.59\% \text{ O}_2/\text{h}$ (from 45 to 100 h). However, there was a peak at the beginning of the oxygen curve at 1 bar, possibly resulting from diffusion of the hydrocarbon into the oxygen-sensitive coating at the tip of the probe. Strangely, only a very slight decrease of n-tetracosane concentration was detected with GC-MS at both pressure conditions.

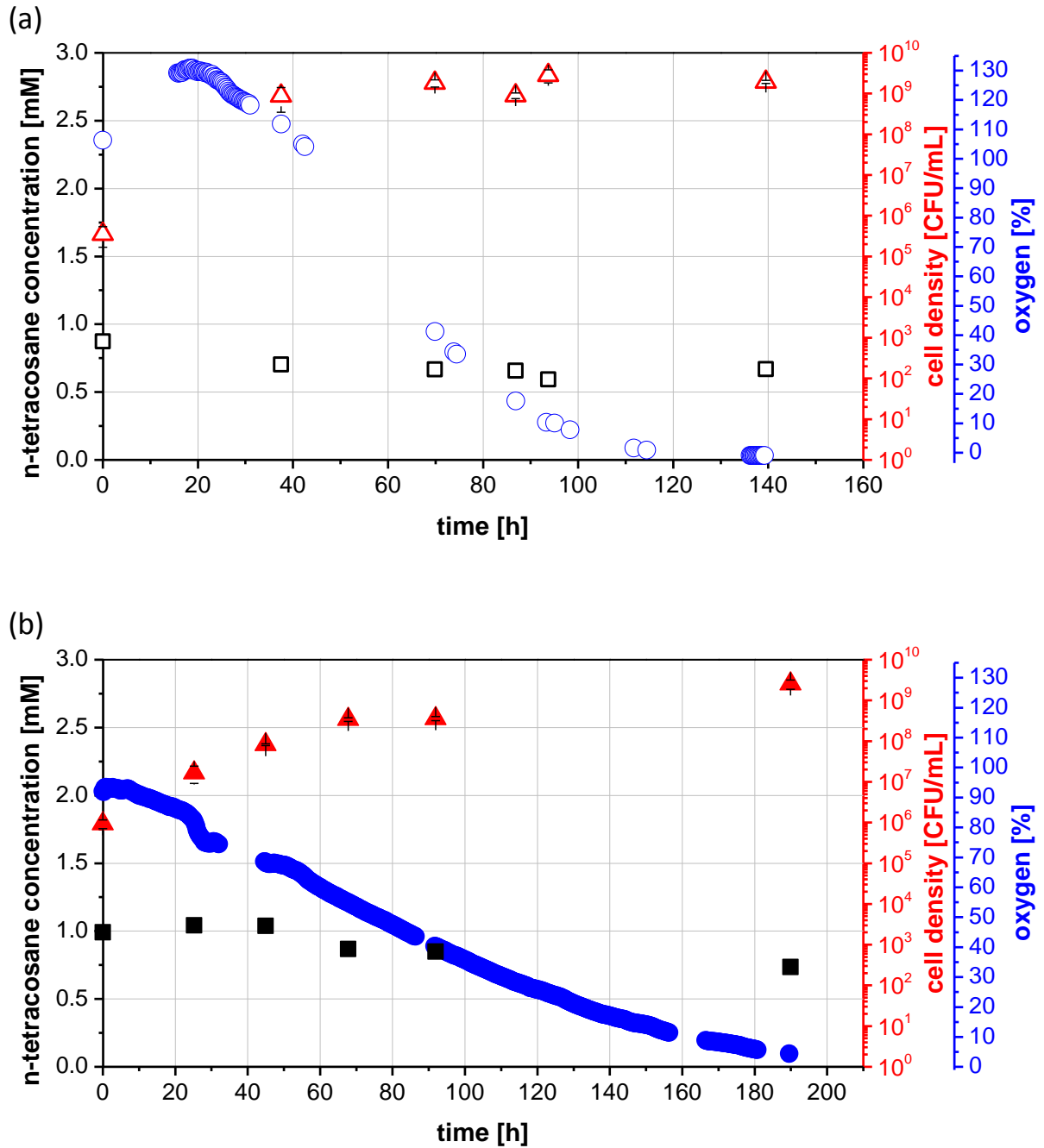


Figure 3.21: Growth of *R. qingshengii* TUHH-12 on 1 mM n-tetracosane at RT at (a) 1 bar vs. (b) 146 bar. Cell density (CFU/mL) was investigated at 1 bar (Δ) and 146 bar (\blacktriangle). n-Tetracosane concentration (mM) was investigated at 1 bar (\square) and 146 bar (\blacksquare). Oxygen partial pressure (%) was measured at 1 bar (\circ) and 146 bar (\bullet) total pressure with O_2 sensors from Ocean Optics GmbH in the gaseous phase. 100% of oxygen corresponds to 20.95% oxygen in air. Cell density was determined in triplicate and standard deviations are shown.

3.3.3 Growth of *R. qingshengii* TUHH-12 with n-decane at ambient and high pressure

The third alkane tested was n-decane. Its degradation by *R. qingshengii* TUHH-12 was determined at 1 bar in ambient pressure reference reactors and at 151 bar in 160 mL high pressure reactors at RT (Figure 3.22). Unfortunately, the experiment was stopped too early so that the growth curve did not reach the stationary phase. At 151 bar, the growth rate (0.269 h^{-1} , 0 to 24 h) was slightly lower than at 1 bar (0.286 h^{-1} , 0 to 24 h). However, n-decane degradation and oxygen consumption at 151 bar (0.182 mM n-decane/h, 0 to 8 h; 2.13% O_2 /h, 31 to 37 h) seemed to be slightly faster than at 1 bar (0.153 mM n-decane/h, 0 to 8 h; 1.58% O_2 /h, 31 to 37 h). The oxygen was not consumed completely and the oxygen curves did not correlate with the substrate degradation curves.

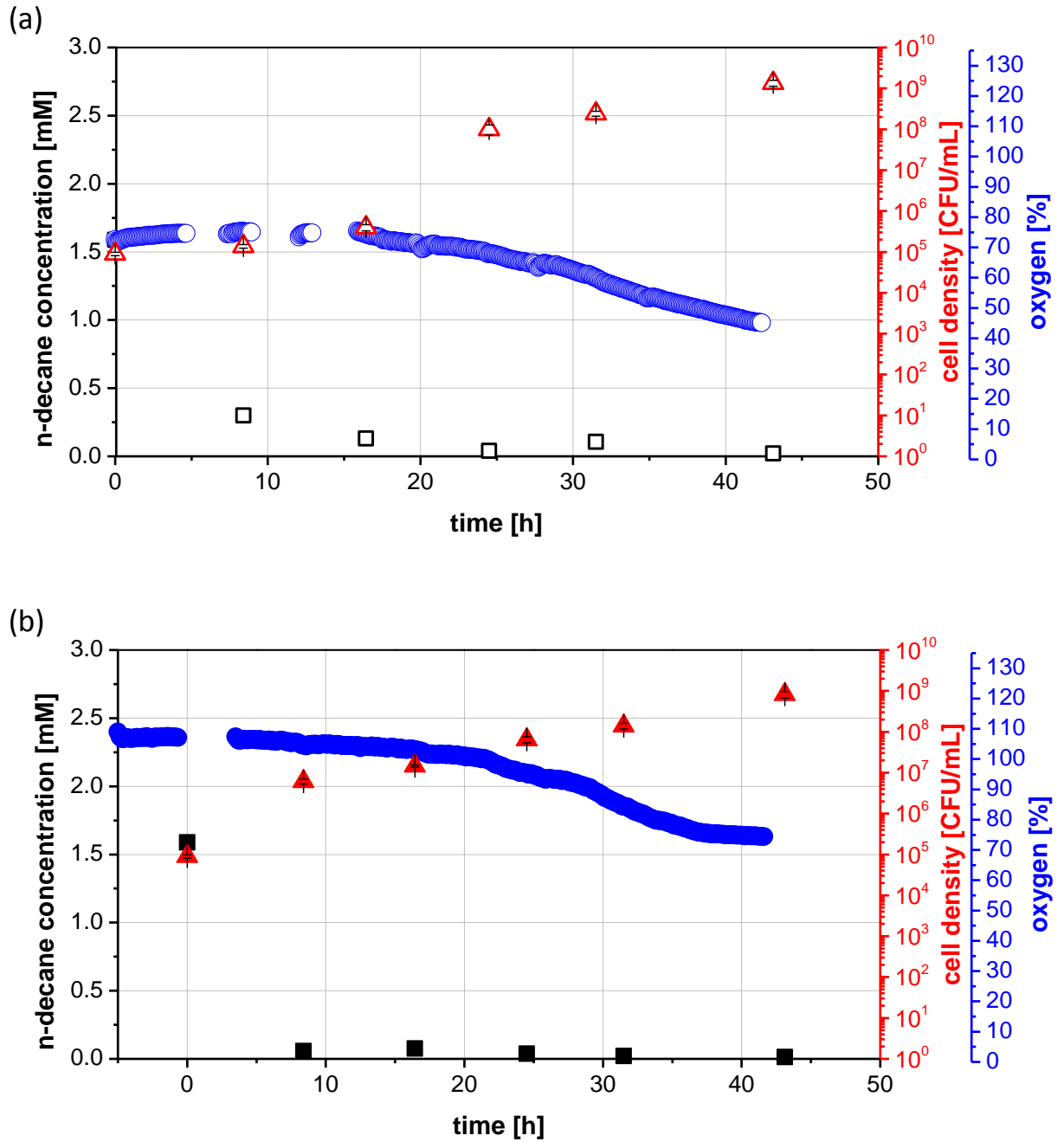


Figure 3.22: Growth of *R. qingshengii* TUHH-12 at RT on 1.59 mM n-decane at (a) 1 bar vs. (b) 151 bar. Cell density (CFU/mL) was investigated at 1 bar (Δ) and 151 bar (\blacktriangle). n-Decane concentration (mM) was investigated at 1 bar (\square) and 151 bar (\blacksquare). Oxygen partial pressure (%) was measured at 1 bar (\circ) and 151 bar (\bullet) total pressure with O_2 sensors from Ocean Optics GmbH in the gaseous phase. 100% of oxygen corresponds to 20.95% oxygen in air. Cell density was determined in triplicate and standard deviations are shown.

3.3.3.1 Incubation of *n*-decane without bacterial inoculum at ambient and high pressure

To verify the influence of high pressure on the concentration of *n*-decane a control experiment was carried out. *n*-Decane was incubated in MMII without bacterial inoculum at 1 bar in the ambient pressure reference reactors, at 1 bar in closed glass vials and at 135 bar in the 160 mL high pressure reactors at RT. As shown in Figure 3.23, the *n*-decane concentration decreased in ambient pressure reference and 160 mL high pressure reactors already after a very short time of incubation. When incubated at 1 bar in the ambient pressure reference reactor, after 12 h 29.9% of the initial *n*-decane was left and after 114 h only 11.9% was left. A greater loss of *n*-decane was observed in incubation at 135 bar in 160 mL high pressure reactors. After 12 h 8.2% was left and after 114 h 0.5% was left from the initial *n*-decane. When *n*-decane was incubated at 1 bar in closed glass vials, which had a

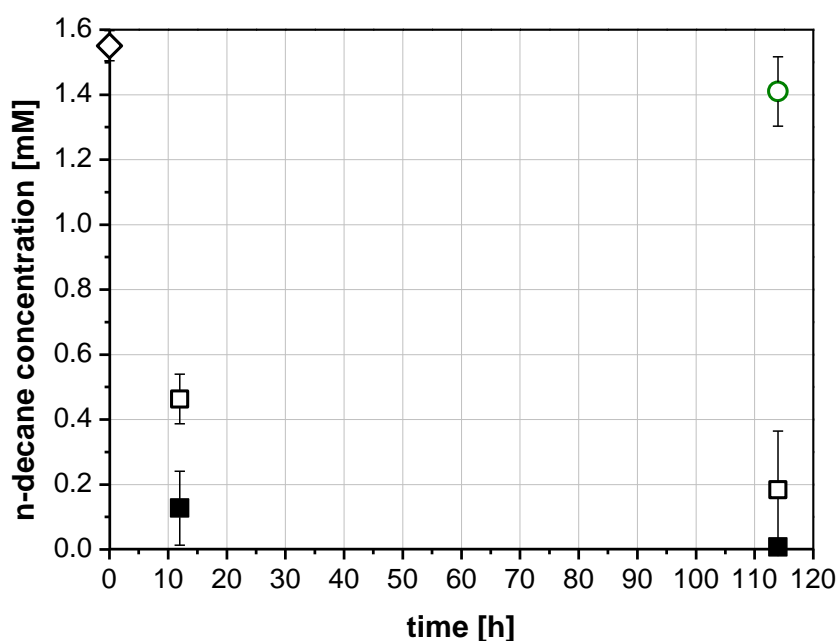


Figure 3.23: Concentration of *n*-decane (mM) during incubation of initially 1.59 mM *n*-decane (◇) in MMII at RT without bacterial inoculation at 1 bar in ambient pressure reference reactors (□), at 1 bar in closed glass vials (○) and at 135 bar in 160 mL high pressure reactors (■). Shown *n*-decane concentrations at 0 h are the mean of analysis of five reactors, *n*-decane concentrations at 12 h are the mean of analysis of two reactors and *n*-decane concentrations at 114 h are the mean of analysis of three reactors/glass vials. Standard deviations are shown. The reactors at the time of 12 h were cooled at 4°C for 5 h prior to opening them.

smaller volume of gaseous phase than the reactors, only 9.1% of the original n-decane was lost after 114 h. Since n-decane has a very low melting temperature of -30°C (GESTIS Substance Database: n-decane), cooling the reactors prior to depressurising them did not help reducing losses.

3.3.4 Degradation of n-hexadecane by *D. aurantiaca* C7.oil.2 at ambient and high pressure

The GoM strain *D. aurantiaca* C7.oil.2 was incubated in the 1 L high pressure reactor at 1 and 154 bar with n-hexadecane at RT (Figure 3.24). In the incubation at 154 bar, samples were taken while the experiment was running. With the current reactor setup, subsampling at 1 bar was not feasible, since a negative pressure would have occurred. Thus, for the incubation at 1 bar, only at the start and at the end of the experiment the cell density was

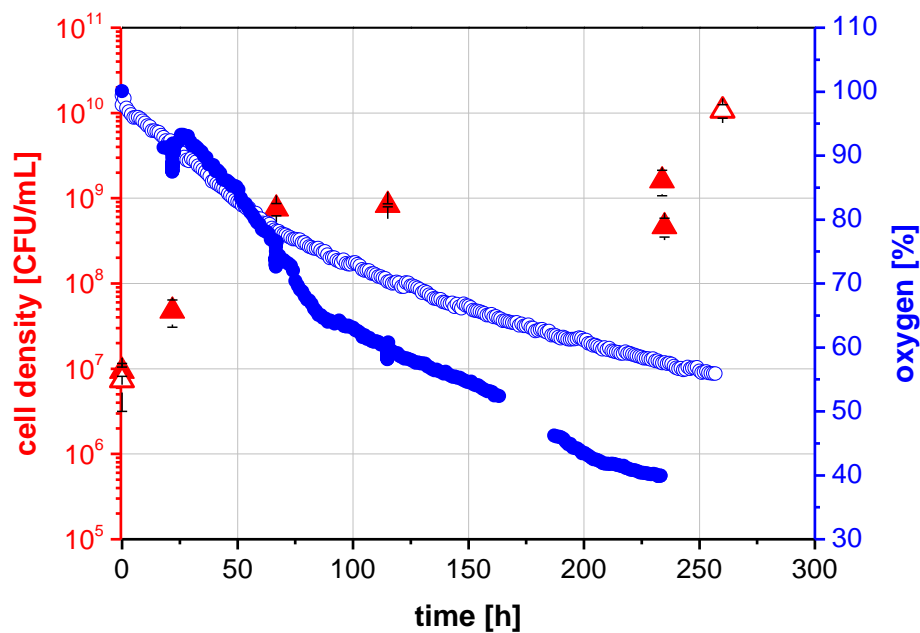


Figure 3.24: Growth of *D. aurantiaca* C7.oil.2 at RT with n-hexadecane at 1 vs. 154 bar. Cell density (CFU/mL) was investigated at 1 bar (Δ) and 154 bar (\blacktriangle). Oxygen partial pressure (%) was measured at 1 bar (\circ) and 154 bar (\bullet) total pressure with the prototype O_2 sensor in the gaseous phase. 100% of oxygen corresponds to 20.95% oxygen in air. Cell density was determined in triplicate and standard deviations are shown. Times of subsampling are apparent in the small peaks in the oxygen decrease curve (Bachelor thesis of Sabrina Felicitas Jesch 2015).

determined. At 154 bar, 18.2% more oxygen was consumed at the end of the incubation than at 1 bar, although a lower cell density was determined.

Unfortunately, after the experiment was finished the strain was found to be contaminated. Besides coral-red colonies, yellow colonies, probably contaminations, were observed. Colonies of *Dietzia* sp. were reported to be orange to coral-red (Koerner *et al.* 2009). Consequently, the strain was purified using streak plate technique. In a later experiment (described in Chapter 3.4.5), again colonies of divergent morphology were observed. Surprisingly, after sequencing of the 16S-rDNA it emerged that the strain has several colony phenotypes.

3.3.5 Influence of Corexit® EC9500A on growth and biodegradation capability of *R. qingshengii* TUHH-12 at ambient and high pressure

As described in the following subsections, the influence of the dispersant Corexit® EC9500A on the n-hexadecane degradation ability and growth of *R. qingshengii* TUHH-12 was investigated at different pressure and temperature conditions. In addition, the growth on the dispersant as sole source of carbon was tested.

3.3.5.1 Influence of Corexit® EC9500A on growth and n-hexadecane biodegradation behaviour of *R. qingshengii* TUHH-12 at ambient and high pressure at RT

To evaluate the effects of the dispersant Corexit® EC9500A on the growth of *R. qingshengii* TUHH-12, the strain was incubated with 1 mM n-hexadecane with addition of Corexit® EC9500A in the ambient pressure reference reactors and 160 mL high pressure reactors at RT. Compared to the incubations with n-hexadecane without Corexit® EC9500A (Figure 3.25 a), the n-hexadecane degradation curve under addition of Corexit® EC9500A had a shortened lag-phase at 1 bar as well as at 147 bar (Figure 3.25 b). The growth and degradation curves for incubations with Corexit® EC9500A at 1 and 147 bar were very similar. Bacteria grew at a rate of 0.434 h^{-1} (from 11 to 29 h) at 1 bar and at a rate of 0.407 h^{-1} (from 11 to 29 h) at 147 bar. n-Hexadecane was degraded at a rate of 0.065 mM/h (from 6 to 22 h) at 1 bar and at a rate of 0.054 mM/h (from 6 to 23 h) at 147 bar. These rates were very similar to the rates in incubations without Corexit® EC9500A, where bacteria grew at a rate of 0.411 h^{-1} (from 11 to 29 h) at 1 bar and at a rate of 0.368 h^{-1} (from 11 to 29 h) at

147 bar and n-hexadecane was degraded at a rate of 0.06 mM/h (from 6 to 22 h) at 1 bar and at a rate of 0.062 mM/h (from 6 to 22 h) at 147 bar.

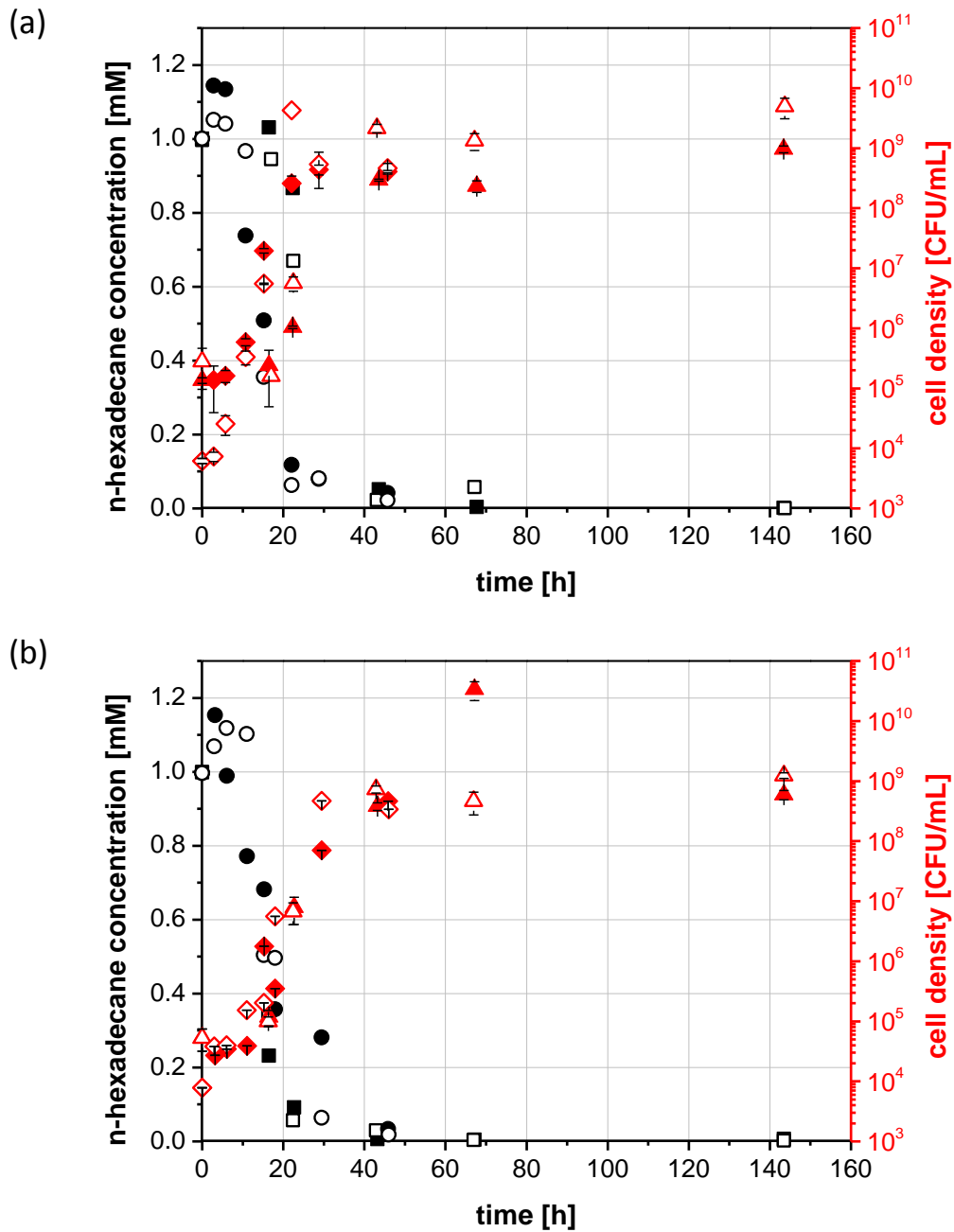


Figure 3.25: Degradation of 1 mM n-hexadecane by *R. qingshengii* TUHH-12 at RT, at ambient and high pressure conditions, (a) without vs. (b) with addition of Corexit® EC9500A. Cell density (CFU/mL) was investigated at 1 bar (Δ , \diamond) and 147 bar (\blacktriangle , \blacklozenge). n-Hexadecane concentration (mM) was investigated at 1 bar (\square , \circ) and 147 bar (\blacksquare , \bullet). Triangles and squares indicate data points from a first experiment (Triangles and squares from (a) are already shown in Figure 3.17.). Rhombi and circles indicate data points from a second run under same conditions. Cell density was determined in triplicate and standard deviations are shown.

3.3.5.2 Growth of *R. qingshengii* TUHH-12 on Corexit® EC9500A at ambient and high pressure

As shown in Figure 3.26, the growth of *R. qingshengii* TUHH-12 on Corexit® EC9500A was tested in the ambient pressure reference and 160 mL high pressure reactors at RT at 1 and 144 bar. The experiment showed that the bacteria grew with Corexit® EC9500A as sole carbon source. The growth rate was slightly faster at 1 bar with 0.208 h^{-1} (from 16 to 66 h) than at 144 bar with 0.138 h^{-1} (from 16 to 66 h).

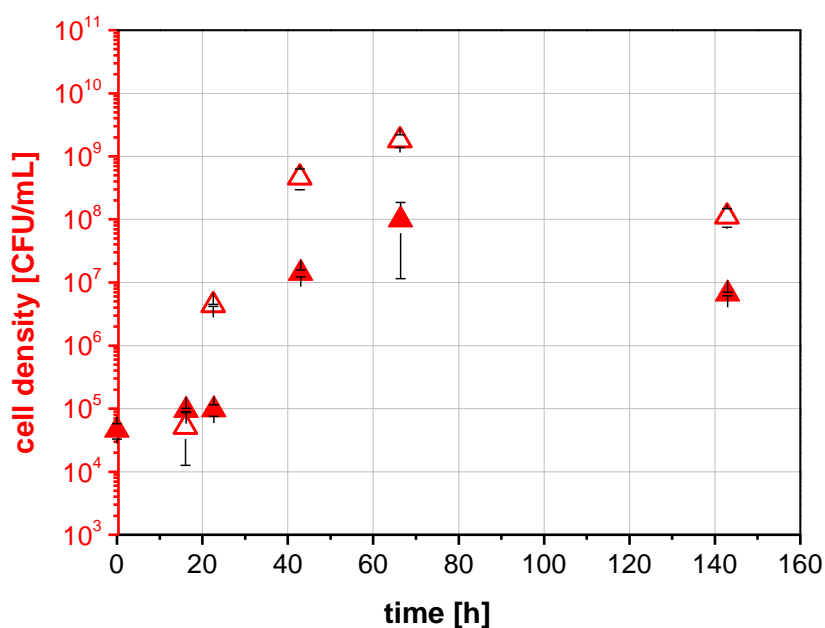


Figure 3.26: Cell density (CFU/mL) of *R. qingshengii* TUHH-12 growing on Corexit® EC9500A at RT at 1 bar (Δ) vs. 144 bar (▲). Cell density was determined in triplicate and standard deviations are shown.

3.3.5.3 Influence of Corexit® EC9500A on growth and *n*-hexadecane degradation of *R. qingshengii* TUHH-12 degradation at 1 bar and 4°C

In the GoM, at 700 m depth below water surface, low temperatures of about 2°C to 5°C are present (Atlas and Hazen 2011). Therefore, to simulate natural conditions, *R. qingshengii* TUHH-12 was incubated at 4°C. The degradation of 1 mM *n*-hexadecane with and without addition of Corexit® EC9500A at 1 bar in the ambient pressure reference reactors and 160 mL high pressure reactors was tested at this temperature (Figure 3.27). The results show a similar growth and degradation behaviour when the mineral medium was supplemented

with Corexit® EC9500A or when no dispersant was added. However, compared to the growth with n-hexadecane at RT (see also Chapter 3.3.1 and 3.3.5.1), degradation of the substrate took much longer and growth was slower at 4°C. The growth rate at 4°C and 1 bar in incubation without as well as with Corexit® EC9500A was 0.037 h^{-1} , from 71 to 189 h of the exponential phase. Without addition of Corexit® EC9500A, the n-hexadecane degradation rate at 4°C and 1 bar, in the exponential phase lasting from 71 to 189 h, was 0.012 mM/h. In incubation with Corexit® EC9500A the degradation rate was 0.007 mM/h (from 71 to 140 h).

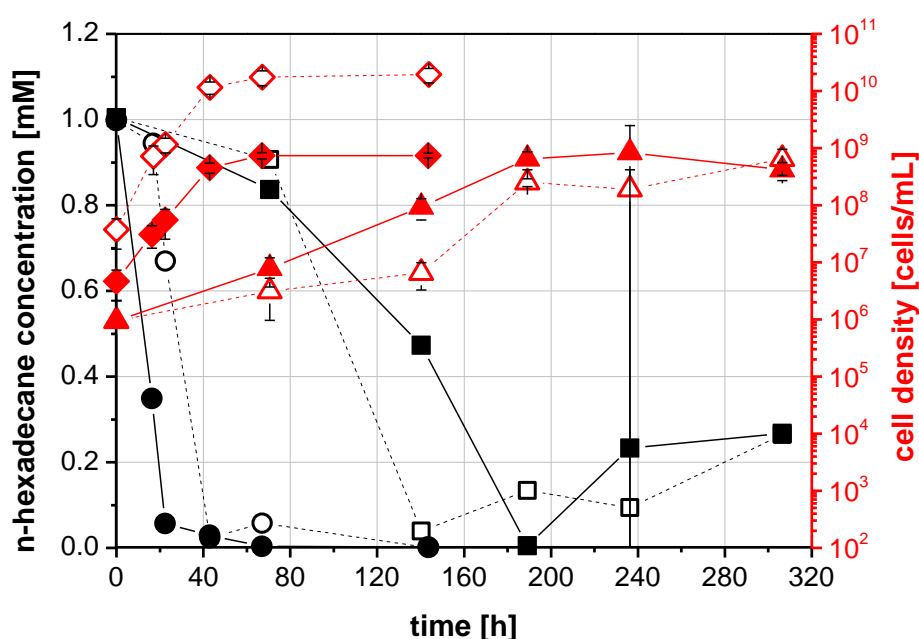


Figure 3.27: Degradation of 1 mM n-hexadecane by *R. qingshengii* TUHH-12 at ambient pressure of 1 bar at RT vs. at 4°C, with vs. without addition of Corexit® EC9500A. Cell density (cells/mL) in incubation without Corexit® EC9500A was investigated at 4°C (Δ) and at RT (\diamond). Cell density in incubation with Corexit® EC9500A was investigated at 4°C (\blacktriangle) and at RT (\blacklozenge). n-Hexadecane concentration (mM) in incubation without Corexit® EC9500A was investigated at 4°C (\square) and at RT (\circ). n-Hexadecane concentration (mM) in incubation with Corexit® EC9500A was investigated at 4°C (\blacksquare) and at RT (\bullet). Data points at RT belong to the experiments shown in Figure 3.17 a and Figure 3.25 a. Cell density was determined in triplicate and standard deviations are shown.

3.4 Biodegradation of aromatic hydrocarbons at ambient and high pressure

R. wratislaviensis Tol3 served as a model bacterium to investigate the degradation of aromatic hydrocarbons at ambient and high pressure in ambient pressure reference and 160 mL high pressure reactors. Toluene served as representative of the aromatic fraction of crude oil. The strain *D. aurantiaca* C7.oil.2 was used as an indigenous model degrader of toluene.

3.4.1 Growth of *R. wratislaviensis* Tol3 with toluene at ambient and high pressure

R. wratislaviensis Tol3 was incubated in the presence of toluene vapour at 1 and 140 bar using the set of ambient pressure reference and 160 mL high pressure reactors at RT (Figure 3.28). High pressure had a positive effect on the initial growth. The strain grew at a rate of

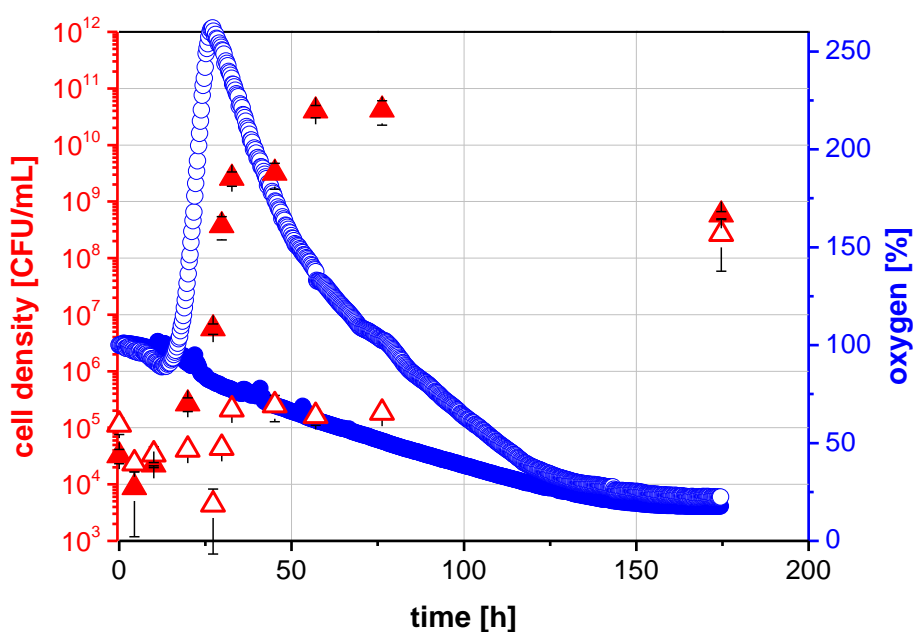


Figure 3.28: Growth of *R. wratislaviensis* Tol3 with toluene (supplied via vapour diffusion) at RT at 1 vs. 140 bar. Cell density (CFU/mL) was investigated at 1 bar (Δ) and 140 bar (\blacktriangle). Oxygen partial pressure (%) was measured at 1 bar (\circ) and 140 bar (\bullet) total pressure with O₂ sensors from Ocean Optics GmbH in the gaseous phase. 100% of oxygen corresponds to 20.95% oxygen in air. Cell density was determined in triplicate and standard deviations are shown (Bachelor thesis of Alexandra Buck-Emden 2015).

0.717 h^{-1} , from 20 to 33 h of the exponential phase, at 140 bar. Strangely, there was only poor growth at 1 bar in the first 76 h. The growth curve at 1 bar had no defined exponential growth phase. Only the last sampling point showed a cell density similar to the cell density at high pressure. However, this could be an outlier.

There was an initial increase in the 1 bar oxygen curve with a maximum at 26 h, which probably was caused by the diffusion of the toluene into the coating of the oxygen probe. Apparently, due to previous experiments, the high pressure oxygen sensor was already accustomed to the toluene vapour. The initial increase complicates the comparison of the oxygen curves. However, at the end of the incubation a similar oxygen level was reached at both pressure conditions.

3.4.2 Growth of *R. wratislaviensis* Tol3 with toluene at different pressures from 1 to 154 bar

To find out whether there is a critical pressure, above which *R. wratislaviensis* Tol3 shows an obviously enhanced growth, the strain was incubated at different pressures in the 160 mL high pressure reactors for 5 days at RT. As shown in Figure 3.29, pressures of 44 to 154 bar had a positive effect on the cell density, whereas at 1 bar cell density decreased. In the high pressure incubations, *R. wratislaviensis* Tol3 reached 8×10^4 to 1×10^6 -fold higher final cell numbers than in the incubation at ambient pressure. As already described in the previous subsection, the inhibited growth at 1 bar is remarkable, since the preculture, used to inoculate the cultures of this experiment, grew well at 1 bar. However, at all tested pressures above ambient pressure, the cell density reached more or less the same level and no critical pressure was found. In the reactor, which was incubated at 1 bar, at the end of the incubation no liquid toluene was left in the open supply beaker, but in reactors, which were incubated at high pressures, still liquid toluene was left.

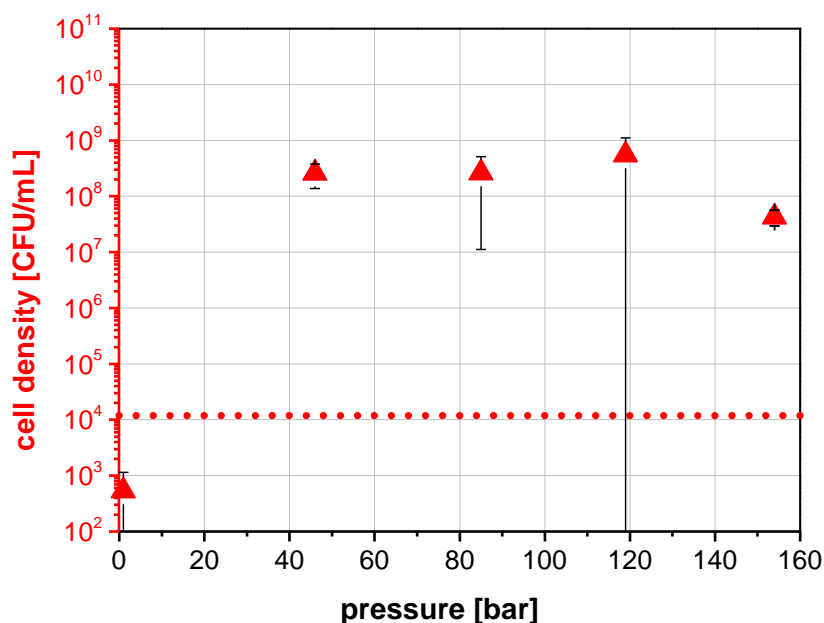


Figure 3.29: Incubation of *R. wratislaviensis* Tol3 at RT at different pressures in the range from 1 to 154 bar with toluene provided via vapour diffusion. The dotted line represents the initial cell density (CFU/mL) at 0 h (• • •). The cell density of samples taken after 5 days of incubation (▲) was investigated. Shown cell densities are the mean of analysis of three 5 mL cultures cultivated together in one reactor, respectively. Standard deviations are shown.

3.4.3 Degradation of α -D glucose by *R. wratislaviensis* Tol3 at different pressures from 1 to 154 bar

Possibly, pressure effects were specific to the toluene degradation pathway in *R. wratislaviensis* Tol3. However, high pressure also could have influenced the growth on a universal carbon source such as glucose. To clarify this question, *R. wratislaviensis* Tol3 was incubated for 5 days at RT with 1% (w/v) α -D glucose in 160 mL high pressure reactors at pressures ranging from 1 to 154 bar, as shown in Figure 3.30. On first sight, it seemed that an increasing pressure had a negative effect on growth but a positive effect on glucose degradation. However, the differences are not significant. Thus, only a trend can be supposed.

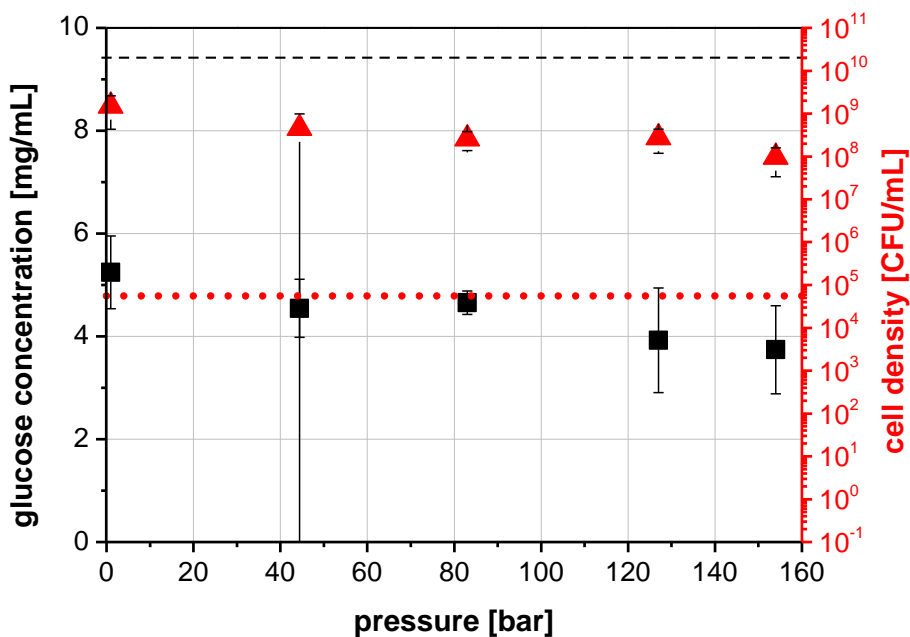


Figure 3.30: Degradation of 1% (w/v) α -D glucose by *R. wratislaviensis* Tol3 at RT at pressures in the range from 1 to 154 bar. The dotted line represents the initial cell density (CFU/mL, ● ● ●) and the dashed line represents the initial glucose concentration (mg/mL, — — —). The cell density (\blacktriangle) and the glucose concentration (\blacksquare) of samples taken after 5 days of incubation were investigated. Measured values are the mean of three 5 mL cultures incubated in one reactor. Standard deviations are shown.

3.4.4 Investigation of the influence of toluene concentration on the growth of *R. wratislaviensis* Tol3

The hypothesis was examined that the solution of nitrogen in liquid toluene led to a lowered toluene vapour pressure and a low toluene concentration in the culture medium, which was preferred by *R. wratislaviensis* Tol3 (see Discussion Chapter 4.3.1). At 1 bar and RT, a vial with the culture and a smaller open vial with a mixture of toluene and decalin were placed inside an airtight Erlenmeyer flask, which had a comparable volume like the 160 mL high pressure reactors. The toluene/decalin mixture had lower vapour pressure than the pure toluene. Different ratios of toluene to decalin were tested. The cultures were incubated for 7 days at ambient pressure. The results (Figure 3.31) showed that with increasing amount of decalin the OD and thus growth of the strain increased significantly. The bacteria seemed to prefer low toluene concentrations.

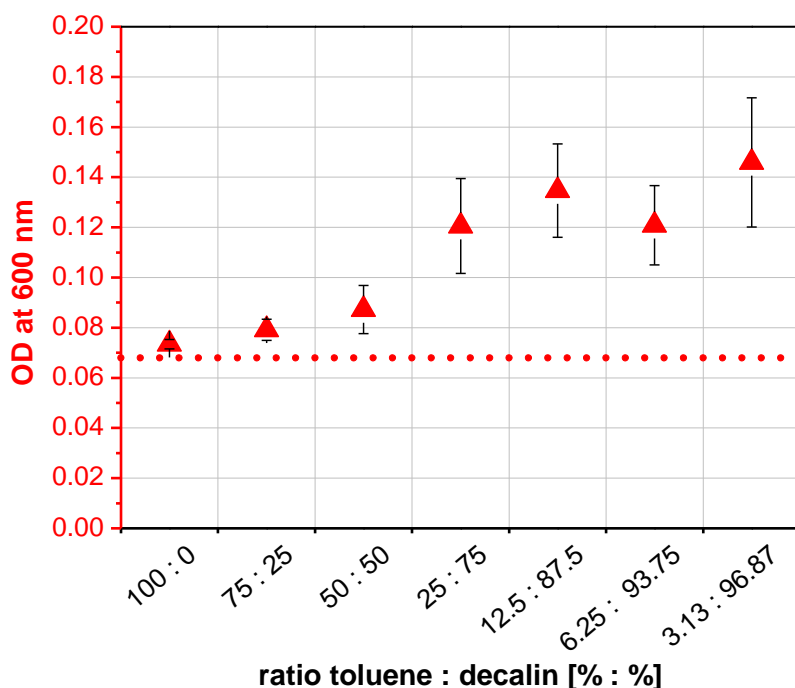


Figure 3.31: Optical density (▲) of *R. wratislaviensis* Tol3 incubated with toluene at 1 bar and RT after 7 days of incubation. The dotted line represents the initial cell density (CFU/mL) (● ● ●). Toluene was provided via vapour diffusion in an extra beaker next to the culture vial. Toluene was mixed at different ratios with decalin to lower the vapour pressure. Measured values are the mean of three 5 mL cultures incubated in one Erlenmeyer flask. Standard deviations are shown.

3.4.5 Growth of *D. aurantiaca* C7.oil.2 with toluene at ambient and high pressure at 4°C

The strain *D. aurantiaca* C7.oil.2, indigenous in the GoM, was incubated at 4°C in 160 mL high pressure reactors at 142 bar and in the ambient pressure reference reactors at 1 bar. At 142 bar, cells grew slightly and slowly, while at 1 bar no growth was observed (Figure 3.32). *D. aurantiaca* C7.oil.2 reached a 1.8×10^4 -fold higher final cell number in the incubation at 142 bar than in the incubation at 1 bar. This phenomenon, which was already observed in above described experiments with *R. qingshengii* Tol3 incubated on toluene (Chapters 3.4.1 and 3.4.2), is contradictory, since the preculture, used to inoculate the experiment, grew well at ambient pressure.

After this experiment, it seemed that the investigated strain was again contaminated, although it had already been purified, as described in Chapter 3.3.4. On agar plates, besides the coral-red colonies, which are typical for *Dietzia* sp. (Koerner *et al.* 2009), there were colonies of other morphologies. Consequently, the strain was purified again using streak

plate technique. To verify the strain's identity, cells from isolated red and orange colonies were used as template for Colony PCR to amplify the 16S-rDNA. The PCR-products were purified and sequenced. All analysed colonies were identified as *Dietzia aurantiaca*, which leads to the conclusion that this strain has a phenotypic heterogeneity of colonies. As described in the review of Ackermann (2015), some bacterial species can show several colony phenotypes.

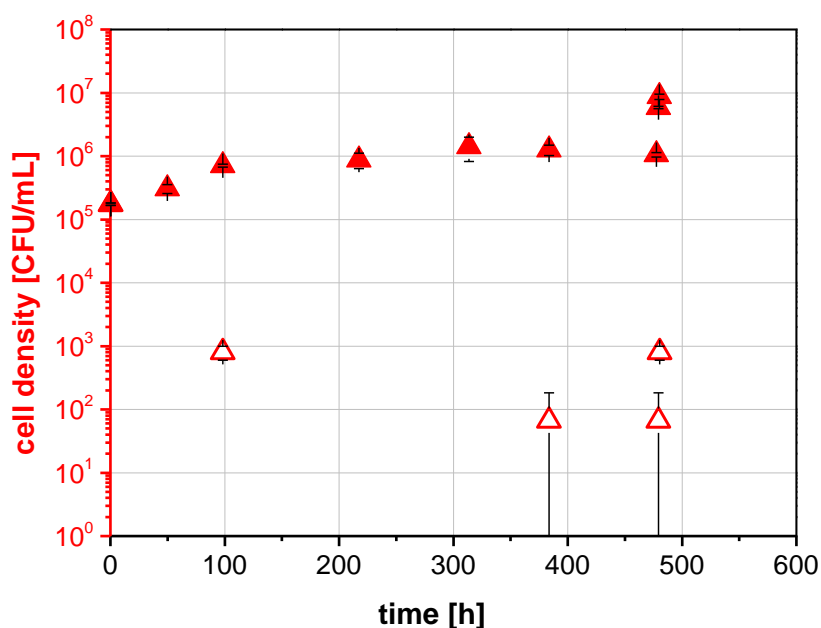


Figure 3.32: Growth of *D. aurantiaca* C7.oil.2 with toluene provided via vapour diffusion at 1 vs. 142 bar at 4°C. Cell density (CFU/mL) at 1 bar (Δ) and 142 bar (\blacktriangle) was determined in triplicate and standard deviations are shown. In incubations at 1 bar, no living cells were counted after 50, 218, 314 and 478 h of incubation. This cannot be displayed in logarithmic scale (Bachelor thesis of Alexandra Buck-Emden 2015).

3.5 Biodegradation of a PAH at ambient and high pressure

S. yanoikuyae B1 was used as a model bacterium to determine the degradation of PAHs at ambient and high pressure in ambient pressure reference and 160 mL high pressure reactors as well as in the high pressure view cell reactor No. 1. Naphthalene served as representative of the PAHs.

3.5.1 Degradation of naphthalene by *S. yanoikuyae* B1 at ambient and high pressure

When *S. yanoikuyae* B1 was incubated at RT with 1.77 mM naphthalene at 139 bar in 160 mL high pressure reactors, the growth was strongly inhibited. The growth rate at ambient pressure, in the exponential phase from 15 to 28 h, was 0.332 h^{-1} , whereas at high pressure, cell density decreased after 15 h cultivation time and no living cells were counted after 66 h. At ambient pressure, the naphthalene was degraded completely at a rate of 0.064 mM/h , from 7 to 19 h (Figure 3.33). Since the bacteria showed no growth at 139 bar, it could be expected that there would be no naphthalene conversion at all. However, a decrease of the naphthalene concentration in the medium was observed. The naphthalene was converted with a rate of 0.054 mM/h , from 7 to 25 h of incubation. After 75 h, 96.6% of the initial naphthalene was converted at 139 bar. In contrast to the culture medium, incubated at ambient pressure, which only changed its colour from transparent to light yellow, the culture medium turned brown in the incubation at 139 bar (Figure 3.34).

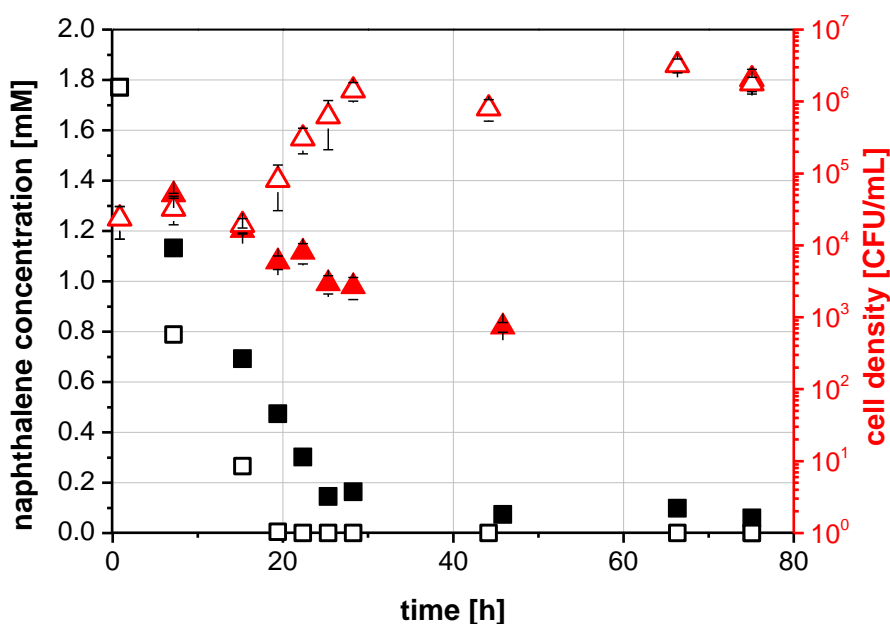


Figure 3.33: Conversion of 1.77 mM naphthalene by *S. yanoikuyae* B1 at RT at 1 vs. 139 bar. Naphthalene concentration (mM) was determined at 1 bar (□) and 139 bar (■). Cell density (CFU/mL) at 1 bar (△) and 139 bar (▲) was determined in triplicate and standard deviations are shown. In incubations at 139 bar, no living cells were counted at 66 h and later. This cannot be displayed in logarithmic scale (Bachelor thesis of Robert Hiessl 2014).

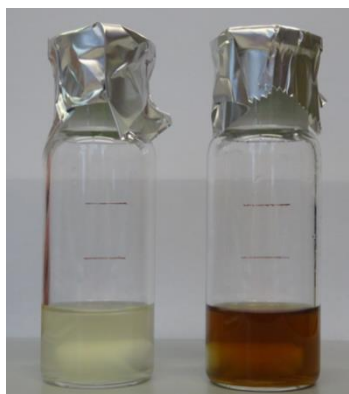


Figure 3.34: Left: turbid, grown *S. yanoikuyae* B1 culture after incubation with naphthalene at 1 bar. Right: clear, brown *S. yanoikuyae* B1 culture after incubation with naphthalene at 139 bar (Bachelor thesis of Robert Hiessl 2014).

3.5.2 Incubation of naphthalene without bacteria at ambient and high pressure

In a control experiment, naphthalene was incubated at RT in Brunner mineral medium without bacteria at 1 and 142 bar in ambient pressure reference and 160 mL high pressure reactors (Figure 3.35). At high pressure, only 20.77% of the initial naphthalene was lost after 451 h. In the incubation at ambient pressure, 25.34% of the initial naphthalene was lost. The difference in losses at 1 and 142 bar is not significant. The medium did not change its colour, neither in the incubation at 1 bar nor at 142 bar.

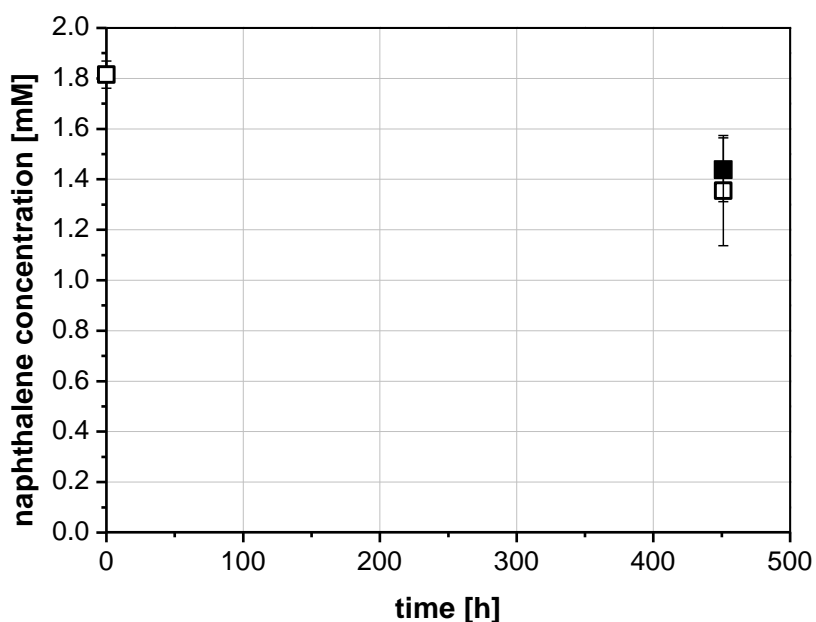


Figure 3.35: Concentration of naphthalene (mM) after incubation of initially 1.77 mM naphthalene in Brunner mineral medium without bacterial inoculum at RT at 1 bar (\square) and 142 bar (\blacksquare). Shown naphthalene concentrations are the mean of analysis of five reactors, respectively. Standard deviations are shown.

3.5.3 Degradation of naphthalene by *S. yanoikuyae* B1 at different pressures from 1 to 130 bar

To determine the maximum pressure up to which growth of *S. yanoikuyae* B1 was possible, the strain was incubated at RT with naphthalene at different pressures, ranging from 1 to 130 bar, in the 160 mL high pressure reactors for 70 h. At pressures between 1 and 88 bar, the cell density remained more or less constant (Figure 3.36). But above this pressure, the cell density decreased markedly. No growth was observed anymore when pressures of 120 bar were reached or exceeded, since viable cell counts dropped below starting values.

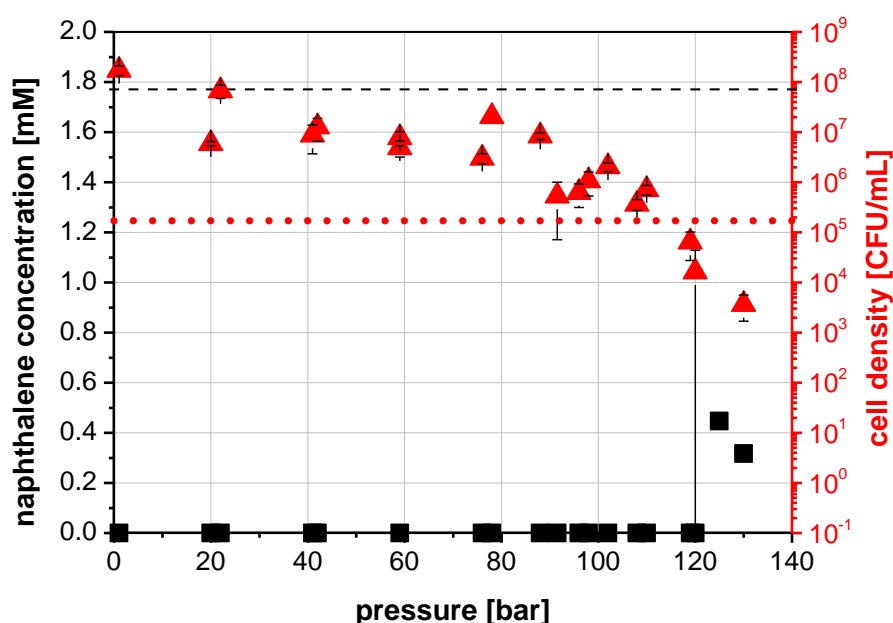


Figure 3.36: Cell density (CFU/mL, ▲) and concentration of remaining naphthalene (mM, ■) after 70 h of incubation of *S. yanoikuyae* B1 cultures with naphthalene at RT at different pressures. The starting cell density is indicated by a dotted line (•••) and the starting naphthalene concentration is indicated by a dashed line (— — —). In the incubation at 125 bar, no living cells were counted after 70 h of incubation. This cannot be displayed in logarithmic scale. Cell density was determined in triplicate and standard deviations are shown (Bachelor thesis of Robert Hiessl 2014).

However, up to pressures of 120 bar, the concentration of naphthalene dropped to below detection limit. Although no growth was observed here, in incubations at 125 and 130 bar, 25.2 and 17.9% of the initial naphthalene concentration remained. At pressures below

120 bar, the colour of the medium turned to a light yellow, whereas above this critical pressure, the colour changed to a dark brown. The results of Chapters 3.5.1 to 3.5.3 were published in Schedler *et al.* 2014.

3.5.4 Investigation of O₂ consumption and CO₂ production by *S. yanoikuyae* B1 growing with naphthalene at ambient and high pressure

S. yanoikuyae B1 was incubated at RT at 1 and at 162 bar (Figure 3.37). The oxygen sensor Fibox 3 and the carbon dioxide sensor pCO₂ mini from PreSens Precision Sensing GmbH (Regensburg, Germany), installed in the high pressure view cell reactor No. 1, were used to monitor oxygen consumption and carbon dioxide production. Again, no growth was observed at high pressure in comparison to ambient pressure. However, a slow consumption of O₂ and a slow production of CO₂ were measured at high pressure. At 1 bar, oxygen was consumed at a rate of 1.39% O₂/h (from 5 to 40 h), whereas at 162 bar oxygen

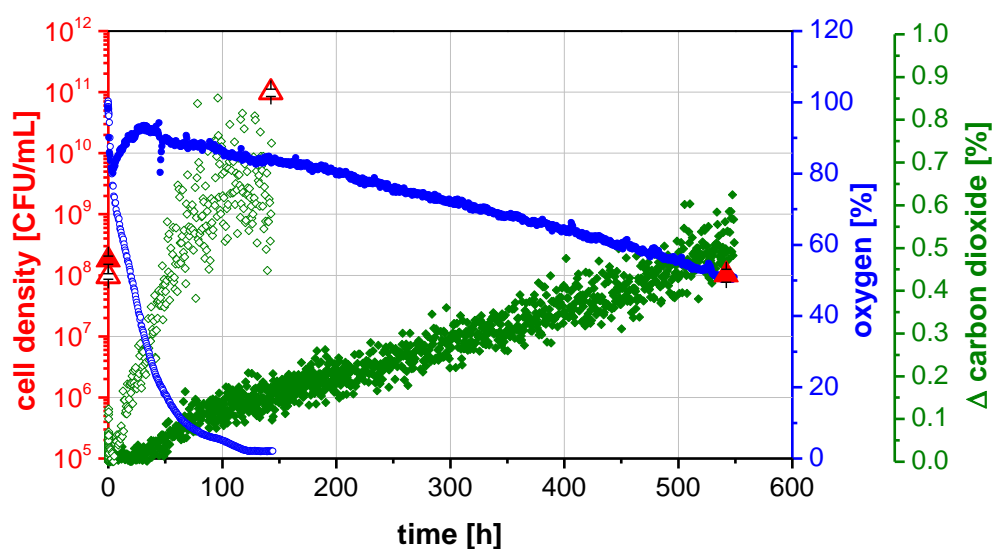


Figure 3.37: Conversion of 1.77 mM naphthalene by *S. yanoikuyae* B1 at RT at 1 vs. 162 bar. Cell density (CFU/mL) was investigated at 1 bar (Δ) and 162 bar (\blacktriangle). O₂ partial pressure (%) was measured at 1 bar (\circ) and 162 bar (\bullet). Difference of CO₂ partial pressure (final minus initial CO₂ partial pressure, in Δ %) was measured at 1 bar (\diamond) and 162 bar (\blacklozenge). Reactions were monitored with O₂ sensor Fibox 3 and pCO₂ mini from PreSens Precision Sensing GmbH in the gaseous phase. 100% of oxygen corresponds to 20.95% oxygen in air. Cell density was determined in triplicate and standard deviations are shown.

was consumed at a rate of 0.08% O₂/h (from 100 to 500 h). At 1 bar, carbon dioxide was produced at a rate of 0.009% CO₂/h (from 5 to 40 h), while at 162 bar it was produced at a rate of 0.0009% CO₂/h (from 100 to 500 h). At ambient pressure after about 100 h, the O₂ and CO₂ partial pressures stopped declining and rising. However, at 162 bar constant O₂ and CO₂ partial pressures were not monitored, since the experiment was abandoned too early.

3.5.5 Analysis of brown culture medium from incubation of *S. yanoikuyae* B1 with naphthalene at high pressure

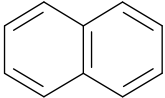
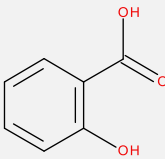
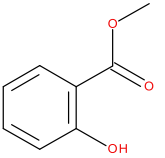
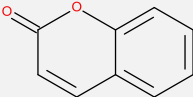
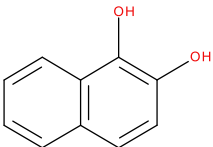
The accumulation of hydroxylated intermediates of the naphthalene degradation pathway could have led to the brown colour of the culture medium, which appeared when *S. yanoikuyae* B1 was incubated with naphthalene at high pressure. To determine whether mono- or dihydroxylated compounds accumulated, the colourimetric test of Arnow (1937) was carried out. A yellow colour was observed after addition of the acid and the nitrite/molybdate reagent, but no colour change to red appeared after addition of NaOH. At 512 nm, no peak was observed in photometric measurements. These results indicate that probably no dihydroxylated compounds (such as catechol or 1,2-dihydroxynaphthalene) were accumulated, but possibly monohydroxylated compounds (such as salicylate or monohydroxynaphthalene). However, it was difficult to evaluate colour changes in this test since the medium was already brownish from the beginning.

To determine whether the reason for the formation of the brown colour was the accumulation of intermediates of the naphthalene degradation pathway, the culture medium of an incubation of *S. yanoikuyae* B1 at 150 bar with naphthalene was extracted with dichloromethane. The brown colour was not transferred completely into the solvent, but a part of it stayed in the medium. The extract was analysed⁸ using GC-MS. The intermediates of the naphthalene degradation pathway found are shown in Table 3.1. Starting from an initial naphthalene mass of 45 mg in the medium, a residual mass of 3.13 mg naphthalene was measured at the end of cultivation. Thus, 93% of the original naphthalene was converted after 192 h of incubation. The most abundant peak of intermediates was salicylic acid, of which 39.92 mg were found in the medium at the end of the incubation by photometric analysis. Furthermore, traces of other intermediates of the

⁸ The extract was kindly analysed by Dr. Jagos Radovic and Prof. Dr. Thomas Oldenburg from University of Calgary, Canada.

naphthalene degradation pathway, such as methyl salicylate, coumarin and dihydroxynaphthalene, were detected by GC-MS.

Table 3.1: Tentatively identified intermediates, sorted by peak abundance from highest to lowest. Compounds were identified by GC-MS analysis of extracted brown medium from incubation of *S. yanoikuyae* B1 with naphthalene at 150 bar (analysis made by Dr. Jagos Radovic and Prof. Dr. Thomas Oldenburg, University of Calgary, Canada). Mass of salicylic acid was determined photometrically.

Intermediate	Structure	Mass of intermediate (mg) found at the end of incubation in 200 mL of culture medium with initial naphthalene mass of 45 mg
Naphthalene		3.13
Salicylic acid		39.92
Methyl salicylate		0.12
Coumarin		0.06
Dihydroxynaphthalene		not evaluated

3.5.6 Degradation of salicylic acid by *S. yanoikuyae* B1 at ambient and high pressure

Since a high amount of salicylic acid was found in the culture medium after incubation with naphthalene at high pressure, *S. yanoikuyae* B1 was incubated with 1.63 mM salicylic acid at 1 bar in ambient pressure reference reactors as well as at 148 bar in 160 mL high pressure reactors at RT (Figure 3.38). At ambient pressure, bacteria grew and the salicylic acid was nearly completely degraded so that only 1.6% of the initial salicylic acid was finally left. In contrast, at 148 bar salicylic acid was only slightly degraded and 81.9% of the initial salicylic acid was left at the end of the incubation. Despite minor degradation, no biomass formation was observed at high pressure. Instead, the viable cell counts dropped below starting cell density.

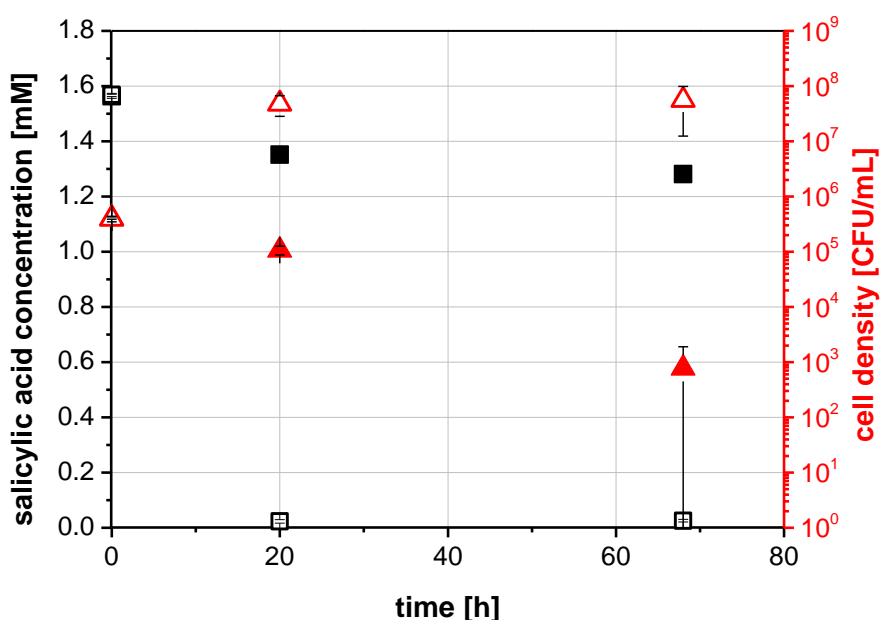


Figure 3.38: Degradation of 1.63 mM salicylic acid by *S. yanoikuyae* B1 at RT at 1 vs. 148 bar. Cell density (CFU/mL) was investigated at 1 bar (Δ) and 148 bar (\blacktriangle). Concentration of salicylic acid (mM) was investigated at 1 bar (\square) and 148 bar (\blacksquare). Shown data points are the mean of analysis of three reactors, respectively. Standard deviations are shown.

3.5.7 Degradation of α -D glucose by *S. yanoikuyae* B1 at ambient and high pressure

Possibly, pressure effects were specific to the naphthalene degradation pathway in *S. yanoikuyae* B1. However, high pressure also could have influenced the growth of the strain on a universal carbon source such as glucose. To clarify this question, *S. yanoikuyae* B1

was incubated at RT with 1% (w/v) α -D glucose in ambient pressure reference and 160 mL high pressure reactors at 1 and 156 bar (Figure 3.39). Similar to the growth with naphthalene, high pressure had a negative effect on the cell density when bacteria were grown on glucose. After 45.5 h the cell density increased at 1 bar, while at 156 bar cell density decreased and thus cells were dying. Furthermore, at 156 bar glucose was only slightly converted and 89.6% of the initial glucose concentration was left, whereas at 1 bar glucose was converted and 56.3% of the initial glucose concentration was left.

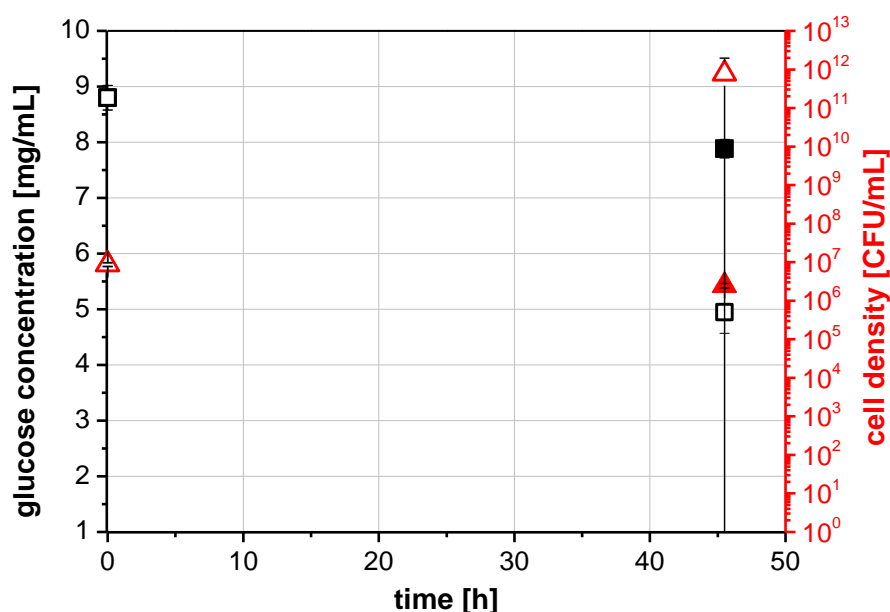


Figure 3.39: Degradation of 1% (w/v) α -D glucose by *S. yanoikuyae* B1 at RT at 1 vs. 156 bar. Cell density (CFU/mL) was investigated at 1 bar (Δ) and 156 bar (\blacktriangle). Glucose concentration (mg/mL) was investigated at 1 bar (\square) and 156 bar (\blacksquare). Shown values are the mean of three 5 mL cultures incubated in one reactor. Standard deviations are shown.

3.5.8 Influence of Corexit® EC9500A on degradation of naphthalene by *S. yanoikuyae* B1 at ambient and high pressure

The influence of Corexit® EC9500A on growth and naphthalene-conversion behaviour of *S. yanoikuyae* B1 was determined at RT at 149 bar in the 160 mL high pressure reactors and compared to results at 1 bar in the ambient pressure reference reactors. Inhibiting effects of high pressure observed in previous experiments (see Chapters 3.5.1 and 3.5.7) were confirmed by the results of this experiment (Figure 3.40 a and b). In contrast to the

incubation at 1 bar, at 149 bar the cell density of *S. yanoikuyae* B1 decreased and no living cells were observed at the end of the incubation. Furthermore, at 149 bar as well as at 1 bar naphthalene was converted, although at 149 bar the conversion was not complete and had a lower rate than at 1 bar. Equal to previous results, a change of colour of the medium from transparent to brown was observed in high pressure incubations. The growth curves show a slightly lower growth in incubations with Corexit® EC9500A (Figure 3.40 a) in comparison to incubations without Corexit® (Figure 3.40 b). However, this trend was not confirmed by the naphthalene conversion curves.

In previous experiments, a pressure of 120 bar was found to be the limit below which growth of *S. yanoikuyae* B1 was only slightly negatively affected. Hence, the experiment was repeated at 89 bar, to exclude the influence of pressure and evaluate the effects of Corexit® EC9500A (see Figure 3.41 a and b). No obvious effect of Corexit® EC9500A on growth and naphthalene conversion was observed at 89 bar. The growth was slightly better at 1 bar than at 89 bar.

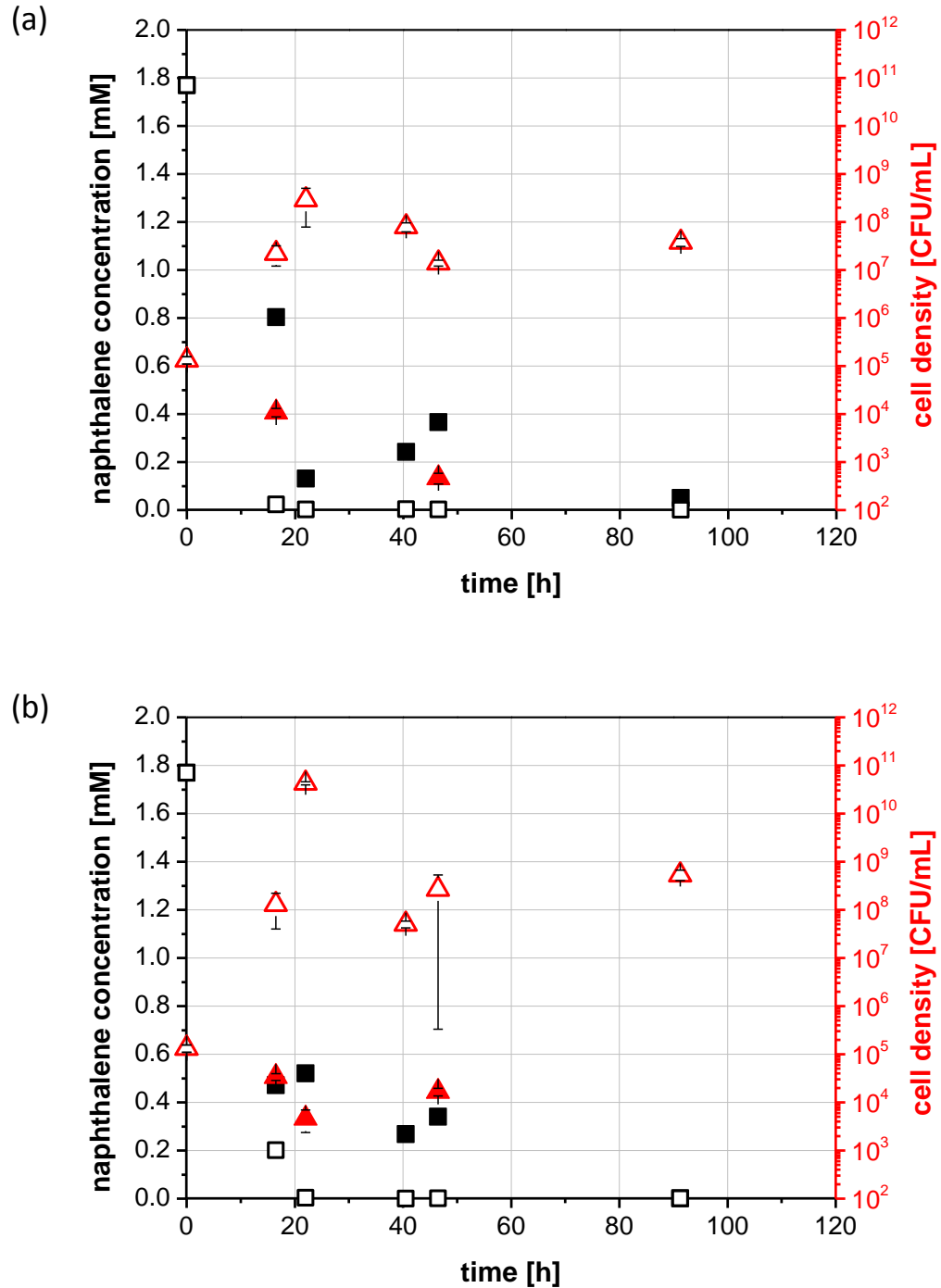


Figure 3.40: Conversion of 1.77 mM naphthalene by *S. yanoikuyae* B1 at RT (a) with vs. (b) without addition of Corexit® EC9500A at 1 vs. 149 bar. Cell density (CFU/mL) was investigated at ambient (Δ) and high pressure (\blacktriangle). Concentration of naphthalene (mM) was investigated at ambient (\square) and high pressure (\blacksquare). In incubations at 149 bar, no living cells were counted after 22, 40.5 and 91.15 h. This cannot be displayed in logarithmic scale. Cell density was determined in triplicate and standard deviations are shown (Bachelor thesis of Sabrina Felicitas Jesch 2015).

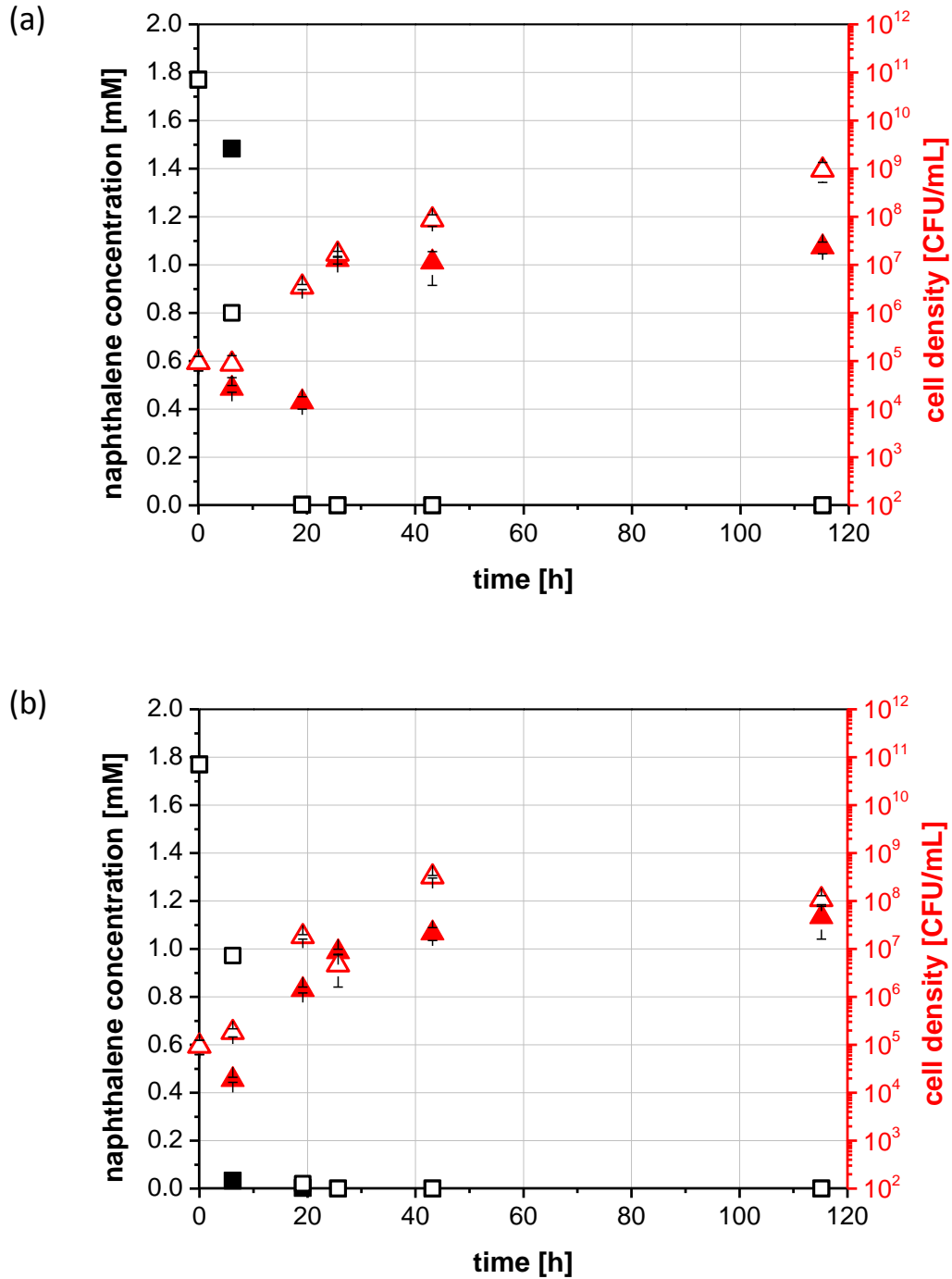


Figure 3.41: Conversion of 1.77 mM naphthalene by *S. yanoikuyae* B1 at RT (a) with vs. (b) without addition of Corexit® EC9500A at 1 vs. 89 bar. Cell density (CFU/mL) was investigated at ambient (Δ) and high pressure (\blacktriangle). Concentration of naphthalene (mM) was investigated at ambient (\square) and high pressure (\blacksquare). Cell density was determined in triplicate and standard deviations are shown (Bachelor thesis of Sabrina Felicitas Jesch 2015).

3.5.9 Growth of *S. yanoikuyae* B1 on Corexit® EC9500A at ambient and high pressure

The growth of *S. yanoikuyae* B1 on Corexit® EC9500A as sole source of carbon was tested at RT at 93 bar and compared to incubations at ambient pressure. As shown in Figure 3.42, the model strain showed a slight growth on the dispersant at both pressure conditions.

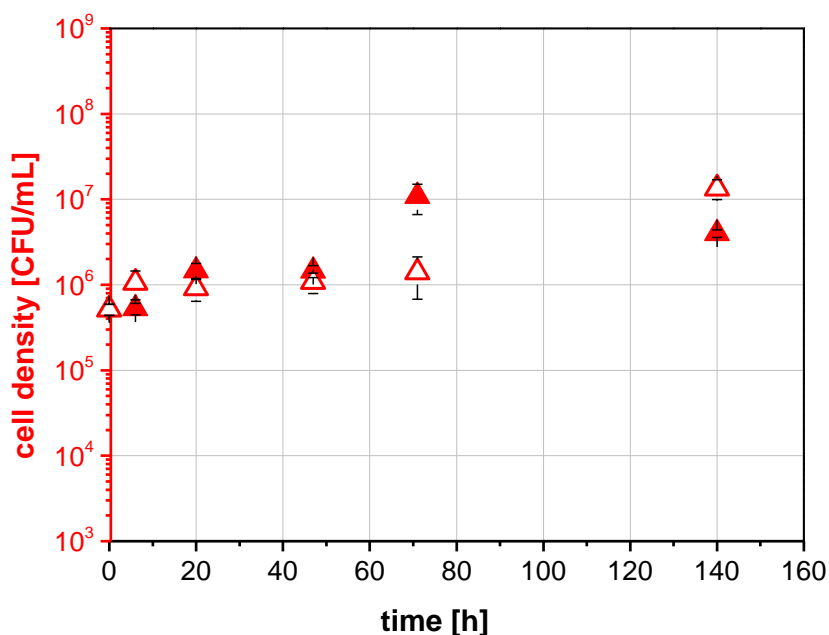


Figure 3.42: Cell density (CFU/mL) of *S. yanoikuyae* B1 growing on Corexit® EC9500A at RT at 1 bar (Δ) and 93 bar (▲). Cell density was determined in triplicate and standard deviations are shown (Bachelor thesis of Sabrina Felicitas Jesch 2015).

3.6 Biodegradation of Louisiana sweet crude oil and natural gas by bacterial communities from deep-sea sediments at ambient and high pressure

The degradation of Louisiana sweet crude oil and natural gas by bacterial communities from different surface sediments, which were sampled in the deep sea of the GoM, was investigated at ambient and deep-sea conditions. For the incubation, high pressure view cell reactors No. 1 and 2 as well as 160 mL high pressure reactors and ambient pressure reference reactors were used.

3.6.1 Comparison of the activity of bacterial communities from deep-sea sediments from 2010 and 2013 at different incubation conditions

Different deep-sea sediments from 2010 and 2013 were incubated in mineral minimal medium II with 0.1% (v/v) Louisiana sweet crude oil in high pressure view cell reactor No. 1 at different temperature, salinity and pressure conditions.

Sediment No. 4 (WB-1103-BC-DSH10), which was collected in August 2010, was incubated with crude oil at high pressure at different temperatures. The oxygen consumption curve of microorganisms in sediment No. 4 showed a shorter lag-phase when the sediment was incubated at 5°C than when it was incubated at 20°C (Figure 3.43 a and b).

Sediment No. 2 (WB-1110-MC-DSH08), which was sampled in December 2010, was incubated with crude oil at high pressure with different salt contents. A salt content of 3% (w/v) NaCl had a positive influence on the growth of the microorganisms in sediment No. 2. More oxygen was consumed and more carbon dioxide was produced than without addition of extra salt (Figure 3.44 a and b).

Sediment No. 3 from December 2010 (WB-1110-MC-DSH10) and No. 8 from August 2013 (WB-0813-MC-DSH10) were incubated with crude oil at different pressures, at 5°C and at a medium salt content of 3% (w/v) NaCl, as shown in Figure 3.45. The bacterial count of sediment No. 3 was higher and showed more culturable types of bacteria than that of sediment No. 8, for both 1 and 150 bar incubations. As shown in Figure 3.45 a, elevated pressure had a positive effect on the oxygen consumption and biomass production of sediment No. 3 from 2010. Sediment No. 8 was collected at the same sampling site, but 3 years later in August 2013. For sediment No. 8, the effect of pressure was reversed, but less distinct.

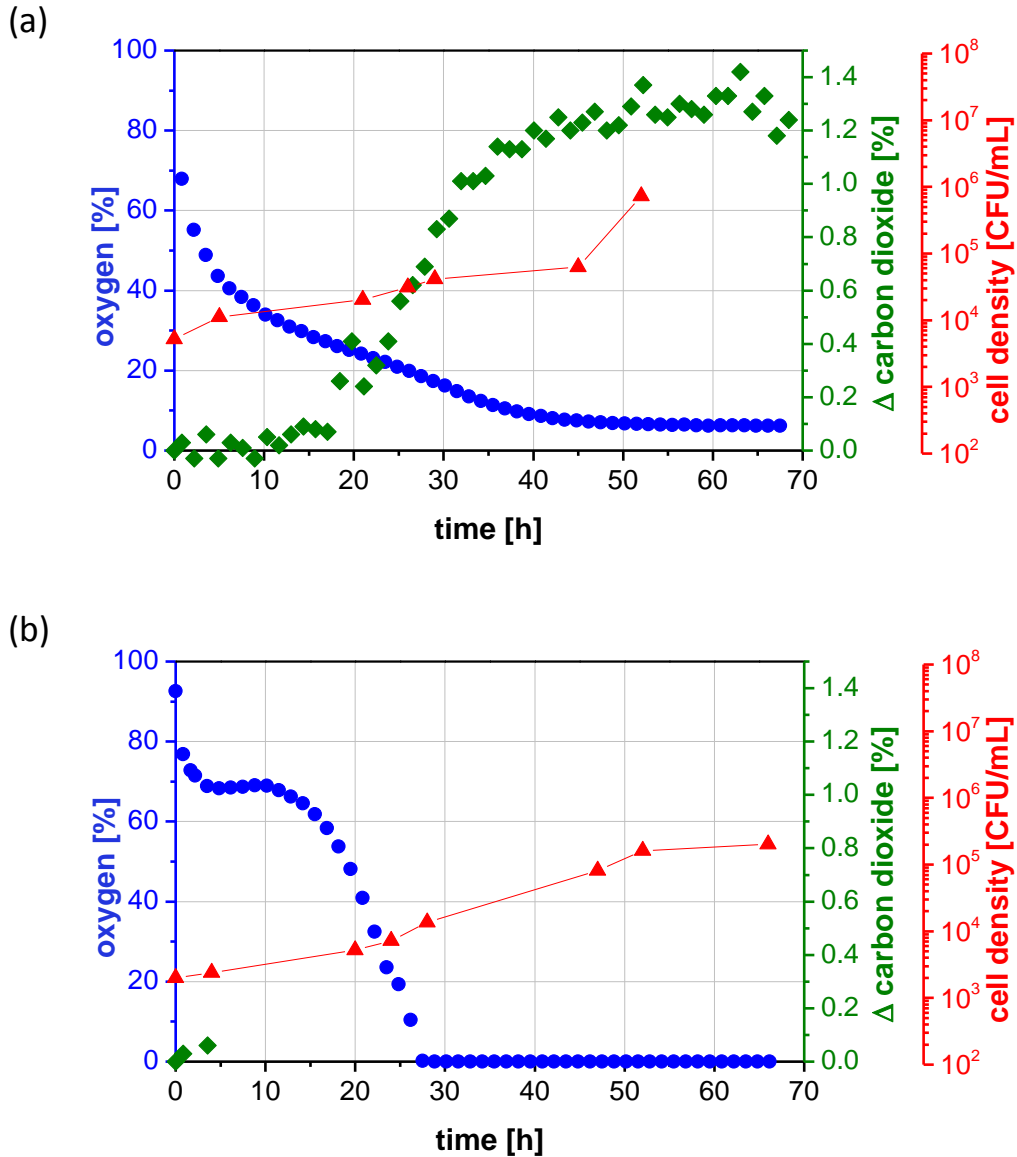


Figure 3.43: Incubation of sediment No. 4 (WB-1103-BC-DSH10) at 150 bar in MMII medium supplemented with crude oil at (a) 5°C vs. (b) 20°C. Cell density (\blacktriangle , in CFU/mL), oxygen partial pressure (\bullet , in %) and difference of carbon dioxide partial pressure (final minus initial partial pressure, \blacklozenge , in Δ %) were measured. Due to measurement problems, the carbon dioxide curve is missing in (b). Reactions were monitored with O₂ sensor Fibox 3 and pCO₂ mini from PreSens Precision Sensing GmbH in the gaseous phase. 100% of oxygen corresponds to 20.95% oxygen in air (Diploma thesis of Judit Martín Juárez 2014).

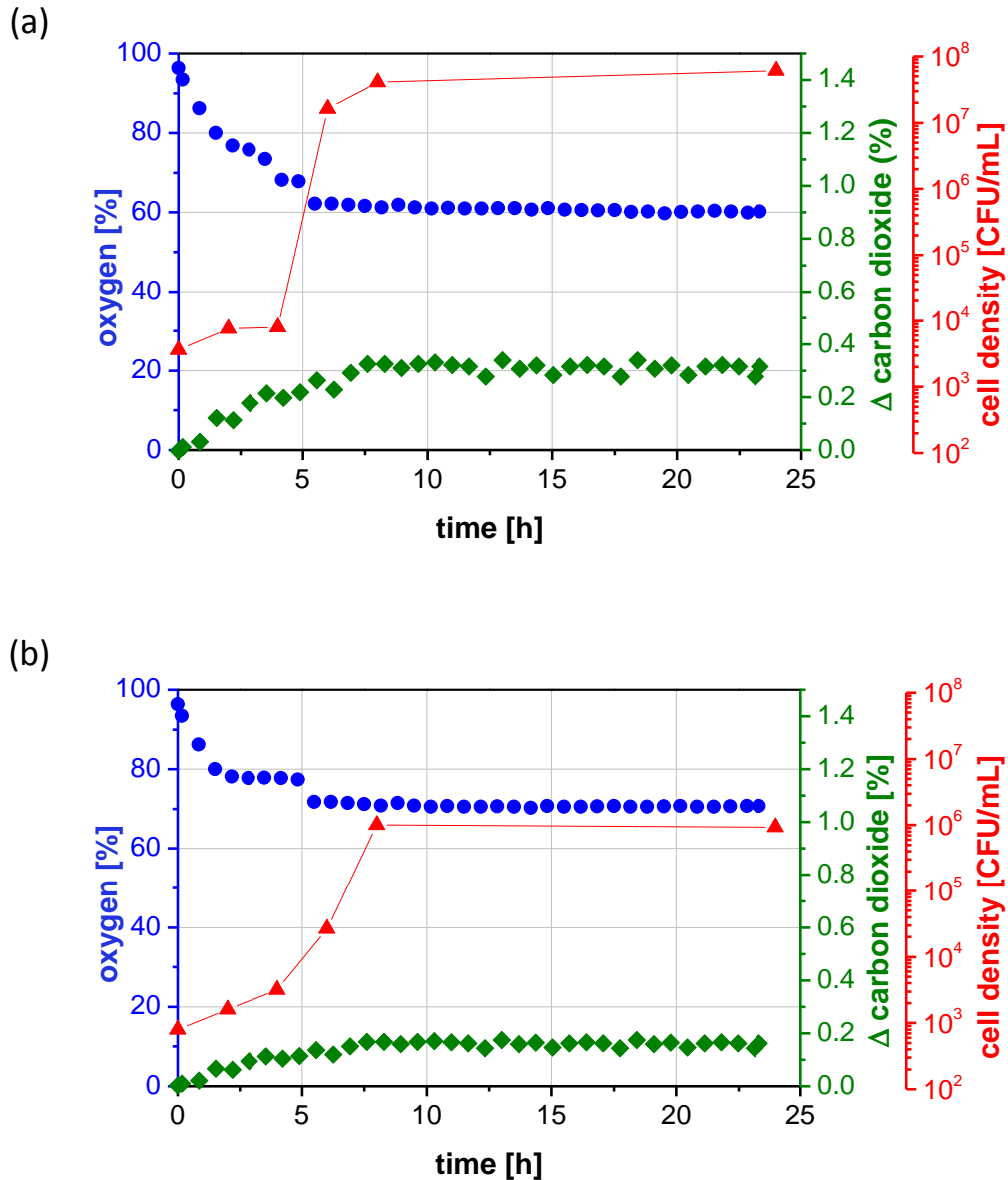


Figure 3.44: Incubation of sediment No. 2 (WB-1110-MC-DSH08) at 5°C and 150 bar in MMII medium with crude oil (a) with vs. (b) without addition of 3% (w/v) NaCl. Cell density (\blacktriangle , in CFU/mL), oxygen partial pressure (\bullet , in %) and difference of carbon dioxide partial pressure (final minus initial partial pressure, \blacklozenge , in $\Delta\%$) were measured. Reactions were monitored with O_2 sensor Fibox 3 and pCO_2 mini from PreSens Precision Sensing GmbH in the gaseous phase. 100% of oxygen corresponds to 20.95% oxygen in air (Diploma thesis of Judit Martín Juárez 2014).

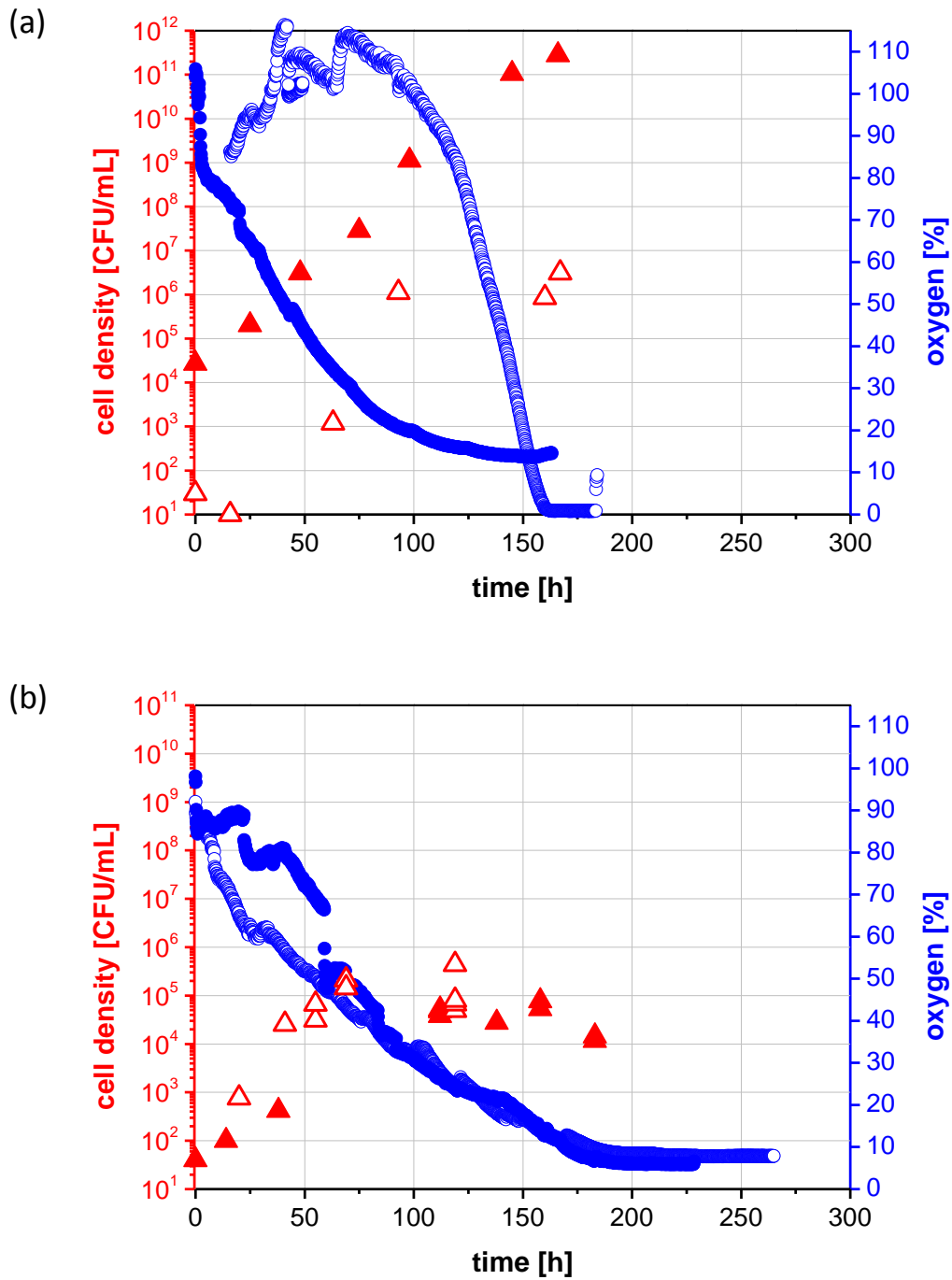


Figure 3.45: Cell density (CFU/mL) of incubations of sediment (a) No. 3 (WB-1110-MC-DSH10) and (b) No. 8 (WB-0813-MC-DSH10) at 5°C, in MMII with 3% (w/v) NaCl supplemented with Louisiana sweet crude oil, at 1 bar (Δ) vs. 150 bar (\blacktriangle). Oxygen partial pressure (%) at 1 bar (\circ) and 150 bar (\bullet) total pressure was measured with O₂ sensor Fibox 3 from PreSens Precision Sensing GmbH in the gaseous phase. 100% of oxygen corresponds to 20.95% oxygen in air (Project work of Eva Mong Su 2014).

3.6.2 Degradation of Louisiana sweet crude oil by bacterial communities from 2010 and 2013 sediments at ambient and high pressure

Deep-sea sediment No. 4 (WB-1103-BC-DSH10) from August 2010 was incubated with 0.1% (v/v) Louisiana sweet crude oil in the high pressure view cell reactor No. 2 at 1 and 150 bar at RT. These incubations were compared to incubations of deep-sea sediment No. 8 (WB-0813-MC-DSH10), which was collected at the same sampling site, but three years later in August 2013. Sediment No. 8 was incubated at RT with 0.1% (v/v) Louisiana sweet crude oil in 160 mL high pressure reactors at 144 bar and in ambient pressure reference reactors at 1 bar.

In the incubation of sediment No. 4, which was carried out by Dr. Ana Gabriela Valladares Juárez, oxygen and carbon dioxide were monitored in the liquid phase with the VisiSens™ O₂ and CO₂ sensors from PreSens Precision Sensing GmbH. Images of colour changes of the VisiSens™ oxygen-sensing patch during oxygen consumption are shown in Figure 3.15. Oxygen was consumed at rates of 0.07 mM/h (from 16 to 27 h) at 1 bar and 0.10 mM/h (from 10 to 17h) at 150 bar. After its depletion, oxygen concentration became stable at both pressures and carbon dioxide started to be produced exponentially (see Figure 3.46 a and b). In contrast to the incubation at 150 bar, at 1 bar the carbon dioxide production started after a delay of 29 h. In total, more carbon dioxide was produced in the 150 bar incubation than in the 1 bar incubation. In addition, carbon dioxide concentration increased faster at 150 bar than at 1 bar. The initial increases in oxygen concentration could have been caused by diffusion of oxygen from the gas phase into the liquid phase.

No subsamples, but an initial and an end sample were taken for analysis of bacterial growth. Corresponding to the decrease in oxygen concentration, the density of bacterial cells increased (Figure 3.47). In the 1 bar incubation, a higher final cell density (2×10^5 CFU/mL) was reached than in the 150 bar incubation (1×10^5 CFU/mL). In blank experiments (data not shown), where medium and crude oil were not inoculated with deep-sea sediment, the oxygen and carbon dioxide concentrations were constant and bacterial concentrations did not increase (Valladares Juárez *et al.* 2015).

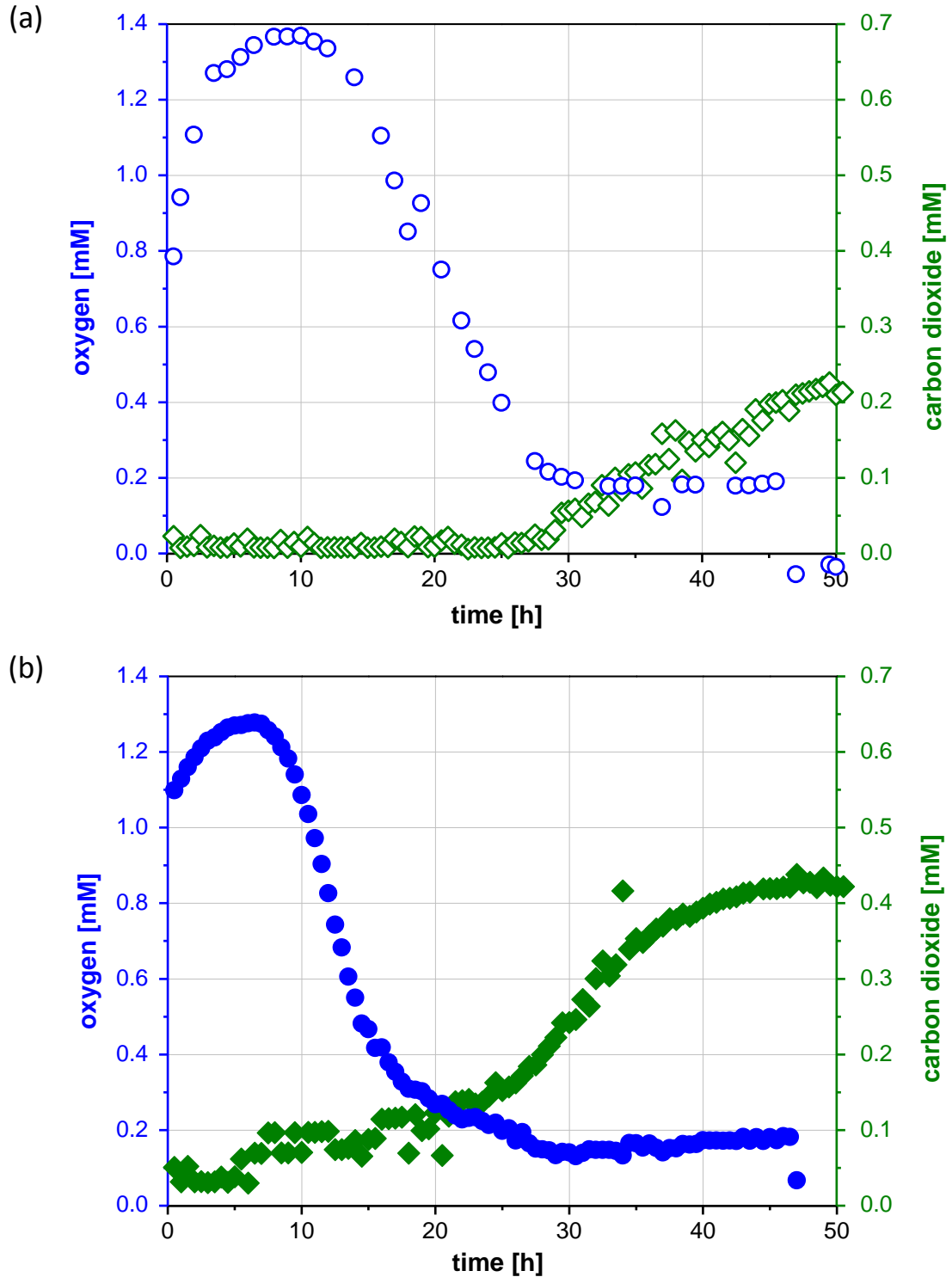


Figure 3.46: Incubation of sediment No. 4 (WB-1103-BC-DSH10) from August 2010 at RT with Louisiana sweet crude oil at (a) ambient vs. (b) high pressure. (a) Oxygen concentration (mM, ○) and carbon dioxide concentration (mM, ◇) were measured at 1 bar. (b) Oxygen concentration (mM, ●) and carbon dioxide concentration (mM, ◆) were measured at 150 bar. Oxygen and carbon dioxide were monitored in the liquid phase with the VisiSens™ O₂ and CO₂ sensors.

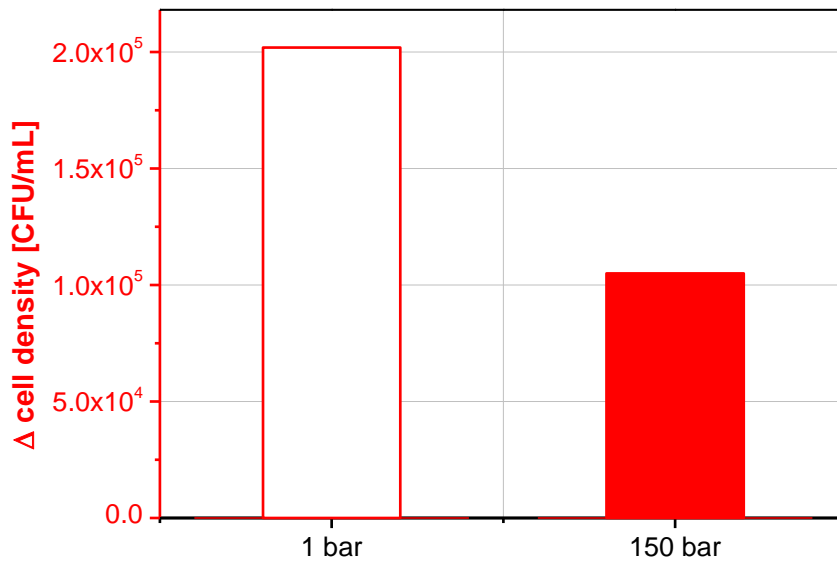


Figure 3.47: Difference of cell density (final minus initial cell density, in Δ CFU/mL) of incubations of sediment No. 4 (WB-1103-BC-DSH10) from August 2010 at RT with crude oil at 1 vs. 150 bar (Valladares Juárez *et al.* 2015).

Compared to the above described incubations of sediment No. 4, in the incubations of sediment No. 8 in 160 mL high pressure reactors the oxygen consumption was delayed (Figure 3.48). Incubations at both pressure conditions showed long lag-phases. The oxygen consumption curve of the incubation at 144 bar showed a longer lag-phase of about 150 h and a slower oxygen consumption rate of 1.22% O₂/h (in exponential phase from 150 to 220 h) compared to a lag-phase of about 120 h and a consumption rate of 1.64% O₂/h at 1 bar (in exponential phase from 120 to 160 h). At both pressure conditions, the cell density increased, but more biomass was produced in the 1 bar incubation. However, this difference in growth was not significant.

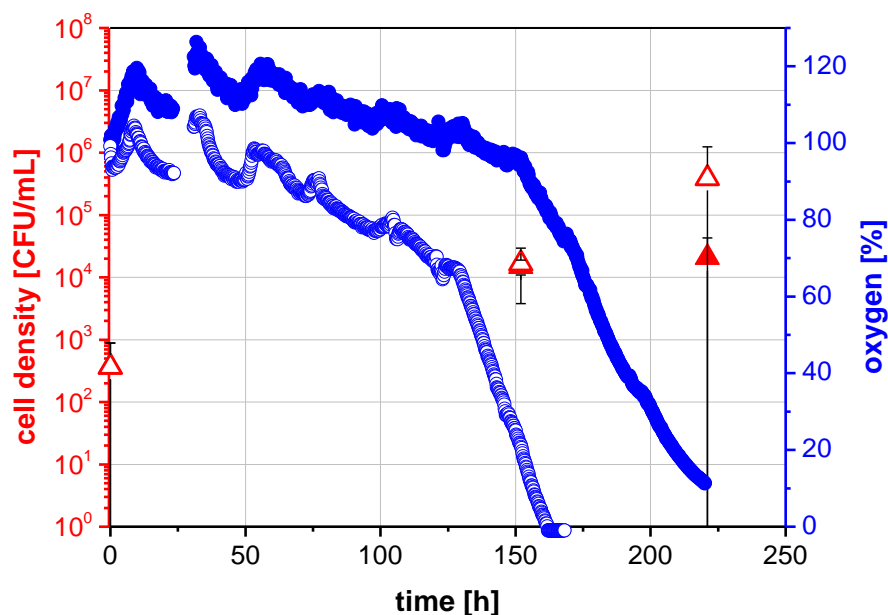


Figure 3.48: Incubation of sediment No. 8 (WB-0813-MC-DSH10) from August 2013 at RT with Louisiana sweet crude oil at ambient vs. high pressure. Cell density (CFU/mL) was investigated at 1 bar (Δ) and 144 bar (\blacktriangle). The cell density at 0 h is the mean of two reactors, at 152 h of four reactors and at 221 h of five or six reactors. Standard deviations are shown. Oxygen partial pressure (%) at 1 bar (\circ) and 144 bar (\bullet) total pressure was measured with O_2 sensors from Ocean Optics GmbH in the gaseous phase. 100% of oxygen corresponds to 20.95% oxygen in air.

3.6.2.1 Analysis of pressure influence on community composition

Samples of the incubations of the sediments No. 4 (from 2010) and No. 8 (from 2013), which were described in the previous subsection, were sent to project partners Prof. Dr. Katherine Freeman and Dr. Sara Lincoln from Pennsylvania State University, USA. To examine changes in the bacterial community composition during biodegradation and to examine differences under low and high pressure, they carried out 16S rDNA amplicon sequencing.

As shown in Figure 3.49, for the 2010 sediment in the 1 bar incubation the diversity declined and at the end, Proteobacteria and Firmicutes dominated. At 150 bar, Acidobacteria declined and Proteobacteria increased at the end. For the 2013 sediment, at 1 bar there was a low initial diversity and finally Proteobacteria and Firmicutes dominated. At 150 bar, Firmicutes declined and Proteobacteria increased.

Results

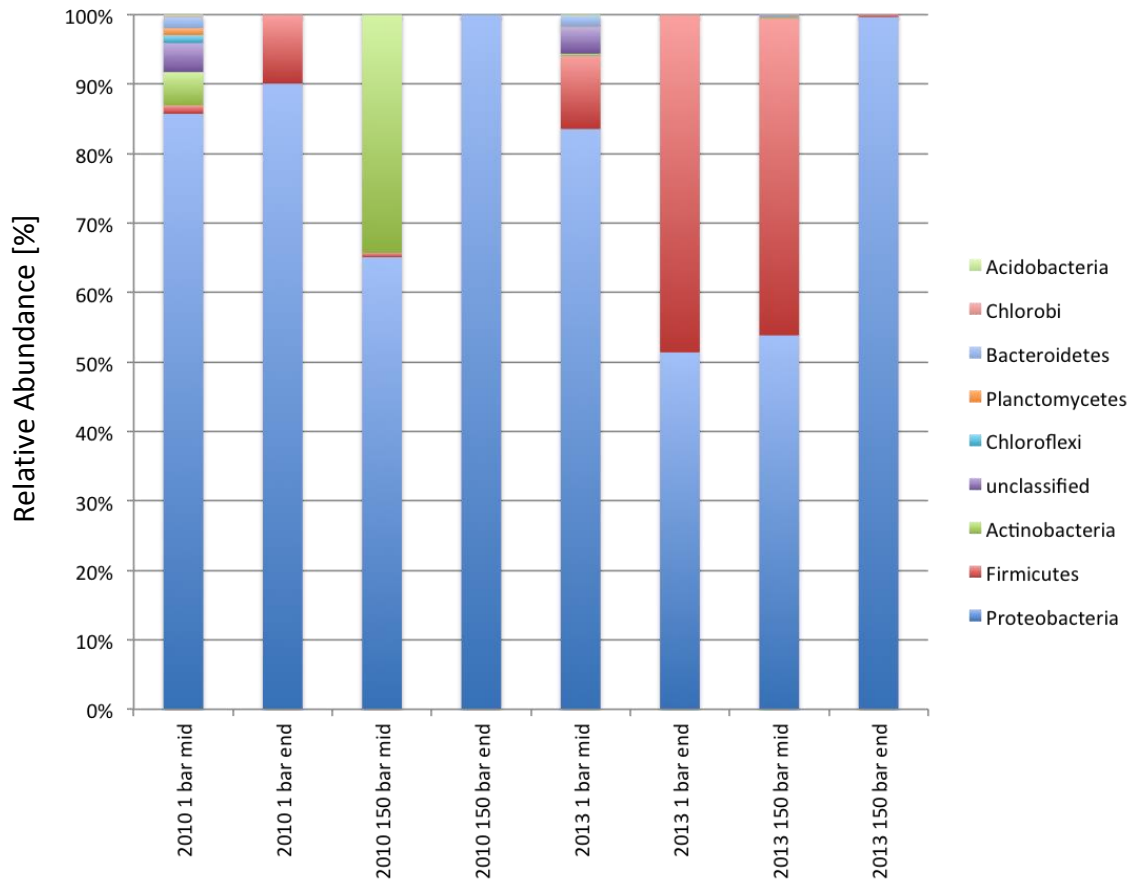


Figure 3.49: Preliminary analysis of community composition in samples from incubations of sediments No. 4 (WB-1103-BC-DSH10) and 8 (WB-0813-MC-DSH10) at 1 vs. 150 bar. The relative abundance (%) of different phylogenetic groups in the samples was analysed.

The tree diagram in Figure 3.50 describes how related the composition of different bacteria in each sample is to the other duplicate- or triplicate-samples of one time/pressure point and also to all other samples. This tree is not a traditional phylogenetic tree, showing the position of organisms, and does not relate to the bar diagram of phyla in Figure 3.49, but it is a tree diagram for whole communities and compares operational taxonomic units, which are clusters based on similarity of sequences.

These community analyses were only preliminary and further analyses are needed to get a more complete picture of the influence of high pressure on bacterial community composition.

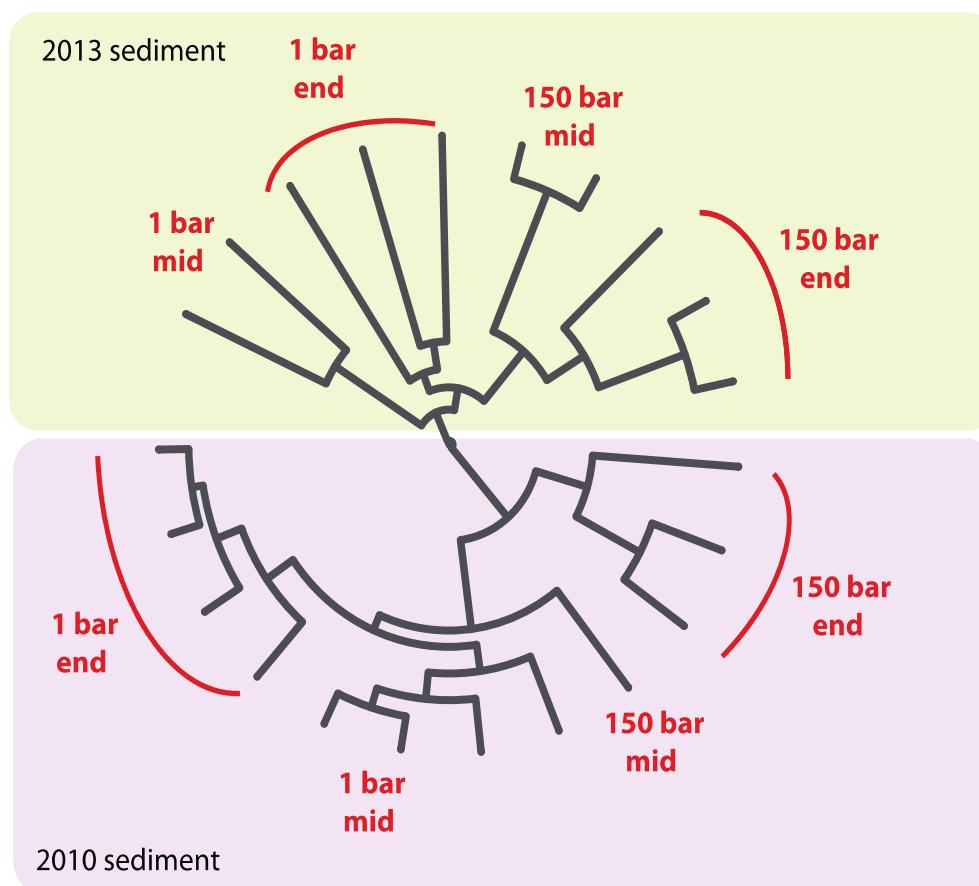


Figure 3.50: Preliminary analysis of community composition in samples from incubations of sediments No. 4 (WB-1103-BC-DSH10) and 8 (WB-0813-MC-DSH10) at 1 and 150 bar. The tree diagram describes the dissimilarity among multiple groups. Ends of the branches represent the different analysed samples. Branch length is meaningful, but none of the concentric connecting lines are. (Unpublished work of Dr. Sara Lincoln and Prof. Dr. Katherine Freeman, Pennsylvania State University, USA).

3.6.3 Degradation of natural gas and crude oil by bacterial communities from a 2010 sediment at ambient and high pressure

Deep-sea sediment No. 4 (WB1103-BC-DSH10) was incubated with Louisiana sweet crude oil at 1 and 153 bar. In addition, it was incubated with natural gas, consisting primarily of methane, as sole source of energy and carbon at 1 and 148 bar at RT in high pressure view cell reactor No. 2. Oxygen consumption rates were monitored online with the O₂ measurement system Fibox 3 from PreSens Precision Sensing GmbH.

In the incubations with crude oil and natural gas, at high pressure oxygen was used up very fast in about 40 h (Figure 3.52 a and b). The consumption rate in the incubation with

crude oil at 153 bar was 6% O₂/h (in the exponential phase from 18 to 23 h) and 6.9% O₂/h in the incubation with natural gas at 148 bar (in the exponential phase from 8 to 15 h). In the experiment at 1 bar with crude oil, a steep oxygen increase occurred at 25 h. In contrast, the oxygen consumption at 1 bar in the experiment with natural gas was very slow and incomplete with an interrupted and atypical course. Thus, in both ambient pressure incubations problems with the oxygen sensors occurred, which could be due to an accidental movement of the sensor, mistakes in the calibration or disturbances by light.

End samples were analysed by DGGE population analysis (jointly with Prof. Dr. Grossart, IGB Neuglobsow). Unfortunately, a mistake occurred and the sample from incubation with crude oil at 153 bar was lost. As shown in Figure 3.51, DGGE analysis revealed that in the bacterial consortium of the analysed sediment No. 4 different bacterial strains were found to be prominent in incubations with crude oil and in the incubations with natural gas. Moreover, some bands were stronger pronounced in the samples filtered with 0.2 µm filters than in samples filtered with 5.0 µm filters and vice versa. Furthermore, different bacterial communities had developed in incubations of sediment No. 4 with natural gas at 1 bar compared to incubation at 148 bar. Thus, pressure had an effect on which strains were enriched with natural gas.

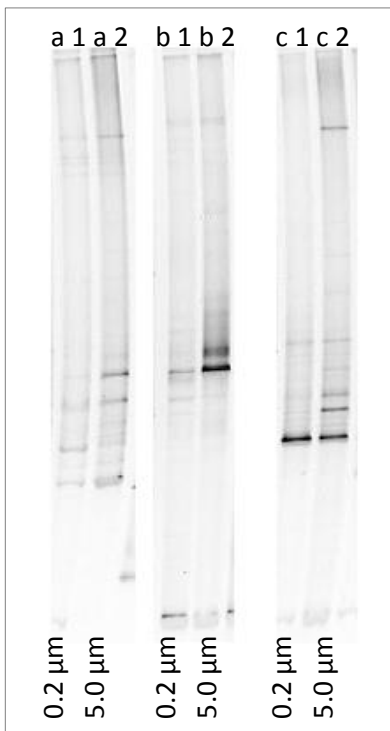


Figure 3.51: DGGE population analysis of incubations of deep-sea sediment No. 4 (WB1103-BC-DSH10) at RT with natural gas at (a) 1 bar and (b) 148 bar, and of incubations with crude oil at (c) 1 bar. DGGE analysis of incubation with crude oil at 153 bar is missing. In preparation for DGGE, samples were filtered at first with a (2) 5.0 µm filter and then with a (1) 0.2 µm filter.

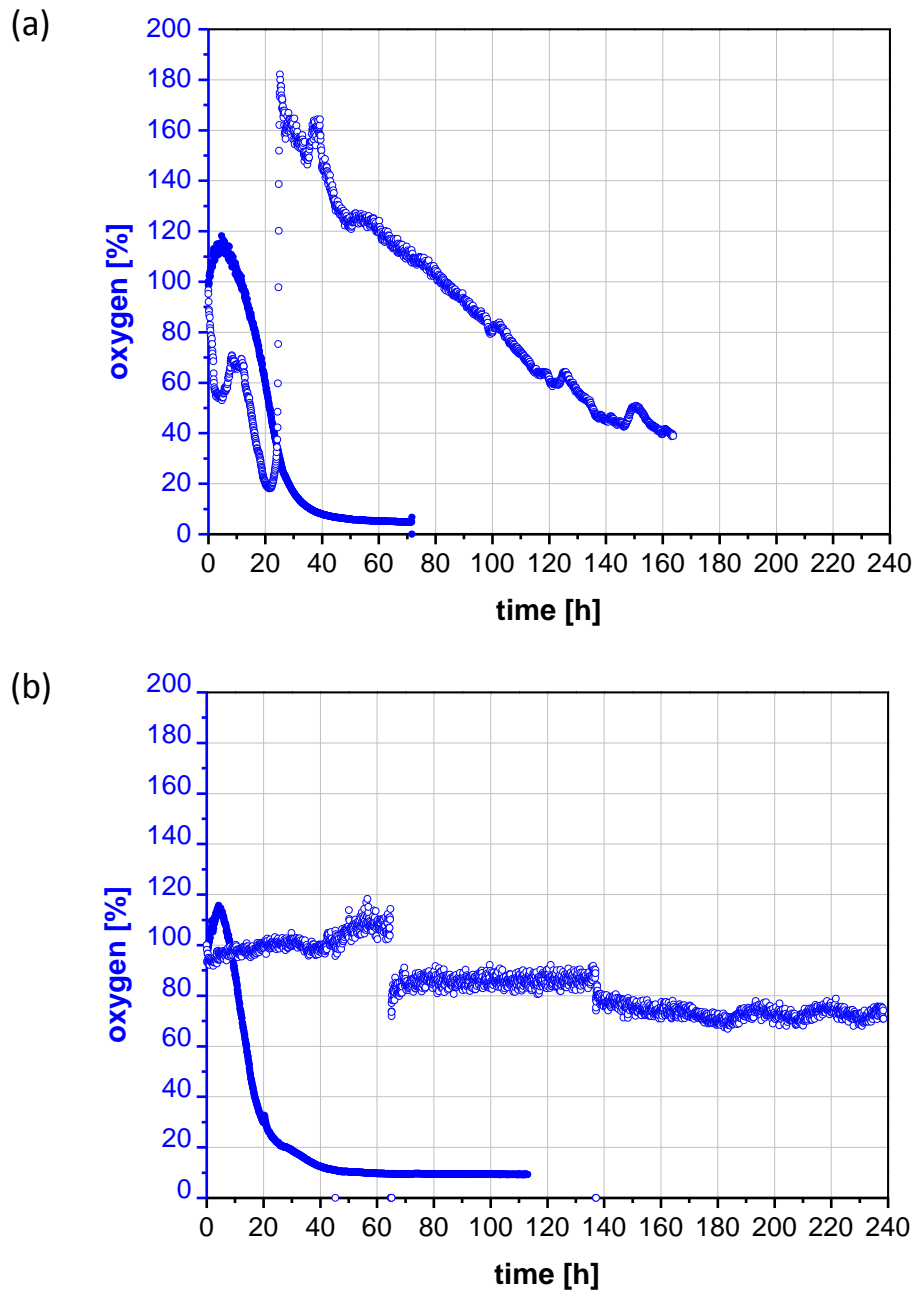


Figure 3.52: Oxygen consumption (oxygen partial pressure in %) of incubation of deep-sea sediment No. 4 (WB1103-BC-DSH10) at RT with (a) Louisiana sweet crude oil at 1 bar (○) vs. 153 bar (●) and (b) natural gas at 1 bar (○) vs. 148 bar (●). O₂ measured with fiber optic O₂ sensor Fibox 3 from PreSens Precision Sensing GmbH. 100% of oxygen corresponds to 20.95% oxygen in air (work of Ana Gabriela Valladares Juárez).

4 Discussion

4.1 Development and optimisation of the high pressure reactors

4.1.1 Optimisation of the oxygen concentration in a high pressure reactor for aerobic biodegradation

Bacteria can grow in a limited range of oxygen concentration. A too low oxygen concentration does not support growth of aerobic bacteria, whereas a too high oxygen concentration is toxic for bacteria. Generally, in the sea, water is saturated with oxygen along the water column. Consumption of oxygen in the water column is balanced by diffusion of oxygen from the atmosphere and sea currents. However, in a closed, completely medium-filled reactor setup, as described in Results Chapter 3.1.1, oxygen dissolved in the medium was not sufficient to permit growth of aerobic bacteria. Thus, an air cushion was needed in the reactor.

However, when the reactor was pressurised mechanically the oxygen partial pressure increased and bacterial growth was inhibited. The high pressure reactor with screw-piston mechanism was used to test the effect of elevated oxygen partial pressure on bacterial growth of the model strains *R. qingshengii* TUHH-12 and *E. coli* (see Results Chapter 3.1.3). *R. qingshengii* TUHH-12 had a slightly lower critical oxygen partial pressure when it was incubated on MMII with n-hexadecane than when it was incubated on LB medium. *E. coli* had a significantly lower critical oxygen partial pressure when it was incubated on MMII with glucose than when it was incubated on LB medium. Thus, the critical oxygen partial pressure was dependent of the respective bacterial strain and culture medium used. Wiseman *et al.* (1966), who tested the effect of hyperbaric oxygen on various bacteria, came to the same conclusion. In literature, much lower critical oxygen partial pressures can be found for growth of *E. coli* on complex media. While McAllister *et al.* (1963) found smaller or stunted colonies of *E. coli* at 1 or 2 bar oxygen compared to controls at 1 bar air on horse-blood-agar plates, Hopkinson and Towers (1963) reported that growth of *E. coli* was inhibited at 2 to 4 bar oxygen on solid medium. Wiseman *et al.* (1966), however, observed a maximum

growth of *E. coli* in liquid broth medium at 3 bar oxygen pressure, which was decreasing rapidly when this pressure was exceeded. As described in the review of Gottlieb (1971), various authors found that oxygen partial pressures of more than 1.3 bar are inhibiting for *E. coli*.

The results of the experiments made clear that for testing the effects of high pressure on the bacterial growth and degradation behaviour, mechanical pressurisation was not suitable. At very low total pressures, the oxygen partial pressure was already too high and inhibited the bacterial growth. However, when the limits of tolerable oxygen partial pressure are known, the initial oxygen partial pressure in an experiment can be adjusted optimally so that sufficient oxygen is available for degradation of hydrocarbons. Thus, anoxic states could be prevented, without poisoning the bacteria.

The problem of toxic oxygen partial pressures was overcome by pressurising the reactor with inert nitrogen gas instead of mechanical pressurisation. Thus, the oxygen partial pressure was kept constant and equivalent to the partial pressure at atmosphere.

4.1.2 Suggestions for the design of an ideal reactor for biodegradation experiments under deep-sea conditions

Resulting from the work of this thesis, the required abilities of a reactor optimal for high pressure biodegradation experiments came clear:

- Such an improved reactor needs to be made of stainless steel (type 1.4571) to avoid corrosion of the material during incubation of bacteria in aqueous media. However, contact between the salts-containing culture medium and the steel should be avoided, since stress corrosion cracking of stainless steel in the presence of chloride ions has been reported in literature (Rhodes 1969, Truman 1977). To avoid this and to ensure sterile conditions, the reactor should be equipped with a glass or Teflon vial, which can be autoclaved.
- Since stirring affects the oxygen supply in the medium and thus the biodegradation rates under aerobic conditions, mixing could be realised e.g. by a magnetic stirrer.
- To avoid de-/repressurisation cycles due to subsampling, oxygen consumption should be measured continuously using a probe, which is fitted into the reactor. The newly developed O₂ prototype sensor seems to be suitable.

- However, if cell density is meant to be monitored, subsampling is still needed. For this, a big culture volume of at least 500 mL would be ideal to have enough material for analysing growth and moreover for different analytical purposes e.g. for extraction of DNA from sediment incubations for community analysis and end-point oil analysis.

The 1 L high pressure reactor already meets the requirements mentioned above. However, certain improvements are desirable to design a reactor, which is ideal for high pressure biodegradation experiments:

- Actually, for calculation of degradation rates a functioning and reliable high pressure oxygen measurement system would be sufficient. However, a disadvantage of a one-pot-reactor-system like the 1 L high pressure reactor is that subsamples cannot be used for generation of a hydrocarbon degradation curve, since mixtures of oil and medium are not homogeneous. Thus, to obtain additional information, a system for measuring the concentration of hydrocarbons (crude oil, crude oil components or methane) at high pressure would be worthwhile.
- For investigation of the degradation of methane at high pressure, a system for introducing defined volumes of methane needs to be developed.
- In addition, construction of a new CO₂ sensor, similar to the O₂ prototype sensor design from PreSens Precision Sensing GmbH and Eurotechnica GmbH, would be conceivable. Alternatively, VisiSens™ CO₂ and O₂ systems (from PreSens Precision Sensing GmbH) could be used and then windows would be needed in the reactor.
- These windows could also be useful to get information about the biomass production by measurement of the optical density.
- For subsampling, for analysis of cell density, the lid would needed to be fitted with an extra connection. To compensate the upcoming pressure loss, another connection would be needed for resupplying nitrogen gas or fresh medium under ambient or high pressure (as already described in Chapter 2.7.2). For instance, this could be managed via a mechanical pressurisation by a spindle pump like it is realised in the high pressure view cell reactor No. 1.
- To accommodate all these connections, a big reactor volume and thus enough space on the reactor's lid is preferable.

- Unfortunately, no valves are available yet that would not be damaged by taking samples from culture medium inoculated with sediments, since they block and break all types of valves. Thus, analysis of bacterial growth of incubations with sediments is only possible with a set of several reactors.
- Mechanical pressure build-up with a spindle pump could also support or replace pressure build-up in the reactor with nitrogen gas.
- To ensure a constant incubation temperature, a cooling jacket connected to a water bath would be needed.
- The reactors described in this thesis were batch reactors, thus biodegradation was limited by oxygen availability. A system regulating a continuous gas exchange (supply with O₂ and discharge of CO₂) could be useful. Thereby, longer incubation times with higher biomass production and higher amounts of degraded hydrocarbons could be achieved.
- With a one-pot system, control incubations at ambient pressure cannot be run in parallel with the high pressure experiment. A second reactor with similar features would be worthwhile for reference.

In conclusion, to construct a reactor ideal for biodegradation experiments at high pressure, properties from the different reactor systems tested in this thesis would need to be combined.

4.2 Biodegradation of n-alkanes at ambient and high pressure

4.2.1 Degradation of n-hexadecane, n-tetracosane and n-decane by *R. qingshengii* TUHH-12 and *D. aurantiaca* C7.oil.2 at ambient and high pressure

R. qingshengii TUHH-12 served as a model organism for degradation of the n-alkanes n-hexadecane, n-decane and n-tetracosane under high pressure conditions. *R. qingshengii* was first described by Xu *et al.* (2007) and was reported to degrade several hydrocarbons such as benzene, toluene, xylenes, naphthalene and n-dodecane (Benedek *et al.* 2013). The genome of the *R. qingshengii* TUHH-12 strain encodes multiple enzymes for alkane and aromatic compound degradation as well as genes for EPS biosynthesis (Lincoln *et al.* 2015). During work on this thesis, *R. qingshengii* TUHH-12 was even found to degrade polysaccharides

contained in two substances used for solidification of culture media: agar and Gelrite™ (Carl Roth GmbH + Co. KG, Karlsruhe, Germany). However, up to now nothing was known about effects of high pressure on hydrocarbon degradation capabilities of this strain.

In this thesis, the strain was found to grow at a pressure of 150 bar, although it was isolated from samples collected at ambient pressure. Compared to incubations at ambient pressure on different alkanes, growth and degradation behaviour at high pressure were only slightly different. Thus, the strain can be classified as a piezotolerant microorganism. This pressure tolerance of the species *Rhodococcus* was already described by Colquhoun *et al.* (1998) and Heald *et al.* (2001). They found that certain *Rhodococcus* strains were tolerant to even higher pressures of 400 and 600 bar, when growing on glucose yeast extract medium. The fact that these strains were isolated from pacific deep-sea sediments indicated a good adaptation to high pressures. Moreover, *R. erythropolis* was found to survive even extreme pressures of 780,000 bar (Burchell *et al.* 2004).

In incubations with 1 mM n-hexadecane, a slightly negative effect of high pressure on the growth, substrate and oxygen consumption of *R. qingshengii* TUHH-12 was observed. Compared to this incubation, where on average one third of the oxygen was used up at the end of the incubation, in incubation with 3 mM n-hexadecane the oxygen was depleted completely. In the incubation with 1 mM n-hexadecane, the oxygen consumption rate was lower at 147 bar than at 1 bar. In contrast, in the incubation with 3 mM n-hexadecane the oxygen consumption rate was slightly higher at 150 bar than at 1 bar.

The few studies available on n-hexadecane biodegradation at high pressure show divergent results as well. Schwarz *et al.* (1974, 1975) found that degradation and growth with n-hexadecane at *in situ* pressure (506.6 bar) by a microbial community was retarded significantly in contrast to the incubation at ambient pressure. Grossi *et al.* (2010) found no significant effects of high pressure on growth and n-hexadecane degradation of *Marinobacter hydrocarbonoclasticus*.

In control experiments without inoculum of *R. qingshengii* TUHH-12, n-hexadecane concentration decreased. At high pressure, the concentration decreased much faster than at ambient pressure. Obviously, the incubation in reactors at high pressure or the (de-)pressurisation had an effect on the concentration of n-hexadecane in the medium. Since contaminations could be excluded, a possible explanation for the loss of n-hexadecane could be that it evaporated and was lost after releasing the gas phase by depressurising and

opening the reactors. The vapour pressure of a substance decreases non-linearly with decreasing temperature according to the Clausius-Clapeyron relation (Todeschini and Consonni 2009). The melting point of n-hexadecane is 18°C (GESTIS Substance Database: n-hexadecane). Cooling of reactors at 4°C before opening helped minimising losses, since n-hexadecane changed to solid aggregate state.

For the incubation of *R. qingshengii* TUHH-12 with n-tetracosane results showed, as already observed with n-hexadecane, that growth and oxygen consumption were slightly negatively affected by high pressure. n-Tetracosane was slightly but not completely degraded in incubations at both pressure conditions.

For the incubation of *R. qingshengii* TUHH-12 with n-decane, the effect of high pressure was different when cell density or oxygen consumption and substrate depletion were monitored. However, the deviations were very small. Already at the second point of sampling, nearly no n-decane was detected anymore in the medium. Similarly, in control experiments without bacteria, n-decane concentration decreased rapidly in the reactors, whereby more n-decane was lost at high pressure. When n-decane was incubated at 1 bar in closed glass vials, which have a smaller volume than the reactor's volume, much less n-decane was lost after the same time. Thus, the loss of n-decane in the reactors is assumed to be caused by evaporation effects.

Bacteria of the genus *Dietzia* were described to degrade various n-alkanes (Alonso-Gutiérrez *et al.* 2011, Bihari *et al.* 2011, Rainey *et al.* 1995, Yumoto *et al.* 2002) and aromatic hydrocarbons such as naphthalene or toluene (Bødtker *et al.* 2009, von der Weid *et al.* 2007). Although, bacteria of the genus *Dietzia* had been, among other things, isolated from deep-sea sediments, for instance from mud samples of the Mariana Trench (Takami *et al.* 1997), nothing was known about the influence of high pressure on their hydrocarbon degradation abilities up to now.

The alkane model degrader *D. aurantiaca* C7.oil.2, which was isolated from GoM deep-sea sediments, was investigated regarding its pressure tolerance while degrading n-hexadecane. No clear effect of high pressure was observed. However, *D. aurantiaca* C7.oil.2 can be classified as a piezotolerant strain, since it was able to grow and consume oxygen at a pressure of 154 bar.

In summary, growth and degradation behaviour of *R. qingshengii* TUHH-12 incubated at high pressure with n-hexadecane, n-tetracosane and n-decane was only slightly different from incubations at ambient pressure. Similarly, biomass production and n-hexadecane degradation of *D. aurantiaca* C7.oil.2 was not clearly affected by high pressure. Hence, both strains are piezotolerant. The obtained degradation rates for incubation of *R. qingshengii* TUHH-12 at high pressure with various alkanes were implemented in a model, describing the fate of the DWH oil. Thereby, the model's predictions of changes in all oil concentrations were improved (Lindo-Atichati *et al.* 2016).

4.2.2 Influence of Corexit® EC9500A on n-hexadecane degradation by *R. qingshengii* TUHH-12 at ambient and high pressure

When Corexit® EC9500A was added to the culture medium at RT, *R. qingshengii* TUHH-12 started to actively metabolise the n-hexadecane faster than without addition of the dispersant, since there was a shortened lag-phase in the degradation curves at ambient and high pressure. Possibly, the enhanced initial degradation was caused by the increased Corexit®-induced bioavailability of n-hexadecane.

Several research groups are reporting about an enhanced bacterial degradation of n-hexadecane or other n-alkanes in the presence of Corexit® EC9500A (e.g. Campo *et al.* 2013, Swannell and Daniel 1999, Davies *et al.* 2001). However, there are contrasting findings as well. Lindstrom and Braddock (2002) reported that the addition of Corexit® EC9500A diminished mineralisation of less soluble substrates (such as hexadecane or phenanthrene) in oil, whereas mineralisation of more soluble components (such as dodecane) was not affected by addition of Corexit® EC9500A. Likewise, Foght and Westlake reported in 1982 that the degradation of n-alkanes was initially retarded in experiments with Corexit® EC9527A. Hamdan and Fulmer (2011) found that Corexit® EC9500A was harmful to all studied hydrocarbon-degrading bacteria. More recently, the addition of dispersants was found to significantly change the composition of a microbial community, so that certain bacterial taxa that can degrade compounds of dispersants were enriched (Kleindienst *et al.* 2015a). Kleindienst *et al.* also observed either suppression or no stimulation of oil biodegradation when a dispersant was present. Overholt *et al.* (2016) found both inhibiting and enhancing effects of Corexit® EC9500A on oil degradation and growth of two model oil

degraders. In conclusion, divergent effects of Corexit® on microorganisms were found, depending on the investigated hydrocarbons and bacterial strains or bacterial populations.

Nothing was known about effects of high pressure on hydrocarbon degradation under the influence of Corexit® up to now. In the incubation of *R. qingshengii* TUHH-12 on n-hexadecane with addition of Corexit® EC9500A at RT no significant differences at ambient and high pressure in the growth and n-hexadecane-degradation rates were found.

When *R. qingshengii* TUHH-12 was incubated at 4°C and 1 bar with n-hexadecane with or without Corexit® EC9500A no clear effect of the dispersant was observed. However, a slower growth and degradation than at RT was observed, since at low temperatures long chain alkanes are in solid state and thus bioavailability is reduced. Similarly, others report a slower degradation of dispersed crude oil at low temperatures in comparison to ambient temperatures (Campo *et al.* 2013, Venosa and Holder 2007).

R. qingshengii TUHH-12 was able to grow on Corexit® EC9500A at RT as sole source of carbon. Thus, Corexit® EC9500A was not toxic to the tested model strain neither at ambient nor at high pressure. Also, others reported that Corexit® EC9500A can be used as sole source of energy and carbon (Overholt *et al.* 2016). Microorganisms can mineralise and grow on certain components of dispersants (Bælum *et al.* 2012, Campo *et al.* 2013, Chakraborty *et al.* 2012, Lindstrom and Braddock 2002, Lindstrom *et al.* 1999).

In summary, addition of Corexit® EC9500A to the *R. qingshengii* TUHH-12 culture at RT was not toxic and did neither change growth rates nor n-hexadecane degradation rates significantly, but shortened the lag-phase of the degradation curves independently of the pressure conditions.

4.3 Biodegradation of an aromatic hydrocarbon at ambient and high pressure

4.3.1 Growth of *R. wratislaviensis* Tol3 and *D. aurantiaca* C7.oil.2 with toluene at ambient and high pressure

R. wratislaviensis Tol3 was used as a model strain to investigate the effect of high pressure on toluene degradation. The genus *Rhodococcus* was described to degrade, among other things, BTEXs hydrocarbons and various PAHs such as naphthalene, phenanthrene or anthracene (Auffret *et al.* 2009, Egorova *et al.* 2013, Pizzul *et al.* 2007). BTEX compounds are

toxic to microorganisms at high concentrations (Dou *et al.* 2008, Mazzeo *et al.* 2010). However, if the substrate concentration is too low, the growth is not supported sufficiently. Thus, in the described experiments toluene was provided via vapour diffusion, to ensure a low concentration and to maintain a constant substrate supply. For this, a small open beaker was filled with toluene and placed in the reactor beside the culture vial. In the experiments, initial and end toluene concentrations were not analysed, since releasing the pressure from high pressure reactors led to losses of gaseous toluene. In future studies, it could be worth considering monitoring toluene concentration online.

Up to now, no research was made on the influence of high pressure on hydrocarbon-degradation abilities of *R. wratislaviensis*. In this thesis, high pressures from 44 to 154 bar were found to influence the growth of the strain positively, whereas at 1 bar nearly no growth was observed. However, the growth was enhanced to the same extent by all tested high pressures and no critical pressure point was found. Possibly, this critical pressure, above which the growth is enhanced, lies between 1 and 44 bar. At first sight, this leads to the conclusion that *R. wratislaviensis* Tol3 is a piezophilic strain. But results are contradictory, since the preculture, used to inoculate these cultures, had grown well at 1 bar. Probably, this was caused by differences in cultivation of the preculture in an air-tight glass vessel (desiccator) compared to cultivation of cultures of the main experiment in the reactors. The desiccator had a bigger volume than the ambient pressure reference reactors. However, the ratio of the volume of air to the volume of liquid toluene in the reactors was adjusted to the ratio in the desiccator. In addition, in contrast to the main culture in the ambient pressure reference reactor, which was inoculated with 10% (v/v) of the grown liquid preculture, the preculture itself was inoculated with one single colony from an agar plate. Possibly, traces of the agar attached to the colony and supported growth of the preculture. Moreover, the preculture was cultivated in an Erlenmeyer flask together with other precultures and agar plates in the desiccator, while in the reactors a single glass vial with another geometry and other surface conditions was used.

At the end of the experiment, in the supply beakers of all 160 mL high pressure reactors more liquid toluene was left than in the ambient pressure reference reactors. Possibly, high pressure had an effect on how much toluene could go into the atmosphere. Thus, it had an effect on the equilibrium between liquid toluene in the supply beaker and gaseous toluene in the atmosphere. Seemingly, at high pressure less toluene was in the atmosphere, causing

that less toluene could dissolve into the culture medium over time, which enhanced bacterial growth. But possibly, this was not directly caused by the high pressure itself, but by the introduced nitrogen and the colligative properties of its solution in toluene. These properties are only depending on the ratio of the number of the solute molecules (nitrogen) to the number of solvent molecules (toluene) in the solution and not on the chemical nature of the substances (Hammel 1976). Mole fraction and solubility of nitrogen in liquid toluene had been reported to rise with increasing pressure (Battino *et al.* 1984, Jabłowiec *et al.* 2007). Colligative properties are e.g. a lower vapour pressure, a lower melting temperature and a higher boiling temperature of the solvent (Hammel 1976). The Raoult's law states that the total vapour pressure over a liquid mixture, containing a non-volatile solute, is equal to the vapour pressure exerted by the pure volatile solvent multiplied by its mole fraction (Jenkins 2008). Thus, solution of nitrogen in toluene could have led to a lowering of the toluene's vapour pressure.

When glucose was used as a universal carbon source, to examine whether central cell functions of *R. wratislaviensis* Tol3 were affected by high pressure, no significant differences in incubations at ambient and high pressure were observed. This result leads to the conclusion that the enhanced growth with toluene at high pressure is not induced by high pressure effects on the central metabolism. Rather, there could be a high pressure effect on the toluene degradation pathway or a preferred, lowered toluene vapour pressure at high pressure, as described above. In conclusion, the investigated model strain is not piezophilic but piezotolerant.

To verify the hypothesis that growth of *R. wratislaviensis* Tol3 was enhanced when less toluene was in the gaseous phase, the strain was incubated with toluene vapour under addition of decalin. Decalin (decahydronaphthalene) is a liquid, bicyclic aromatic hydrocarbon, which is miscible with toluene. Decalin has a low volatility. Similar to the solution of nitrogen in toluene, when decalin and toluene are mixed, the vapour pressure of the final solution will be lower than the vapour pressure of the pure toluene, according to Raoult's law. Thus, toluene's concentration in the gaseous phase would be lowered and less toluene could dissolve in the culture medium. The results of this experiment showed that indeed growth was better when decalin was added to the toluene supply beaker than with pure toluene. From these results, it can be concluded that high pressure had no effect on the toluene degradation pathway. The theory was affirmed that introduction of nitrogen in

high pressure incubations lowered the toluene vapour pressure. Thereby, the subsequent delivery and the concentration of toluene in the atmosphere were lowered. Hence, less toluene could dissolve in the culture medium over time, which was preferred by the bacteria.

Similar results were observed when *D. aurantiaca* C7.oil.2 was incubated with toluene at ambient and high pressure. The indigenous strain grew slightly at high pressure in the 160 mL high pressure reactors but not at ambient pressure in the ambient pressure reference reactors. However, the preculture used to inoculate the experiment grew well at ambient pressure in the desiccator. Thus, most likely this strain can be classified as a piezotolerant strain too and the explanation for the enhanced growth of *R. wratislaviensis* Tol3 at high pressure is true for this strain as well.

In summary, growth of *R. wratislaviensis* Tol3 as well as *D. aurantiaca* C7.oil.2 incubated with toluene was enhanced by high pressure. Strangely, no growth was observed in incubations at ambient pressure in the ambient pressure reference reactors, although the precultures grew well at 1 bar in a desiccator. Enhanced growth at high pressure most likely resulted from increased solubility of nitrogen in liquid toluene, leading to a lowered toluene vapour pressure and a low toluene concentration in the culture medium, which was preferred by the model strains.

4.4 Biodegradation of a PAH at ambient and high pressure

4.4.1 Degradation of naphthalene by *S. yanoikuyae* B1 at ambient and high pressure

As sole source of carbon and energy *S. yanoikuyae* B1 can assimilate and mineralise aromatic compounds such as biphenyl, anthracene, phenanthrene, naphthalene, toluene, cyclohexene and 1,3,5-trimethylbenzene (Gibson *et al.* 1973, Lang 1996). In this thesis its capability to grow with naphthalene was tested under elevated pressure conditions, which was not investigated before.

High pressure was found to have a slightly negative effect on the naphthalene degradation and a strong negative effect on growth of *S. yanoikuyae* B1. In first experiments, no increase in cell density was observed at all when the strain was incubated

at a pressure of 139 bar, instead bacteria were dying. In contrast, the bacteria grew well at ambient pressure.

Others also found that growth and hydrocarbon degradation are limited by high pressure. Schwarz *et al.* (1975) determined that the rate of n-hexadecane utilisation by a microbial community from a sediment sample of 4,940 m depth was much slower under deep-sea conditions at 506.6 bar and 4°C than the rate observed at 1 bar and 4°C. Likewise, the utilisation of n-hexadecane at 20°C and 506.6 bar was considerably slower than the utilisation at ambient conditions of 20°C and 1 bar (Schwarz *et al.* 1974). In both studies, bacteria took longer to reach maximum growth at high pressure than at ambient pressure. From these data, Colwell and Walker (1977) suggested that oil entering the deep sea will be most probably degraded at very slow rates by the microbial community and that specific fractions of the oil, such as PAHs, may persist for years or even decades. In contrast, Grossi *et al.* (2010) found no significant effects of high pressure on growth and n-hexadecane degradation of deep-sea strain *Marinobacter hydrocarbonoclasticus*, which is thus piezotolerant. Scoma *et al.* (2016) found a reduction of growth yields of two piezosensitive strains of the genus *Alcanivorax* incubated with n-dodecane already at pressures of 50 and 100 bar. The strain *Alcanivorax dieselolei* KS_293 showed an unaffected carbon degradation capacity at 100 bar, as the CO₂ production per cell did not significantly change. Similarly, O₂ respiration per cell was not affected at high pressure. Besides these studies, up to now only a limited number of reports are available determining the effects of high pressure on biodegradation by deep-sea bacteria. However, they do not concentrate specifically on degradation of hydrocarbons but on the degradation of organic matter, detritus or glucose (Jannasch *et al.* 1971, Turley and Lochte 1990, ZoBell and Johnson 1949). They found inhibiting as well as enhancing effects of high pressure, as discussed in Chapter 4.5.2.

Interestingly, at 139 bar *S. yanoikuyae* B1 still was able to convert naphthalene, although at a slightly lower rate than at 1 bar and not completely, so that at the end of the incubation 3.4% of initial naphthalene was left. This special type of piezosensitivity, where the hydrocarbon-degradation ability is less sensitive to high pressure than growth is, was, to the best of my knowledge, not described in literature before.

In incubations of naphthalene in Brunner mineral medium without bacterial inoculum, at both ambient and high pressure a certain amount of naphthalene was lost at the end of the

incubation. However, there was no significant difference at both pressure conditions and thus high pressure had no significant effect on the concentration of naphthalene in the medium. Since contaminations could be excluded, the losses were most probably caused by evaporation of the naphthalene. This experiment showed that in the experiment, described above, evaporation was responsible for the decrease of naphthalene concentration over time only to a small degree and that bacteria must have made a major contribution to the decrease.

In order to find the critical pressure point, above which no growth was possible anymore, *S. yanoikuyae* B1 was incubated with naphthalene at pressures ranging from 1 to 130 bar. Significant differences in growth at different pressures were observed. Up to 88 bar, the cell density remained more or less constant after 70 h of incubation. Above this pressure, the density of viable cells decreased and already at 120 bar no viable cells were counted by determination of CFUs. This result is in contrast to values described in literature, where piezosensitive bacteria stopped growth at pressures of 300 to 500 bar (Nogi 2008). Furthermore, the findings are surprising given the fact that in literature the majority of high pressure effects on cellular components and processes of bacterial cells are proposed to occur at pressures much higher than 200 bar (Follonier *et al.* 2012) (see Introduction Chapter 1.3.2). Thus, in this thesis effects on bacterial growth were observed at pressures lower than those typically assumed to be the threshold for pressure effects. However, it has to be taken into account that in literature effects of pressure were not investigated on hydrocarbon-degrading bacteria, but, among other things, on model organisms such as *E. coli*.

Pressures of up to 10 bar had been described as already indirectly affecting microorganisms by increasing gas solubility and hence dissolved gas concentrations (e.g. of oxygen or carbon dioxide), according to Henry's law (Follonier *et al.* 2012, Wiebe and Gaddy 1940). This can lead to oxidative stress, acidification of the internal pH or it may affect the function of membranes and physicochemical properties of enzymes (Follonier *et al.* 2012, Stretton and Goodman 1998). However, in the used experimental setup no increase of oxygen partial pressure was to be expected, since the reactors were pressurised with nitrogen gas. Another physical consequence of elevated pressures is the change in substrate solubility, since Sawamura *et al.* (1993) found that the solubility of naphthalene in water

decreased with increasing pressure. Contribution of solubility changes of naphthalene to the observed differences in growth and degradation cannot be excluded.

Interestingly, 120 bar corresponds to the depth range of 1,000 to 1,200 m, at which a large oil plume was detected in June 2010 in the aftermath of the DWH blowout (Camilli *et al.* 2010, Hazen *et al.* 2010). This plume was characterised by increased concentrations of aromatic hydrocarbons (Camilli *et al.* 2010, Hazen *et al.* 2010). The finding that bacterial growth can be impacted by pressure corresponding to this depth suggests that pressure-related enhancement or inhibition may have influenced biodegradation of the DWH oil plume.

Strikingly, in the cultivations of *S. yanoikuyae* B1 the naphthalene concentration decreased to below the limit of detection, not only under surface pressure conditions but also in incubations up to 120 bar, although here increasingly reduced growth occurred. *S. yanoikuyae* B1 may have assimilated and partially degraded naphthalene, but possibly another part in the metabolism or certain cell structures were disturbed by the elevated pressure. Consequently, the substrate may not have been used efficiently as source of carbon and energy, and cells were not able to grow and divide in normal fashion. Even in incubations above 120 bar, where no growth was observed and cells started dying or remaining in an inactive stage, naphthalene was depleted, although to a lower extent than at 1 bar. This means the cell division was now inhibited completely by the elevated pressure, but the resting cells were still able to break down naphthalene. ZoBell and Cobet (1962, 1964) found that cell division was sensitive to pressure and stopped before increase in cell size did. They observed this retarding effect on cell division and cell size increase of *E. coli* at pressures between about 200 and 500 bar. However, the pressure effect on substrate degradation was not investigated.

The reduced naphthalene depletion in the experiments at more than 120 bar could also result from death or inactivity of an increasing number of bacteria. Moreover, a pressure-induced decrease of the fluidity and a disruption of the permeability of the cell membrane for water-soluble proteins is possible (Hauben *et al.* 1996, Kato *et al.* 2002) and could influence substrate transport across the cell membrane (Oger and Jebbar 2010). However, these modifications of fluidity were found to occur at about 1,000 bar (Kato *et al.* 2002). Loss of membrane integrity was found to occur between 1,000 and 2,000 bar (Pagán and Mackey 2000).

In order to find out whether at high pressure the naphthalene could be converted to CO₂ by *S. yanoikuyae* B1, the experiment was repeated in high pressure view cell reactor No. 1 and CO₂ as well as O₂ were monitored continuously. Again, as in previous experiments, high pressure had an inhibitory effect and no growth was observed in comparison to the incubation at ambient pressure. But interestingly, not only at ambient pressure but also at high pressure O₂ was consumed and CO₂ was produced, even though at much lower rates. In conclusion, at least a part of the provided naphthalene was converted completely to CO₂. Most likely, the upper part of the naphthalene degradation pathway was not affected by high pressure. Naphthalene was oxidised and probably, after cleavage of the first aromatic ring, pyruvate was formed, which can be converted to acetyl-CoA under production of NADH and CO₂. However, the lower part of the naphthalene pathway seemed to be, at least partly, inhibited at a certain step. For example, the enzyme salicylate hydroxylase, responsible for conversion of salicylate, could have been inhibited.

Scoma *et al.* (2016) found similar results. While growth yields of *Alcanivorax dieselolei* KS_293 incubated with n-dodecane were reduced at pressures of 100 bar, the CO₂ production and O₂ respiration per cell did not significantly change at high pressure.

Moreover, the colour of the *S. yanoikuyae* B1 culture medium turned to a dark brown during incubations with naphthalene above the critical pressure of 120 bar, while below this pressure the colour of the medium did only turn to a light yellow. The yellow coloration was most likely due to the formation of 2-hydroxymuconic acid semialdehyde, a product of *meta*-cleavage dioxygenase activity. When the medium with naphthalene was incubated at more than 120 bar without bacterial inoculum no change of colour was observed. Thus, the colour change was caused by the bacterial metabolism.

This colour change again indicated that the naphthalene degradation pathway was inhibited by high pressure at a certain step. The brown colour can be explained by the accumulation of degradation intermediates. This could be caused by inhibition of an involved enzyme, either in its formation or function. The conformation of an enzyme can be modified by pressure, which can have consequences for its substrate affinity (Follonier *et al.* 2012). Penniston (1971) described that multimeric enzymes are inhibited by high pressure since their protein multimers dissociate. However, such dissociations of multimeric proteins

start to occur at pressures of about 2,000 bar, while at pressures of more than 4,000 bar most proteins are denatured (Aertsen *et al.* 2009).

Accumulation of catechol or 1,2-dihydroxynaphthalene, intermediates in the naphthalene degradation pathway, could be responsible for the brownish colour of the culture medium incubated at high pressure. By colorimetric method of Arnow (1937) neither of them were found. Probably, catechol and dihydroxynaphthalene concentrations were under the detection limit of this test. However, the test indicated that possibly monohydroxylated compounds (such as salicylate or monohydroxynaphthalene) accumulated.

In a GC-MS analysis of the brown culture medium by project partners at the University of Calgary, Canada, no catechol but, against the results from the colorimetric test, traces of 1,2-dihydroxynaphthalene were detected. Thus, the change of colour of the medium at pressures of above 120 bar emerged probably due to accumulation of 1,2-dihydroxynaphthalene or due to polymerisation of quinones or other aromatic ring cleavage products. Moreover, the GC-MS analysis revealed that besides unutilised naphthalene, high amounts of salicylate accumulated in the medium. In addition, other metabolites of the naphthalene degradation pathway, such as methyl salicylate and coumarin, were found in traces. Thus, it seemed that the second part of the naphthalene degradation pathway after formation of salicylate, which accumulated, was inhibited by high pressure.

In order to investigate this hypothesis, the ability of *S. yanoikuyae* B1 to degrade salicylic acid at high pressure was tested. The strain could not grow on salicylic acid, but it died, since the density of viable cells dropped under the starting cell density already after 20 h of incubation. The degradation of salicylic acid was strongly inhibited at high pressure. After 68 h of incubation, 81.9% of the initial substrate was not degraded. In contrast, at ambient pressure *S. yanoikuyae* B1 grew well with salicylic acid and degraded it almost completely. In conclusion, the enzyme for conversion of salicylic acid to catechol, the salicylate hydroxylase, could not work properly at high pressure. This experiment confirmed that the lower part of the naphthalene degradation pathway was at least partly inhibited by high pressure.

In the following experiment, *S. yanoikuyae* B1 was incubated with glucose as sole carbon source to examine whether central functions were affected by high pressure as well. Again, at a high pressure no growth occurred, while at ambient pressure the strain grew well. In

addition, at 156 bar the glucose was degraded to a much lower extent than at 1 bar, which indicated that also a central cell function was inhibited. Possibly, a central function (such as the glycolysis, citric acid cycle, protein synthesis, RNA transcription or cell division) was affected by high pressure, which led to restriction of biomass production. One can only speculate about the reasons for the inhibitory effect of high pressure. Most likely high pressure affected several functions of the cell.

In summary, when *S. yanoikuyae* B1 was growing with naphthalene at pressures of 120 bar or higher, the upper part of the naphthalene degradation pathway functioned. But, since the lower naphthalene degradation pathway from salicylate onwards was partly inhibited by high pressure, the conversion stopped at salicylate, which accumulated. However, cells could metabolise the pyruvate emerging from cleavage of the first aromatic ring of naphthalene (in the upper part of the pathway) to CO₂. In addition, a central cell function (e.g. an anabolic process) was inhibited by high pressure, which prevented production of biomass. After a certain time of incubation at high pressure, maintenance of cell functions was no longer possible and cells were dying. Most likely, at a pressure above 150 bar other effects on cell functions will appear and *S. yanoikuyae* B1 will not be able to convert naphthalene at all. In conclusion, *S. yanoikuyae* B1 can be classified as a piezosensitive strain, which is growing and utilising substrates best at ambient pressure conditions.

4.4.2 Influence of Corexit® EC9500A on degradation of naphthalene by *S. yanoikuyae* B1 at ambient and high pressure

The significant negative effect of high pressure on biomass production and the only slightly negative effect on the degradation behaviour, as described in the previous subsection, was also observed with addition of Corexit® EC9500A to the culture of *S. yanoikuyae* B1 with naphthalene. There was no significant difference in the naphthalene degradation with or without addition of the dispersant and, in contrast to the incubation of *R. qingshengii* TUHH-12 with n-hexadecane and Corexit® EC9500A (Chapter 4.2.2), no clear effect on the lag-phase of the degradation curve was observed with the dispersant. The growth was only slightly negatively affected in comparison to incubations without the dispersant. Accordingly, Foght and Westlake (1982) reported that Corexit® EC9527A had less effect on

degradation of the aromatic fraction than on degradation of n-alkanes by a marine oil-degrading population.

S. yanoikuyae B1 was able to use Corexit® EC9500A as sole carbon source. Corexit® EC9500A was not harmful to the model strain neither at ambient nor at high pressure. This observation was already made for incubations of other bacterial strains or consortia at ambient pressure by others (Lindstrom and Braddock 2002, Overholt *et al.* 2016).

In conclusion, addition of Corexit® EC9500A to the bacterial culture did not change growth or naphthalene degradation rates significantly and had no toxic effects.

4.5 Biodegradation of Louisiana sweet crude oil and natural gas by bacterial communities from deep-sea sediments at ambient and high pressure

The determination of high pressure effects on biodegradation was expanded from pure model strains, degrading single oil components, to degradation of total crude oil by bacterial communities in the sediments. All used sediments were surface scrapes from the top of sediment cores, which is the aerobic zone of the sea floor. The sea-floor sediments contained aerobic bacteria, which settled the bottom of the sea. Oxygen consumption and carbon dioxide production are corresponding to the degradation of crude oil. Therefore, when crude oil is biodegraded aerobically, oxygen, as a key substrate, is consumed. Consequently, carbon dioxide, as a major product, is produced and cell density increases. Aerobic microbial activity was observed in all analysed sediments.

4.5.1 Comparison of the activity of bacterial communities from deep-sea sediments from 2010 and 2013 at different incubation conditions

Aerobic bacteria in tested sediments (No. 2 and 4), which were collected in the GoM in 2010, grew best at a temperature of 5°C and in mineral minimal medium II supplemented with 3% (w/v) NaCl. These preferred conditions are similar to the temperature and salt content in the sea. As reported in the review of DeLaue and Wright (2011), most marine microorganisms were found to have an optimum salinity range of 2.5 to 3.5% and bacteria show reduced growth or hydrocarbon degradation if salinity exceeds or falls below this range.

However, influence of elevated pressure on oil-degrading bacteria remains unclear. Microorganisms in one tested sediment (No. 3), which was collected in 2010, consumed O₂ faster and produced more biomass at 150 bar than when they were incubated at ambient pressure. In incubation of another sediment (No. 8), collected in 2013 at the same site, the effect of pressure was reverse, but less distinct. In sediment No. 3 from 2010 more different strain morphologies and higher biomass production were observed than in sediment No. 8 from 2013 at both 1 and 150 bar. This indicates that three years after the DWH oil spill, with declining availability of crude oil, less oil-degrading microorganisms were present in the sea-floor sediments than directly after the spill. Accordingly, Kimes *et al.* (2014) concluded in their review that corresponding to the availability of hydrocarbon compounds temporal, successional shifts in the indigenous microbial community composition were observed in numerous studies following the DWH (e.g. Redmond and Valentine 2012, Hazen *et al.* 2010, Mason *et al.* 2012, Valentine *et al.* 2010, Kessler *et al.* 2011, Dubinsky *et al.* 2013). After the spill, in September and October 2010, the bacterial community resembled its predecessor prior to the spill. However, bacteria, capable of oil degradation, persisted in the water column near the DWH wellhead (Yang *et al.* 2014).

In summary, while the influence of high pressure on crude oil-degrading microbial communities in sediments remains unclear, the deep-sea conditions of low temperature and 3% salinity of the medium were preferred by the tested microbial communities. However, time of sediment sampling in the GoM made a difference in bacterial activity.

4.5.2 Degradation of Louisiana sweet crude oil by bacterial communities from 2010 and 2013 sediments at ambient and high pressure

In both analysed sediments (No. 4 from 2010 and No. 8 from 2013), which were compared in this experiment, aerobic microbial activity was observed. Only when deep-sea sediments were added as bacterial source, the oxygen concentration decreased and the carbon dioxide concentration and cell density increased, whereas in blank experiments without sediments the values remained constant. This proved that there was no biodegradation of oil without bacteria.

Certain differences were observed between the incubations of the two sediments. On the one hand, the date of sediment collection made a difference. The incubation of the

sediment, sampled three years after the DWH accident in 2013, showed a longer lag-phase in the oxygen consumption curve than the sediment collected in 2010 at the same site. In conclusion, possibly three years after the spill less and/or less active hydrocarbon-degraders were present in the analysed surface sediment, which needed longer to adapt to the crude oil. A similar result was found in the experiment described in Chapter 3.6.1. Right after the DWH oil spill, the excess supply of crude oil caused a bloom of adapted oil-degrading bacteria, which were able to degrade the hydrocarbons at fast rates (Bælum *et al.* 2012, Hazen *et al.* 2010, Kessler *et al.* 2011, Redmond and Valentine 2012, Valentine *et al.* 2010 and 2012). The rapid oil degradation by the bacterial community in sediment No. 4, sampled in 2010, confirmed this assumption. Thus, it can be assumed that when the availability of oil decreased, less of these microorganisms were present in the sediment. Moreover, possibly they needed longer to adapt to the oil and thus the bacterial community in the 2013 sediment No. 8 showed a longer lag-phase in the oxygen consumption curve.

Furthermore, different pressure conditions made a difference. In the incubation with the 2010 sediment No. 4, oxygen was consumed faster at 150 bar than at 1 bar, but this difference was only very small. The carbon dioxide production rates matched with this result. In the incubation with sediment No. 8 from 2013 it was vice versa. At 144 bar, bacteria needed longer to start oxygen consumption and consumed oxygen at a lower rate than at 1 bar. For the 2013 as well as for the 2010 sediment incubations, more biomass was produced in the 1 bar incubations than in the 150 bar incubations. Only for the 2013 sediment incubation, tendencies in cell counts agree with the tendencies in oxygen consumption at different pressure conditions.

Only the results from the incubation of sediment No. 8 from 2013 are in accordance to the results of Schwarz *et al.* (1974, 1975), who found that growth and hydrocarbon degradation of a deep-sea bacterial community was clearly retarded at 506.6 bar in contrast to 1 bar. In 1971, Jannasch *et al.* found that microbial degradation of organic matter in the deep sea was greatly restricted compared to ambient pressure degradation. In contrast, Turley and Lochte reported in 1990 that deep-sea bacteria degraded organic carbon from detritus at a faster rate at 456 bar than at 1 bar, but the amount of produced biomass was not significantly different. Similarly, ZoBell and Johnson (1949) found that deep-sea bacterial communities grew on glucose faster at 405 to 608 bar than at 1 bar. Thus, like the results

from the experiments with the 2010 and 2013 sediments, divergent effects of high pressure can be found in literature.

In preliminary analyses of the community composition and succession of the 2010 and 2013 sediment incubations, high pressure was found to change the bacterial consortium in sediments that degrade oil, so that completely different bacterial populations evolved compared to incubations at ambient pressure. The samples cluster by year of sediment collection, pressure and time of sampling. During incubation the diversity declined. In conclusion, at the phylum level, Proteobacteria and Firmicutes dominated at the end of 1 bar incubations and Proteobacteria dominated at the end of 150 bar incubations. Likewise, Kimes *et al.* (2013), who analysed the metagenome of sediments from the GoM following the DHW spill, found that Proteobacteria and Firmicutes were dominating. Similarly, others reported that bacterial communities, dominating in the deep-water oil plume, belonged to the phylum of Gammaproteobacteria (Hazen *et al.* 2010, Mason *et al.* 2012, Redmond and Valentine 2012, Valentine *et al.* 2010). Members of the Alpha-, Beta-, Gamma- and Deltaproteobacteria and Firmicutes are known to play a major role in aerobic hydrocarbon conversion (Head *et al.* 2006, Kim and Kwon 2010, Prince *et al.* 2010). To get more knowledge on how high pressure affects the composition of bacterial communities, further analyses are needed.

Possibly, in addition to the effects of pressure also the inherent heterogeneity of the sediments, which were used for inoculation, played a certain role in the observed differences of the O₂ and CO₂ curves in the incubations at the two pressure conditions. Bacteria are not distributed evenly in sediments and grow at different rates. Similarly, Lowit *et al.* 2000 stated that the reproducibility of an experiment is depending on the variability of the measurement tool as well as on the inhomogeneous distribution of bacterial community members among collected environmental samples.

In summary, for the analysed bacterial communities in sediments, divergent effects of high pressure on their growth and degradation behaviour were found. Also, the date of sampling of the sediments made a difference in bacterial activity. However, from the results it is very clear that high pressure changed the crude-oil degrading bacterial consortium in sediments and that diversity declined during the incubation.

4.5.3 Degradation of natural gas and crude oil by bacterial communities from a 2010 sediment at ambient and high pressure

The experiment, described in Chapter 3.6.3, showed that bacteria contained in deep-sea sediments are able to degrade not only crude oil but also natural gas at high pressure. At high pressure, incubations with crude oil and natural gas showed similar oxygen consumption rates. A comparison of different pressure conditions was unfortunately not possible from the results of this experiment due to problems with the oxygen sensors in incubations at ambient pressure.

In DGGE population analysis, theoretically each band represents one bacterial strain and thus different band patterns represent different bacterial community compositions. DGGE analysis of end samples revealed that the bacterial community evolved differently in incubations with natural gas depending on the respective pressure conditions. Other bacterial strains degraded natural gas at ambient than at high pressure and other bacterial strains degraded crude oil than natural gas. Furthermore, in some cases bacterial strains that were attached to sediment particles (pretreatment of the sample with 5.0 μm filter) were more prominent than the unattached bacterial strains (pretreatment of the sample with 0.2 μm filter) and vice versa. Unfortunately, due to a mistake, the DGGE results of the incubation with oil at ambient pressure cannot be compared to the incubation at high pressure. This experiment needs to be repeated and subsequently the dominant bacterial strains should be identified and compared with bacteria that were already found to be present at the DWH site by metagenomic analysis in literature (e.g. Bælum *et al.* 2012, Dubinsky *et al.* 2013 Gutierrez *et al.* 2013b, Hazen *et al.* 2010, Kimes *et al.* 2013, Kessler *et al.* 2011, Kleindienst *et al.* 2015a and b, Mason *et al.* 2012 and 2014, Redmond and Valentine 2012, Valentine *et al.* 2010, Yergeau *et al.* 2015).

In summary, the results of this thesis show that indeed high pressure has an effect on the composition, growth and hydrocarbon-degradation capability of deep-sea bacterial consortia. However, growth- and degradation-enhancing as well as -retarding effects of high pressure were found, pointing out that pressure effects are dependent on various factors such as the respective bacterial community composition in the sediments, the respective carbon source as well as experimental conditions. Thus, at this point no definite statement can be made regarding effects of high pressure on bacterial communities, apart from that

high pressure is a crucial factor in investigations of crude oil biodegradation in deep waters that cannot be neglected.

5 Conclusion

The influence of high pressure on the degradation of crude oil components and crude oil by bacterial model strains and bacterial communities was investigated. In summary, it can be concluded that the effects of high pressure and Corexit® on degradation behaviour and growth were manifold:

- In case of n-alkane biodegradation by *R. qingshengii* TUHH-12 only slight effects of high pressure on growth and biodegradation were observed.
- Growth of *S. yanoikuyae* B1 with naphthalene was inhibited at a pressure of 120 bar, while substrate conversion was nearly not affected.
- Growth of *R. wratislaviensis* Tol3 and *D. aurantiaca* C7.oil.2 with toluene was enhanced under elevated pressure conditions.
- Addition of Corexit® EC9500A had no harmful effect on the tested model strains. In case of *R. qingshengii* TUHH-12 the n-hexadecane-degradation curve had a shortened lag-phase.
- High pressure had enhancing or inhibiting effects on growth and crude oil biodegradation by bacterial communities from GoM surface sediments, dependent on the respective analysed sediment and its sampling time. High pressure changed the bacterial consortium in sediments that degrade oil and natural gas.

In conclusion, the effects of high pressure were dependent on the investigated model strain or bacterial community, on the analysed hydrocarbon as well as on the experimental conditions.

Several reactor systems for simulation of deep sea conditions as well as different gas concentration monitoring devices were tested. From the gained experiences, requirements for a new improved high pressure reactor were formulated and a new prototype sensor for oxygen measurement under high pressure was constructed in cooperation with two companies.

Up to now, the deep-sea condition of high pressure was, apart from a few exceptions, neglected in marine hydrocarbon biodegradation studies due to the high technical effort.

However, this thesis proves that pressure is a crucial factor that needs to be considered when estimating the biodegradation and ultimate fate of deep-sea oil releases such as the Deepwater Horizon oil spill. This thesis proved that there is still a high demand for research on high pressure effects on marine bacteria.

6 References

- Abbott BJ, Gledhill WE (1971) The Extracellular Accumulation of Metabolic Products by Hydrocarbon-Degrading Microorganism. In: Perlman D (ed) ADVANCES IN APPLIED MICROBIOLOGY. Academic Press, New York, London, pp 249–388.
- Abe F, Horikoshi K (2001) The biotechnological potential of piezophiles. Trends in Biotechnology 19:102–108.
- Ackermann M (2015) A functional perspective on phenotypic heterogeneity in microorganisms. Nature Reviews Microbiology 13:497–508.
- Aertsen A, Meersman F, Hendrickx MEG, Vogel RF, Michiels CW (2009) Biotechnology under high pressure: applications and implications. Trends in Biotechnology 27:434–441.
- Agteren MH van, Keuning S, Oosterhaven J (1998) Handbook on Biodegradation and Biological Treatment of Hazardous Organic Compounds. Springer Science & Business Media, Dordrecht.
- Allredge AL, Silver MW (1988) Characteristics, dynamics and significance of marine snow. Progress in Oceanography 20:41–82.
- Allen EE, Banfield JF (2005) Community genomics in microbial ecology and evolution. Nature Reviews Microbiology 3:489–498.
- Alonso-Gutiérrez J, Teramoto M, Yamazoe A, Harayama S, Figueras A, Novoa B (2011) Alkane-degrading properties of *Dietzia* sp. H0B, a key player in the Prestige oil spill biodegradation (NW Spain). Journal of Applied Microbiology 111:800–810.
- Aman ZM, Paris CB, May EF, Johns ML, Lindo-Atichati D (2015) High-pressure visual experimental studies of oil-in-water dispersion droplet size. Chemical Engineering Science 127:392–400.
- Arnou LE (1937) Colorimetric Determination of the Components of 3,4-Dihydroxyphenylalaninetyrosine Mixtures. Journal of Biological Chemistry 118:531–537.

- Arsène F, Tomoyasu T, Bukau B (2000) The heat shock response of *Escherichia coli*. *International Journal of Food Microbiology* 55:3–9.
- Atlas RM (1975) Effects of Temperature and Crude Oil Composition on Petroleum Biodegradation. *Applied Microbiology* 30:396–403.
- Atlas RM (1981) Microbial degradation of petroleum hydrocarbons: an environmental perspective. *Microbial Reviews* 45:180–209.
- Atlas RM, Bartha R (1972) Degradation and mineralization of petroleum in sea water: Limitation by nitrogen and phosphorous. *Biotechnology and Bioengineering* 14:309–318.
- Atlas RM, Hazen TC (2011) Oil Biodegradation and Bioremediation: A Tale of the Two Worst Spills in U.S. History. *Environmental Science & Technology* 45:6709–6715.
- Auffret M, Labbé D, Thouand G, Greer CW, Fayolle-Guichard F (2009) Degradation of a Mixture of Hydrocarbons, Gasoline, and Diesel Oil Additives by *Rhodococcus aetherivorans* and *Rhodococcus wratislaviensis*. *Applied and Environmental Microbiology* 75:7774–7782.
- Azam F, Malfatti F (2007) Microbial structuring of marine ecosystems. *Nature Reviews Microbiology* 5:782–791.
- Bælum J, Borglin S, Chakraborty R, Fortney JL, Lamendella R, Mason OU, Auer M, Zemla M, Bill M, Conrad ME, Malfatti SA, Tringe SG, Holman H-Y, Hazen TC, Jansson JK (2012) Deep-sea bacteria enriched by oil and dispersant from the Deepwater Horizon spill. *Environmental Microbiology* 14:2405–2416.
- Balny C, Mozhaev VV, Lange R (1997) Hydrostatic Pressure and Proteins: Basic Concepts and New Data. *Comparative Biochemistry and Physiology Part A: Physiology* 116:299–304.
- Bartlett D, Wright M, Yayanos AA, Silverman M (1989) Isolation of a gene regulated by hydrostatic pressure in a deep-sea bacterium. *Nature* 342:572–574.
- Battino R, Rettich TR, Tominaga T (1984) The Solubility of Nitrogen and Air in Liquids. *Journal of Physical and Chemical Reference Data* 13:563–600.

- Bean JW (1945) EFFECTS OF OXYGEN AT INCREASED PRESSURE. *Physiological Reviews* 25:715–715.
- Beazley MJ, Martinez RJ, Rajan S, Powell J, Piceno YM, Tom LM, Andersen GL, Hazen TC, Nostrand JDV, Zhou J, Mortazavi B, Sobecky PA (2012) Microbial Community Analysis of a Coastal Salt Marsh Affected by the Deepwater Horizon Oil Spill. *PLoS one* 7:e41305.
- Benedek T, Vajna B, Táncsics A, Márialigeti K, Lányi S, Máthé I (2013) Remarkable impact of PAHs and TPHs on the richness and diversity of bacterial species in surface soils exposed to long-term hydrocarbon pollution. *World Journal of Microbiology and Biotechnology* 29:1989–2002.
- Bihari Z, Szvetnik A, Szabó Z, Blastyák A, Zombori Z, Balázs M, Kiss I (2011) Functional analysis of long-chain n-alkane degradation by *Dietzia* spp. *FEMS Microbiology Letters* 316:100–107.
- Bødtker G, Hvidsten IV, Barth T, Torsvik T (2009) Hydrocarbon degradation by *Dietzia* sp. A14101 isolated from an oil reservoir model column. *Antonie van Leeuwenhoek* 96:459–69.
- Bowles MW, Samarkin VA, Joye SB (2011) Improved measurement of microbial activity in deep-sea sediments at in situ pressure and methane concentration. *Limnology and Oceanography: Methods* 9:499–506.
- Brakstad OG (2008) Natural and Stimulated Biodegradation of Petroleum in Cold Marine Environments. In: Margesin R, Schinner F, Marx J-C, Gerday C (eds) *Psychrophiles: from Biodiversity to Biotechnology*. Springer Verlag, Berlin, Heidelberg, pp 389–407.
- Brenner K, You L, Arnold FH (2008) Engineering microbial consortia: a new frontier in synthetic biology. *Trends in Biotechnology* 26:483–489.
- Brooks GR, Larson RA, Schwing PT, Romero I, Moore C, Reichart G-J, Jilbert T, Chanton JP, Hastings DW, Overholt WA, Marks KP, Kostka JE, Holmes CW, Hollander D (2015) Sedimentation Pulse in the NE Gulf of Mexico Following the 2010 DWH Blowout. *PLoS one* 10:e0132341.

- Buck-Emden A (2015) Biologischer Abbau eines aromatischen Kohlenwasserstoffes unter hydrostatischen Druckbedingungen durch *Rhodococcus wratislaviensis* und *Dietzia spec.* Bachelor's thesis, Hamburg University of Technology, Institute of Technical Biocatalysis.
- Burchell MJ, Mann JR, Bunch AW (2004) Survival of bacteria and spores under extreme shock pressures. *Monthly Notices of the Royal Astronomical Society* 352:1273–1278.
- Cabiscol E, Tamarit J, Ros J (2000) Oxidative stress in bacteria and protein damage by reactive oxygen species. *International Microbiology* 3:3–8.
- Camilli R, Reddy CM, Yoerger DR, Mooy BASV, Jakuba MV, Kinsey JC, McIntyre CP, Sylva SP, Maloney JV (2010) Tracking Hydrocarbon Plume Transport and Biodegradation at Deepwater Horizon. *Science* 330:201–204.
- Campo P, Venosa AD, Suidan MT (2013) Biodegradability of Corexit 9500 and Dispersed South Louisiana Crude Oil at 5 and 25 °C. *Environmental Science & Technology* 47:1960–1967.
- Cerniglia CE (1984) Microbial Metabolism of Polycyclic Aromatic Hydrocarbons. In: Laskin AI (ed) *Advances in Applied Microbiology*. Academic Press, Orlando, London, pp 31–65.
- Chakraborty R, Borglin SE, Dubinsky EA, Andersen GL, Hazen TC (2012) Microbial Response to the MC-252 Oil and Corexit 9500 in the Gulf of Mexico. *Frontiers in Microbiology* 3:357.
- Chanton J, Zhao T, Rosenheim BE, Joye S, Bosman S, Brunner C, Yeager KM, Diercks AR, Hollander D (2015) Using Natural Abundance Radiocarbon To Trace the Flux of Petrocarbon to the Seafloor Following the Deepwater Horizon Oil Spill. *Environmental Science & Technology* 49:847–854.
- Coates JD, Woodward J, Allen J, Philp P, Lovley DR (1997) Anaerobic degradation of polycyclic aromatic hydrocarbons and alkanes in petroleum-contaminated marine harbor sediments. *Applied and Environmental Microbiology* 63:3589–3593.
- Colquhoun JA, Heald SC, Li L, Tamaoka J, Kato C, Horikoshi K, Bull AT (1998) Taxonomy and biotransformation activities of some deep-sea actinomycetes. *Extremophiles* 2:269–277.

- Colwell RR, Walker JD, Cooney JJ (1977) Ecological Aspects of Microbial Degradation of Petroleum in the Marine Environment. *Critical Reviews in Microbiology* 5:423–445.
- Crespo-Medina M, Meile CD, Hunter KS, Diercks A-R, Asper VL, Orphan VJ, Tavormina PL, Nigro LM, Battles JJ, Chanton JP, Shiller AM, Joung D-J, Amon RMW, Bracco A, Montoya JP, Villareal TA, Wood AM, Joye SB (2014) The rise and fall of methanotrophy following a deepwater oil-well blowout. *Nature Geoscience* 7:423–427.
- Cui Z, Lai Q, Dong C, Shao Z (2008) Biodiversity of polycyclic aromatic hydrocarbon-degrading bacteria from deep sea sediments of the Middle Atlantic Ridge. *Environmental Microbiology* 10:2138–2149.
- Daly KL, Passow U, Chanton J, Hollander D (2016) Assessing the impacts of oil-associated marine snow formation and sedimentation during and after the Deepwater Horizon oil spill. *Anthropocene*. <http://dx.doi.org/10.1016/j.ancene.2016.01.006>.
- Davies L, Daniel F, Swannell R, Braddock J (2001) Biodegradability of Chemically-Dispersed Oil - A report produced for the Minerals Management Service (MMS), Alaska Department of Environmental Conservation (ADEC) and United States Coast Guard (USCG).
- Davis BD (2014) Taxonomic and Metabolic Characterization of Bacteria isolated from Gulf of Mexico sediments affected by the Deepwater Horizon Oil Spill. Master's thesis, University of West Florida.
- Delaune RD, Wright AL (2011) Projected Impact of Deepwater Horizon Oil Spill on U.S. Gulf Coast Wetlands. *Soil Science Society of America Journal* 75:1602–1612.
- DeLong EF, Yayanos AA (1985) Adaptation of the membrane lipids of a deep-sea bacterium to changes in hydrostatic pressure. *Science* 228:1101–1103.
- Diercks A-R, Highsmith RC, Asper VL, Joung D, Zhou Z, Guo L, Shiller AM, Joye SB, Teske AP, Guinasso N, Wade TL, Lohrenz SE (2010) Characterization of subsurface polycyclic aromatic hydrocarbons at the Deepwater Horizon site. *Geophysical Research Letters* 37:L20602.

- Dou J, Liu X, Hu Z, Deng D (2008) Anaerobic BTEX biodegradation linked to nitrate and sulfate reduction. *Journal of Hazardous Materials* 151:720–729.
- DSMZ GmbH (2012a) 141 METHANOGENIUM MEDIUM. http://www.dsmz.de/microorganisms/medium/pdf/DSMZ_Medium141.pdf. Accessed 30 Oct. 2015.
- DSMZ GmbH (2012b) 457 MINERAL MEDIUM (BRUNNER). http://www.dsmz.de/microorganisms/medium/pdf/DSMZ_Medium457.pdf. Accessed 30 Oct. 2015.
- DSMZ GmbH (2012c) 830 R2A MEDIUM. http://www.dsmz.de/microorganisms/medium/pdf/DSMZ_Medium830.pdf. Accessed 30 Oct. 2015.
- Dubinsky EA, Conrad ME, Chakraborty R, Bill M, Borglin SE, Hollibaugh JT, Mason OU, M. Piceno Y, Reid FC, Stringfellow WT, Tom LM, Hazen TC, Andersen GL (2013) Succession of Hydrocarbon-Degrading Bacteria in the Aftermath of the Deepwater Horizon Oil Spill in the Gulf of Mexico. *Environmental Science & Technology* 47:10860–10867.
- Egger LS (2013) Einfluss erhöhter Sauerstoffpartialdrücke auf das Wachstum von Bakterien. Bachelor's thesis, Hamburg University of Technology, Institute of Technical Biocatalysis
- Egorova DO, Korsakova ES, Demakov VA, Plotnikova EG (2013) Degradation of aromatic hydrocarbons by the *Rhodococcus wratislaviensis* KT112-7 isolated from waste products of a salt-mining plant. *Applied Biochemistry and Microbiology* 49:244–255.
- Eisenmenger MJ, Reyes-De-Corcuera JI (2009) High pressure enhancement of enzymes: A review. *Enzyme and Microbial Technology* 45:331–347.
- Eurotechnica GmbH (2014) Operating Manual HP-VC 300.
- Fan T, Buckley JS (2002) Rapid and Accurate SARA Analysis of Medium Gravity Crude Oils. *Energy & Fuels* 16:1571–1575.
- Fang J, Zhang L, Bazylinski DA (2010) Deep-sea piezosphere and piezophiles: geomicrobiology and biogeochemistry. *Trends in Microbiology* 18:413–422.
- Foght JM, Westlake DWS (1982) Effect of the dispersant Corexit 9527 on the microbial degradation of Prudhoe Bay oil. *Canadian Journal of Microbiology* 28:117–122.

- Follonier S, Panke S, Zinn M (2012) Pressure to kill or pressure to boost: a review on the various effects and applications of hydrostatic pressure in bacterial biotechnology. *Applied Microbiology and Biotechnology* 93:1805–1815.
- Fuchs G (1999) Oxidation of Organic Compounds. In: Lengeler JW, Drews G, Schlegel HG (eds) *Biology of the Prokaryotes*. Georg Thieme Verlag, Stuttgart, New York, pp 187–233.
- Gardner JV, Armstrong AA (2011) The Mariana Trench: A new view based on multibeam echosounding. *AGU Fall Meeting Abstracts* 1:1517.
- GESTIS Substance database: n-decane. [http://gestis-en.itrust.de/nxt/gateway.dll?f=templates\\$fn=default.htm\\$vid=gestiseng:sdbeng\\$3.0](http://gestis-en.itrust.de/nxt/gateway.dll?f=templates$fn=default.htm$vid=gestiseng:sdbeng$3.0). Accessed 4 April 2016.
- GESTIS Substance database: n-hexadecane. [http://gestis-en.itrust.de/nxt/gateway.dll?f=templates\\$fn=default.htm\\$vid=gestiseng:sdbeng\\$3.0](http://gestis-en.itrust.de/nxt/gateway.dll?f=templates$fn=default.htm$vid=gestiseng:sdbeng$3.0). Accessed 30 Oct. 2015.
- Gibson DT, Roberts RL, Wells MC, Kobal VM (1973) Oxidation of biphenyl by a *Beijerinckia* species. *Biochemical and Biophysical Research Communications* 50:211–219.
- Gottlieb SF (1971) Effect of Hyperbaric Oxygen on Microorganisms. *Annual Review of Microbiology* 25:111–152.
- Gross M, Lehle K, Jaenicke R, Nierhaus KH (1993) Pressure-induced dissociation of ribosomes and elongation cycle intermediates. *European Journal of Biochemistry* 218:463–468.
- Grossi V, Yakimov MM, Al Ali B, Tapilatu Y, Cuny P, Goutx M, La Cono V, Giuliano L, Tamburini C (2010) Hydrostatic pressure affects membrane and storage lipid compositions of the piezotolerant hydrocarbon-degrading *Marinobacter hydrocarbonoclasticus* strain #5. *Environmental Microbiology* 12:2020–2033.
- Gulf of Mexico Research Initiative (GoMRI). <http://gulfresearchinitiative.org>. Accessed 4 April 2016.

- Gutierrez T, Berry D, Yang T, Mishamandani S, McKay L, Teske A, Aitken MD (2013a) Role of Bacterial Exopolysaccharides (EPS) in the Fate of the Oil Released during the Deepwater Horizon Oil Spill. PLoS ONE 8:e67717.
- Gutierrez T, Singleton DR, Berry D, Yang T, Aitken MD, Teske A (2013b) Hydrocarbon-degrading bacteria enriched by the Deepwater Horizon oil spill identified by cultivation and DNA-SIP. The ISME Journal 7:2091–2104.
- Hamdan LJ, Fulmer PA (2011) Effects of COREXIT® EC9500A on bacteria from a beach oiled by the Deepwater Horizon spill. Aquatic microbial ecology 63:101–109.
- Hammel HT (1976) Colligative properties of a solution. Science 192:748–756.
- Hassanshahian M, Cappello S (2013) Crude Oil Biodegradation in the Marine Environments. In: Rolando Chamy (ed) Biodegradation - Engineering and Technology. InTech, pp 101–135.
- Hauben KJA, Wuytack EY, Soontjens CCF, Michiels CW (1996) High-Pressure Transient Sensitization of *Escherichia coli* to Lysozyme and Nisin by Disruption of Outer-Membrane Permeability. Journal of Food Protection 59:350–355.
- Hauf K (2012) Abbau von Hexadekan durch *Pseudomonas frederiksbergensis* in einer Hochdruckzelle. Bachelor's thesis, Hamburg University of Technology, Institute of Technical Biocatalysis.
- Hawley ER, Piao H, Scott NM, Malfatti S, Pagani I, Huntemann M, Chen A, Glavina del Rio T, Foster B, Copeland A, Jansson J, Pati A, Tringe S, Gilbert JA, Lorenson TD, Hess M (2014) Metagenomic analysis of microbial consortium from natural crude oil that seeps into the marine ecosystem offshore Southern California. Standards in Genomic Sciences 9:1259–1274.
- Hazen TC, Dubinsky EA, DeSantis TZ, Andersen GL, Piceno YM, Singh N, Jansson JK, Probst A, Borglin SE, Fortney JL, Stringfellow WT, Bill M, Conrad ME, Tom LM, Chavarria KL, Alusi TR, Lamendella R, Joyner DC, Spier C, Baelum J, Auer M, Zemla ML, Chakraborty R, Sonnenthal EL, D'haeseleer P, Holman H-YN, Osman S, Lu Z, Nostrand JDV, Deng Y, Zhou J,

- Mason OU (2010) Deep-Sea Oil Plume Enriches Indigenous Oil-Degrading Bacteria. *Science* 330:204–208.
- Head IM, Jones DM, Røling WFM (2006) Marine microorganisms make a meal of oil. *Nature Reviews Microbiology* 4:173–182.
- Heald SC, Brandão PFB, Hardicre R, Bull AT (2001) Physiology, biochemistry and taxonomy of deep-sea nitrile metabolising *Rhodococcus* strains. *Antonie Van Leeuwenhoek* 80:169–183.
- Heider J, Schühle K (2013) Anaerobic Biodegradation of Hydrocarbons Including Methane. In: Rosenberg E, DeLong EF, Lory S, Stackebrandt E, Thompson F (eds) *The Prokaryotes*. Springer Verlag, Berlin, Heidelberg, pp 605–634.
- Hiessl R (2014) Biologischer Abbau eines polycyclischen, aromatischen Kohlenwasserstoffs unter erhöhtem Druck durch *Sphingobium yanoikuyae*. Bachelor's thesis, Hamburg University of Technology, Institute of Technical Biocatalysis.
- Hollander DJ, Freeman KH, Ellis G, Diefendorf AF, Peebles EB, Paul J (2010) Long-Lived, Sub-Surface Layers of Toxic Oil in the Deep-Sea: A Molecular Organic and Isotopic Geochemical Approach to Understanding their Nature, Molecular Distribution, Origin and Impact to the Northern Gulf of Mexico. AGU Fall Meeting San Francisco, CA (Abstract OS21G-02).
- Hopkinson WI, Towers AG (1963) EFFECTS OF HYPERBARIC OXYGEN ON SOME COMMON PATHOGENIC BACTERIA. *The Lancet* 282:1361–1363.
- Horikoshi K (1998) Barophiles: deep-sea microorganisms adapted to an extreme environment. *Current Opinion in Microbiology* 1:291–295.
- Horikoshi K, Bull AT (2010) Prologue: Definition, Categories, Distribution, Origin and Evolution, Pioneering Studies, and Emerging Fields of Extremophiles. In: Horikoshi K (ed) *Extremophiles Handbook*. Springer Science & Business Media, Tokyo, Dordrecht, Heidelberg, London, New York, pp 3–15.

- Jabłoniec A, Horstmann S, Gmehling J (2007) Experimental Determination and Calculation of Gas Solubility Data for Nitrogen in Different Solvents. *Industrial & Engineering Chemistry Research* 46:4654–4659.
- Jannasch HW, Eimhjellen K, Wirsen C O, Farmanfarmaian A (1971) Microbial Degradation of Organic Matter in the Deep Sea. *Science* 171:672–675.
- Jannasch HW, Taylor CD (1984) Deep-Sea Microbiology. *Annual Review of Microbiology* 38:487–487.
- Jenkins HDB (2008) Ideal Liquid Mixtures. Vapour Pressure and Raoult's Law. In: *Chemical Thermodynamics at a Glance*. Blackwell Publishing Ltd, pp 94–97.
- Jesch SF (2015) Biologischer Abbau von Hexadekan und Naphthalin unter hohem Druck und dem Einfluss des Dispersionsmittel Corexit EC9500A. Bachelor's thesis, Hamburg University of Technology, Institute of Technical Biocatalysis.
- Jiménez Juárez JM (2015) Degradation of hydrocarbons by bacteria from the Gulf of Mexico. Bachelor's thesis, Hamburg University of Technology, Institute of Technical Biocatalysis.
- Joye SB (2015) Deepwater Horizon, 5 years on. *Science* 349:592–593.
- Joye SB, Leifer I, MacDonald IR, Chanton JP, Meile CD, Teske AP, Kostka JE, Chistoserdova L, Coffin R, Hollander D, Kastner M, Montoya JP, Rehder G, Solomon E, Treude T, Villareal TA (2011a) Comment on "A Persistent Oxygen Anomaly Reveals the Fate of Spilled Methane in the Deep Gulf of Mexico." *Science* 332:1033–1033.
- Joye SB, MacDonald IR, Leifer I, Asper V (2011b) Magnitude and oxidation potential of hydrocarbon gases released from the BP oil well blowout. *Nature Geoscience* 4:160–164.
- Joye SB, Teske AP, Kostka JE (2014) Microbial Dynamics Following the Macondo Oil Well Blowout across Gulf of Mexico Environments. *BioScience* 64:766–777.
- Kato C (1999) Barophiles (Piezophiles). In: Horikoshi K, Tsujii K (eds) *Extremophiles in Deep-Sea Environments*. Springer Verlag, Japan, pp 91–111.
- Kato M, Hayashi R, Tsuda T, Taniguchi K (2002) High pressure-induced changes of biological membrane. *European Journal of Biochemistry* 269:110–118.

- Kator H, Oppenheimer CH, Miget RJ (1971) Microbial degradation of a Louisiana crude oil in closed flasks and under simulated field conditions. *International Oil Spill Conference Proceedings* 1971:287–296.
- Kessler JD, Valentine DL, Redmond MC, Du M, Chan EW, Mendes SD, Quiroz EW, Villanueva CJ, Shusta SS, Werra LM, Yvon-Lewis SA, Weber TC (2011) A Persistent Oxygen Anomaly Reveals the Fate of Spilled Methane in the Deep Gulf of Mexico. *Science* 331:312–315.
- Kim S-J, Kwon KK (2010) Marine, Hydrocarbon-Degrading Alphaproteobacteria. In: Timmis KN (ed) *Handbook of Hydrocarbon and Lipid Microbiology*. Springer Verlag, Berlin, Heidelberg, pp 1707–1714.
- Kimes NE, Callaghan AV, Aktas DF, Smith WL, Sunner J, Golding B, Drozdowska M, Hazen TC, Suflita JM, Morris PJ (2013) Metagenomic analysis and metabolite profiling of deep-sea sediments from the Gulf of Mexico following the Deepwater Horizon oil spill. *Frontiers in Microbiology* 4:50.
- Kimes NE, Callaghan AV, Suflita JM, Morris PJ (2014) Microbial transformation of the Deepwater Horizon oil spill—past, present, and future perspectives. *Frontiers in Microbiology* 5:603.
- King GM, Kostka JE, Hazen TC, Sobecky PA (2015) Microbial Responses to the Deepwater Horizon Oil Spill: From Coastal Wetlands to the Deep Sea. *Annual Review of Marine Science* 7:377–401.
- Kleindienst S, Grim S, Sogin M, Bracco A, Crespo-Medina M, Joye SB (2015b) Diverse, rare microbial taxa responded to the Deepwater Horizon deep-sea hydrocarbon plume. *The ISME Journal* 10:400–415.
- Kleindienst S, Seidel M, Ziervogel K, Grim S, Loftis K, Harrison S, Malkin SY, Perkins MJ, Field J, Sogin ML, Dittmar T, Passow U, Medeiros P, Joye SB (2016) Reply to Prince *et al.*: Ability of chemical dispersants to reduce oil spill impacts remains unclear. *Proceedings of the National Academy of Sciences* 201600498.
- Kleindienst S, Seidel M, Ziervogel K, Grim S, Loftis K, Harrison S, Malkin SY, Perkins MJ, Field J, Sogin ML, Dittmar T, Passow U, Medeiros PM, Joye SB (2015a) Chemical dispersants can

suppress the activity of natural oil-degrading microorganisms. Proceedings of the National Academy of Sciences 201507380.

Koerner RJ, Goodfellow M, Jones AL (2009) The genus *Dietzia*: a new home for some known and emerging opportunist pathogens. FEMS Immunology & Medical Microbiology 55:296–305.

Kostka JE, Prakash O, Overholt WA, Green SJ, Freyer G, Canion A, Delgardio J, Norton N, Hazen TC, Huettel M (2011) Hydrocarbon-Degrading Bacteria and the Bacterial Community Response in Gulf of Mexico Beach Sands Impacted by the Deepwater Horizon Oil Spill. Applied and Environmental Microbiology 77:7962–7974.

Kromm A (2014) Das Verhalten von Mikroorganismen unter erhöhtem Sauerstoffpartialdruck. Bachelor's thesis, Hamburg University of Technology, Institute of Technical Biocatalysis.

Kujawinski EB, Kido Soule MC, Valentine DL, Boysen AK, Longnecker K, Redmond MC (2011) Fate of Dispersants Associated with the Deepwater Horizon Oil Spill. Environmental Science & Technology 45:1298–1306.

Lang E (1996) Diversity of bacterial capabilities in utilizing alkylated benzenes and other aromatic compounds. Letters in Applied Microbiology 23:257–260.

Leahy JG, Colwell RR (1990) Microbial degradation of hydrocarbons in the environment. Microbiological reviews 54:305–315.

Lehr B, Bristol S, Possolo A (2010) Oil Budget Calculator: Deepwater Horizon: Technical Documentation - A Report by The Federal Interagency Solutions Group, Oil Budget Calculator Science and Engineering Team. A Report to the National Incident Command.

Lincoln SA, Hamilton TL, Valladares Juárez AG, Schedler M, Macalady JL, Müller R, Freeman KH (2015) Draft Genome Sequence of the Piezotolerant and Crude Oil-Degrading Bacterium *Rhodococcus qingshengii* Strain TUHH-12. Genome Announcements 3:e00268-15.

- Lindo-Atichati D, Paris CB, Le Hénaff M, Schedler M, Valladares Juárez AG, Müller R (2016) Simulating the effects of droplet size, high-pressure biodegradation, and variable flow rate on the subsea evolution of deep plumes from the Macondo blowout. *Deep Sea Research Part II: Topical Studies in Oceanography*. <http://dx.doi.org/10.1016/j.dsr2.2014.01.011>.
- Lindstrom JE, Braddock JF (2002) Biodegradation of petroleum hydrocarbons at low temperature in the presence of the dispersant Corexit 9500. *Marine Pollution Bulletin* 44:739–747.
- Linstrom JE, White DM, Braddock JF (1999) Biodegradation of Dispersed Oil Using COREXIT 9500 - A Report Produced for the Alaska Department of Environmental Conservation Division of Spill Prevention and Response.
- Liu Z, Liu J (2013) Evaluating bacterial community structures in oil collected from the sea surface and sediment in the northern Gulf of Mexico after the Deepwater Horizon oil spill. *MicrobiologyOpen* 2:492–504.
- Liu Z, Liu J, Zhu Q, Wu W (2012) The weathering of oil after the Deepwater Horizon oil spill: insights from the chemical composition of the oil from the sea surface, salt marshes and sediments. *Environmental Research Letters* 7:35302–35315.
- Louvado A, Gomes NCM, Simões MMQ, Almeida A, Cleary DFR, Cunha A (2015) Polycyclic aromatic hydrocarbons in deep sea sediments: Microbe–pollutant interactions in a remote environment. *Science of the Total Environment* 526:312–328.
- Lowit MB, Blum LK, Mills AL (2000) Determining replication for discrimination among microbial communities in environmental samples using community-level physiological profiles. *FEMS Microbiology Ecology* 32:97–102.
- Macgregor RB (2002) The interactions of nucleic acids at elevated hydrostatic pressure. *Biochimica et Biophysica Acta (BBA) - Protein Structure and Molecular Enzymology* 1595:266–276.
- Madigan MT, Martinko JM (2009) *Brock Mikrobiologie*, 11th edn. Pearson Studium, Munich.

- Marshall AG, Rodgers RP (2003) Petroleomics: The Next Grand Challenge for Chemical Analysis. *Accounts of Chemical Research* 37:53–59.
- Martín Juárez J (2014) Biodegradation of oil by sediments collected from different sea-sites in the Gulf of Mexico. Diploma thesis, Hamburg University of Technology, Institute of Technical Biocatalysis.
- Mason OU, Hazen TC, Borglin S, Chain PSG, Dubinsky EA, Fortney JL, Han J, Holman H-YN, Hultman J, Lamendella R, Mackelprang R, Malfatti S, Tom LM, Tringe SG, Woyke T, Zhou J, Rubin EM, Jansson JK (2012) Metagenome, metatranscriptome and single-cell sequencing reveal microbial response to Deepwater Horizon oil spill. *The ISME Journal* 6:1715–1727.
- Mason OU, Scott NM, Gonzalez A, Robbins-Pianka A, Bælum J, Kimbrel J, Bouskill NJ, Prestat E, Borglin S, Joyner DC, Fortney JL, Jurelevicius D, Stringfellow WT, Alvarez-Cohen L, Hazen TC, Knight R, Gilbert JA, Jansson JK (2014) Metagenomics reveals sediment microbial community response to Deepwater Horizon oil spill. *The ISME Journal* 8:1464–1475.
- Mazzeo DEC, Levy CE, de Angelis D de F, Marin-Morales MA (2010) BTEX biodegradation by bacteria from effluents of petroleum refinery. *Science of the Total Environment* 408:4334–4340.
- McAllister TA, Stark JM, Norman JN, Ross RM (1963) INHIBITORY EFFECTS OF HYPERBARIC OXYGEN ON BACTERIA AND FUNGI. *The Lancet* 282:1040–1042.
- McInerney MJ, Struchtemeyer CG, Sieber J, Mouttaki H, Stams AJM, Schink B, Rohlin L, Gunsalus RP (2008) Physiology, Ecology, Phylogeny, and Genomics of Microorganisms Capable of Syntrophic Metabolism. *Annals of the New York Academy of Sciences* 1125:58–72.
- McNutt MK, Camilli R, Crone TJ, Guthrie GD, Hsieh PA, Ryerson TB, Savas O, Shaffer F (2012) Review of flow rate estimates of the Deepwater Horizon oil spill. *Proceedings of the National Academy of Sciences* 109:20260–20267.
- Meganathan R, Marquis RE (1973) Loss of Bacterial Motility under Pressure. *Nature* 246:525–527.

- Michel J, Owens EH, Zengel S, Graham A, Nixon Z, Allard T, Holton W, Reimer PD, Lamarche A, White M, Rutherford N, Childs C, Mauseth G, Challenger G, Taylor E (2013) Extent and Degree of Shoreline Oiling: Deepwater Horizon Oil Spill, Gulf of Mexico, USA. *PLoS one* 8:e65087.
- Montagna PA, Baguley JG, Cooksey C, Hartwell I, Hyde LJ, Hyland JL, Kalke RD, Kracker LM, Reuscher M, Rhodes ACE (2013) Deep-Sea Benthic Footprint of the Deepwater Horizon Blowout. *PLoS one* 8:e70540.
- Mota MJ, Lopes RP, Delgadillo I, Saraiva JA (2013) Microorganisms under high pressure — Adaptation, growth and biotechnological potential. *Biotechnology Advances* 31:1426–1434.
- Mozhaev VV, Heremans K, Frank J, Masson P, Balny C (1996) High pressure effects on protein structure and function. *Proteins* 24:81–91.
- Müller R (2006) Umweltbiotechnologie. In: Antranikian G (ed) *Angewandte Mikrobiologie*. Springer Verlag, Berlin, Heidelberg, pp 445–458.
- Muyzer G (1999) DGGE/TGGE a method for identifying genes from natural ecosystems. *Current Opinion in Microbiology* 2:317–322.
- Muyzer G, Waal EC de, Uitterlinden AG (1993) Profiling of complex microbial populations by denaturing gradient gel electrophoresis analysis of polymerase chain reaction-amplified genes coding for 16S rRNA. *Applied and Environmental Microbiology* 59:695–700.
- Nagata T, Tamburini C, Arístegui J, Baltar F, Bochdansky AB, Fonda-Umani S, Fukuda H, Gogou A, Hansell DA, Hansman RL, Herndl GJ, Panagiotopoulos C, Reinthaler T, Sohrin R, Verdugo P, Yamada N, Yamashita Y, Yokokawa T, Bartlett DH (2010) Emerging concepts on microbial processes in the bathypelagic ocean – ecology, biogeochemistry, and genomics. *Deep Sea Research Part II: Topical Studies in Oceanography* 57:1519–1536.
- National Commission on the BP Deepwater Horizon Oil Spill and Offshore Drilling (2011) *Deep Water: The Gulf Oil Disaster and the Future of Offshore Drilling - Report to the President (BP Oil Spill Commission Report)*.

- National Research Council (2003) Oil in the Sea III: Inputs, Fates, and Effects. The National Academies Press, Washington, DC.
- Nercessian O, Noyes E, Kalyuzhnaya MG, Lidstrom ME, Chistoserdova L (2005) Bacterial Populations Active in Metabolism of C1 Compounds in the Sediment of Lake Washington, a Freshwater Lake. *Applied and Environmental Microbiology* 71:6885–6899.
- Niven GW, Miles CA, Mackey BM (1999) The effects of hydrostatic pressure on ribosome conformation in *Escherichia coli*: an in vivo study using differential scanning calorimetry. *Microbiology* 145:419–425.
- Nogi Y (2008) Bacteria in the Deep Sea: Psychropiezophiles. In: Margesin R, Schinner F, Marx J-C, Gerday C (eds) *Psychrophiles: from Biodiversity to Biotechnology*. Springer Berlin Heidelberg, pp 73–82.
- Ocean Optics GmbH (2012) Catalog of Products-Spectrometers, Accessories and More.
- Oger PM, Jebbar M (2010) The many ways of coping with pressure. *Research in Microbiology* 161:799–809.
- Overholt WA, Marks KP, Romero IC, Hollander DJ, Snell TW, Kostka JE (2016) Hydrocarbon-Degrading Bacteria Exhibit a Species-Specific Response to Dispersed Oil while Moderating Ecotoxicity. *Applied and Environmental Microbiology* 82:518–527.
- Pagán R, Mackey B (2000) Relationship between Membrane Damage and Cell Death in Pressure-Treated *Escherichia coli* Cells: Differences between Exponential- and Stationary-Phase Cells and Variation among Strains. *Applied and Environmental Microbiology* 66:2829–2834.
- Passow U (2014) Formation of rapidly-sinking, oil-associated marine snow. *Deep Sea Research Part II: Topical Studies in Oceanography* <http://dx.doi.org/10.1016/j.dsr2.2014.10.001>.
- Passow U, Ziervogel K, Asper V, Diercks A (2012) Marine snow formation in the aftermath of the Deepwater Horizon oil spill in the Gulf of Mexico. *Environmental Research Letters* 7:35301.

- Peng F, Wang Y, Sun F, Liu Z, Lai Q, Shao Z (2008) A novel lipopeptide produced by a Pacific Ocean deep-sea bacterium, *Rhodococcus* sp. TW53. *Journal of Applied Microbiology* 105:698–705.
- Penniston JT (1971) High hydrostatic pressure and enzymic activity: Inhibition of multimeric enzymes by dissociation. *Archives of Biochemistry and Biophysics* 142:322–332.
- Pérez-Pantoja D, González B, Pieper DH (2010) Aerobic Degradation of Aromatic Hydrocarbons. In: Timmis KN (ed) *Handbook of Hydrocarbon and Lipid Microbiology*. Springer Verlag, Berlin, Heidelberg, pp 799–837.
- Pizzul L, Castillo M del P, Stenström J (2007) Effect of rapeseed oil on the degradation of polycyclic aromatic hydrocarbons in soil by *Rhodococcus wratislaviensis*. *International Biodeterioration & Biodegradation* 59:111–118.
- PreSens Precision sensing Brochure: Imaging Solutions-VisiSens.
- Prieur D, Marteinsson VT (1998) Prokaryotes living under elevated hydrostatic pressure. In: Antranikian G (ed) *Biotechnology of Extremophiles*. Springer Verlag, Berlin, Heidelberg, pp 23–35.
- Prince RC (1993) Petroleum Spill Bioremediation in Marine Environments. *Critical Reviews in Microbiology* 19:217–240.
- Prince RC, Coolbaugh TS, Parkerton TF (2016) Oil dispersants do facilitate biodegradation of spilled oil. *Proceedings of the National Academy of Sciences* 201525333.
- Prince RC, Gramain A, McGenity TJ (2010) Prokaryotic Hydrocarbon Degradation. In: Timmis KN (ed) *Handbook of Hydrocarbon and Lipid Microbiology*. Springer Verlag, Berlin, Heidelberg, pp 1669–1692.
- Rainey FA, Klatte S, Kroppenstedt R-M, Stackebrandt E (1995) *Dietzia*, a New Genus Including *Dietzia maris* comb. no., Formerly *Rhodococcus maris*. *INTERNATIONAL JOURNAL OF SYSTEMATIC BACTERIOLOGY* 45:32–36.
- Ramseur JL (2010) Deepwater Horizon Oil Spill: The Fate of the Oil - CRS Report for Congress.

- Reddy CM, Arey JS, Seewald JS, Sylva SP, Lemkau KL, Nelson RK, Carmichael CA, McIntyre CP, Fenwick J, Ventura GT, Van Mooy BAS, Camilli R (2012) Composition and fate of gas and oil released to the water column during the Deepwater Horizon oil spill. *Proceedings of the National Academy of Sciences of the United States of America* 109:20229–20234.
- Redmond MC, Valentine DL (2012) Natural gas and temperature structured a microbial community response to the Deepwater Horizon oil spill. *Proceedings of the National Academy of Sciences* 109:20292–20297.
- Reference oil team (2012) Meeting summary - Oil Samples Available to GoMRI Funded Researchers. BP Knox Storage Facility.
- Rhodes PR (1969) Mechanism of Chloride Stress Corrosion Cracking of Austenitic Stainless Steels. *Corrosion* 25:462–472.
- Rojey A, Jaffret C (1997) *Natural Gas: production, processing, transport*. Editions Technip, Paris.
- Romero IC, Schwing PT, Brooks GR, Larson RA, Hastings DW, Ellis G, Goddard EA, Hollander DJ (2015) Hydrocarbons in Deep-Sea Sediments following the 2010 Deepwater Horizon Blowout in the Northeast Gulf of Mexico. *PLoS one* 10:e0128371.
- Ron EZ, Rosenberg E (2014) Enhanced bioremediation of oil spills in the sea. *Current Opinion in Biotechnology* 27:191–194.
- Rosenberg E, Navon-Venezia S, Zilber-Rosenberg I, Ron EZ (1998) Rate-Limiting Steps in the Microbial Degradation of Petroleum Hydrocarbons. In: Rubin PH, Narkis PN, Carberry DJ (eds) *Soil and Aquifer Pollution*. Springer Verlag, Berlin, Heidelberg, pp 159–172.
- Ryerson TB, Aikin KC, Angevine WM, Atlas EL, Blake DR, Brock CA, Fehsenfeld FC, Gao R-S, de Gouw JA, Fahey DW, Holloway JS, Lack DA, Lueb RA, Meinardi S, Middlebrook AM, Murphy DM, Neuman JA, Nowak JB, Parrish DD, Peischl J, Perring AE, Pollack IB, Ravishankara AR, Roberts JM, Schwarz JP, Spackman JR, Stark H, Warneke C, Watts LA (2011) Atmospheric emissions from the Deepwater Horizon spill constrain air-water partitioning, hydrocarbon fate, and leak rate. *Geophysical Research Letters* 38:L07803.

- Ryerson TB, Camilli R, Kessler JD, Kujawinski EB, Reddy CM, Valentine DL, Atlas E, Blake DR, de Gouw J, Meinardi S, Parrish DD, Peischl J, Seewald JS, Warneke C (2012) Chemical data quantify Deepwater Horizon hydrocarbon flow rate and environmental distribution. *Proceedings of the National Academy of Sciences of the United States of America* 109:20246–20253.
- Sammarco PW, Kolian SR, Warby RAF, Bouldin JL, Subra WA, Porter SA (2013) Distribution and concentrations of petroleum hydrocarbons associated with the BP/Deepwater Horizon Oil Spill, Gulf of Mexico. *Marine pollution bulletin* 73:129–143.
- Sawamura S, Tsuchiya M, Ishigami T, Taniguchi Y, Suzuki K (1993) Effect of pressure on the solubility of naphthalene in water at 25°C. *Journal of Solution Chemistry* 22:727–732.
- Schedler M, Hiessl R, Valladares Juárez AG, Gust G, Müller R (2014) Effect of high pressure on hydrocarbon-degrading bacteria. *AMB Express* 4:77.
- Schrope M (2010) Oil cruise finds deep-sea plume. *Nature News* 465:274–275.
- Schrope M (2013) Dirty blizzard buried Deepwater Horizon oil. *Nature News* doi:10.1038/nature.2013.12304.
- Schwarz JR, Walker JD, Colwell RR (1974) Deep-Sea Bacteria: Growth and Utilization of Hydrocarbons at Ambient and In Situ Pressure. *Applied Microbiology* 28:982–986.
- Schwarz JR, Walker JD, Colwell RR (1975) Deep-sea bacteria: growth and utilization of n-hexadecane at in situ temperature and pressure. *Canadian Journal of Microbiology* 21:682–687.
- Schwing PT, Romero IC, Brooks GR, Hastings DW, Larson RA, Hollander DJ (2015) A Decline in Benthic Foraminifera following the Deepwater Horizon Event in the Northeastern Gulf of Mexico. *PLoS one* 10:e0120565.
- Scoma A, Barbato M, Hernandez-Sanabria E, Mapelli F, Daffonchio D, Borin S, Boon N (2016) Microbial oil-degradation under mild hydrostatic pressure (10 MPa): which pathways are impacted in piezosensitive hydrocarbonoclastic bacteria? *Scientific Reports* 6:23526.

- Seo JS, Keum YS, Li QX (2009) Bacterial degradation of aromatic compounds. *International Journal of Environmental Research and Public Health* 6:278–309.
- Shiller AM, Joung D (2012) Nutrient depletion as a proxy for microbial growth in Deepwater Horizon subsurface oil/gas plumes. *Environmental Research Letters* 7:45301.
- Socolofsky SA, Adams EE, Boufadel MC, Aman ZM, Johansen Øistein, Konkel WJ, Lindo D, Madsen MN, North EW, Paris CB, Rasmussen D, Reed M, Rønningen P, Sim LH, Uhrenholdt T, Anderson KG, Cooper C, Nedwed TJ (2015) Intercomparison of oil spill prediction models for accidental blowout scenarios with and without subsea chemical dispersant injection. *Marine Pollution Bulletin* 96:110–126.
- Speight JG (2007) *Natural Gas: A Basic Handbook*. Gulf Publishing Company, Houston, Texas.
- Spormann AM, Widdel F (2000) Metabolism of alkylbenzenes, alkanes, and other hydrocarbons in anaerobic bacteria. *Biodegradation* 11:85–105.
- Stanier RY, Ornston LN (1973) The β -ketoacid pathway. In: Rose AH, Tempest DW (eds) *Advances in Microbial Physiology*. Academic Press, London and New York, pp 89–151.
- Stretton S, Goodman AE (1998) Carbon dioxide as a regulator of gene expression in microorganisms. *Antonie Van Leeuwenhoek* 73:79–85.
- Su EM (2014) Comparison of two sediments collected from different sea-sites in the Gulf of Mexico on bacterial growth under different pressures. Project work, Hamburg University of Technology, Institute of Technical Biocatalysis.
- Swannell RPJ, Daniel F (1999) Effect of Dispersants on Oil Biodegradation Under Simulated Marine Conditions. *International Oil Spill Conference Proceedings 1999*:169–176.
- Takami H, Inoue A, Fuji F, Horikoshi K (1997) Microbial flora in the deepest sea mud of the Mariana Trench. *FEMS Microbiology Letters* 152:279–285.
- Tapilatu Y, Acquaviva M, Guigue C, Miralles G, Bertrand J-C, Cuny P (2010) Isolation of alkane-degrading bacteria from deep-sea Mediterranean sediments. *Letters in Applied Microbiology* 50:234–236.

- The Center for the Integrated Modeling and Analysis of the Gulf Ecosystem (CIMAGE II). <http://www.marine.usf.edu/c-image/>. Accessed 4 April 2016.
- Todeschini R, Consonni V (2009) Molecular Descriptors for Chemoinformatics, Vol 41 (2 Volume Set), 2nd edn. Wiley-VCH Verlag GmbH & Co, Weinheim.
- Truman JE (1977) The influence of chloride content, pH and temperature of test solution on the occurrence of stress corrosion cracking with austenitic stainless steel. *Corrosion Science* 17:737–746.
- Turley CM, Lochte K (1990) Microbial response to the input of fresh detritus to the deep-sea bed. *Palaeogeography, Palaeoclimatology, Palaeoecology* 89:3–23.
- Valentine DL, Fisher GB, Bagby SC, Nelson RK, Reddy CM, Sylva SP, Woo MA (2014) Fallout plume of submerged oil from Deepwater Horizon. *Proceedings of the National Academy of Sciences* 111:15906–15911.
- Valentine DL, Kessler JD, Redmond MC, Mendes SD, Heintz MB, Farwell C, Hu L, Kinnaman FS, Yvon-Lewis S, Du M, Chan EW, Tigreros FG, Villanueva CJ (2010) Propane Respiration Jump-Starts Microbial Response to a Deep Oil Spill. *Science* 330:208–211.
- Valentine DL, Mezić I, Maćešić S, Črnjarić-Žic N, Ivić S, Hogan PJ, Fonoberov VA, Loire S (2012) Dynamic autoinoculation and the microbial ecology of a deep water hydrocarbon irruption. *Proceedings of the National Academy of Sciences* 109:20286–20291.
- Valladares Juárez AG, Kadimesetty HS, Achatz DE, Schedler M, Müller R (2015) Online Monitoring of Crude Oil Biodegradation at Elevated Pressures. *IEEE Journal of Selected Topics in Applied Earth Observations and Remote Sensing* 8:872–878.
- Venosa AD, Holder EL (2007) Biodegradability of dispersed crude oil at two different temperatures. *Marine Pollution Bulletin* 54:545–553.
- von der Weid I, Marques JM, Cunha CD, Lippi RK, dos Santos SCC, Rosado AS, Lins U, Seldin L (2007) Identification and biodegradation potential of a novel strain of *Dietzia cinnamea* isolated from a petroleum-contaminated tropical soil. *Systematic and Applied Microbiology* 30:331–339.

- Wang YP, Gu J-D (2006) Degradability of dimethyl terephthalate by *Variovorax paradoxus* T4 and *Sphingomonas yanoikuyae* DOS01 isolated from deep-ocean sediments. *Ecotoxicology* 15:549–557.
- Welch TJ, Farewell A, Neidhardt FC, Bartlett DH (1993) Stress response of *Escherichia coli* to elevated hydrostatic pressure. *Journal of Bacteriology* 175:7170–7177.
- White HK, Lyons SL, Harrison SJ, Findley DM, Liu Y, Kujawinski EB (2014) Long-Term Persistence of Dispersants following the Deepwater Horizon Oil Spill. *Environmental Science & Technology Letters* 1:295–299.
- Wiebe R, Gaddy VL (1940) The Solubility of Carbon Dioxide in Water at Various Temperatures from 12 to 40° and at Pressures to 500 Atmospheres. *Critical Phenomena. Journal of the American Chemical Society* 62:815–817.
- Wirsen CO, Jannasch DHW, Wakeham SG, Canuel EA (1986) Membrane lipids of a psychrophilic and barophilic deep-sea bacterium. *Current Microbiology* 14:319–322.
- Wiseman GM, Violago FC, Roberts E, Penn I (1966) The Effect of Hyperbaric Oxygen Upon Aerobic Bacteria: I. in Vitro Studies. *Canadian Journal of Microbiology* 12:521–529.
- Xu J-L, He J, Wang Z-C, Wang K, Li W-J, Tang S-K, Li S-P (2007) *Rhodococcus qingshengii* sp. nov., a carbendazim-degrading bacterium. *International Journal Of Systematic And Evolutionary Microbiology* 57:2754–2757.
- Yakimov MM, Timmis KN, Golyshin PN (2007) Obligate oil-degrading marine bacteria. *Current Opinion in Biotechnology* 18:257–266.
- Yang T, Nigro LM, Gutierrez T, D'Ambrosio L, Joye SB, Highsmith R, Teske A (2014) Pulsed blooms and persistent oil-degrading bacterial populations in the water column during and after the Deepwater Horizon blowout. *Deep Sea Research Part II: Topical Studies in Oceanography* <http://dx.doi.org/10.1016/j.dsr2.2014.01.014>.
- Yayanos AA, Pollard EC (1969) A Study of the Effects of Hydrostatic Pressure on Macromolecular Synthesis in *Escherichia coli*. *Biophysical Journal* 9:1464–1482.

- Yergeau E, Maynard C, Sanschagrin S, Champagne J, Juck D, Lee K, Greer CW (2015) Microbial Community Composition, Functions, and Activities in the Gulf of Mexico 1 Year after the Deepwater Horizon Accident. *Applied and Environmental Microbiology* 81:5855–5866.
- Yumoto I, Kojima K, Matsuyama H, Kusumoto K, Iwata H, Nakamura A, Nodasaka Y (2002) *Dietzia psychralcaliphila* sp. nov., a novel, facultatively psychrophilic alkaliphile that grows on hydrocarbons. *International Journal of Systematic and Evolutionary Microbiology* 52:85–90.
- Yvon-Lewis SA, Hu L, Kessler J (2011) Methane flux to the atmosphere from the Deepwater Horizon oil disaster. *Geophysical Research Letters* 38:L01602.
- Zhang Y, McEwen RS, Ryan JP, Bellingham JG, Thomas H, Thompson CH, Rienecker E (2011) A peak-capture algorithm used on an autonomous underwater vehicle in the 2010 Gulf of Mexico oil spill response scientific survey. *Journal of Field Robotics* 28:484–496.
- Ziervogel K, McKay L, Rhodes B, Osburn CL, Dickson-Brown J, Arnosti C, Teske A (2012) Microbial Activities and Dissolved Organic Matter Dynamics in Oil-Contaminated Surface Seawater from the Deepwater Horizon Oil Spill Site. *PLoS one* 7:e34816.
- ZoBell CE (1946) ACTION OF MICROÖRGANISMS ON HYDROCARBONS. *Bacteriological Reviews* 10:1–49.
- ZoBell CE, Cobet AB (1962) Growth, Reproduction, and Death Rates of *Escherichia Coli* at Increased Hydrostatic Pressures. *Journal of Bacteriology* 84:1228–1236.
- ZoBell CE, Cobet AB (1964) Filament Formation by *Escherichia Coli* at Increased Hydrostatic Pressures. *Journal of Bacteriology* 87:710–719.
- ZoBell CE, Hittle LL (1967) Some Effects of Hyperbaric Oxygenation on Bacteria at Increased Hydrostatic Pressures. *Canadian Journal of Microbiology* 13:1311–1319.
- ZoBell CE, Johnson FH (1949) THE INFLUENCE OF HYDROSTATIC PRESSURE ON THE GROWTH AND VIABILITY OF TERRESTRIAL AND MARINE BACTERIA 1. *Journal of Bacteriology* 57:179–189.

Appendix

Overview of the experiments

Table A.1: Summary of the setup and conditions of the biodegradation experiments carried out in this thesis.

Bacterial strain or bacterial community from sediment	Medium for liquid culture	Substrate		Corexit® EC9500A	Reactor	Probe	Pressure (bar)	Temperature (°C)	Chapter	
		Concentration (mM)	Hydrocarbon						Results	Discussion
<i>R. qingshengii</i> TUHH-12	MM II	1	n-Hexadecane	-	160 mL high pressure reactor with screw-piston mechanism for mechanical pressurisation	-	1 and 150	RT	3.1.1	4.1
<i>R. qingshengii</i> TUHH-12 and <i>E. coli</i>	MM II or LB medium	1mM C ₁₆ H ₃₄ , 1% (w/v) α-D glucose	n-Hexadecane or α-D glucose	-	High pressure reactor with screw-piston for mechanical press.	-	Different oxygen partial pressures	RT or 37	3.1.3	4.1

Table continued on next page.

Table A.1 - continued

<i>R. qingshengii</i> TUHH-12	MM II	1 or 3	n- Hexadecane	-	160 ml high pressure + ambient pressure reactors	O ₂ sensors (Ocean Optics GmbH)	1, 147 and 150	RT	3.3.1	4.2.1
<i>R. qingshengii</i> TUHH-12 or without inoculum	MM II	1	n- Hexadecane	-	160 ml high pressure + ambient pressure reactors	-	1, 135 and 152	RT	3.3.1.1	4.2.1
<i>R. qingshengii</i> TUHH-12	MM II	1	n- Tetracosane	-	160 ml high pressure + ambient pressure reactors	O ₂ sensors (Ocean Optics GmbH)	1 and 146	RT	3.3.2	4.2.1
<i>R. qingshengii</i> TUHH-12	MM II	1.59	n-Decane	-	160 ml high pressure + ambient pressure reactors	O ₂ sensors (Ocean Optics GmbH)	1 and 151	RT	3.3.3	4.2.1
-	MM II	1.59	n-Decane	-	160 ml high pressure + ambient pressure reactors	O ₂ sensors (Ocean Optics GmbH)	1 and 135	RT	3.3.3.1	4.2.1
<i>D. aurantiaca</i> C7.oil.2	MM II	1	n- Hexadecane	-	1 L high pressure reactor	Prototype O ₂ sensor	1 and 154	RT	3.3.4	4.2.1

Table continued on next page.

Table A.1 - continued

<i>R. qingshengii</i> TUHH-12	MM II	1	n- Hexadecane	With and without	160 mL high pressure + ambient pressure reactors	-	1 and 147	RT	3.3.5.1	4.2.2
<i>R. qingshengii</i> TUHH-12	MM II	-	-	With	160 mL high pressure + ambient pressure reactors	-	1 and 144	RT	3.3.5.2	4.2.2
<i>R. qingshengii</i> TUHH-12	MM II	1	n- Hexadecane	With and without	160 mL high pressure + ambient pressure reactors	-	1	4	3.3.5.3	4.2.2
<i>R. wratislaviensis</i> Tol3	Brunner		Toluene vapour	-	160 mL high pressure + ambient pressure reactors	O ₂ sensors Ocean (Optics GmbH)	1 and 140	RT	3.4.1	4.3.1
<i>R. wratislaviensis</i> Tol3	Brunner		Toluene vapour	-	160 mL high pressure reactors	-	1-154	RT	3.4.2	4.3.1
<i>R. wratislaviensis</i> Tol3	Brunner	1% (w/v)	α -D Glucose	-	160 mL high pressure reactors	-	1-154	RT	3.4.3	4.3.1

Table continued on next page.

Table A.1 - continued

<i>R. wratislaviensis</i> Tol3	Brunner		Toluene vapour (and decalin)	-	Airtight Erlenmeyer flask	-	1	RT	3.4.4	4.3.1
<i>D. aurantiaca</i> C7.oil.2	MMIII		Toluene vapour	-	160 ml high pressure + ambient pressure reactors	-	1 and 142	4	3.4.5	4.3.1
<i>S. yanoikuyae</i> B1	Brunner	1.77	Naph-thalene	-	160 ml high pressure + ambient pressure reactors	-	1 and 139	RT	3.5.1	4.4.1
-	Brunner	1.77	Naph-thalene	-	160 ml high pressure + ambient pressure reactors	-	1 and 142	RT	3.5.2	4.4.1
<i>S. yanoikuyae</i> B1	Brunner	1.77	Naph-thalene	-	160 ml high pressure reactors	-	1-130	RT	3.5.3	4.4.1
<i>S. yanoikuyae</i> B1	Brunner	1.77	Naph-thalene	-	High pressure view cell reactor No. 1	Fibox 3 + pCO ₂ mini (PreSens Precision Sensing)	1 and 162	RT	3.5.4	4.4.1

Table continued on next page.

Table A.1 - continued

<i>S. yanoikuyae</i> B1	Brunner	1.77	Naph- thalene	-	1 L high pressure reactor	-	1 and 150	RT	3.5.5	4.4.1
<i>S. yanoikuyae</i> B1	Brunner	1.63	Salicylic acid	-	160 mL high pressure + ambient pressure reactors	-	1 and 148	RT	3.5.6	4.4.1
<i>S. yanoikuyae</i> B1	Brunner	1% (w/v)	α -D Glucose	-	160 mL high pressure + ambient pressure reactors	-	1 and 156	RT	3.5.7	4.4.1
<i>S. yanoikuyae</i> B1	Brunner	1.77	Naph- thalene	With and without	160 mL high pressure + ambient pressure reactors	-	1, 89 and 149	RT	3.5.8	4.4.2
<i>S. yanoikuyae</i> B1	Brunner	-	-	With	160 mL high pressure + ambient pressure reactors	-	1 and 93	RT	3.5.9	4.4.2
Sediment No. 2 and 4	MM II with or without 3% NaCl	0.1% (v/v)	Crude oil	-	High pressure view cell reactor No. 1	Fibox 3 + pCO ₂ mini (PreSens)	150	5 or 20	3.6.1	4.5.1

Table continued on next page.

Table A.1 - continued

Sediment No. 3 and 8	MM II with 3% NaCl	0.1% (v/v)	Crude oil	-	High pressure view cell reactor No. 1	Fibox 3 (PreSens Precision Sensing GmbH)	1 and 150	5	3.6.1	4.5.1
Sediment No. 4	MM II	0.1% (v/v)	Crude oil	-	High pressure view cell reactor No. 2	VisiSens™ O ₂ and CO ₂ sensors (PreSens Precision Sensing GmbH)	1 and 150	RT	3.6.2	4.5.2
Sediment No. 8	MM II	0.1% (v/v)	Crude oil	-	160 mL high pressure + ambient pressure reactors	O ₂ sensors (Ocean Optics GmbH)	1 and 144	RT	3.6.2	4.5.2
Sediment No. 4	MM II	0.1% (v/v) crude oil	Crude oil or natural gas	-	High pressure view cell reactor No. 2	Fibox 3 (PreSens Precision Sensing GmbH)	1, 148 and 153	RT	3.6.3	4.5.3

Lebenslauf

Persönliche Daten

Name	Schedler
Vorname	Martina
Geburtsdatum	18.06.1986
Geburtsort, -land	Rostock, Deutschland

Schulbildung

09.1993 – 07.1995	Jürgen-Reichen-Grundschule in Rostock
09.1995 – 07.1997	Grundschule am Margaretenplatz in Rostock
09.1997 – 07.2006	Goethegymnasium Rostock (seit 2005 umbenannt in Innerstädtisches Gymnasium Rostock), Abitur am 01.07.2006

Hochschulstudium

10.2006 – 02.2012	Studium der Biologie an der Universität Rostock, Abschluss mit dem Diplom am 10.02.2012
07.2012 – 07.2016	Doktorarbeit am Institut für Technische Biokatalyse der Technischen Universität Hamburg-Harburg